MESOTHELIAL PHYSIOLOGY AND PATHOPHYSIOLOGY

EDITED BY: Sotirios G. Zarogiannis
PUBLISHED IN: Frontiers in Physiology

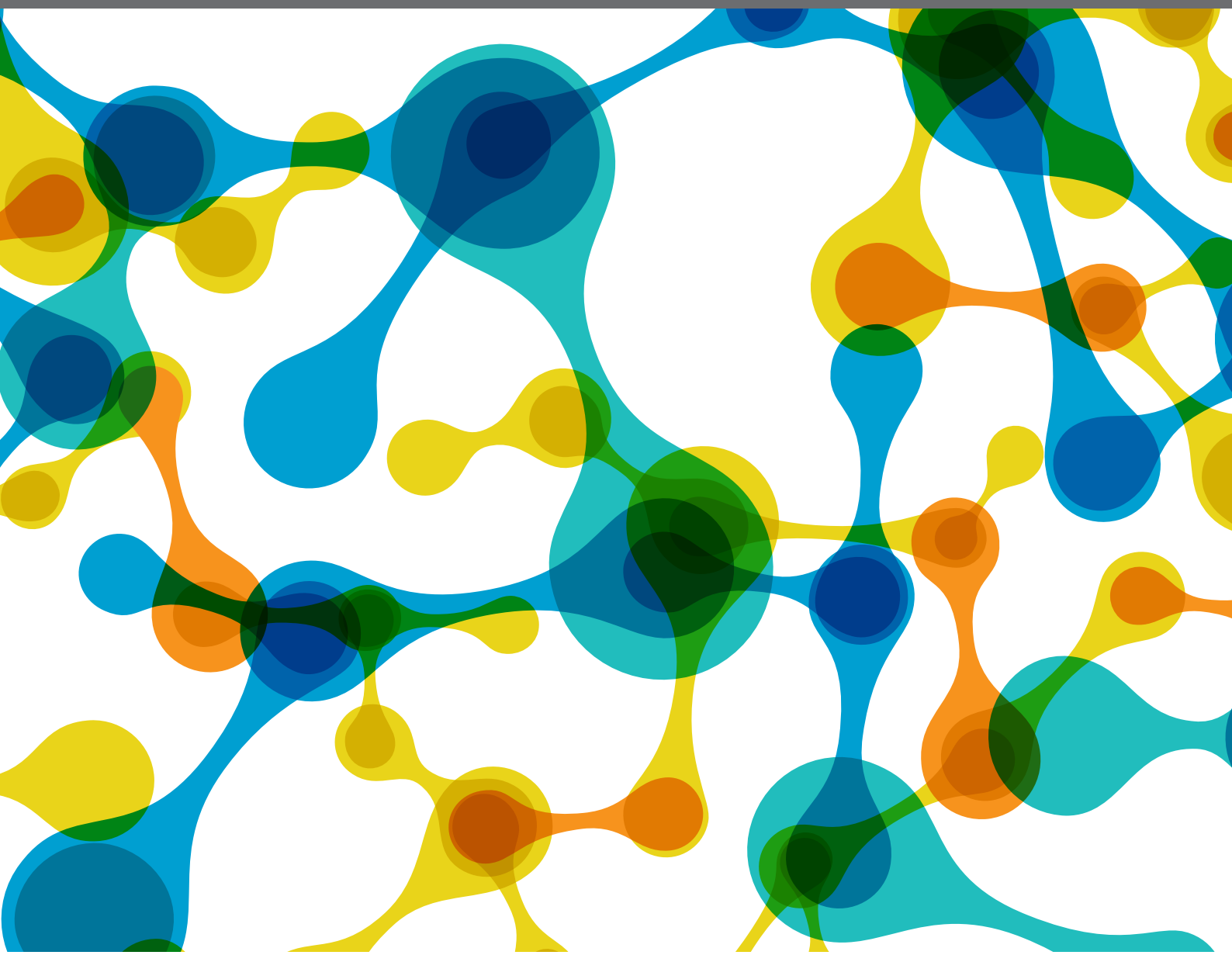

frontiers Research Topics

ISSN 1664-8714
ISBN 978-2-88945-541-6
DOI 10.3389/978-2-88945-541-6

About Frontiers

Frontiers is more than just an open-access publisher of scholarly articles: it is a pioneering approach to the world of academia, radically improving the way scholarly research is managed. The grand vision of Frontiers is a world where all people have an equal opportunity to seek, share and generate knowledge. Frontiers provides immediate and permanent online open access to all its publications, but this alone is not enough to realize our grand goals.

Frontiers Journal Series

The Frontiers Journal Series is a multi-tier and interdisciplinary set of open-access, online journals, promising a paradigm shift from the current review, selection and dissemination processes in academic publishing. All Frontiers journals are driven by researchers for researchers; therefore, they constitute a service to the scholarly community. At the same time, the Frontiers Journal Series operates on a revolutionary invention, the tiered publishing system, initially addressing specific communities of scholars, and gradually climbing up to broader public understanding, thus serving the interests of the lay society, too.

Dedication to Quality

Each Frontiers article is a landmark of the highest quality, thanks to genuinely collaborative interactions between authors and review editors, who include some of the world's best academicians. Research must be certified by peers before entering a stream of knowledge that may eventually reach the public - and shape society; therefore, Frontiers only applies the most rigorous and unbiased reviews.
Frontiers revolutionizes research publishing by freely delivering the most outstanding research, evaluated with no bias from both the academic and social point of view. By applying the most advanced information technologies, Frontiers is catapulting scholarly publishing into a new generation.

What are Frontiers Research Topics?

Frontiers Research Topics are very popular trademarks of the Frontiers Journals Series: they are collections of at least ten articles, all centered on a particular subject. With their unique mix of varied contributions from Original Research to Review Articles, Frontiers Research Topics unify the most influential researchers, the latest key findings and historical advances in a hot research area! Find out more on how to host your own Frontiers Research Topic or contribute to one as an author by contacting the Frontiers Editorial Office: researchtopics@frontiersin.org

MESOTHELIAL PHYSIOLOGY AND PATHOPHYSIOLOGY

Topic Editor:
Sotirios G. Zarogiannis, University of Thessaly, Greece

The mesothelium is composed by a single layer of mesothelial cells that vest the serosal cavities (pleural, peritoneal and pericardial) and internal organs of the body. The mesothelial cells have a mixed phenotype of epithelial cells and fibroblasts rendering them remarkable plasticity. Besides providing a slippery surface for the frictionless movement of internal organs, the mesothelium participates in a wide range of physiological and pathophysiological processes. Some of its functions include lung development, trans-cellular and para-cellular transport of ions and water, secretion of glycoproteins (mainly hyaluronan), secretion of cytokines and growth factors, wound healing, response to inflammatory stimuli and induction of inflammation, mesothelial to mesenchymal transition and formation of tunneling nanotubes. Many of these functions are pivotal to physiological conditions such as respiratory development, maintenance of steady volume of serosal fluids and serosal permeability, cell-to-cell communication, re-mesotheliazation of serosal membranes after mechanical (e.g. by asbestos or nanoparticles) or inflammatory injury and participation in immune responses. Deviation from the physiological threshold of these functions results in the development of serosal effusions, induction of serosal and lung fibrosis, induction of mesothelial tumorigenesis, leading thus to devastating pathologies. Treatment of pathologies like mesothelioma, pleural and peritoneal fibrosis (in cases of patients under Peritoneal Dialysis) or lung fibrosis still pose a great challenge for researchers.

Citation: Zarogiannis, S. G., ed (2018). Mesothelial Physiology and Pathophysiology. Lausanne: Frontiers Media. doi: 10.3389/978-2-88945-541-6

Table of Contents

frontiers in Physiology

EDITORIAL
published: 22 March 2018
doi: 10.3389/fphys.2018.00263

Editorial: Mesothelial Physiology and Pathophysiology

*Sotirios G. Zarogiannis**

Department of Physiology, Faculty of Medicine, BIOPOLIS, University of Thessaly, Larissa, Greece

Keywords: mesothelium, pleura, peritoneum, pericardium, physiology, serosal membranes, mesothelial cells

Editorial on the Research Topic

Mesothelial Physiology and Pathophysiology

The Research Topic "Mesothelial Physiology and Pathophysiology" aimed at providing a forum for investigations conducted in all fields of serosal membranes research. The physiology and pathophysiology of mesothelial cells and membranes is a research field with a growing community given that many of the clinical entities that involve serosal contribution, require the detailed understanding of the underlying biological processes in order to provide effective treatments. The research production volume in the field of mesothelial physiology and pathophysiology is a function of the frequency of the clinical entities that they are involved into. Thus, the most active area is pleural research followed by peritoneal and lastly pericardial. Pleural effusions are a common entity that involves the abnormal accumulation of pleural fluid in the pleural cavity due to abnormal turnover, and the underlying diseases stem from congestive heart failure to infectious lung diseases and several intra- and extra- thoracic malignancies (Zarogiannis and Kalomenidis, 2015). It is therefore easily conceived that the water and solute transport systems of the pleural membrane comprising the transcellular and paracellular mesothelial permeability can be altered in pathophysiological conditions. These mechanisms are thoroughly reviewed in this Research Topic with a special focus on the tight junction component that regulates the paracellular permeability of the pleural mesothelium (Markov and Amasheh). The authors provide a detailed description of the electrophysiological studies that yield the knowledge around the transmesothelial permeability and the set of studies on paracellular permeability that provide significant evidence of tight junction switch in the inflamed human pleural mesothelium. During inflammation a protein expression change from sealing to pore forming claudins in the tight junctions occurs, a finding that could be prone to therapeutic intervention. In the same context an experimental study demonstrated the calcium dependent effects of increased paracellular permeability induced by bradykinin, histamine and thrombin in rat primary mesothelial monolayers (Kuwahara). This study provides further evidence of paracellular permeability changes due to the effects of inflammation related molecules attributable to reorganization of mesothelial cell F-actin cytoskeleton and increased actin polymerization. These aspects of pleural membrane permeability changes can supplement the understanding of the pathophysiology of pleural effusion dynamics.

A Perspective on the pleural mesothelium in development and disease provided an overview on the mesothelial contribution of lung development and also highlighted the ability of mesothelial cells to differentiate into several types of cells depending on the underlying stimuli (Batra and Antony). This process renders new roles to pleural mesothelial cells in the context of lung injury and repair mechanisms that can contribute to the development of lung mesenchymal pathologies such as interstitial pulmonary fibrosis. The authors also focus on the therapeutic potential of modulation pleural mesothelial activation and thus parenchymal disease progression. From a different angle the pleural mesothelium is sensitive to the effects of environmental or engineered nanoparticles that through inhalation reach the pleural cavity by disrupting the lung parenchyma and transmigration

OPEN ACCESS

Edited by:
Mario Diaz,
Universidad de La Laguna, Spain

Reviewed by:
Kausar Begam Riaz Ahmed,
United States Food and Drug Administration, United States

Correspondence:
Sotirios G. Zarogiannis
szarog@med.uth.gr

Specialty section:
This article was submitted to Membrane Physiology and Membrane Biophysics, a section of the journal Frontiers in Physiology

Received: *05 February 2018*
Accepted: *07 March 2018*
Published: *22 March 2018*

Citation:
Zarogiannis SG (2018) Editorial: Mesothelial Physiology and Pathophysiology. Front. Physiol. 9:263. doi: 10.3389/fphys.2018.00263

or in the case of smaller particles through the circulation. A well characterized such pathology is the malignant pleural mesothelioma (MPM) due to asbestos fibers exposure. Currently there is increasing evidence that engineered nanoparticles such as carbon nanotubes (CNTs) can cause a similar pleural pathology. Lohcharoenkal et al. demonstrated that single-walled CNTs induced neoplastic-like transformation in human mesothelial cells after prolonged exposure. The observed effects were due to H-Ras upregulation and ERK1/2 activation that led to increased expression of cortactin, a protein implicated in cell motility and neoplastic development, and thus a more aggressive transformation phenotype (Lohcharoenkal et al.). In another experimental study Ady et al. investigated the role of Tunneling Nanotubes (TnTs) in MPM cell communication (Ady et al.). The authors in very well designed studies demonstrated TnT occurrence in ex vivo preparations of MPM patient tumor tissues as well as in 2D and 3D MPM cell cultures. Furthermore they provided some interesting preclinical evidence of decreased tumor growth and survival of immunodeficient mice implanted with TnT-primed human MPM cells.

TnTs between peritoneal mesothelial cells in physiological and pathophysiological conditions in the peritoneal cavity has also been the theme of a Mini Review article (Ranzinger et al.). The research in the peritoneal mesothelium has stemmed from questions that have risen due to its use as a dialyzing membrane during the Peritoneal Dialysis (PD) modality in End Stage Renal Disease patients. In such a modality the peritoneal membrane is in a chronic state of inflammation caused by the PD fluids that are daily introduced in the peritoneal cavity. The authors discuss the influence of several insults to the mesothelial cells that are due to the effects of PD fluids, such as increased oxidative stress or increased osmotic stress, that can lead to differences in the mesothelial cells propensity to exhibit intercellular communication via TnTs and highlight the open questions in the field of PD and mesothelial cells TnTs. Pertinent to this is also the Review article of Moinuddin et al., regarding a severe form of peritoneal related disease which is the Encapsulating Peritoneal Sclerosis (EPS). The authors provide a global presentation of EPS in terms of etiology, risk factors, diagnosis and the underlying pathophysiology along with all the available treatment and prevention options. Another manuscript regarding PD was a Mini Review on the available *in vivo* and *ex vivo* animal models for the study of PD effects on the peritoneal mesothelial membrane (Nikitidou et al.). Nikitidou et al. critically discuss the advantages and disadvantages of each model and present the parameters studied in each one concluding in the need for establishment of standardized protocols in order to yield clinically relevant and applicable results.

Pericardium is the most neglected research field of mesothelial membranes. A Mini Review that filled an important gap in the literature was centered on the physiology of pericardial fluid production and drainage (Vogiatzidis et al.). The authors provide detailed information on the anatomy and histology of the pericardium, the composition of the pericardial fluid and the physiology underlying its dynamic turnover in the pericardial cavity.

AUTHOR CONTRIBUTIONS

The author confirms being the sole contributor of this work and approved it for publication.

ACKNOWLEDGMENTS

Since this is the first collection of articles published in a physiology journal that focuses on Mesothelial Physiology and Pathophysiology, I would like to deeply thank all the contributing authors, the reviewers of the manuscripts and the staff of Frontiers in Physiology for their excellent work and dedication.

REFERENCES

Zarogiannis, S.G., and Kalomenidis, I. (2015). Can pharmacologic agents speed the rate of resorption of pleural fluid? *Curr. Opin. Pulm. Med.* 21, 372–375. doi: 10.1097/MCP.0000000000000170

Conflict of Interest Statement: The author declares that the research was conducted in the absence of any commercial or financial relationships that could be construed as a potential conflict of interest.

frontiers in Physiology

MINI REVIEW
published: 01 September 2015
doi: 10.3389/fphys.2015.00244

Animal models in peritoneal dialysis

*Olga Nikitidou[1], Vasiliki I. Peppa[2], Konstantinos Leivaditis[1], Theodoros Eleftheriadis[1], Sotirios G. Zarogiannis[2] and Vassilios Liakopoulos[1]**

[1] Division of Nephrology and Hypertension, 1st Department of Internal Medicine, School of Medicine, American Hellenic Educational Progressive Association Hospital, Aristotle University of Thessaloniki, Thessaloniki, Greece, [2] Department of Physiology, Faculty of Medicine, BIOPOLIS, University of Thessaly, Larissa, Greece

Peritoneal dialysis (PD) has been extensively used over the past years as a method of kidney replacement therapy for patients with end stage renal disease (ESRD). In an attempt to better understand the properties of the peritoneal membrane and the mechanisms involved in major complications associated with PD, such as inflammation, peritonitis and peritoneal injury, both *in vivo* and *ex vivo* animal models have been used. The aim of the present review is to briefly describe the animal models that have been used, and comment on the main problems encountered while working with these models. Moreover, the differences characterizing these animal models, as well as, the differences with humans are highlighted. Finally, it is suggested that the use of standardized protocols is a necessity in order to take full advantage of animal models, extrapolate their results in humans, overcome the problems related to PD and help promote its use.

Keywords: animal models, ion and water transport, membrane physiology, peritoneal dialysis, ussing chamber

OPEN ACCESS

Edited by:
Ali Mobasheri,
University of Surrey, UK

Reviewed by:
Martin Diener,
Giessen University, Germany
David Marples,
University of Leeds, UK

****Correspondence:***
Vassilios Liakopoulos,
Division of Nephrology and Hypertension, 1st Department of Internal Medicine, School of Medicine, American Hellenic Educational Progressive Association Hospital, Aristotle University of Thessaloniki, 1 St. Kyriakidi street, 54636, Thessaloniki, Greece
liakopul@otenet.gr

Specialty section:
This article was submitted to Membrane Physiology and Membrane Biophysics, a section of the journal Frontiers in Physiology

Received: *21 June 2015*
Accepted: *17 August 2015*
Published: *01 September 2015*

Citation:
Nikitidou O, Peppa VI, Leivaditis K, Eleftheriadis T, Zarogiannis SG and Liakopoulos V (2015) Animal models in peritoneal dialysis. Front. Physiol. 6:244. doi: 10.3389/fphys.2015.00244

Peritoneal dialysis (PD) is a well-established method of kidney replacement therapy. It is currently estimated that the end stage renal disease (ESRD) patients receiving PD worldwide are approximately 200,000 and that they represent 11% of the total number of patients receiving any modality of dialysis (Jain et al., 2012). It is worth mentioning that Putman in 1923 made the first attempt for PD in a canine model (Putnam, 1923).

The extended use of PD over the years makes the in depth understanding of the physiology of the peritoneal membrane, the transport of solute and water across it and the mechanisms influencing inflammation, peritonitis, peritoneal injury and encapsulating peritonitis, a necessity. Moreover, many therapeutic interventions, new PD solutions, and pharmaceutical agents need to be tested before their implementation in the daily clinical practice. Research on humans could probably provide the necessary answers to the aforementioned topics, but it is complicated with many technical problems and ethical concerns (Stojimirovic et al., 2007). The scientific community in order to overcome this problem has exploited the observed similarities among humans and animal models. More precisely, the similar transport properties of solute and water across the peritoneal membrane in humans and animal models was an important foundation for the conduction of series of experiments in a variety of animal models.

Small animals such as rats, rabbits, and genetically modified mice have mostly been used for experimental models, although larger animals such as dogs, sheep, or even kangaroos have been used, as well. The use of each animal model comes with different advantages and disadvantages (**Table 1**). More precisely, rats are easy to breed and affordable, but have a short life expectancy, small size that increases the risk of complications during the insertion of a peritoneal catheter and large size of peritoneal membrane when at the same time only small quantities of dialysate can be introduced in their peritoneal cavity (Lameire et al., 1998). On the other hand, rabbits have a longer life expectancy, can survive longer on PD and the insertion of the peritoneal catheter is easier,

TABLE 1 | Main advantages and disadvantages of different animals used in animal models.

Animals		Advantages	Disadvantages
Small	Rats	• Easy and affordable breeding • Fast generation and maturation	• Short life expectancy • Small size—increased risk of complications • Higher ratio of peritoneal surface area compared to humans • Large size of parietal peritoneum • High intraperitoneal amylase levels
	Rabbits	• Adequate life expectancy • Adequate survival on PD • Easy peritoneal catheter insertion • Similar size of parietal peritoneum to humans • Similar ratio of peritoneal surface area to humans	• Delicate animals—difficult to breed
	Genetically modified mice	• Easy and affordable breeding • Fast generation and maturation • Ability to explore the role of single proteins	• Extremely small size
Large	Dogs Sheep Kangaroos etc	• Long life expectancy • Easy peritoneal catheter insertion	• Difficult and expensive breeding • Large time frame for obtaining results

but are very delicate animals and difficult to breed (Garosi and Di Paolo, 2001). Regarding larger animals, their life expectancy is long and could approximate PD on humans, but their breeding is difficult and expensive and a large time frame is needed for results to be obtained (Van Biesen et al., 2006).

As for the genetically modified mice, both knockout and transgenic models have been used over the past few years in order to provide important information in many different molecular pathways that are significant for PD (Nishino et al., 2007). The ability to modify the genome of mice enabled the scientists to explore the expression of different genes and the results of the modification of their expression. The role of single proteins such as aquaporin-1 in the transport of water across the peritoneal membrane (Yang et al., 1999; Ni et al., 2006) or NOS (Nitric oxide synthase) isoforms in peritonitis (Ni et al., 2010), as well as, IL-6 in inflammation (Hurst et al., 2001; McLoughlin et al., 2004) and TGF-β in encapsulating peritonitis (Park et al., 2008) were explored using genetically modified mice. The extremely small size of these animal makes manipulations difficult (Ni et al., 2003), but over the past few years the development of new molecular techniques provide significant tools to overcome this disadvantage (Devuyst et al., 2010).

Acute and chronic animal models have been developed (Hoff, 2005; Pawlaczyk et al., 2015) (**Table 2**). Acute models describe experiments that have short duration and can study the impact of a single dwell on the peritoneal membrane. They provide crucial information regarding mainly the transport characteristics of the peritoneal membrane and its function. Its permeability to water and solute, the interaction with different dialysis solutions, certain substances, therapeutic agents or even inflammation mediators can be extensively studied this way. On the other hand, chronic models can evaluate the chronic impact of PD resembling the impact of the method on humans due to the longer duration of the experiments. They can focus on changes of the structure and the function of the peritoneal membrane. For example, the effect of glucose used as an osmotic agent in dialysis solutions or the effect of the newer biocompatible solutions with lower GDPs' (Glucose degradation products) concentration, neutral pH or replacement of glucose with icodextrin on the morphology of the peritoneal membrane can be analyzed. Fibrosis, encapsulating peritoneal sclerosis, repeated episodes of peritonitis, and morphological alterations can be in depth studied using the chronic models. In this way, an important background for targeted therapeutic interventions is provided.

In the acute model the animal is anesthetized, a temporary catheter is inserted in the peritoneal cavity and during a 4-h dwell samplings of the peritoneal fluid and blood are obtained (Lameire et al., 1998). In the chronic model, on the other hand, three are the most common methods used (Mortier et al., 2005). The first method includes the direct blind injection of the dialysate into the peritoneal cavity with or without anesthesia. The repeated injections are related to increased risk of intraperitoneal bleeding and infection that could probably interfere with the results of the experiment. The second method is called "open system" and is characterized by the subcutaneous insertion of a permanent indwelling peritoneal catheter from the neck to the peritoneal cavity of the animal. This catheter can be used for the introduction of dialysate into the peritoneal cavity and the drain of the dwell directly or indirectly as it can be used as the tunnel through which another sterile catheter is inserted during every exchange. In this method anesthesia is not required but the rate of peritonitis episodes remains high and the malfunction of the catheter as a result of omental wrapping, adhesions and fibrosis is frequent. Finally, the third method is called "closed system." In this method, as in the "open-system," a permanent indwelling peritoneal catheter is inserted subcutaneously from the neck to the peritoneal cavity of the animal. The catheter is attached to a subcutaneous reservoir in the neck of the animal and the dialysate remains in the peritoneal cavity until it is fully absorbed. This method results in lower rates of peritonitis,

TABLE 2 | The main studied parameters in acute and chronic animal models.

Animal models	Studied parameters	
Acute	Transport characteristics and function of the PM	Permeability to water and solutes Lymphatic drainage Interaction with different dialysis solutions Acute effect of glucose Inflammatory response—effect of inflammation mediators Interaction with various therapeutic agents
Chronic	Changes of structure and function of the PM	Effect of biocompatible solutions (lower GDP and neutral pH) Effect of icodextrin Peritonitis—defense mechanisms Mesothelial cell damage PM thickness Vascular alterations Fibrosis Encapsulating peritoneal sclerosis Therapeutic interventions

PM, peritoneal membrane.

although the malfunction of the catheter still remains a problem.

In any case, even if it is tempting, before applying the extrapolated results of animal models in humans we should point out the differences between these models and humans and the related technical problems. The most important differences concern the visceral, parietal and diaphragm surfaces. It seems that the diaphragm, which is directly related to the lymphatic drainage responsible for the clearance of macromolecules, extends to a larger area in humans than in animal models (Pawlaczyk et al., 2015). On the other hand, the parietal peritoneum that is directly related to the solute transport is larger in rats than in humans, while in rabbits it is similar to humans (Pawlaczyk et al., 1996). Moreover, it is known that the intraperitoneal levels of amylase that are elevated in rats can locally degrade icodextrin, an osmotic agent used in several dialysis fluids, rapidly (de Waart et al., 2001). To these differences one must add the higher ratio of peritoneal surface area to dialysate that is observed in rats, while in rabbits it is similar to the one observed in humans (Stojimirovic et al., 2007). Finally, in rats changes in the permeability and the surface area of the peritoneal membrane are encountered as they grow up, resulting in changes in the kinetics of the peritoneal membrane (Kuzlan et al., 1997). As Van Biesen et al highlights multiple experiments in different animal models and comparison of the results obtained could overcome those differences and provide a more realistic approach of the mechanisms that characterize PD in humans (Van Biesen et al., 2006).

Among the technical problems that have to be faced when handling animal models, tissue-sampling problems must be highlighted. The peritoneal tissue is quite fragile, dries quickly when exposed to the air and can easily be damaged even after delicate contact with surgical gloves or instruments (Duman and Sen, 2009). Furthermore, in patients on PD the visceral peritoneum exhibits more pronounced alterations than the parietal peritoneum, while in many of the studies conducted in animal models the biopsy samples are obtained by the parietal peritoneum. This inconsistency could be misleading if extrapolating results of animal studies to humans.

Catheter obstruction, peritonitis, and anesthesia use represent other major problems. In an attempt to minimize catheter dysfunction, omentectomy, and heparin have been used, but both methods have important pitfalls. On one hand the omentum is considered to be an important immune defense organ of the peritoneal cavity (Beelen, 1992), while on the other heparin is known to have many pleiotropic actions besides being an anticoagulant (De Vriese et al., 2001; Gozdzikiewicz et al., 2009). Therefore, both of these interventions could result in undesirable functional and morphological changes in the peritoneum (Mortier et al., 2005). The use of heparin coated catheters that has been suggested seems to be a good solution, since it reduces the rate of malfunction without inducing changes in the peritoneum (De Vriese et al., 2002). Regarding peritonitis, many investigators have administered antibiotics in order to prevent infections, an intervention that has been proven successful and simultaneously not leading to morphological and function changes in the peritoneum (Mortier et al., 2003; Choi et al., 2006). Finally, the use of anesthesia when handling animals has been related to changes in the peritoneum kinetics, probably through a direct reduction of the lymphatic drainage (Tran et al., 1993) and an increase of ultrafiltration and decrease of the absorption rates from the peritoneal membrane (Shin et al., 2006).

There are some important differences in animal model studies (Mortier et al., 2005; Topley, 2005). There are differences related to the volume of dialysate instilled and the time it remains in the peritoneal cavity, the frequency of the exchanges, and the total time the animals undergo PD before the termination of the study. The drainage of the dialysate is also an issue. More precisely, there are animal models characterized by the presence of the dialysate in the peritoneal cavity until it is fully absorbed, while in other animal models drainage after every dwell is performed. The last model resembles chronic PD in humans and offers the ability to better understand transportation through the peritoneal membrane and at the same time examine the dialysate for the presence of cells and substances (Pawlaczyk et al., 2015). Moreover, differences in the use of anesthesia, heparin or even the definition of peritonitis have been described. A common finding in most studies is the use of high concentration glucose solutions although in humans other lower glucose concentration solutions may also be used. Finally, the high rate of dropout due to catheter malfunction must be highlighted. It is obvious that there are many limitations when analyzing the results of the studies conducted on animal models, nevertheless the information they provide are very important and necessary to better understand this method of renal replacement therapy.

One field of special interest for nephrologists is encapsulating peritoneal sclerosis (EPS) which is a rare but life threatening complication of PD. Several animal models have been used

in order to understand the underlying pathophysiological mechanisms that lead to EPS (Hoff, 2005; Park et al., 2008; Hirahara et al., 2015). Chlorexidine and acidic dialysis solutions, povidone iodine, formaldehyde, and even bleach and talc are some of the agents that have been used in an attempt to induce peritoneal injury and development of EPS in animal models. At the same time many different inhibitors of inflammation, angiogenesis, and fibrosis, as well as, inhibitors of the renin angiotensin system have been studied as potential therapeutic interventions in an attempt to resolve EPS (Kitamura et al., 2014).

The *in vivo* animal models provide useful information for future PD solutions that are yet to be tested or promote our understanding of their effects on the peritoneal membrane of ESRD patients undergoing PD. To this end an *ex vivo* sheep and human model of the peritoneal ionic and water permeability can further provide useful information that can be applied in the PD solution improvement and development area (Liakopoulos et al., 2006, 2009). In these studies the membrane specimens are mounted in the Ussing System that measures the transmembrane ionic permeability (Zarogiannis et al., 2004; Stefanidis et al., 2005). The majority of such investigations involved electrophysiological experiments in sheep visceral or parietal peritoneum specimens and some of the results have been tested in human specimens yielding identical findings, thus rendering this model a powerful tool for PD solution assessment as to the ion and water transport drug induced alterations (Zarogiannis et al., 2005, 2007; Stefanidis et al., 2007). The focus of these electrophysiological investigations was the identification of ion channels, as well as, hormonal receptors present in the mesothelial compartment of the peritoneum (Kourti et al., 2007, 2013; Zarogiannis et al., 2007; Karioti et al., 2008, 2009). Most of these findings remain yet to be investigated in human specimens and subsequently tested in *in vivo* animal models.

In conclusion, *in vivo* and *ex vivo* animal models have been extensively used for the understanding of the properties of the peritoneal membrane and results of these experiments have been extrapolated in humans. For the time being, the fundamental differences in the animal models used, as already described, remains the main problem when it comes to comparing results of different models and especially using these results in order to evaluate the use of PD in humans. At the same time, the necessity of in depth understanding of PD brings into perspective the importance of establishing standardized protocols that could overcome the aforementioned differences and obstacles.

References

Beelen, R. H. (1992). Role of omental milky spots in the local immune response. *Lancet* 339, 689. doi: 10.1016/0140-6736(92)90857-Y

Choi, J., Credit, K., Henderson, K., Deverkadra, R., Vanpelt, H. M., He, Z., et al. (2006). Antibiotic prophylaxis in an animal model of chronic peritoneal exposure. *Perit. Dial. Int.* 26, 249–258.

De Vriese, A. S., Mortier, S., Cornelissen, M., Palmans, E., Vanacker, N. J., Leyssens, A., et al. (2002). The effects of heparin administration in an animal model of chronic peritoneal dialysate exposure. *Perit. Dial. Int.* 22, 566–572.

De Vriese, A. S., Mortier, S., and Lameire, N. H. (2001). Non anticoagulant effects of heparin: implications for animal models of peritoneal dialysis. *Perit. Dial. Int.* 21(Suppl. 3), S354–S356.

Devuyst, O., Margetts, P. J., and Topley, N. (2010). The pathophysiology of the peritoneal membrane. *J. Am. Soc. Nephrol.* 21, 1077–1085. doi: 10.1681/ASN.2009070694

de Waart, D. R., Zweers, M. M., Struijk, D. G., and Krediet, R. T. (2001). Icodextrin degradation products in spent dialysate of CAPD patients and the rat, and its relation with dialysate osmolality. *Perit. Dial. Int.* 21, 269–274.

Duman, S., and Sen, S. (2009). Technical aspects in studying peritoneal morphology in animal models of peritoneal dialysis. *Perit. Dial. Int.* 29(Suppl. 2), S40–S44.

Garosi, G., and Di Paolo, N. (2001). The rabbit model in evaluating the biocompatibility in peritoneal dialysis. *Nephrol. Dial. Transplant* 16, 664–665. doi: 10.1093/ndt/16.3.664

Gozdzikiewicz, J., Borawski, J., and Mysliwiec, M. (2009). Pleiotropic effects of heparin and heparinoids in peritoneal dialysis. *Clin. Appl. Thromb. Hemost.* 15, 92–97. doi: 10.1177/1076029607304722

Hirahara, I., Sato, H., Imai, T., Onishi, A., Morishita, Y., Muto, S., et al. (2015). Methylglyoxal induced basophilic spindle cells with podoplanin at the surface of peritoneum in rat peritoneal dialysis model. *Biomed Res. Int.* 2015:289751. doi: 10.1155/2015/289751

Hoff, C. M. (2005). Experimental animal models of encapsulating peritoneal sclerosis. *Perit. Dial. Int.* 25(Suppl. 4), S57–S66.

Hurst, S. M., Wilkinson, T. S., Mcloughlin, R. M., Jones, S., Horiuchi, S., Yamamoto, N., et al. (2001). Il-6 and its soluble receptor orchestrate a temporal switch in the pattern of leukocyte recruitment seen during acute inflammation. *Immunity* 14, 705–714. doi: 10.1016/S1074-7613(01)00151-0

Jain, A. K., Blake, P., Cordy, P., and Garg, A. X. (2012). Global trends in rates of peritoneal dialysis. *J. Am. Soc. Nephrol.* 23, 533–544. doi: 10.1681/ASN.2011060607

Karioti, A., Hatzoglou, C., Zarogiannis, S., Deligiorgi, T., Kourti, P., Giannopoulou, M., et al. (2009). Spironolactone increases permeability of visceral sheep peritoneum. *Adv. Perit. Dial.* 25, 16–19.

Karioti, A., Hatzoglou, C., Zarogiannis, S., Deligiorgi, T., Liakopoulos, V., Kourti, P., et al. (2008). Rapid effect of dexamethasone on the permeability of visceral sheep peritoneum. *Adv. Perit. Dial.* 24, 2–6.

Kitamura, M., Nishino, T., Obata, Y., Ozono, Y., Koji, T., and Kohno, S. (2014). New insights into therapeutic strategies for the treatment of peritoneal fibrosis: learning from histochemical analyses of animal models. *Acta Histochem. Cytochem.* 47, 133–143. doi: 10.1267/ahc.14025

Kourti, P., Zarogiannis, S., Liakopoulos, V., Hatzoglou, C., Giannopoulou, M., Chronopoulou, I., et al. (2007). Effect of endothelin-1 on the transmesothelial resistance of isolated visceral sheep peritoneum. *Adv. Perit. Dial.* 23, 38–42.

Kourti, P., Zarogiannis, S. G., Liakopoulos, V., Karioti, A., Eleftheriadis, T., Hatzoglou, C., et al. (2013). Endothelin-1 acutely reduces the permeability of visceral sheep peritoneum in vitro through both endothelin-A and endothelin-B receptors. *Artif. Organs* 37, 308–312. doi: 10.1111/j.1525-1594.2012.01565.x

Kuzlan, M., Pawlaczyk, K., Wieczorowska-Tobis, K., Korybalska, K., Breborowicz, A., and Oreopoulos, D. G. (1997). Peritoneal surface area and its permeability in rats. *Perit. Dial. Int.* 17, 295–300.

Lameire, N., Van Biesen, W., Van Landschoot, M., Wang, T., Heimbürger, O., Bergström, J., et al. (1998). Experimental models in peritoneal dialysis: a European experience. *Kidney Int.* 54, 2194–2206. doi: 10.1046/j.1523-1755.1998.00179.x

Liakopoulos, V., Zarogiannis, S., Hatzoglou, C., Kourti, P., Poultsidi, A., Eleftheriadis, T., et al. (2006). Inhibition by mercuric chloride of aquaporin-1 in the parietal sheep peritoneum: an electrophysiologic study. *Adv. Perit. Dial.* 22, 7–10.

Liakopoulos, V., Zarogiannis, S., Kourti, P., Hatzoglou, C., Karioti, A., Arampatzis, S., et al. (2009). Effect of cimetidine on the electrophysiologic profile of isolated visceral sheep peritoneum. *Adv. Perit. Dial.* 25, 20–23.

McLoughlin, R. M., Hurst, S. M., Nowell, M. A., Harris, D. A., Horiuchi, S., Morgan, L. W., et al. (2004). Differential regulation of neutrophil-activating chemokines by IL-6 and its soluble receptor isoforms. *J. Immunol.* 172, 5676–5683. doi: 10.4049/jimmunol.172.9.5676

Mortier, S., De Vriese, A. S., Leyssens, A., Vanacker, N. J., Faict, D., Cornelissen, M., et al. (2003). Antibiotic administration in an animal model of chronic peritoneal dialysate exposure. *Perit. Dial. Int.* 23, 331–338.

Mortier, S., Lameire, N. H., and De Vriese, A. S. (2005). Animal models in peritoneal dialysis research: a need for consensus. *Perit. Dial. Int.* 25, 16–24.

Ni, J., McLoughlin, R. M., Brodovitch, A., Moulin, P., Brouckaert, P., Casadei, B., et al. (2010). Nitric oxide synthase isoforms play distinct roles during acute peritonitis. *Nephrol. Dial. Transplant* 25, 86–96. doi: 10.1093/ndt/gfp415

Ni, J., Moulin, P., Gianello, P., Feron, O., Balligand, J. L., and Devuyst, O. (2003). Mice that lack endothelial nitric oxide synthase are protected against functional and structural modifications induced by acute peritonitis. *J. Am. Soc. Nephrol.* 14, 3205–3216. doi: 10.1097/01.ASN.0000099382.18284.57

Ni, J., Verbavatz, J. M., Rippe, A., Boisdé, I., Moulin, P., Rippe, B., et al. (2006). Aquaporin-1 plays an essential role in water permeability and ultrafiltration during peritoneal dialysis. *Kidney Int.* 69, 1518–1525. doi: 10.1038/sj.ki.5000285

Nishino, T., Ni, J., and Devuyst, O. (2007). Transgenic mouse models. *Perit. Dial. Int.* 27, 625–633.

Park, S. H., Kim, Y. L., and Lindholm, B. (2008). Experimental encapsulating peritoneal sclerosis models: pathogenesis and treatment. *Perit. Dial. Int.* 28(Suppl. 5), S21–S28.

Pawlaczyk, K., Baum, E., Schwermer, K., Hoppe, K., Lindholm, B., and Breborowicz, A. (2015). Animal models of peritoneal dialysis: thirty years of our own experience. *Biomed Res. Int.* 2015: 261813. doi: 10.1155/2015/261813

Pawlaczyk, K., Kuzlan, M., Wieczorowska-Tobis, K., Pawlik-Juzków, H., Breborowicz, A., Knapowski, J., et al. (1996). Species-dependent topography of the peritoneum. *Adv. Perit. Dial.* 12, 3–6.

Putnam, T. (1923). The living peritoneum as a dialyzing membrane. *Am. J. Physiol.* 63, 548–565.

Shin, S. K., Kamerath, C. D., Gilson, J. F., and Leypoldt, J. K. (2006). Effects of anaesthesia on fluid and solute transport in a C57BL6 mouse model of peritoneal dialysis. *Nephrol. Dial. Transplant* 21, 2874–2880. doi: 10.1093/ndt/gfl368

Stefanidis, I., Liakopoulos, V., Kourti, P., Zarogiannis, S., Poultsidi, A., Mertems, P. R., et al. (2007). Amiloride-sensitive sodium channels on the parietal human peritoneum: evidence by ussing-type chamber experiments. *ASAIO J.* 53, 335–338. doi: 10.1097/MAT.0b013e3180317908

Stefanidis, I., Zarogiannis, S., Hatzoglou, C., Liakopoulos, V., Kourti, P., Poultsidi, A., et al. (2005). Enhancement of the transmesothelial resistance of the parietal sheep peritoneum by epinephrine *in vitro*: ussing-type chamber experiments. *Artif. Organs* 29, 919–922. doi: 10.1111/j.1525-1594.2005.00157.x

Stojimirovic, B., Trbojevic-Stankovic, J., and Nesic, D. (2007). Animal models in peritoneal dialysis. *Scand J. Lab. Anim. Sci.* 34, 283–289.

Topley, N. (2005). Animal models in peritoneal dialysis: more questions than answers? *Perit. Dial. Int.* 25, 33–34.

Tran, L., Rodela, H., Abernethy, N. J., Yuan, Z. Y., Hay, J. B., Oreopoulos, D., et al. (1993). Lymphatic drainage of hypertonic solution from peritoneal cavity of anesthetized and conscious sheep. *J. Appl. Physiol. (1985)* 74, 859–867.

Van Biesen, W., Vanholder, R., and Lameire, N. (2006). Animal models in peritoneal dialysis: a story of kangaroos and ostriches. *Perit. Dial. Int.* 26, 571–573.

Yang, B., Folkesson, H. G., Yang, J., Matthay, M. A., Ma, T., and Verkman, A. S. (1999). Reduced osmotic water permeability of the peritoneal barrier in aquaporin-1 knockout mice. *Am. J. Physiol.* 276, C76–C81.

Zarogiannis, S., Kourti, P., Hatzoglou, C., Liakopoulos, V., Poultsidi, A., Gourgoulianis, K., et al. (2005). Influence of the sodium transport inhibition by amiloride on the transmesothelial resistance of isolated visceral sheep peritoneum. *Adv. Perit. Dial.* 21, 5–8.

Zarogiannis, S., Liakopoulos, V., Hatzoglou, C., Kourti, P., Vogiatzidis, K., Potamianos, S., et al. (2007). Effect of sodium-potassium pump inhibition by ouabain on the permeability of isolated visceral sheep peritoneum. *Adv. Perit. Dial.* 23, 43–47.

Zarogiannis, S., Stefanidis, I., Hatzoglou, C., Liakopoulos, V., Gourgoulianis, K., and Molyvdas, P. A. (2004). Effect of adrenaline on the electrophysiologic profile of isolated visceral sheep peritoneum. *Adv. Perit. Dial.* 20, 23–26.

Conflict of Interest Statement: The authors declare that the research was conducted in the absence of any commercial or financial relationships that could be construed as a potential conflict of interest.

frontiers in Physiology

MINI REVIEW
published: 18 March 2015
doi: 10.3389/fphys.2015.00062

Physiology of pericardial fluid production and drainage

Konstantinos Vogiatzidis[1], *Sotirios G. Zarogiannis*[1]*, *Isaac Aidonidis*[1], *Evgeniy I. Solenov*[2], *Paschalis-Adam Molyvdas*[1], *Konstantinos I. Gourgoulianis*[3] and *Chrissi Hatzoglou*[1]

[1] Department of Physiology, Faculty of Medicine, School of Health Sciences, University of Thessaly, Larissa, Greece, [2] Laboratory of Physiological Genetics, Institute of Cytology and Cytogenetics, Siberian Branch of the Russian Academy of Sciences, Novosibirsk, Russia, [3] Department of Respiratory Medicine, Faculty of Medicine, School of Health Sciences, University of Thessaly, Larissa, Greece

The pericardium is one of the serosal cavities of the mammals. It consists of two anatomical structures closely connected, an external sac of fibrous connective tissue, that is called fibrous pericardium and an internal that is called serous pericardium coating the internal surface of the fibrous pericardium (parietal layer) and the heart (visceral layer) forming the pericardial space. Between these two layers a small amount of fluid exists that is called pericardial fluid. The pericardial fluid is a product of ultrafiltration and is considered to be drained by lymphatic capillary bed mainly. Under normal conditions it provides lubrication during heart beating while the mesothelial cells that line the membrane may also have a role in the absorption of the pericardial fluid along with the pericardial lymphatics. Here, we provide a review of the the current literature regarding the physiology of the pericardial space and the regulation of pericardial fluid turnover and highlight the areas that need to be further investigated.

Keywords: mesothelium, pericardiac fluid turnover, pericardium, serosal membranes, transmembrane transport

OPEN ACCESS

Edited by:
Ali Mobasheri,
University of Surrey, UK

Reviewed by:
Martin Diener,
University Giessen, Germany
Salah Amasheh,
Freie Universität Berlin, Germany

***Correspondence:**
Sotirios G. Zarogiannis,
Department of Physiology,
Faculty of Medicine,
School of Health Sciences,
University of Thessaly,
3rd Panapistimiou Str., BIOPOLIS,
41500 Larissa, Greece
szarog@med.uth.gr

Specialty section:
This article was submitted to Membrane Physiology and Membrane Biophysics, a section of the journal Frontiers in Physiology

Received: *01 December 2014*
Accepted: *16 February 2015*
Published: *18 March 2015*

Citation:
Vogiatzidis K, Zarogiannis SG, Aidonidis I, Solenov EI, Molyvdas P-A, Gourgoulianis KI and Hatzoglou C (2015) Physiology of pericardial fluid production and drainage. Front. Physiol. 6:62. doi: 10.3389/fphys.2015.00062

Introduction

The pericardium is one of the serosal cavities of mammals (Michailova and Usunoff, 2006). It is a fibrous—serosal conical sac enclosing the roots of the aorta and the pulmonary artery (Chinchoy, 2005). In humans, pericardium is located inside the middle mediastinum posteriorly to the sternum and the cartilages of the third to seventh left rib. Normally, it is not in contact with the frontal wall of the thoracic cavity (Frick et al., 1985; Chinchoy, 2005). Laterally, it is held together with the mediastinal parietal pleura. Pericardium isolates the heart from the adjacent tissues, allowing it's free movement within the boundaries of the pericardial cavity and is filled with a small amount of fluid which is called pericardial fluid (Chinchoy, 2005).

Anatomy and Histology

The pericardium consists of an external sac of fibrous connective tissue, called fibrous pericardium and an internal called serous pericardium. The latter coats the internal surface of the fibrous pericardium and the heart. Arterial branches from thoracic aorta, right and left pericardiophrenic artery (internal mammary artery branches), are responsible for the blood supply of the whole pericardium while the venous drainage is accomplished through the venae pericardiales which drain to the azygos vein, to the superior vena cava or to the brachiocephalic (Chinchoy, 2005). The pericardium

is innervated by the two phrenic nerves, each one giving an afferent branch (pericardial branch) (Randall and Ardell, 1985; Ardell and Randall, 1986; Chiou et al., 1997).

The thickness of the pericardium increases proportionally to the size of the heart and the pericardial cavity, with the exception of humans who have considerably thicker pericardium compared to the mammals with the same heart size (human 1–3.5 mm, sheep 0.32 ± 0.01 mm, pig 0.20 ± 0.01 mm) (D'Avila, 2003). The serous pericardial membrane covers the outside of the heart (visceral pericardium), extending a short distance beyond the atria and ventricles on the great vessels and lines the inside of the fibrous sac (parietal pericardium). The visceral pericardium is also refered to as epicardium and is in continuance with the parietal pericardium (Chinchoy, 2005; Jöbsis et al., 2007).

The parietal lamina of the serous pericardium is composed of a monolayer of flattened, squamous-like, mesothelial cells. Mesothelial cells rest on a thin basement membrane supported by connective tissue stroma in a narrow submesothelial space. The connective tissue stroma contains variously oriented layers of collagen fibrils and small elastic fibers (Ishihara et al., 1980; Mutsaers, 2002). The luminal surface of the mesothelial cells has well developed microvillous border with occasional cilia. The latter bear friction and increase the surface area for fluid transport. There are junctional complexes between adjacent mesothelial cells that consist of desmosomes, which reinforce intercellular adhesion and zonulae occludentes. All of these morphological characteristics form permeability barriers. Actin-like filaments are present in microvilli and in immediate subjacent regions of the cells. These filaments mediate changes on cell shape. Intermediate filaments are associated with desmosomes and form bundles in the perinuclear regions, which provide structural support to the cytoplasm (Ishihara et al., 1980).

Between the mesothelial cells of the parietal pericardium, not the epicardium, there are milky spots, similar to those in the omentum and mediastinal pleura, bulging toward the pericardial cavity. These structures are enclosed with cuboidal mesothelial cells (Takada et al., 1991; Mutsaers, 2002; Michailova and Usunoff, 2006). These openings provide direct access to the underlying submesothelial lymphatic system allowing rapid removal of fluid and cells from the pericardial cavity (Takada et al., 1991). Inside the pericardial cavity and submesothelial layers of the pericardium, there are resident macrophages, readily available in case of immunological response (Ishihara et al., 1980; Mutsaers, 2002; Michailova and Usunoff, 2006).

Histological studies on parietal pericardium of rodents have shown the presence of circular fenestrations ("pores"; diameter up to 50 μm), which connect the pericardial cavity with the adjacent mediastinal pleural cavities, except the positions that are held by the adipose tissue (Nakatani et al., 1988; Mohrman and Heller, 2006). Both their stomata and lumen are covered with mesothelial cells and below them elastin and collagen fibers (Fukuo et al., 1988; Nakatani et al., 1988). The functional significance of the pericardial "pores" remains unclear, however labeled erythrocytes have shown to pass through them from one cavity to the other (Fukuo et al., 1988).

The epicardium has common morphological features with the parietal pericardium but there are some functional differences. On the laminal surface there is a monolayer of mesothelial cells, lying on a thin basal membrane (Mutsaers, 2002; Jöbsis et al., 2007). The proportion of cuboidal cells is greater in the epicardium than in the parietal pericardium (Michailova and Usunoff, 2006). Underneath the basal membrane there is a dense network of collagen and elastic fibers, full of hydroxyproline, which embryologically stems from extracardiac tissue and doesn't infiltrate the underlying myocardium. The fibers are parallel to each other, in multiple layers and crossing the heart surface from diagonally to vertically, compared to the myocardial cells (Simionescu et al., 1993; Jöbsis et al., 2007). These mechanical properties play a role in the residual stress and passive stiffness of the heart (Przyklenk et al., 1987; Jöbsis et al., 2007).

Pericardial Fluid

The composition of the normal human pericardial fluid is difficult to define. All available data have been obtained either by cardiothoracic surgery patients or from animals. This probably compromises the data validity (Ben-Horin et al., 2005). However, the pericardial fluid is a plasma ultrafiltrate having specific characteristics just like the pleura fluid (Mauer et al., 1940; Holt, 1970). Volumetric studies have shown that the pericardial fluid volume is directly analogous to the animal size: in rabbits 0.4–1.9 mL, in dogs 0.5–2.5 mL and in adult humans about 20–60 mL (average 15–35 mL) (Vesely and Cahill, 1986; Ben-Horin et al., 2005).

Pericardial fluid coloring studies report that the fluid distribution inside the cavity is heterogeneous. The largest amount is inside the atrioventricular and the intraventricular sulcus, the superior and the transversal sinus, especially on the supine position (D'Avila, 2003). Nevertheless, there are some pharmacokinetic studies that show that the pericardial fluid is stirring up constantly and thus the supplement's composition is the same regardless the position (Chinchoy, 2005).

Regarding the cell population, studies in human normal pericardial fluid have shown the presence of a heterogenous cell population. There are mesothelial cells, lymphocytes (53%), glanulocytes (31%), macrophages (12%), eosinophils (1.7%), and basophils (1.2%). This means that the pericardial fluid "lymphocytosis" should always be under critical consideration and characterized as pathological only when it exceeds 60% of the whole cell population (Gibson and Segal, 1978a; Benhaiem-Sigaux et al., 1985).

The pericardial fluid is considered to be a plasma ultrafiltration product, like other serosal cavity fluids. Studies in greyhounds showed that the concentrations (in mmole kgr H_2O^{-1}) of Na^+ (150.5 ± 0.72), Cl^- (123.2 ± 0.71), Ca^{2+} (1.92 ± 0.04), and Mg^{2+} (0.85 ± 0.09) were lower in the pericardial fluid than in the plasma. On the contrary, the concentration of K^+ (3.81 ± 0.07) was higher than the plasma, which was attributed to the K^+ leakage from the myocardial interstitium toward the pericardial cavity, during systole (Holt, 1970; Gibson and Segal, 1978b). The protein concentration was also lower with different proportion of protein fractions; from higher to lower concentration being albumin, globulins, macroglobulins, and fibrinogen. Finally, the pericardial fluid osmomolarity was lower than the plasma (Gibson and Segal, 1978b). Given the net filtration gradients of the

substances above, it is obvious that the normal pericardial fluid is a transudate (Holt, 1970; Gibson and Segal, 1978b). However the relatively high protein and LDH concentrations raise caution as far as the applicability of Light's criteria is concerned (Gibson and Segal, 1978b; Meyers et al., 1997; Burgess et al., 2002; Ben-Horin et al., 2005).

Physiology

The normal pericardium contributes in important functions. In is necessary for: (1) lubricating the moving surfaces of the heart, (2) stabilizing the heart anatomic position, (3) isolating the heart from the adjacent anatomical structures, prohibiting the adhesion formation, the inflammatory or neoplastic extention, (4) limiting heart dilatation during diastole, reducing the endomyocardial tension, (5) preventing cardiac hypertrophy in pressure overload conditions, (6) reducing the right ventricular impulse work in left ventricular overload conditions, (7) the ventriculoatrial blood retrogression prevention during high end-diastolic ventricular pressures, (8) the preservation of the negative endothoracic pressure, which is crucial for the atria blood filling, (9) the nervous stimulation response and regulation of the cardiac frequency and arterial blood pressure, (10) the formation of a hydrostatic compensation system ensuring that end-diastolic pressure remains the same at all hydrostatic levels and the Frank–Starling mechanism is functional (Holt, 1970; Goto and LeWinter, 1990; Cinca and Rodriguez-Sinovas, 2000).

Many studies in both parietal and visceral pericardium (human, canine, pig) have shown the same mechanical properties, only with quantitative differences. *In vitro* studies in canine parietal pericardium demonstrated the presence of viscoelastic response, mainly attributed to the presence and the arrangement of the elastic and collagen fibers (Lee and Boughner, 1981, 1985). These parietal pericardium properties are responsible for (1) its participation to ventricular volume modulation, (2) the intraventricular interaction, and (3) the participation to the ventricular diastolic pressure/volume relatioships (Lee and Boughner, 1981; Maruyama et al., 1982; Takata et al., 1997; Gibbons Kroeker et al., 2003).

In vitro epicardial studies (humans, pigs), proved the presence of elastic properties that have been attributed to the composition and orientation of the connective tissue. Specifically, the human epicardium undergoes an oblong and circumferential systolic shortening, therebe the energy gathering during the diastolic period may contribute to the passive mechanical properties of the myocardium (Lorenz et al., 2000; Jöbsis et al., 2007). In this way, the epicardium seems to be participating in the ventricular end-diastolic volume control (Jöbsis et al., 2007).

Hydrodynamics

Under normal conditions, the human pericardial cavity contains 20–60 ml of fluid (Chinchoy, 2005). Moreover, it has been determined that the whole amount of pericardial fluid drains through the lymphatic capillary bed every 5–7 h, in sheep (Yuan et al., 2000). The pericardial fluid volume is determined by the equilibrium between production and drainage. There is strong evidence that the pericardial fluid is derived by plasma ultrafiltration through the epicardial capillaries (and probably the parietal's pericardium), as well as a small amount of interstitial fluid from the underlying myocardium, during the cardiac circle (Stewart et al., 1997). The fluid drainage is mainly accomplished through the parietal pericardium lymphatic capillary bed (Yuan et al., 2000). Nevertheless, the whole procedure is not fully elucidated because of the difficulty to study pericardial fluid dynamics under normal conditions (Shabetai, 2003).

The fluid movement through the pericardial laminae is a hydrostatic/osmotic pressure equilibrium, between the microvasculature and the cavity (Yuan et al., 2000). As shown in **Figure 1**, according to the Starling equilibrium:

$$\text{Fluid Movement} = L \times S[(P_{cap} - P_p) - \sigma \times (\Pi_{cap} - \Pi_p)]$$

P and Π stand for hydrostatic and osmotic pressures inside the capillaries (cap) and pericardial cavity (p), respectively. L is a membrane conductance constant for liquids, S is the surface area and σ is the osmotic constant of the endothelium/interstitial tissue barrier for proteins (Yuan et al., 2000).

The P_p measurement is challenging. The main problems for the direct measurement of the P_p were the small cavity size (<0.34 mm) as well as the sac deformation that provoved by the catheter insertion. The P_p depends on the pericardial fluid volume and accumulation velocity, the cardiac and respiration circle phase and the measurement position. The large amount and the fluid rapid accumulation results in rapid and great increase in P_p. This is not present during the gradual fluid accumulation, which allows greater ammounts of fluid without hemodynamic instability. This phenomenon is due to the viscoelastic properties of the parietal pericardium (Holt, 1970). During the diastole (laminae approach) the P_p increases and during the systole it decreases (Smiseth et al., 1985; DeVries et al., 2001; Hamilton et al., 2004). The P_p becomes more negative during inspiration and less during expiration (in humans ∼ 3 mmHg endexpiration and −5 mmHg

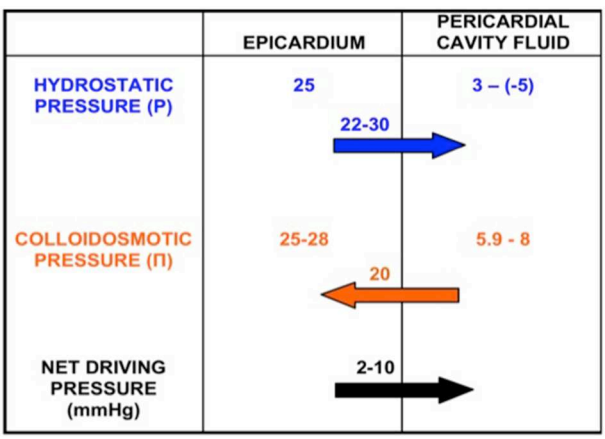

FIGURE 1 | Production of pericardial fluid as a net pressure phenomenon. Epicardial and pericardial cavity hydrostatic (P) and colloidosmotic (Π) pressures. There is a net pressure difference of 2–10 mmHg that drives the fluid from the epicardium toward the pericardial cavity.

endinspiration) (Kenner and Wood, 1966; Spodick, 1997). Finally, the P_p is about 20 mmHg above the free ventricular wall and almost zero inside the great sulcus (atrioventricular, intraventricular), during the enddiastole (Traboulsi et al., 1992). This ensures the constant fluid movement and homogenous composition, regardless the gathering position (Santamore et al., 1990). The pericardial capillaries stem from the systematic circulation. The venous drainage is accomplished through the superior vena cava (high pressure system). Thus, the P_{cap} is about 25 mmHg, the Π_{cap} is about 25–28 mmHg (Mohrman and Heller, 2006) and the Π_p is calculated near 5.9–8 mmHg by using the van't Hoff equation (Ben-Horin et al., 2005).

Pericardial Lymph Drainage

The lympatics have high absorbing capacity due to the smooth myocytes, placed circumferentially around the lumen that transforms them into a pump. This pump has a diastolic and systolic period that is controlled by the Frank–Starling mechanism, like the cardiac pump, increasing the absorbing capacity under increased "preload" conditions (Yuan et al., 2000; Quick et al., 2007).

The initial studies on the role of lympatic vessels during pericardial fluid drainage were controversial (Hollenberg and Dougherty, 1969; Miller et al., 1988). Finally, the leading role of the lymphatics was established (Boulanger et al., 1999). The thoracic duct ligation decreased the fluid drainage, without completely blocking it. That was attributed to the complicated structure of the lymphatic capillary bed (Eliskova et al., 1995; Boulanger et al., 1999).

In vivo studies in sheep support the notion that the fluid drainage through the lympatics increases proportionally to the volume or pressure increase, as much as four times. This property has been related to the effect of external factors on the lymphatics function as well as to the functional alterations due to the neurohormonal stimulation. These characteristics are extremely important under conditions of fluid accumulation like cardiac tamponade (Miserocchi, 1989; Yuan et al., 2000). Also, in rabbits and mice, but not in sheep, there is a proven communication between the pericardial and the pleural cavity, through "pores" (diameter up to 50 μm), enabling fluid leakage toward the pleural cavity in certain conditions (Nakatani et al., 1988; Boulanger et al., 1999).

Water, Electrolyte, and Protein Transport

The common mesodermal origin and the simplicity of its isolation established the parietal pericardium as a surrogate tissue for pleural mesothelial tissue studies in small animals (Ishihara et al., 1980; Zocchi et al., 1998). Early studies showed data consistent with the passive diffusion of water, Na^+, Cl^- and small molecules (sucrose, mannitol) through "small" pores and later it was shown that there is a passive paracellular diffusion of macromolecules (albumin, dextranes) through "large" pores (either like permanent channels or like transient cystic formations). In both cases the main morphological and functional barrier proved to be the mesothelium. However, by that time active ion trasport through the parietal pericardium was thought to be minimal (Zocchi et al., 1998; Bodega et al., 2000).

However, a later study that examined this aspect showed that the electrical resistance of the rabbit parietal pericardium is measurable and attributed to the mesothelial barrier since it had greater resistance ($10.1 \pm 0.9\ \Omega\times\ cm^2$) compared to the underlying connective tissue alone ($1 \pm 0.2\ \Omega\times\ cm^2$) (Bodega et al., 2001). This established the mesothelium as the main barrier for molecular transfer. Furthermore, another study shed more light to the active electrolyte transport through the parietal pericardium showing that it is directed from the basal to the apical surface with a net driving pressure of $\sim$3 cmH_2O, which is 5-fold higher than the one through the pleural lamenae (Tang and Lai-Fook, 2005). In this study it was also shown that the diffusion constant of the rabbit parietal pericardium for albumin ($0.26–0.96 \times 10^{-8}\ cm^2/s$), is independent from its concentration. This finding contradicted the previous data regarding rabbit pericardium, pleura and omentum where the reference values were higher and directly proportional to albumin concentration (Parameswaran et al., 1999a,b; Bodega et al., 2002). This discrepancy was attributed to the experimental conditions and the tissue differences. The pericardium contains a larger proportion of collagen fibers compared to the elastic ones and a higher concentration of hyaluronic acid that render it more stiff as well as less permeable than the other serosal membranes (Tang and Lai-Fook, 2005). Moreover, the characteristics above are related to the higher values of hydraulic and electrical resistance of the pericardium and mainly the mesothelial layer (Bodega et al., 2002; Tang and Lai-Fook, 2005). There are *in vitro* data that the hydraulic permeability of the parietal pericardium is independent of the hydrostatic pressure over the range from 6 to 15 cmH_2O and directly proportional to the membrane thickness, among the species (Fingerote et al., 1980).

Variance among species seems to be the case also in terms of transmesothelial electrical resistance, an index of ion transport. As mentioned above rabbit parietal pericardium had values in the range of $10.1 \pm 0.9\ \Omega\times\ cm^2$, while in sheep these values were nearly double ($22.83 \pm 0.4\ \Omega\times\ cm^2$) (Vogiatzidis et al., 2006). Moreover, in the last study the effects of morphine on the pericardium were assessed and it was shown that the electrical resistance of the pericardium is increased by the application of morphine. The same results were found in the pleura and the peritoneum indicating a common opoidergic influence of the ionic transport capacity of the three serosal membranes (Vogiatzidis et al., 2006; Zarogiannis et al., 2007).

Conclusions

The study of pericardial space physiology is an area with many things to be discovered. The mechanism of pericardial fluid production is straightforward in physiological conditions, however it needs to be identified what is the exact role of the mesothelial cells both in the recycling of the pericardial fluid as well as with respect to the paracrine function that they possess. Another important challenge would be to dissect the exact contribution and magnitude of each mechanism regulating the recycling of the pericardial fluid.

Finally, few things are known about the interplay of mesothelial cells and pericardial fluid. These areas will increase our understanding of the physiology of the pericardial space once explored as well as they will provide us with new insights regarding drug development in the context of pericardial effusions.

References

Ardell, J. L., and Randall, W. C. (1986). Selective vagal innervation of sinoatrial and atrioventricular nodes in canine heart. *Am. J. Physiol.* 251, 764–773.

Benhaiem-Sigaux, N., Mina, E., Sigaux, F., Lambre, C. R., Valensi, F., Allegret, C., et al. (1985). Characterization of human pericardial macrophages. *J. Leukoc. Biol.* 38, 709–721.

Ben-Horin, S., Shinfeld, A., Kachel, E., Chetrit, A., and Livneh, A. (2005). The composition of normal pericardial fluid and its implications for diagnosing pericardial effusions. *Am. J. Med.* 118, 636–640. doi: 10.1016/j.amjmed.2005.01.066

Bodega, F., Zocchi, L., and Agostoni, E. (2000). Macromolecule transfer through mesothelium and connective tissue. *J. Appl. Physiol.* 89, 2165–2173.

Bodega, F., Zocchi, L., and Agostoni, E. (2002). Albumin transcytosis in mesothelium. *Am. J. Physiol. Lung Cell. Mol. Physiol.* 282, 3–11. doi: 10.1152/ajplung.00157.2001

Bodega, F., Zocchi, L., Cremaschi, D., and Agostoni, E. (2001). Electrical resistance and ion diffusion through mesothelium. *Respir. Physiol.* 124, 231–241. doi: 10.1016/S0034-5687(00)00213-9

Boulanger, B., Yuan, Z., Flessner, M., Hay, J., and Johnston, M. (1999). Pericardial fluid absorption into lymphatic vessels in sheep. *Microvasc. Res.* 57, 174–186. doi: 10.1006/mvre.1998.2127

Burgess, L. J., Reuter, H., Taljaard, J. J. F., and Doubell, A. F. (2002). Role of biochemical tests in the diagnosis of large pericardial effusions. *Chest* 121, 495–499. doi: 10.1378/chest.121.2.495

Chinchoy, E. (2005). *Handbook of Cardiac Anatomy, Physiology and Devices*. Totowa, NJ: Humana Press Inc. 101–110. doi: 10.1007/978-1-59259-835-9_7

Chiou, C. W., Eble, J. N., and Zipes, D. P. (1997). Efferent vagal innervation of the canine atria and sinus and atrioventricular nodes. The third fat pad. *Circulation* 95, 2573–2584. doi: 10.1161/01.CIR.95.11.2573

Cinca, J., and Rodriguez-Sinovas, A. (2000). Cardiovascular reflex responces induced by epicardial chemoreceptor stimulation. *Cardiovasc. Res.* 45, 163–171. doi: 10.1016/S0008-6363(99)00319-3

D'Avila, A. (2003). Pericardial anatomy for the interventional electrophysiologists. *J. Cardiovasc. Electrophysiol.* 14, 422–430. doi: 10.1046/j.1540-8167.2003.02487.x

DeVries, G., Hamilton, D. R., Ter Keurs, H. E. D. J., Beyar, R., and Tyberg, J. V. (2001). A novel technique for measurement of pericardial pressure. *Am. J. Physiol. Heart Circ. Physiol.* 280, 2815–2822.

Eliskova, M., Eliska, O., and Miller, A. J. (1995). The lymphatic drainage of the parietal pericardium in man. *Lymphology* 28, 208–217.

Fingerote, R., Fung, H. Y., and Rabkin, S. W. (1980). Hydraulic permeability of canine and human pericardium *in vitro*. *Basic Res. Cardiol.* 75, 764–771. doi: 10.1007/BF01910454

Frick, H., Leonhardt, H., and Starck, D. (1985). *Human Anatomy, Greek edn.* Athens: Parisianos Publication.

Fukuo, Y., Nakatani, T., Shinohara, H., and Matsuda, T. (1988). The mouse pericardium: it allows passage of particulate matter from the pleural to the pericardial cavity. *Anat. Rec.* 222, 1–5. doi: 10.1002/ar.1092220102

Gibbons Kroeker, C. A., Shrive, N. G., Belenkie, I., and Tyberg, J. V. (2003). Pericardium modulates left and right ventricular stroke volumes to compensate for sudden changes in atrial volume. *Am. J. Physiol. Heart Circ. Physiol.* 284, 2247–2254. doi: 10.1152/ajpheart.00613.2002

Gibson, A. T., and Segal, M. B. (1978a). A study of the composition of pericardial fluid, with special reference to the probable mechanism of fluid formation. *J. Physiol.* 277, 367–377. doi: 10.1113/jphysiol.1978.sp012277

Gibson, A. T., and Segal, M. B. (1978b). A study of the routes by which protein passes from the pericardial cavity to the blood in rabbits. *J. Physiol.* 280, 423–433.

Goto, Y., and LeWinter, M. M. (1990). Nonuniform regional deformation of the pericardium during the cardiac cycle in dogs. *Circ. Res.* 67, 1107–1114. doi: 10.1161/01.RES.67.5.1107

Hamilton, D. R., Sas, R., and Tyberg, J. V. (2004). Atrioventricular nonuniformity of pericardial constraint. *Am. J. Physiol. Heart Circ. Physiol.* 287, 1700–1704. doi: 10.1152/ajpheart.00117.2004

Hollenberg, M., and Dougherty, J. (1969). Lymph flow and131-I-albumin resorption from pericardial effusions in man. *Am. J. Cardiol.* 24, 514–522. doi: 10.1016/0002-9149(69)90494-9

Holt, J. P. (1970). The normal pericardium. *Am. J. Cardiol.* 26, 455–465. doi: 10.1016/0002-9149(70)90702-2

Ishihara, T., Ferrans, V. J., Jones, M., Boyce, S. W., Kawanami, O., and Roberts, W. C. (1980). Histologic and ultrastructure features of normal human parietal pericardium. *Am. J. Cardiol.* 46, 744–753. doi: 10.1016/0002-9149(80)90424-5

Jõbsis, P. D., Ashikaga, H., Wen, H., Rothstein, E. C., Horvath, K. A., McVeigh, E. R., et al. (2007).The visceral pericardium: macromolecular structure and contribution to passive mechanical properties of the left ventricle. *Am. J. Physiol. Heart Circ. Physiol.* 293, 3379–3387. doi: 10.1152/ajpheart.00967.2007

Kenner, H. M., and Wood, E. H. (1966). Intrapericardial, intrapleural, and intracardiac pressures during acute heart failure in dogs studied without thoracotomy. *Circ. Res.* 19, 1071–1079. doi: 10.1161/01.RES.19.6.1071

Lee, J. M., and Boughner, D. R. (1981). Tissue mechanics of canine pericardium in differenttest environments. Evidence for time-dependent accommodation, absence of plasticity, and new roles for collagen and elastin. *Circ. Res.* 49, 533–544. doi: 10.1161/01.RES.49.2.533

Lee, J. M., and Boughner, D. R. (1985). Mechanical properties of human pericardium. Differences in viscoelastic response when compared with canine pericardium. *Circ. Res.* 57, 475–481. doi: 10.1161/01.RES.57.3.475

Lorenz, C. H., Pastorek, J. S., and Bundy, J. M. (2000). Delineation of normal human left ventricular twist throughout systole by tagged cine magnetic resonance imaging. *J. Cardiovasc. Magn. Reson.* 2, 97–108. doi: 10.3109/10976640009148678

Maruyama, Y., Ashikawa, K., Isoyama, S., Kanatsuka, H., Ino-Oka, E., and Takishima, T. (1982). Mechanical interactions between four heart chambers with and without the pericardium in canine hearts. *Circ. Res.* 50, 86–100. doi: 10.1161/01.RES.50.1.86

Mauer, F. W., Warren, M. F., and Drinker, C. K. (1940). The composition of mammalian pericardial and peritoneal fluids. *Am. J. Physiol.* 129, 635–644.

Meyers, D. G., Meyers, R. E., and Prendergast, T. W. (1997). The usefulness of diagnostic tests on pericardial fluid. *Chest* 111, 1213–1221. doi: 10.1378/chest.111.5.1213

Michailova, K. N., and Usunoff, K. G. (2006). Seposal membranes (Pleura, Pericardium, Peritoneum): normal sructure, development and experimental pathology. *Adv. Anat. Embryol. Cell Biol.* 183, 1–144.

Miller, A. J., DeBoer, A., Pick, R., Van Pelt, L., Palmer, A. S., and Huber, M. P. (1988). The lymphatic drainage of the pericardial space in the dog. *Lymphology* 21, 227–233.

Miserocchi, G. (1989). Effect of diaphragmatic contraction or relaxation on size and shape of lymphatic stomata on the peritoneal surface in anesthetized rabbits. *Proc. Physiol. Soc.* 417, 132P.

Mohrman, D. E., and Heller, L. J. (2006). *Cardiovascular Physiology 6th edn.* New York, NY: Lange Physiology Series.

Mutsaers, S.E. (2002). Mesothelial cells: their structure, function and role in serosal repair. *Respirology* 7, 171–191. doi: 10.1046/j.1440-1843.2002.00404.x

Nakatani, T., Shinohara, H., Fukuo, Y., Morisawa, S., and Matsuda, T. (1988). Pericardium of rodents: pores connect the pericardial and pleural cavities. *Anat. Rec.* 220, 132–137. doi: 10.1002/ar.1092200204

Parameswaran, S., Brown, L. V., Ibbott, G. S., and Lai-Fook, S. J. (1999a). Hydraulic conductivity, albumin reflection and diffusion coefficients of pig mediastinal pleura. *Microvasc. Res.* 58, 114–127. doi: 10.1006/mvre.1999.2168

Parameswaran, S., Brown, L. V., Ibbott, G. S., and Lai-Fook, S. J. (1999b). Effect of concentration and hyaluronidase on albumin diffusion across rabbit mesentery. *Microcirculation* 6, 117–126. doi: 10.1111/j.1549-8719.1999.tb00094.x

Przyklenk, K., Connelly, C. M., McLaughlin, R. J., Kloner, R. A., and Apstein, C. S. (1987). Effect of myocyte necrosis on strength, strain, and stiffness of isolated myocardial strips. *Am. Heart J.* 114, 1349–1359. doi: 10.1016/0002-8703(87)90536-9

Quick, C. M., Venugopal, A. M., Gashev, A. A., Zawieja, D. C., and Stewart, R. H. (2007). Intrinsic pump-conduit behavior of lymphangions. *Am. J. Physiol. Regul. Integr. Comp. Physiol.* 292, 1510–1518. doi: 10.1152/ajpregu.00258.2006

Randall, W. C., and Ardell, J. L. (1985). Selective parasympathectomy of automatic and conductile tissues of the canine heart. *Am. J. Physiol.* 248, 61–68.

Santamore, W. P., Constantinescu, M. S., Bogen, D., and Johnston, W. E. (1990). Nonuniform distribution of normal pericardial fluid. *Basic Res. Cardiol.* 85, 541–549. doi: 10.1007/BF01907889

Shabetai, R. (2003). *The Pericardium (Developments in Cardiovascular Medicine)*, Boston, MA: Kluwer Academic Publishers.

Simionescu, D., Simionescu, A., and Deac, R. (1993). Mapping of glutaraldehyde-treated bovine pericardium and tissue selection for bioprosthetic heart valves. *J. Biomed. Mater. Res.* 27, 697–704. doi: 10.1002/jbm.820270602

Smiseth, O.A., Frais, M. A., Kingma, I., Smith, E. R., and Tyberg, J. V. (1985). Assessment of pericardial constraint in dogs. *Circulation* 71, 158–164. doi: 10.1161/01.CIR.71.1.158

Spodick, D. H. (1997). *The Pericardium: A Comprehensive Textbook Chapter 3, Marcel Dekker Inc*. New York, NY.

Stewart, R. H., Rohn, D. A., Allen, S. J., and Laine, G. A. (1997). Basic determinants of epicardial transudation. *Am. J. Physiol.* 273, 1408–1414.

Takada, K., Otsuki, Y., and Magari, S. (1991). Lymphatics and pre-lymphatics of the rabbit pericardium and epicardium with special emphasis on particulate absorption and milky spot-like structures. *Lymphology* 24, 116–124.

Takata, M., Harasaw, Y., Beloucif, S., and Robotham, J. L. (1997). Coupled vs. uncoupled pericardial constraint: effects on cardiac chamber interaction. *J. Appl. Physiol.* 83, 1799–1813.

Tang, S. M., and Lai-Fook, S. J. (2005). Transport properties of the mesothelium and interstitium measured in rabbit pericardium. *Microvasc. Res.* 70, 152–164. doi: 10.1016/j.mvr.2005.10.003

Traboulsi, M., Scott-Douglas, N. W., Smith, E. R., and Tyberg, J. V. (1992). The right and left ventricular intracavitary and transmural pressure-strain relationships. *Am. Heart J.* 123, 1279–1287. doi: 10.1016/0002-8703(92)91034-X

Vesely, T. M., and Cahill, D. R. (1986). Cross-sectional anatomy of the pericardial sinuses, recesses and adjacent structures. *Surg. Radiol. Anat.* 8, 221–227. doi: 10.1007/BF02425071

Vogiatzidis, K., Hatzoglou, C., Zarogiannis, S., Matafia, G., Gourgoulianis, K., and Molyvdas, P. A. (2006). μ-opioid influence on the transmesothelial resistance of isolated sheep pleura and parietal pericardium. *Eur. J. Pharm.* 530, 276–280. doi: 10.1016/j.ejphar.2005.11.050

Yuan, Z., Boulanger, B., Flessner, M., and Johnston, M. (2000). Relationship between pericardial pressure and lymphatic pericardial fluid transport in sheep. *Microvasc. Res.* 60, 28–36. doi: 10.1006/mvre.2000.2239

Zarogiannis, S., Vogiatzidis, K., Hatzoglou, C., Liakopoulos, V., Potamianos, S., Eleftheriadis, T., et al. (2007). μ-opioid stimulation of isolated parietal sheep peritoneum decreases peritoneal permeability *in vitro*. *Adv. Perit. Dial.* 23, 34–37.

Zocchi, L., Raffaini, A., Agostoni, E., and Cremaschi, D. (1998). Diffusional permeability of rabbit mesothelium. *J. Appl. Physiol.* 85, 471–477.

Conflict of Interest Statement: The authors declare that the research was conducted in the absence of any commercial or financial relationships that could be construed as a potential conflict of interest.

frontiers in
PHYSIOLOGY

REVIEW ARTICLE
published: 05 January 2015
doi: 10.3389/fphys.2014.00470

Encapsulating peritoneal sclerosis—a rare but devastating peritoneal disease

Zia Moinuddin[1,2], Angela Summers[1], David Van Dellen[1], Titus Augustine[1] and Sarah E. Herrick[2]*

[1] *Department of Transplantation, Manchester Royal Infirmary, Manchester, UK*
[2] *Faculty of Medical and Human Sciences, Institute of Inflammation and Repair, University of Manchester, Manchester Academic Health Science Centre, Manchester, UK*

Edited by:
Sotirios G. Zarogiannis, University of Thessaly, Greece

Reviewed by:
Theodoros Eleftheriadis, University of Thessaly, Greece
Antonios Helias Tzamaloukas, U.S. Department of Veterans Affairs, USA

***Correspondence:**
Sarah E. Herrick, Faculty of Medical and Human Sciences, Institute of Inflammation and Repair, University of Manchester, Room 3.106 Stopford Building, Oxford Road, Manchester M13 9PT, UK
e-mail: sarah.herrick@manchester.ac.uk

Encapsulating peritoneal sclerosis (EPS) is a devastating but, fortunately, rare complication of long-term peritoneal dialysis. The disease is associated with extensive thickening and fibrosis of the peritoneum resulting in the formation of a fibrous cocoon encapsulating the bowel leading to intestinal obstruction. The incidence of EPS ranges between 0.7 and 3.3% and increases with duration of peritoneal dialysis therapy. Dialysis fluid is hyperosmotic, hyperglycemic, and acidic causing chronic injury and inflammation in the peritoneum with loss of mesothelium and extensive tissue fibrosis. The pathogenesis of EPS, however, still remains uncertain, although a widely accepted hypothesis is the "two-hit theory," where, the first hit is chronic peritoneal membrane injury from long standing peritoneal dialysis followed by a second hit such as an episode of peritonitis, genetic predisposition and/or acute cessation of peritoneal dialysis, leading to EPS. Recently, EPS has been reported in patients shortly after transplantation suggesting that this procedure may also act as a possible second insult. The process of epithelial–mesenchymal transition of mesothelial cells is proposed to play a central role in the development of peritoneal sclerosis, a common characteristic of patients on dialysis, however, its importance in EPS is less clear. There is no established treatment for EPS although evidence from small case studies suggests that corticosteroids and tamoxifen may be beneficial. Nutritional support is essential and surgical intervention (peritonectomy and enterolysis) is recommended in later stages to relieve bowel obstruction.

Keywords: encapsulating peritoneal sclerosis, peritoneal dialysis, mesothelium, epithelial–mesenchymal transition, fibrosis

INTRODUCTION

Encapsulating peritoneal sclerosis (EPS) is a chronic clinical syndrome of insidious onset, presenting late as chronic malnourishment with signs and symptoms of intermittent, acute or sub-acute gastrointestinal obstruction (Augustine et al., 2009). It appears to be a multifactorial disease with several initiating factors that are significant at the different stages of the disease. Diagnosis is confirmed by macroscopic and/or radiological observation of sclerosis, calcification, peritoneal thickening or encapsulation of the intestines (Kawaguchi et al., 2000). EPS can be fatal but, fortunately, it is a rare complication predominantly of long-term peritoneal dialysis (PD). Since the first case of EPS was reported in 1980 (Gandhi et al., 1980), there has been a steady rise in the incidence of the disease from 0.9% in 1996 to 3.3% in 2005 as patients stay on PD for longer and awareness of this complication has increased. The data obtained over the years from several retrospective studies performed to investigate this potentially fatal condition estimate the worldwide incidence of EPS at 0.7–3.3% in patients on PD (Brown et al., 2009). The mortality rate for patients with EPS is great at 25–55%, predominately in the year after diagnosis and is directly proportional to the duration of PD treatment (Rigby and Hawley, 1998; Kawanishi et al., 2004; Kawanishi and Moriishi, 2005; Brown et al., 2009).

AETIOLOGY

EPS is usually seen in end-stage renal disease (ESRD) patients who have been on long-term PD therapy. Dialysis fluid is damaging to the peritoneum due to the high glucose concentration and acidic pH. A high glucose concentration facilitates the osmosis and diffusion gradient across the peritoneum and the low pH acts to prevent the formation of glucose degradation products (GDPs) which are damaging agents (Jorres et al., 1992). Heat sterilization of PD fluid leads to the formation of GDPs (Wieslander, 1996) and these in the presence of glucose cause the formation of advanced glycation end products (AGEs) (Mortier et al., 2002). More biocompatible solutions are now being used that contain less GDPs which results in reduced peritoneal damage (Boulanger, 2008).

Interestingly, EPS can also develop in patients not on PD but associated with other conditions such as autoimmune diseases, sarcoidosis, peritoneal and intra-abdominal malignancies, chronic peritoneal ascites, intra-peritoneal chemotherapy, intraperitoneal exposure to particulate matter or disinfectant, abdominal surgery, endometriosis, intra-peritoneal infections (tuberculosis), and beta-blocker administration (Pollock, 2001; Kawanishi and Moriishi, 2005) (**Table 1**). Chronic renal failure itself could also induce peritoneal changes including thickening

before PD therapy (Williams et al., 2002) and uremia, a contributory factor in all PD patients, is known to lead to a pro-inflammatory state (Baroni et al., 2012).

RISK FACTORS

The duration of PD therapy seems to be the most important risk factor for the development of EPS. In an Australian survey, the incidence of EPS increased with the duration of PD, being 1.9, 6.4, 10.8, and 19.4% in patients on PD for more than 2, 5, 6, and 8 years respectively (Rigby and Hawley, 1998).

A Japanese prospective study reported similar findings, in which the incidence of EPS was 0.7% after 5 years, 2.1% after 8 years, 5.9% after 10 years, and 17.2% after 15 years of PD therapy (Kawanishi et al., 2004). A more recent Scottish study also reported an increase in incidence of EPS from 2% at 2–3 years to 8.8% at 5–6 years of PD therapy (Brown et al., 2009). However, most cases of EPS are diagnosed after discontinuation of PD therapy. A Japanese prospective study reported that 69% of EPS cases occurred after discontinuation of PD therapy (Kawanishi et al., 2004). This suggests that despite PD being a major risk factor for EPS, lavage of the peritoneal cavity during PD may possibly limit the accumulation of factors that encourage the development of the disease (Yamamoto et al., 2005, 2010).

Interestingly, organ transplantation appears to increase the risk of developing EPS as some studies have reported a high incidence shortly after renal transplantation (Fieren et al., 2007; Balasubramaniam et al., 2009). This could either be due to the acute cessation of PD or due to the profibrotic effect of immunosuppressive medication (calcineurin inhibitors). Calcineurin inhibitors, like Tacrolimus and Cyclosporin, cause up-regulation of transforming growth factor-beta (TGF-β), and other profibrogenic factors potentiating matrix accumulation (Khanna et al., 2002). In experimental rat models, Cyclosporin combined with chronic peritoneal exposure to dialysis solution was associated with increased peritoneal fibrosis and angiogenesis (Van Westrhenen et al., 2007). However, the exact mechanism of post-transplantation EPS still remains unknown.

Peritonitis is a common complication of PD and plays a complex part in the development of EPS with the number of peritonitis episodes linked to incidence of EPS (Yamamoto et al., 2005). Recurrent peritonitis due to bacterial contamination including *Pseudomonas* spp., *Staphylococcus aureus*, and certain fungal organisms have been particularly implicated in the development of EPS (Flanigan et al., 1984; Chew et al., 1997; Rigby and Hawley, 1998). Other risk factors suggested to be involved in EPS onset are the composition of dialysis fluid and generation of GDPs, young age, ultrafiltration failure and the exposure to PD catheter cleaning reagent, chlorhexidine (Pollock, 2001) (**Table 2**).

Table 1 | Non-peritoneal dialysis related causes of EPS.

- Autoimmune diseases
- Sarcoidosis
- Peritoneal and intra-abdominal malignancies
- Chronic peritoneal ascites
- Intra-peritoneal chemotherapy
- Intraperitoneal exposure to particulate matter or disinfectant
- Abdominal surgery
- Endometriosis
- Intra-peritoneal infections (tuberculosis)
- Beta-blocker administration

CLINICAL FEATURES OF EPS

Patients usually present with abdominal symptoms like early satiety, anorexia, nausea, vomiting, and altered bowel habit (constipation or diarrhea in the early stages of EPS) (Nakamoto, 2005; Augustine et al., 2009). These symptoms may be accompanied by signs of inflammation (pyrexia and raised CRP) and/or blood stained ascites in the early stages (Nakamoto, 2005; Maruyama and Nakayama, 2008). Late stages of EPS are associated with abdominal pain, fullness, overt bowel obstruction and presence of an abdominal mass). This is caused by the development of a fibrous cocoon that gradually covers the intestines and leads to malnutrition, weight loss, bowel obstruction, ischemia and strangulation, infection and death (Kawaguchi et al., 2000).

CLASSIFICATION OF EPS

Based on the clinical presentation, Nakamoto categorized EPS into four groups (Nakamoto, 2005). The following are the proposed clinical stages:

Stage 1- Pre-EPS stage: Asymptomatic with mild ascites and no inflammation.
Stage 2- Inflammatory stage: Patients are symptomatic with nausea and diarrhea consistent with partial encapsulation of the bowel and intestinal swelling. Mild inflammation with fibrin exudation is present.
Stage 3- Encapsulation: Symptoms of bowel obstruction due to the formation of the fibrous cocoon causing encapsulation. It can be associated with mild to severe inflammation.
Stage 4- Chronic stage of ileus: Patients have absolute bowel obstruction caused by thickening of the encapsulating fibrous cocoon. There is little, if any, inflammation at this stage.

DIAGNOSIS OF EPS

The diagnosis of EPS relies on clinical findings, radiological tests and pathological appearance of the diseased tissue. Clinically, the diagnosis of EPS is based on recognizing the signs and symptoms (nausea, anorexia, early satiety, weight loss, altered bowel habit, and ascites) in the patients at risk of developing the condition (Nakamoto, 2005). Blood tests may also reveal high CRP and low

Table 2 | Risk factors for EPS in the peritoneal dialysis (PD) population.

- Duration of PD
- Acute cessation of PD
- Organ transplantation
- Peritonitis
- Composition of dialysis fluid (low pH, high glucose)
- Young age
- Ultrafiltration failure
- Exposure to chlorhexidine

albumin levels. These presenting symptoms and signs are vague and non-localizing. However, the insidious nature and chronicity of development can be a distinguishing feature of EPS (Kawaguchi et al., 2000). As a consequence, EPS is often not recognized in its early stages and requires a high index of suspicion to pursue a diagnosis.

As the clinical picture of EPS can vary considerably, various investigations are necessary to further evaluate a suspected case (Kawaguchi et al., 2005). Ultrasonography, water-soluble contrast studies and computed tomography (CT) scanning are the most widely used radiological tests to aid the diagnosis of EPS. CT scanning, however, is the investigation of choice in patients with established EPS and helps monitor disease progression. Peritoneal enhancement, peritoneal thickening, calcification, bowel tethering, bowel wall thickening, signs of bowel obstruction, and loculated collections are the most common CT findings of EPS (Vlijm et al., 2009). But, given the rare, complex nature of the disease and with most of the CT scan appearances being non-specific, interpretation and diagnosis can be difficult. Surgery (Laparoscopy/Laparotomy and peritoneal biopsy) therefore may be needed to confirm the diagnosis (Kawaguchi et al., 2005). At surgery, macroscopically, advanced cases of EPS typically exhibit a thickened brownish peritoneum with a cocoon-like encapsulation of the entire intestine by the visceral peritoneum (**Figure 1**). The intestinal loops are adherent to one another and the visceral peritoneum is severely thickened with fibrosis. Adhesions between the visceral and parietal peritoneum are rare, except in cases of severe inflammation (Honda and Oda, 2005). Macroscopic evidence of peritoneal calcification is also a feature but is not necessarily present in all cases of EPS (Park et al., 2008).

Numerous studies have been performed searching for potential biomarkers in PD effluent to aid the early diagnosis of EPS. Low CA125 levels (denoting mesothelial cell loss) and high levels of the inflammatory cytokine Interleukin-6 (IL-6) in PD effluent have been noted several years before the diagnosis of EPS suggesting that these factors could be potential early diagnostic markers (Sampimon et al., 2010). However, further research is necessary to identify definite biomarkers for early diagnosis of EPS. Current imaging techniques are also not useful at reliably detecting EPS in its early stages. CT scan screening of asymptomatic PD patients is not recommended as EPS may occur within a year of a normal CT scan. Also, not all long-term PD patients with peritoneal abnormalities on CT go on to develop established EPS (Goodlad et al., 2011). Dynamic cinematographic magnetic resonance (cine-MR) scanning with advanced image analysis may be useful in early detection of EPS. However, more studies are required to validate the efficacy of this imaging modality (Wright et al., 2011). Laparoscopy performed in suspected cases may have an important role to play in the early diagnosis of EPS. Our current lack of understanding of the pathophysiology limits our ability to detect EPS early or prevent its occurrence.

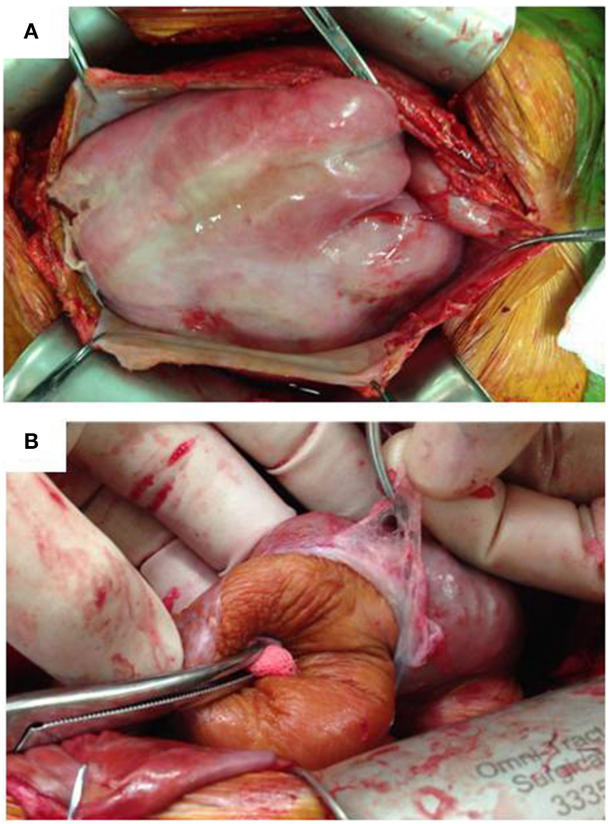

FIGURE 1 | Macroscopic appearance of EPS at surgery. (A) Thickened parietal peritoneum is held up by surgical clips. Visceral peritoneum is thickened forming a fibrous cocoon encapsulating the bowel. **(B)** Visceral peritoneum peeled off the small bowel which has a brownish, tanned leathery appearance.

HISTOLOGICAL FEATURES OF ENCAPSULATING PERITONEAL SCLEROSIS

The two most relevant pathologies of long-term PD are simple sclerosis and EPS. Simple sclerosis is characterized by the thickening of parietal peritoneum in the absence of encapsulation. The uremic state and continuing PD leads to a gradual loss of mesothelium (mesothelial denudation). Medial sclerosis and hyalinization of the peritoneal vasculature (vasculopathy) is also seen along with neoangiogenesis (Honda et al., 1996). The sub-mesothelial compact zone thickens and is composed of myofibroblasts and fibrous collagen (Mateijsen et al., 1999). In addition, AGEs are found to be present in the mesothelial and sub-mesothelial layer of PD patients (Yamada et al., 1994; Nakayama et al., 1997). Of note the amount of angiogenesis was found to be proportional to the severity of intestinal fibrosis (Mateijsen et al., 1999; Plum et al., 2001) and the level of mesothelial deudation correlated with sub-mesothelial thickening and vasculopathy (Williams et al., 2003). Simple sclerosis is a fairly common finding in long-term PD patients while EPS is rare. Therefore, studies analysing the histological differences in the peritoneum from EPS and simple sclerosis patients are limited. Of these, only one study performed by Garosi et al. (2005) analyzed both visceral and parietal peritoneum, and Braun and colleagues analyzed only visceral peritoneum (Braun et al., 2012) while the remaining studies did not specify the type of peritoneum analyzed (**Table 3**). Garosi and colleagues investigated 180 peritoneal biopsies of PD patients with simple sclerosis and

Table 3 | Comparative histopathology of EPS patients and non-EPS PD patients.

	Braun et al., 2012	Braun et al., 2009	Sherif et al., 2008	Garosi et al., 2005	Honda et al., 2003
EPS patients (*n*)	31	9	12	39	12
Non-EPS PD patients (*n*)	27	10	30	180	57
Visceral (V) or parietal (P)	–	V	–	V and P	–
Histologic parameters	**Significance between EPS and non-EPS PD patients**				
Fibrosis	S	S	S	–	NS
Degenerated layer thickness	–	–	S	–	–
Fibroblast like cells	S	–	–	–	–
Inflammation	NS	–	–	S	S
Mesothelial denudation	S	–	NS	–	NS
Vasculopathy	NS	S	–	S	NS
Fibrin deposition	S	–	S	–	S
Vessel density	NS	S	–	–	–
Fe deposits	S	–	–	–	–
Decreased cellularity	S	–	–	–	–
Fibroblast enlargement	–	–	–	–	S
Capillary angiogenesis	–	–	–	–	S
Calcification	NS	–	–	S	–

(S) and (NS) denote significance and non-significance, respectively. (–) denotes data not being measured or recorded.

compared morphological findings with those from biopsies of 39 patients with EPS (Garosi et al., 2005). Significant findings in patients with EPS were thickening of the sub-mesothelial cell layer, vasculopathy, arterial occlusion, inflammation, tissue and arterial calcification, and ossification. In a similar study, fibrin deposition, increase in the size of fibroblasts, capillary angiogenesis, and mononuclear cell infiltration were more common features of EPS than simple sclerosis (Honda et al., 2003). Sherif and colleagues compared the peritoneum of EPS with simple sclerosis and showed that the sub-mesothelial compact zone was thinner in early-EPS than late-EPS (Sherif et al., 2008). In a more recent study, fibroblast-like cells, mesothelial denudation, calcification, decreased cellularity and positive iron staining were more common in the peritoneum of EPS patients. Positive immunohistochemical staining for podoplanin, a lymphatic endothelial marker expressed by peritoneal mesothelial cells, was significantly more prevalent in EPS peritoneum (Braun et al., 2012). Up-regulation of vascular endothelial growth factor (VEGF) and down-regulation of mast cells (Alscher et al., 2007; Braun et al., 2009) also appeared to be a feature of EPS peritoneum. However, as the above findings are not always specific to EPS tissue, reliable histological diagnosis is difficult. Further studies are therefore necessary to explore the presence of additional unique immunohistochemical markers to aid the diagnosis.

PATHOPHYSIOLOGY OF ENCAPSULATING PERITONEAL SCLEROSIS

Although a number of risk factors have been identified, there are currently no means of preventing EPS development or recognizing earlier stages of the disease. Furthermore, it is a matter of debate whether EPS is a natural progression of simple sclerosis or a completely separate entity. However, it is clear that having simple sclerosis does not predispose to developing EPS. It is generally now accepted that a two-hit theory explains EPS development. It is well established that chronic exposure to bio-incompatible dialysate causes damage to the peritoneum of all patients on PD. This first hit causes mesothelial disruption which can trigger a fibrotic process which is referred to as "simple sclerosis."

The subsequent exposure to a second insult, in some patients, triggers the development of EPS. This can be either an episode of peritonitis, acute cessation of PD, transplantation, any other acute intra-abdominal event or maybe a genetic predisposition (**Figure 2**). A number of genetic polymorphisms with functional effects have been described in patients on PD and these may partially explain the propensity to develop EPS (Pletinck et al., 2012). A number of rodent models of EPS have been developed using chronic chemical irritation to induce peritoneal sclerosis and bowel encapsulation (Hoff, 2005; Summers et al., 2008). Such models replicate the cycles of tissue injury with fibrin deposition and inflammation leading to subsequent repair with mesothelial cell and fibroblast activation, proliferation and matrix deposition that are proposed to drive the development of EPS. Some of these mechanisms of induction are described in more detail below.

INFLAMMATORY PROFILE

The PD catheter can itself trigger inflammation either directly as a foreign material or by acting as a site of bacterial biofilm formation leading to PD peritonitis (Flessner et al., 2007). Various characteristics of PD fluid such as low pH, high glucose levels, hyperosmolarity, presence of GDPs, and AGEs promote the release of several growth factors such as Transforming Growth Factor-β (TGF-β) and Platelet Derived Growth Factor (PDGF) and pro-inflammatory cytokines, IL-1, IL-6, IL-18, and Tumor Necrosis Factor-alpha (TNF-α) potentiating fibrosis (Margetts and Bonniaud, 2003; Baroni et al., 2012).

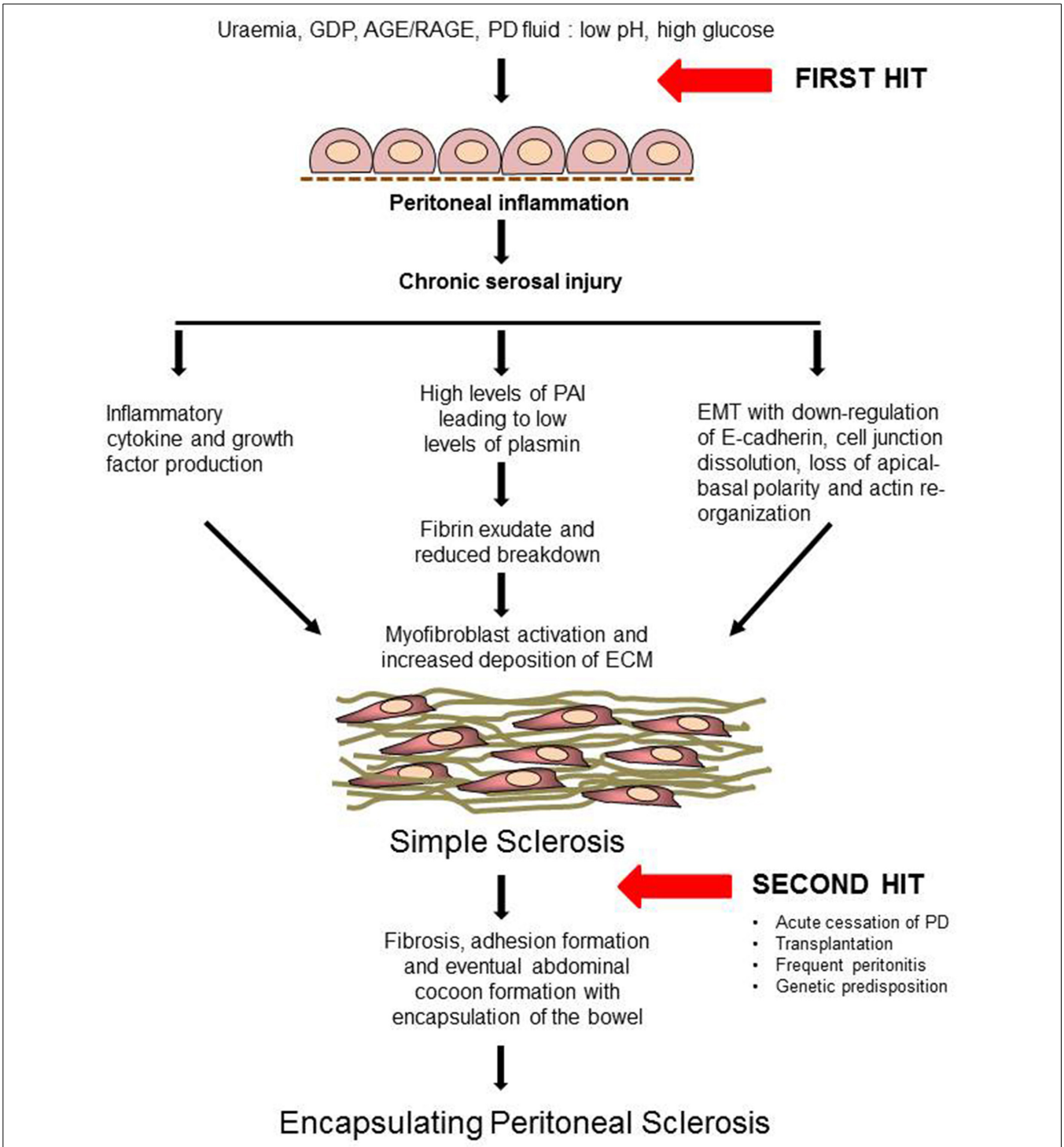

FIGURE 2 | Proposed pathogenesis of EPS: "Two-hit" theory (Modified from Augustine et al., 2009). AGE, Advanced Glycation End-products; RAGE, Receptors for Advanced Glycation End-products; IL-1, Interleukin-1; TNF, Tumor Necrosis Factor; TGF-β, Transforming Growth Factor-β; VEGF, Vascular Endothelial Growth Factor; EMT, Epithelial to Mesenchymal Transdifferentiation; MMP, Matrix Metalloproteinases; ECM, Extracellular Matrix.

Clinical studies have found elevated levels of IL-1β, IL-6, IL-8, TGF-β1, Hepatocyte Growth Factor (HGF), and PDGF in ascites from EPS patients in comparison with non-EPS controls (Masunaga et al., 2003). As EPS develops, patients also suffer from subclinical bowel ischemia which may cause translocation of bacteria across the bowel wall into the peritoneal cavity leading to infection, further inflammation and fibrosis (Augustine et al., 2009).

FIBRIN DEPOSITION AND FIBRINOLYSIS

Peritoneal inflammation initiates fibrin exudation that can either be lysed or remodeled by invading fibroblasts leading to fibrosis and adhesion formation (Holmdahl, 1997; Sulaiman et al., 2002). Plasmin plays a key role not only in fibrin degradation but also in the turnover of extracellular matrix and activation of matrix metalloproteinases. Plasmin is formed from the inactive zymogen plasminogen under the influence of plasminogen activators: tissue plasminogen activator (tPA) and urokinase-like plasminogen activator (uPA), whereas, plasminogen activation inhibitors (PAI-1 and PAI-2) reduce plasminogen activation. Low levels of plasmin and high levels of PAI were found in serum of patients on PD compared with hemodialysis (HD) patients suggesting a higher degree of hypercoagulation (Tomura et al., 1996). Mesothelial cells express PAI-1 and 2 under the influence of TGF-β (Rougier et al., 1998; Holmdahl et al., 2001) and such an inappropriate balance between fibrin deposition and breakdown increases the probability of fibrous adhesion formation possibly contributing to the development of EPS.

EPITHELIAL–MESENCHYMAL TRANSITION (EMT) OF MESOTHELIAL CELLS

In terms of peritoneal fibrosis, substantial evidence points to mesothelial cells (MCs) as being the principle source of myofibroblasts via a process of epithelial–mesenchymal transition (EMT) (Aroeira et al., 2007). MCs are unique in their expression of both epithelial and mesenchymal markers, and when exposed to injurious agents, they lose cell-cell contact and apical-basal cell polarity and invade the basal lamina changing to a mesenchymal phenotype expressing α-smooth muscle actin and depositing extracellular matrix (Aguilera et al., 2005). EMT occurs during normal embryo development and tumor cell invasion and metastasis and is a complex process that requires the correct spatiotemporal expression, interaction and modification of a multitude of intra-and extracellular factors to allow a change in cell phenotype (Thiery et al., 2009). Loss of cell surface E-cadherin is a prerequisite for EMT and primarily controlled by three main families of transcription factors: zinc finger Snail, basic helix-loop-helix, and ZEB (Kalluri and Weinberg, 2009). Several groups have shown the presence of mesothelial markers (ICAM-1 and cytokeratin) localized with spindle-shaped fibroblast- like cells in the sub-mesothelial layer in peritoneal biopsies from patients undergoing PD suggesting EMT had occurred (Yanez-Mo et al., 2003; Jimenez-Heffernan et al., 2004). Mesothelial cells isolated from dialysis fluid effluents from patients undergoing peritoneal dialysis also undergo a transition from epithelial to mesenchymal with a loss of E-cadherin (Zhang et al., 2013) and induction of snail (Yanez-Mo et al., 2003). Furthermore, AGE products (De Vriese et al., 2006) and dialysate (Selgas et al., 2006) induce human mesothelial EMT in culture. The process of EMT can occur under the influence of a number of pro-inflammatory and profibrotic cytokines, however TGF-β is proposed to be a principle mediator of mesothelial EMT as demonstrated both *in vitro* (Hung et al., 2003; Yang et al., 2003) and *in vivo* (Margetts et al., 2005). In terms of therapeutic strategy, blocking TGF-β1 (Loureiro et al., 2011), or addition of tamoxifen (Loureiro et al., 2013a) bone morphogenic protein-7 (Yu et al., 2009), or microRNA30a (Zhou et al., 2013) have all been found to protect the peritoneum from dialysate—induced damage in experimental models. Although strong evidence suggests that mesothelial EMT is important for the development of peritoneal sclerosis, the role this process plays in EPS, is a matter of debate (Loureiro et al., 2013b).

GROWTH FACTORS POTENTIALLY INVOLVED IN THE DEVELOPMENT OF EPS

The pathways involved in the development of EPS are likely to be complex and involve the interaction of a number of important growth factors leading to sub-mesothelial thickening and cocooning of the bowels. The level of the pro-neoangiogenic growth factor, Vascular Endothelial Growth Factor (VEGF), detected in peritoneal effluent has been found to directly correlate with length of time the patients are on PD (Zweers et al., 2001). Furthermore, treatment with VEGF blocking antibody reduced the thickness of the sub-mesothelial layer and reduced vasculopathy in a rat model of EPS (Io et al., 2004) suggesting a key role for this factor in EPS development. VEGF is produced by cultured human peritoneal mesothelial cells in response to various stimuli such as GDPs known to be present in PD fluid (Mandl-Weber et al., 2002). TGF-β, another important growth factor in wound healing and fibrosis, has also been shown to be present in peritoneal dialysate from patients (Lin et al., 1998; Yanez-Mo et al., 2003) Exposure of human mesothelial cells to TGF-β1 induced procollagen type 1 expression (Hung et al., 2003) and in rodent models, TGF-β1 administration caused peritoneal fibrosis (Margetts et al., 2005), and adhesion formation (Williams et al., 1992; Gorvy et al., 2005). Moreover, studies in a hyperglycemia-induced rodent model showed that AGEs upregulate TGF-β and induce submesothelial fibrosis with interstitial accumulation of collagen (De Vriese et al., 2003). Furthermore, intraperitoneal administration of a first generation adenovirus overexpressing TGF-β1 in mice resulted in submesothelial thickening and angiogenesis up to 10 days after administration (Margetts et al., 2005). However, a helper dependent adenovirus subsequently used with longer term expression of TGF-β1 led to encapsulation of the bowels in a thick cocoon in a similar manner to the final stages of EPS (Liu et al., 2009). Over-expression of TGF-β also increased levels of matrix metalloproteinase-2 (MMP-2) and high amounts of this protease found in PD effluent has been considered a potential marker of peritoneal injury and progression to EPS (Hirahara et al., 2007). In a mouse model, inhibition of MMP-2, TGF-β, and VEGF significantly improved peritoneal fibrosis and angiogenesis (Ro et al., 2007). Many other growth factors including HGF, PDGF, Connective Tissue Growth Factor (CTGF), and Fibroblast Growth Factor (FGF), shown to be involved in the development of fibrosis in other organs, may also influence the onset of EPS (Korte et al., 2011a).

THERAPEUTIC MANAGEMENT OF EPS

DISCONTINUATION OF PD

Cessation of PD should be done as soon as the diagnosis of EPS has been established. However, as cessation of PD is a known risk factor for the development and progression of EPS, this approach has been under much debate. Regular peritoneal lavage after discontinuation of PD has been tried in Japan with varying results. A

recent retrospective study performed by Yamamoto et al. (2010) has demonstrated that regular peritoneal lavage helps mesothelial cell layer recovery and prevention of EPS. However, given the risk of peritonitis with peritoneal lavage and the increased association of peritonitis and prolonged PD therapy with EPS progression, it is best to stop PD at the time of diagnosis of EPS along with removal of the PD catheter (Habib et al., 2011; Kawanishi, 2012).

NUTRITIONAL SUPPORT

As most patients with EPS suffer from malnutrition, appropriate nutritional support is imperative in the management of these patients. Studies from our centre have demonstrated poor pre-operative nutritional status and improved survival with peri-operative Total Parenteral Nutrition (TPN) in patients with advanced EPS who underwent surgery (peritonectomy and enterolysis) (De Freitas et al., 2007; Campbell et al., 2014). However, TPN therapy on its own does not have any curative effect as demonstrated by a study from Japan which showed no recovery in patients treated with TPN alone (Kawanishi and Moriishi, 2005). TPN therapy is therefore best used as an adjunct to more definite treatment in EPS patients with malnutrition or peri-operatively until gut function recovers.

MEDICAL TREATMENT

The evaluation of the efficacy of pharmacological treatments for EPS is difficult due to the lack of good evidence based data. However, the treatment options currently in vogue are as follows:

Immunosuppressive therapy

Corticosteroids are the drugs of choice in the management of EPS. They are particularly useful in the treatment of EPS in its early inflammatory stages (Kuriyama and Tomonari, 2001; Kawanishi, 2012). Steroids possibly act by suppressing inflammation, preventing fibrin deposition and collagen synthesis and maturation (Habib et al., 2011). Steroids also help in preventing the formation and reducing the accumulation of ascites (Mori et al., 1997; Jung and Cho, 2013). Various case reports and series have reported good prognosis and improved survival with the use of steroids compared to any other immunosuppressive agent (Junor and McMillan, 1993; Rajani, 2002). However, in a study from Japan, the rate of clinical improvement with isolated steroid treatment was only 38.5% (Kawanishi et al., 2004). Nevertheless, steroids are effective in treating the early stages of EPS but the clinical response tends to reduce in the later stages that are associated with increased fibrosis and bowel obstruction. A variety of other immunosuppressive medications like azathioprine, rapamycin, mycophenalate mofetil, sirolimus, and cyclosporine have also been used to treat EPS either alone or in combination with steroids (Rajani, 2002; Wong et al., 2005; Lafrance et al., 2008). However, apart from steroids, evidence regarding the efficacy of any other immunosuppressive therapy in EPS remains weak due to lack of robust randomized clinical trials (Bozkurt et al., 2009).

Tamoxifen

Tamoxifen is a Selective Estrogen Receptor Modulator (SERM) with antifibrotic properties and has been used in the treatment of various fibrotic disorders like retroperitoenal fibrosis, fibrosing mediastinitis, fibrosing cerivicitis, and desmoid tumors (Cornelis and Oreopoulos, 2011). Various case reports and small series have reported satisfactory outcomes following the use of Tamoxifen in the treatment of EPS (Guest, 2009; Cornelis and Oreopoulos, 2011). A recent large retrospective Dutch study has demonstrated significantly reduced mortality in EPS patients that were treated with Tamoxifen (45.8%) when compared to those that were not treated with Tamoxifen (74.4%) (Korte et al., 2011b). Tamoxifen appears to exert its effect through inhibition and modulation of TGF-β. *In vitro* and animal models showed that Tamoxifen treatment blocked EMT induced by TGF-β, preserved the fibrinolytic activity and reduced the migration capacity of mesothelial cells leading to reduced fibrosis and reduced PD effluent levels of VEGF leading to reduced angiogenesis in the peritoneum (Loureiro et al., 2013a). However, Tamoxifen has almost always been used in combination with corticosteroids, therefore the efficacy and safety of Tamoxifen alone in the treatment of EPS still remains to be evaluated. The potential side-effects of Tamoxifen (deep vein thrombosis, endometrial cancer, and calciphylaxis) also need to be considered (Del Peso et al., 2003). Further prospective trials are therefore necessary to establish the safety and efficacy of Tamoxifen in the treatment of EPS.

SURGERY

Surgical techniques in the management of EPS have evolved over the last decade. Surgery is routinely performed in patients with advanced EPS in Japan and in the UK at specialist referral centers by surgeons experienced in the management of EPS (Augustine et al., 2009; Kawanishi, 2012). Surgery is usually performed in the late stages of EPS, in patients that present with absolute bowel obstruction or as surgical emergencies with an acute abdomen. Currently favored surgical techniques are peritonectomy and careful enterolysis which involves resection of the peritoneum and fibrous tissue together with division of adhesions to release the bowel (**Figure 1**). Mortality post-surgery ranges from 19 to 34.5% (Summers et al., 2005; Kawanishi, 2012; Latus et al., 2013) and is mainly seen in patients with advanced EPS presenting as surgical emergencies (Augustine et al., 2009). Although surgery is the most successful form of treatment for patients with advanced disease, recurrence rates post-surgery tend to be high at around 25%. However, in Japan, the recent introduction of Noble plication (suturing of the intestines to each other to prevent obstruction) along with routine enterolysis has reduced the recurrence rate to 12.3% (Kawanishi, 2012). Tamoxifen and steroids may also be continued post-operatively as they may have a role in preventing recurrence of EPS (Lo and Kawanishi, 2009).

PREVENTION

Although various studies have demonstrated possible mechanisms in the development of EPS, we still have no strategy to prevent the occurrence of this condition. As the risk of developing EPS increases with the duration of PD, there has been much debate on an "expiry date" for PD in patients. Studies from Japan have suggested 8 years to be a safe period to continue PD beyond which patients should be switched to hemodialysis (Kawanishi et al., 2004). However, setting an expiry date is

not recommended as it could have a negative impact on the quality of life and could increase the risk of complications of tunneled lines used for hemodialysis in patients who were symptom free on PD (Garosi et al., 2005). A more rational approach would be to assess peritoneal membrane function. The commonly used method to assess peritoneal deterioration is the Peritoneal Equilibration Test (PET) with a high transport of solutes across the peritoneal membrane being indicative of failing function. There has been a suggestion of cessation of PD in all patients that show a high transport status (Kawanishi, 2012). However, not all patients that are high transporters develop EPS. Therefore, this approach has been under much debate. Peritoneal lavage could potentially be used in patients who have been on long-term PD (>8 years), with high transport status and increased levels of markers of inflammation (IL-6) and low levels of Ca-125 in their PD effluent in order to delay the development of EPS (Moriishi et al., 2002). However, this approach is not universally practiced due to the associated risk of infective peritonitis. Other proposed methods of possible prevention are by using more bio-compatible PD fluid and taking care to reduce the incidence of infective peritonitis. Addition of therapeutic agents such as, Tamoxifen and Angiotensin Converting Enzyme (ACE) inhibitors, may show promise to ameliorate peritoneal membrane function and fibrosis (Kolesnyk et al., 2007). Further studies are therefore necessary to investigate possible therapeutic strategies to prevent the exacerbated fibrotic process which culminates in EPS.

CONCLUSION

Despite the increase in incidence and awareness over the last decade, EPS still remains a rare but much feared complication of long-term PD. Prolonged PD therapy is the most important risk factor in the development of EPS. Uremia, inflammation, EMT and loss of mesothelial fibrinolytic response are possible mechanisms of peritoneal fibrosis which could influence the development of EPS. However, the aetiopathogenesis still remains poorly understood. Currently a high index of suspicion in at risk groups is required to make the diagnosis of EPS. CT scan is the investigation of choice to aid the diagnosis, but the use of newer imaging modalities like cine-MRI, that shows promising signs, still needs to be validated. Low levels of Ca-125 and high levels of IL-6 in PD effluent have been suggested as early markers of development of EPS. However, further research needs to be done to validate this claim and look for other potential bio-markers to detect EPS early. The treatment of EPS in its early stages is largely medical with corticosteroids, tamoxifen and nutritional support. However, surgery (peritonectomy and enterolysis) is the treatment of choice for advanced cases presenting with overt bowel obstruction. Peri-operative nutritional support with TPN and post-operative steroids with or without Tamoxifen is recommended to prevent recurrence. Improvement in surgical technique has vastly improved survival of patients with EPS. However, despite successful surgery these patients remain at increased risk of mortality due to ongoing renal replacement therapy. Many clinicians are reticent toward transplantation in these patients due to a perception that transplantation might not be feasible given the complex surgical history. Although, the risk of developing recurrent disease post transplantation exists, the chances of survival are much improved with a functioning kidney transplant. These patients should therefore be assessed and worked up for renal transplantation in order to improve long-term survival.

REFERENCES

Aguilera, A., Yáñez-Mo, M., Selgas, R., Sánchez-Madrid, F., and López-Cabrera, M. (2005). Epithelial to mesenchymal transition as a triggering factor of peritoneal membrane fibrosis and angiogenesis in peritoneal dialysis patients. *Curr. Opin. Investig. Drugs* 6, 262–268.

Alscher, D. M., Braun, N., Biegger, D., and Fritz, P. (2007). Peritoneal mast cells in peritoneal dialysis patients, particularly in encapsulating peritoneal sclerosis patients. *Am. J. Kidney Dis.* 49, 452–461. doi: 10.1053/j.ajkd.2006.11.040

Aroeira, L. S., Aguilera, A., Sánchez-Tomero, J. A., Bajo, M. A., del Peso, G., Jiménez-Heffernan, J. A., et al. (2007). Epithelial to mesenchymal transition and peritoneal membrane failure in peritoneal dialysis patients: pathologic significance and potential therapeutic interventions. *J. Am. Soc. Nephrol.* 18, 2004–2011. doi: 10.1681/ASN.2006111292

Augustine, T., Brown, P. W., Davies, S. D., Summers, A. M., and Wilkie, M. E. (2009). Encapsulating peritoneal sclerosis: clinical significance and implications. *Nephron. Clin. Pract.* 111, 149–154. doi: 10.1159/000191214

Balasubramaniam, G., Brown, E. A., Davenport, A., Cairns, H., Cooper, B., Fan, S. L., et al. (2009). The Pan-Thames EPS study: treatment and outcomes of encapsulating peritoneal sclerosis. *Nephrol. Dial. Transplant.* 24, 3209–3215. doi: 10.1093/ndt/gfp008

Baroni, G., Schuinski, A., de Moraes, T. P., Meyer, F., and Pecoits-Filho, R. (2012). Inflammation and the peritoneal membrane: causes and impact on structure and function during peritoneal dialysis. *Mediators Inflamm.* 2012:912595. doi: 10.1155/2012/912595

Boulanger, E. (2008). Peritoneal and systemic inflammation: the benefits of using biocompatible peritoneal dialysis fluids. *Perit. Dial. Int.* 28, 28–31.

Bozkurt, D., Sipahi, S., Cetin, P., Hur, E., Ozdemir, O., Ertilav, M., et al. (2009). Does immunosuppressive treatment ameliorate morphology changes in encapsulating peritoneal sclerosis? *Perit. Dial. Int.* 29(Suppl. 2), S206–S210.

Braun, N., Fritz, P., Ulmer, C., Latus, J., Kimmel, M., Biegger, D., et al. (2012). Histological criteria for encapsulating peritoneal sclerosis—a standardized approach. *PLoS ONE* 7:e48647. doi: 10.1371/journal.pone.0048647

Braun, N., Reimold, F., Biegger, D., Fritz, P., Kimmel, M., Ulmer, C., et al. (2009). Fibrogenic growth factors in encapsulating peritoneal sclerosis. *Nephron. Clin. Pract.* 113, c88–c95. doi: 10.1159/000228540

Brown, M. C., Simpson, K., Kerssens, J. J., and Mactier, R. (2009). Encapsulating peritoneal sclerosis in the new millennium: a national cohort study. *Clin. J. Am. Soc. Nephrol.* 4, 1222–1229. doi: 10.2215/CJN.01260209

Campbell, R. F., Augustine, T., Hurst, H., Pararajasingam, R., Van Dellen, D., Armstrong, S., et al. (2014). Anthropometrics identify wasting in patients undergoing surgery for encapsulating peritoneal sclerosis. *Perit. Dial. Int.* doi: 10.3747/pdi.2013.00098. [Epub ahead of print].

Chew, C. G., Clarkson, A. R., and Faull, R. J. (1997). Relapsing CAPD peritonitis with rapid peritoneal sclerosis due to *Haemophilus influenzae*. *Nephrol. Dial. Transplant.* 12, 821–822. doi: 10.1093/ndt/12.4.821

Cornelis, T., and Oreopoulos, D. G. (2011). Update on potential medical treatments for encapsulating peritoneal sclerosis; human and experimental data. *Int. Urol. Nephrol.* 43, 147–156. doi: 10.1007/s11255-010-9744-5

De Freitas, D., Jordaan, A., Williams, R., Alderdice, J., Curwell, J., Hurst, H., et al. (2007). Nutritional management of patients undergoing surgery following diagnosis with encapsulating peritoneal sclerosis. *Perit. Dial. Int.* 28, 271–276.

Del Peso, G., Bajo, M. A., Gil, F., Aguilera, A., Ros, S., Costero, O., et al. (2003). Clinical experience with tamoxifen in peritoneal fibrosing syndromes. *Adv. Perit. Dial.* 19, 32–35.

De Vriese, A. S., Flyvbjerg, A., Mortier, S., Tilton, R. G., and Lameire, N. H. (2003). Inhibition of the interaction of AGE-RAGE prevents hyperglycemia-induced fibrosis of the peritoneal membrane. *J. Am. Soc. Nephrol.* 14, 2109–2118.

De Vriese, A. S., Tilton, R. G., Mortier, S., and Lameire, N. H. (2006). Myofibroblast transdifferentiation of mesothelial cells is mediated by RAGE and contributes to peritoneal fibrosis in uraemia. *Nephrol. Dial. Transplant.* 21, 2549–2555. doi: 10.1093/ndt/gfl271

Fieren, M. W. J. A., Betjes, M. G. H., Korte, M. R., and Boer, W. H. (2007). Posttransplant encapsulating peritoneal sclerosis: a worrying new trend? *Perit. Dial. Int*. 27, 619–624.

Flanigan, M., Anderson, D., and Freeman, R. M. (1984). Peritoneal dialysis complicated by fungal peritonitis and peritoneal fibrosis. *Am. J. Med*. 76, A113, A125.

Flessner, M. F., Credit, K., Henderson, K., Vanpelt, H. M., Potter, R., He, Z., et al. (2007). Peritoneal changes after exposure to sterile solutions by catheter. *J. Am. Soc. Nephrol*. 18, 2294–2302. doi: 10.1681/ASN.2006121417

Gandhi, V. C., Humayun, H. M., Ing, T. S., Daugirdas, J. T., Jablokow, V. R., Iwatsuki, S., et al. (1980). Sclerotic thickening of the peritoneal membrane in maintenance peritoneal dialysis patients. *Arch. Intern. Med*. 140, 1201–1203. doi: 10.1001/archinte.1980.00330200077024

Garosi, G., Di Paolo, N., Sacchi, G., and Gaggiotti, E. (2005). Sclerosing peritonitis: a nosological entity. *Perit. Dial. Int*. 25(Suppl. 3), S110–S112.

Goodlad, C., Tarzi, R., Gedroyc, W., Lim, A., Moser, S., and Brown, E. A. (2011). Screening for encapsulating peritoneal sclerosis in patients on peritoneal dialysis: role of CT scanning. *Nephrol. Dial. Transplant*. 26, 1374–1137. doi: 10.1093/ndt/gfq533

Gorvy, D. A., Herrick, S. E., Shah, M., and Ferguson, M. W. (2005). Experimental manipulation of transforming growth factor-beta isoforms significantly affects adhesion formation in a murine surgical model. *Am. J. Pathol*. 167, 1005–1019. doi: 10.1016/S0002-9440(10)61190-X

Guest, S. (2009). Tamoxifen therapy for encapsulating peritoneal sclerosis: mechanisms of action and update of clinical experiences. *Perit. Dial. Int*. 29, 252–255.

Habib, S. M., Betjes, M. G. H., Fieren, M. W. J. A., Boeschoten, E. W., Abrahams, A. C., Boer, W. H., et al. (2011). Management of encapsulating peritoneal sclerosis: a guideline on optimal and uniform treatment. *Neth. J. Med*. 69, 500–507.

Hirahara, I., Inoue, M., Okuda, K., Ando, Y., Muto, S., and Kusano, E. (2007). The potential of matrix metalloproteinase-2 as a marker of peritoneal injury, increased solute transport, or progression to encapsulating peritoneal sclerosis during peritoneal dialysis–a multicentre study in Japan. *Nephrol. Dial. Transplant.* 22, 560–567. doi: 10.1093/ndt/gfl566

Hoff, C. M. (2005). Experimental animal models of encapsulating peritoneal sclerosis. *Perit. Dial. Int. J. Int. Soc. Perit. Dial*. 25(Suppl. 4), S57–S66.

Holmdahl, L. (1997). The role of fibrinolysis in adhesion formation. *Eur. J. Surg. Suppl*. 163, 24–31.

Holmdahl, L., Kotseos, K., Bergstrom, M., Falk, P., Ivarsson, M. L., and Chegini, N. (2001). Overproduction of transforming growth factor-beta1 (TGF-beta1) is associated with adhesion formation and peritoneal fibrinolytic impairment. *Surgery* 129, 626–632. doi: 10.1067/msy.2001.113039

Honda, K., Nitta, K., Horita, S., Tsukada, M., Ifashi, M., Nihei, H., et al. (2003). Histologic criteria for diagnosing encapsulating peritoneal sclerosis in continuous ambulatory peritoneal dialysis patients. *Adv. Perit. Dial. Conf. Perit. Dial*. 19, 169–175.

Honda, K., Nitta, K., Horita, S., Yumura, W., and Nihei, H. (1996). Morphological changes in the peritoneal vasculature of patients on CAPD with ultrafiltration failure. *Nephron* 72, 171–176. doi: 10.1159/000188837

Honda, K., and Oda, H. (2005). Pathology of encapsulating peritoneal sclerosis. *Perit. Dial. Int*. 25(Suppl. 4), S19–S29.

Io, H., Hamada, C., Ro, Y., Ito, Y., Hirahara, I., and Tomino, Y. (2004). Morphologic changes of peritoneum and expression of VEGF in encapsulated peritoneal sclerosis rat models. *Kidney Int*. 65, 1927–1936. doi: 10.1111/j.1523-1755.2004.00599.x

Jimenez-Heffernan, J. A., Aguilera, A., Lara-Pezzi, E., Bajo, M. A., del Peso, G., Ramirez, M., et al. (2004). Immunohistochemical characterization of fibroblast subpopulations in normal peritoneal tissue and in peritoneal dialysis-induced fibrosis.*Virchows Arch*. 444, 247–256. doi: 10.1007/s00428-003-0963-3

Jorres, A., Topley, N., and Gahl, G. M. (1992). Biocompatibility of peritoneal dialysis fluids. *Int. J. Artif. Organs* 15, 79–83.

Jung, J. Y., and Cho, J. T. (2013). A case of fulminant sclerosing peritonitis presented like acute culture-negative peritonitis and successfully treated with corticosteroid therapy. *J. Korean Med. Sci*. 28, 620–623. doi: 10.3346/jkms.2013.28.4.620

Junor, B. J., and McMillan, M. A. (1993). Immunosuppression in sclerosing peritonitis. *Adv. Perit. Dial*. 9, 187–189.

Kalluri, R., and Weinberg, R. A. (2009). The basics of epithelial-mesenchymal transition. *J. Clin. Invest*. 119, 1420–1428. doi: 10.1172/JCI39104

Kawaguchi, Y., Kawanishi, H., Mujais, S., Topley, N., and Oreopoulos, D. G. (2000). Encapsulating peritoneal sclerosis: definition, etiology, diagnosis, and treatment. International Society for Peritoneal Dialysis Ad Hoc Committee on Ultrafiltration Management in Peritoneal Dialysis. *Perit. Dial. Int*. 20 (Suppl. 4), S43–S55.

Kawaguchi, Y., Saito, A., Kawanishi, H., Nakayama, M., Miyazaki, M., Nakamoto, H., et al. (2005).Recommendations on the management of encapsulating peritoneal sclerosis in Japan, 2005: diagnosis, predictive markers, treatment, and preventive measures. *Perit. Dial. Int*. 25(Suppl. 4), S83–S95.

Kawanishi, H. (2012). Surgical and medical treatments of encapsulation peritoneal sclerosis. *Contrib. Nephrol.* 177, 38–47. doi: 10.1159/000336934

Kawanishi, H., Kawaguchi, Y., Fukui, H., Hara, S., Imada, A., Kubo, H., et al. (2004). Encapsulating peritoneal sclerosis in Japan: a prospective, controlled, multicenter study. *Am. J. Kidney Dis*. 44, 729–737. doi: 10.1053/j.ajkd.2004.06.020

Kawanishi, H., and Moriishi, M. (2005). Epidemiology of encapsulating peritoneal sclerosis in Japan. *Perit. Dial. Int*. 25(Suppl. 4), S14–S18.

Khanna, A., Plummer, M., Bromberek, C., Bresnahan, B., and Hariharan, S. (2002). Expression of TGF-beta and fibrogenic genes in transplant recipients with tacrolimus and cyclosporine nephrotoxicity. *Kidney Int*. 62, 2257–2263. doi: 10.1046/j.1523-1755.2002.00668.x

Kolesnyk, I., Dekker, F. W., Noordzij, M., Ie Cessie, S., Struijk, D. G., and Krediet, R. (2007). Impact of ACE inhibitors and AII receptor blockers on peritoneal membrane transport characteristics in long-term peritoneal dialysis patients. *Perit. Dial. Int*. 27, 446–453.

Korte, M. R., Fieren, M. W., Sampimon, D. E., Lingsma, H. F., Weimar, W., and Betjes, M. G. H. (2011b). Tamoxifen is associated with lower mortality of encapsulating peritoneal sclerosis: results of the Dutch Multicentre EPS Study. *Nephrol. Dial. Transplant.* 26, 691–697. doi: 10.1093/ndt/gfq362

Korte, M. R., Sampimon, D. E., Betjes, M. G. H., and Krediet, R. T. (2011a). Encapsulating peritoneal sclerosis: the state of affairs. *Nat. Rev. Nephrol*. 7, 528–538. doi: 10.1038/nrneph.2011.93

Kuriyama, S., and Tomonari, H. (2001). Corticosteroid therapy in encapsulating peritoneal sclerosis. *Nephrol. Dial. Transplant* 16, 1304–1305. doi: 10.1093/ndt/16.6.1304

Hung, K. Y., Huang, J. W., Chen, C. T., Lee, P. H., and Tsai, T. J. (2003). Pentoxifylline modulates intracellular signalling of TGF-β in cultured human peritoneal mesothelial cells: implications for prevention of encapsulating peritoneal sclerosis. *Nephrol. Dial. Transplant*. 18, 670–676. doi: 10.1093/ndt/gfg141

Lafrance, J.-P., Letourneau, I., Ouimet, D., Bonnardeaux, A., Leblanc, M., Mathieu, N., et al. (2008). Successful treatment of encapsulating peritoneal sclerosis with immunosuppressive therapy. *Am. J. Kidney Dis*. 51, e7–e10. doi: 10.1053/j.ajkd.2007.07.036

Latus, J., Ulmer, C., Fritz, P., Rettenmaier, B., Biegger, D., Lang, T., et al. (2013). Encapsulating peritoneal sclerosis: a rare, serious but potentially curable complication of peritoneal dialysis-experience of a referral centre in Germany. *Nephrol. Dial. Transplant*. 28, 1021–1030. doi: 10.1093/ndt/gfs159

Lin, C. Y., Chen, W. P., Yang, L. Y., Chen, A., and Huang, T. P. (1998). Persistent transforming growth factor-beta 1 expression may predict peritoneal fibrosis in CAPD patients with frequent peritonitis occurrence. *Am. J. Nephrol.* 6, 513–519. doi: 10.1159/000013397

Liu, L., Shi, C.-X., Ghayur, A., Zhang, C., Su, J. Y., Hoff, C. M., et al. (2009). Prolonged peritoneal gene expression using a helper-dependent adenovirus. *Perit. Dial. Int*. 29, 508–516.

Lo, W. K., and Kawanishi, H. (2009). Encapsulating peritoneal sclerosis–medical and surgical treatment. *Perit. Dial. Int*. 29(Suppl. 2), S211–S214.

Loureiro, J., Aguilera, A., Selgas, R., Sandoval, P., Albar-Vizcaíno, P., Pérez-Lozano, M. L., et al. (2011). Blocking TGF-β1 protects the peritoneal membrane from dialysate-induced damage. *J. Am. Soc. Nephrol*. 22, 1682–1695. doi: 10.1681/ASN.2010111197

Loureiro, J., Gónzalez-Mateo, G., Jimenez-Heffernan, J., Selgas, R., López-Cabrera, M., and Aguilera Peralta, A. (2013b). Are the mesothelial-to-mesenchymal transition, sclerotic peritonitis syndromes, and encapsulating peritoneal sclerosis part of the same process? *Int. J. Nephrol.* 2013:263285. doi: 10.1155/2013/263285

Loureiro, J., Sandoval, P., del Peso, G., Gónzalez-Mateo, G., Fernández-Millara, V., Santamaria, B., et al. (2013a). Tamoxifen ameliorates peritoneal membrane damage by blocking mesothelial to mesenchymal transition in peritoneal dialysis. *PLoS ONE* 23:e61165. doi: 10.1371/journal.pone.0061165

Mandl-Weber, S., Cohen, C. D., Haslinger, B., Kretzler, M., and Sitter, T. (2002). Vascular endothelial growth factor production and regulation in human peritoneal mesothelial cells. *Kidney Int.* 61, 570–578. doi: 10.1046/j.1523-1755.2002.00143.x

Margetts, P. J., and Bonniaud, P. (2003). Basic mechanisms and clinical implications of peritoneal fibrosis. *Perit. Dial. Int.* 23, 530–541.

Margetts, P. J., Bonniaud, P., Liu, L., Hoff, C. M., Holmes, C. J., West-Mays, J. A., et al. (2005). Transient overexpression of TGF-{beta}1 induces epithelial mesenchymal transition in the rodent peritoneum. *J. Am. Soc. Nephrol.* 16, 425–436. doi: 10.1681/ASN.2004060436

Maruyama, Y., and Nakayama, M. (2008). Encapsulating peritoneal sclerosis in Japan. *Perit. Dial. Int.* 28(Suppl. 3), S201–S204.

Masunaga, Y., Muto, S., Asakura, S., Akimoto, T., Homma, S., Kusano, E., et al. (2003).Ascites from patients with encapsulating peritoneal sclerosis augments NIH/3T3 fibroblast proliferation. *Ther. Apher. Dial.* 7, 486–493. doi: 10.1046/j.1526-0968.2003.00087.x

Mateijsen, M. A., van der Wal, A. C., Hendricks, P. M. E. M., Zweers, M. M., Mulder, J., Struijk, D. G., et al. (1999). Vascular and interstitial changes in the peritoneum of CAPD patients with peritoneal sclerosis. *Perit. Dial. Int.* 19, 517–525.

Mori, Y., Matsuo, S., Sutoh, H., Toriyama, T., Kawahara, H., and Hotta, N. (1997). A case of a dialysis patient with sclerosing peritonitis successfully treated with corticosteroid therapy alone. *Am. J. Kidney Dis.* 30, 275–278. doi: 10.1016/S0272-6386(97)90064-0

Moriishi, M., Kawanishi, H., Kawai, T., Takahashi, S., Hirai, T., Shishida, M., et al. (2002). Preservation of peritoneal catheter for prevention of encapsulating peritoneal sclerosis. *Adv. Perit. Dial.* 18, 149–153.

Mortier, S., De Vriese, A.,S., Van de Voorde, J., Schaub, T. P., Passlick-Deetjen J., and Lameire, N. H. (2002). Hemodynamic effects of peritoneal dialysis solutions on the rat peritoneal membrane: role of acidity, buffer choice, glucose concentration, and glucose degradation products. *J. Am. Soc. Nephrol.* 13, 480–489.

Nakamoto, H. (2005). Encapsulating peritoneal sclerosis—a clinician's approach to diagnosis and medical treatment. *Perit. Dial. Int. Suppl* 4, S30–S38.

Nakayama, M., Kawaguchi, Y., Yamada, K., Hasegawa, T., Takazoe, K., Katoh, N., et al. (1997). Immunohistochemical detection of advanced glycosylation end-products in the peritoneum and its possible pathophysiological role in CAPD. *Kidney Int.* 51, 182–186. doi: 10.1038/ki.1997.22

Park, S.-H., Kim, Y.-L., and Lindholm, B. (2008). Experimental encapsulating peritoneal sclerosis models: pathogenesis and treatment. *Perit. Dial. Int.* 28(Suppl. 5), S21–S28.

Pletinck, A., Vanholder, R., Veys, N., and Van Biesen, W. (2012). Protecting the peritoneal membrane: factors beyond peritoneal dialysis solutions. *Nat. Rev. Nephrol.* 8, 542–550. doi: 10.1038/nrneph.2012.144

Plum, J., Hermann, S., Fussholler, A., Schoenicke, G., Donner, A., Rohrborn, A., et al. (2001). Peritoneal sclerosis in peritoneal dialysis patients related to dialysis settings and peritoneal transport properties. *Kidney Int. Suppl.* 78, S42–S47. doi: 10.1046/j.1523-1755.2001.07801.x

Pollock, C. A. (2001). Diagnosis and management of encapsulating peritoneal sclerosis. *Perit. Dial. Int.* 21(Suppl. 3), S61–S66.

Rajani, R. (2002). Differential Effect of sirolimus vs prednisolone in the treatment of sclerosing encapsulating peritonitis. *Nephrol. Dial. Transplant.* 17, 2278–2280. doi: 10.1093/ndt/17.12.2278

Rigby, R. J., and Hawley, C. M. (1998). Sclerosing peritonitis: the experience in Australia. *Nephrol. Dial. Transplant.* 13, 154–159. doi: 10.1093/ndt/13.1.154

Ro, Y., Hamada, C., Inaba, M., Io, H., Kaneko, K., and Tomino, Y. (2007). Inhibitory effects of matrix metalloproteinase inhibitor ONO-4817 on morphological alterations in chlorhexidine gluconate-induced peritoneal sclerosis rats. *Nephrol. Dial. Transplant.* 22, 2838–2848. doi: 10.1093/ndt/gfm323

Rougier, J. P., Guia, S., Hagège, J., Nguyen, G., and Ronco, P. M., (1998). PAI-1 secretion and matrix deposition in human peritoneal mesothelial cell cultures: transcriptional regulation by TGF-beta 1. *Kidney Int.* 54, 87–98. doi: 10.1046/j.1523-1755.1998.00955.x

Sampimon, D. E., Korte, M. R., Barreto, D. L., Vlijm, A., de Waart, R., Struijk, D. G., et al. (2010). Early diagnostic markers for encapsulating peritoneal sclerosis: a case-control study. *Perit. Dial. Int.* 30, 163–169. doi: 10.3747/pdi.2009.00022

Selgas, R., Bajo, A., Jiménez-Heffernan, J. A., Sánchez-Tomero, J. A., Del Peso, G., Aguilera, A., et al. (2006). Epithelial-to-mesenchymal transition of the mesothelial cell–its role in the response of the peritoneum to dialysis. *Nephrol. Dial. Transplant.* 21(Suppl. 2), ii2–ii7. doi: 10.1093/ndt/gfl183

Sherif, A. M., Yoshida, H., Maruyama, Y., Yamamoto, H., Yokoyama, K., Hosoya, T., et al. (2008). Comparison between the pathology of encapsulating sclerosis and simple sclerosis of the peritoneal membrane in chronic peritoneal dialysis. *Ther. Apher. Dial.* 12, 33–41. doi: 10.1111/j.1744-9987.2007.00538.x

Sulaiman, H., Dawson, L., Laurent, G. J., Bellingan, G. J., and Herrick, S. E. (2002). Role of plasminogen activators in peritoneal adhesion formation. *Biochem. Soc. Trans.* 30, 126–131. doi: 10.1042/BST0300126

Summers, A., Clancy, M. J., Syed, F., Harwood, N., Augustine, T., Riad, H., et al. (2005). Single-center experience of encapsulating peritoneal sclerosis in patients on peritoneal dialysis for end-stage renal failure. *Kidney Int.* 68, 2381–2388. doi: 10.1111/j.1523-1755.2005.00701.x

Summers, A. M., Hoff, C. M., and Topley, N. (2008). How can genetic advances impact on experimental models of encapsulating peritoneal sclerosis? *Perit. Dial. Int.* 28(Suppl. 5), S16–S20.

Thiery, J. P., Acloque, H., Huang, R. Y., and Nieto, M. A. (2009). Epithelial-mesenchymal transitions in development and disease. *Cell* 139, 871–890. doi: 10.1016/j.cell.2009.11.007

Tomura, S., Nakamura, Y., Doi, M., Ando, R., Ida, T., Chida, Y., et al. (1996). Fibrinogen, coagulation factor VII, tissue plasminogen activator, plasminogen activator inhibitor-1, and lipid as cardiovascular risk factors in chronic hemodialysis and continuous ambulatory peritoneal dialysis patients. *Am. J. Kidney Dis.* 27, 848–854. doi: 10.1016/S0272-6386(96)90523-5

Van Westrhenen, R., Aten, J., Hajji, N., de Boer, O. J., Kunne, C., de Waart, D. K., et al. (2007). Cyclosporin A induces peritoneal fibrosis and angiogenesis during chronic peritoneal exposure to a glucose-based, lactate-buffered dialysis solution in the rat. *Blood Purif.* 25, 466–472. doi: 10.1159/000112475

Vlijm, A., Stoker, J., Bipat, S., Spijkerbower, A. M., Phoa, S. S. K. S., Maes, R., et al. (2009). Computed tomographic findings characteristic for encapsulating peritoneal sclerosis: a case-control study. *Perit. Dial. Int.* 29, 517–522.

Wieslander, A. P. (1996). Cytotoxicity of peritoneal dialysis fluid—is it related to glucose breakdown products? *Nephrol. Dial. Transplant.* 11, 958–959. doi: 10.1093/oxfordjournals.ndt.a027512

Williams, J. D., Craig, K. J., von Ruhland, C., Topley, N., and Williams, G. T. (2003). The natural course of peritoneal membrane biology during peritoneal dialysis. *Kidney Int. Suppl.* 88, S43–S49. doi: 10.1046/j.1523-1755.2003.08805.x

Williams, J. D., Craig, K., Topley, N., Von Ruhland, C., Fallon, M., Newman, G. R., et al. (2002). Morphologic changes in the peritoneal membrane of patients with renal disease. *J. Am. Soc. Nephrol.* 13, 470–479.

Williams, R. S., Rossi, A. M., Chegini, N., and Schultz, G. (1992). Effect of transforming growth factor beta on postoperative adhesion formation and intact peritoneum. *J. Surg. Res.* 52, 65–70. doi: 10.1016/0022-4804(92)90280-D

Wong, C. F., Beshir, S., Khalil, A., Pai, P., and Ahmad, R. (2005). Successful treatment of encapsulating peritoneal sclerosis with azathioprine and prednisolone. *Perit. Dial. Int.* 25, 285–287.

Wright, B., Summers, A., Fenner, J., Gillott, R., Hutchinson, C. E., Spencer, P. A., et al. (2011). Initial observations using a novel "cine" magnetic resonance imaging technique to detect changes in abdominal motion caused by encapsulating peritoneal sclerosis. *Perit. Dial. Int.* 31, 287–290. doi: 10.3747/pdi.2010.00078

Yamada, K., Miyahara, Y., Hamaguchi, K., Nakayama, M., Nakano, H., Nozaki, O., et al. (1994). Immunohistochemical study of human advanced glycosylation end-products (AGE) in chronic renal failure. *Clin. Nephrol.* 42, 354–361.

Yamamoto, R., Otsuka, Y., Nakayama, M., Maruyama, Y., Katoh, N., Ikeda, M., et al. (2005). Risk factors for encapsulating peritoneal sclerosis in patients who have experienced peritoneal dialysis treatment. *Clin. Exp. Nephrol.* 9, 148–152. doi: 10.1007/s10157-005-0349-8

Yamamoto, T., Nagasue, K., Okuno, S., and Yamakawa, T. (2010). The role of peritoneal lavage and the prognostic significance of mesothelial cell area in preventing encapsulating peritoneal sclerosis. *Perit. Dial. Int.* 30, 343–52. doi: 10.3747/pdi.2008.00273

Yanez-Mo, M., Lara-Pezzi, E., Selgas, R., Ramírez-Huesca, M., Dominguez-Jimenez, C., Jimenez-Heffernan, J. A., et al. (2003). Peritoneal dialysis and epithelial-to- mesenchymal transition of mesothelial cells. *N. Engl. J. Med.* 348, 403–413. doi: 10.1056/NEJMoa020809

Yang, A. H., Chen, J. Y., and Lin, J. K. (2003). Myofibroblastic conversion of mesothelial cells. *Kidney Int*. 63, 1530–1539. doi: 10.1046/j.1523-1755.2003.00861.x

Yu, M. A., Shin, K. S., Kim, J. H., Kim, Y. I., Chung, S. S., Park, S. H., et al. (2009). HGF and BMP-7 ameliorate high glucose-induced epithelial-to-mesenchymal transition of peritoneal mesothelium. *J. Am. Soc. Nephrol*. 20, 567–581. doi: 10.1681/ASN.2008040424

Zhang, L., Liu, F., Peng, Y., Sun, L., and Chen, G. (2013). Changes in expression of four molecular marker proteins and one microRNA in mesothelial cells of the peritoneal dialysate effluent fluid of peritoneal dialysis patients. *Exp. Ther. Med*. 6, 1189–1193. doi: 10.3892/etm.2013.1281

Zhou, Q., Yang, M., Lan, H., and Yu, X. (2013). miR-30a negatively regulates TGF-β1-induced epithelial-mesenchymal transition and peritoneal fibrosis by targeting Snai1. *Am. J. Pathol*. 183, 808–819. doi: 10.1016/j.ajpath.2013.05.019

Zweers, M. M., Struijk, D. G., Smit, W., and Krediet, R. T. (2001). Vascular endothelial growth factor in peritoneal dialysis: a longitudinal follow-up. *J. Lab. Clin. Med*. 137, 125–132. doi: 10.1067/mlc.2001.112235

Conflict of Interest Statement: The authors declare that the research was conducted in the absence of any commercial or financial relationships that could be construed as a potential conflict of interest.

Received: 15 September 2014; accepted: 16 November 2014; published online: 05 January 2015.

*Citation: Moinuddin Z, Summers A, Van Dellen D, Augustine T and Herrick SE (2015) Encapsulating peritoneal sclerosis—a rare but devastating peritoneal disease. Front. Physiol. **5**:470. doi: 10.3389/fphys.2014.00470*

This article was submitted to Membrane Physiology and Membrane Biophysics, a section of the journal Frontiers in Physiology.

frontiers in PHYSIOLOGY

ORIGINAL RESEARCH ARTICLE
published: 31 October 2014
doi: 10.3389/fphys.2014.00400

Intercellular communication in malignant pleural mesothelioma: properties of tunneling nanotubes

Justin W. Ady[1], Snider Desir[2,3], Venugopal Thayanithy[2], Rachel I. Vogel[4], André L. Moreira[5], Robert J. Downey[1], Yuman Fong[1,†], Katia Manova-Todorova[6], Malcolm A. S. Moore[7] and Emil Lou[2]*

[1] Department of Surgery, Memorial Sloan-Kettering Cancer Center, New York, NY, USA
[2] Division of Hematology, Oncology and Transplantation, University of Minnesota, Minneapolis, MN, USA
[3] Integrative Biology and Physiology Program, University of Minnesota, Minneapolis, Minnesota, USA
[4] Department of Biostatistics and Bioinformatics, Masonic Cancer Center, University of Minnesota, Minneapolis, MN, USA
[5] Department of Pathology, Memorial Sloan-Kettering Cancer Center, New York, NY, USA
[6] Molecular Cytology, Memorial Sloan-Kettering Cancer Center, New York, NY, USA
[7] Department of Cell Biology, Sloan-Kettering Institute, Memorial Sloan-Kettering Cancer Center, New York, NY, USA

Edited by:
Sotirios G. Zarogiannis, University of Thessaly, Greece

Reviewed by:
Chiara Zurzolo, Pasteur Institute, France
Xiang Wang, University of Bergen, Norway

****Correspondence:***
Emil Lou, Division of Hematology, Oncology and Transplantation, University of Minnesota, Mayo Mail Code 480, 420 Delaware Street SE, Minneapolis, MN 55455, USA
e-mail: emil-lou@umn.edu

†Present address:
Yuman Fong, Department of Surgery, City of Hope, Duarte, CA, USA

Malignant pleural mesothelioma is a particularly aggressive and locally invasive malignancy with a poor prognosis despite advances in understanding of cancer cell biology and development of new therapies. At the cellular level, cultured mesothelioma cells present a mesenchymal appearance and a strong capacity for local cellular invasion. One important but underexplored area of mesothelioma cell biology is intercellular communication. Our group has previously characterized in multiple histological subtypes of mesothelioma a unique cellular protrusion known as tunneling nanotubes (TnTs). TnTs are long, actin filament-based, narrow cytoplasmic extensions that are non-adherent when cultured *in vitro* and are capable of shuttling cellular cargo between connected cells. Our prior work confirmed the presence of nanotube structures in tumors resected from patients with human mesothelioma. In our current study, we quantified the number of TnTs/cell among various mesothelioma subtypes and normal mesothelial cells using confocal microscopic techniques. We also examined changes in TnT length over time in comparison to cell proliferation. We further examined potential approaches to the *in vivo* study of TnTs in animal models of cancer. We have developed novel approaches to study TnTs in aggressive solid tumor malignancies and define fundamental characteristics of TnTs in malignant mesothelioma. There is mounting evidence that TnTs play an important role in intercellular communication in mesothelioma and thus merit further investigation of their role *in vivo*.

Keywords: tunneling nanotubes, malignant pleural mesothelioma, intercellular transfer, intercellular communication

INTRODUCTION

Malignant pleural mesothelioma (MPM) is a clinically devastating and locally invasive malignancy. Patients with this disease uniformly carry a poor prognosis despite advances in understanding of cancer cell biology and development of new therapies. Unlike other solid tumor malignancies, mesothelioma is highly refractory to all forms of current treatment including surgery, radiation, and chemotherapy. Treatment of mesothelioma and other invasive solid tumor malignancies such as cancers of the colon, pancreas, and ovaries is limited by an inadequate understanding of the modes and functions of intercellular communication in the tumor microenvironment (Axelrod et al., 2006; Ruckert et al., 2012). Intercellular communication is critical to tumor formation, organization, and treatment resistance (Kenny et al., 2007; Bissell and Hines, 2011; Ruckert et al., 2012). Mounting evidence suggests that tumor-stromal cell interactions are important to the invasive phenotype. Stromal cells, once seen as passive structural components of the tumor infrastructure, are now viewed as dynamic components of tumor initiation, progression, and invasion (Mueller and Fusenig, 2004; Tlsty and Coussens, 2006; Pietras and Ostman, 2010). Invasive tumors are composed of a large proportion of stroma; in MPM this proportion can be as high as 34–45% depending on the histologic subtype (Motta et al., 2006). The proportion is highest in biphasic and sarcomatoid tumors, the latter of which is associated with even worse prognosis than other subtypes (Motta et al., 2006). This tumor-stroma balance creates a heterogeneous microenvironment composed of, among other things, malignant cells, cancer-associated fibroblasts, vascular endothelial cells, macrophages, and other inflammatory infiltrates. In a study of MPM, inflammatory or

Abbreviations: MPM, malignant pleural mesothelioma; TnTs, tunneling nanotubes; nm, nanometers; EMT, epithelial-to-mesenchymal transition; IF, immunofluorescence; FBS, fetal bovine serum; HA, hyaluronic acid; GFP, green fluorescent protein; EM, electron microscopy; TNFaip2, tumor necrosis factor-alpha-induced protein 2 (also called M-Sec), MSKCC, Memorial Sloan-Kettering Cancer Center.

desmoplastic stroma types correlated with worse patient prognosis, as compared with fibrous or myxoid forms of stroma (Cerruto et al., 2006).

The most commonly studied avenues of cellular transfer among cancer cells include gap junctions, chemokines, cytokine messengers, and microvesicles/exosomes (Bissell and Radisky, 2001; Hegmans et al., 2004; Cottin et al., 2010; Naus and Laird, 2010; Bobrie et al., 2011; Pap et al., 2011; Strassburg et al., 2012). These forms of intercellular communication are most effective over short distances. Furthermore, cell-cell junctions are disrupted upon epithelial-mesenchymal transition, a precursor to metastasis (Lamorte et al., 2002; Huber et al., 2005), making intercellular communication via these junctions impossible for separated cells. Additionally, effective cell-cell "cross-talk" via diffusible factors could be difficult to achieve because of an increase in interstitial fluid pressure in the tumor microenvironment. There remains considerable uncertainty regarding how tumor-stroma exchange of cellular information takes place and how distant cells that are not in close proximity are able to communicate within a three-dimensional matrix composed of a significant proportion of stromatous material. A better understanding of the mechanisms and cellular structures that underlie intercellular communication among distant cells in the tumor matrix of malignant tumors is expected to lead to new targeted treatments that block progression of mesothelioma and other invasive solid tumor malignancies.

Our group has investigated tunneling nanotubes (TnTs), a previously underexplored form of cellular protrusions that are distinctly unique from other filamentous cellular extensions. TnTs are long, narrow, actin-based cytoplasmic extensions that form *de novo in vitro*. Nano-sized in width (50–800 nm), TnTs can stretch the length of several cell diameters or longer (as long as several hundred microns) to form direct cell-to-cell cytoplasmic connections. TnTs display non-adherence to the substratum when cultivated *in vitro* (Rustom et al., 2004). These characteristics differentiate TnTs from other, well-known actin-based cytoplasmic extensions including lamellopodia, filopodia, and invadopodia (Rustom et al., 2004). TnTs are open-ended "intercellular bridges" whose walls consist of a contiguous lipid bilayer that can establish a direct connection between the cytoplasm of connected cells, or in some cases interface with gap junctions in plasma membranes (Wang et al., 2010). TnT formation is largely generated by actin-driven membranous protrusions extending to outlying cells. They have been noted to form either by one cell extending a tubular cytoplasmic connection to another cell located at some distance (in contrast with gap junctions, which connect cells in immediate proximity) or to form between cells in close proximity that then move apart via usual mechanisms of cell motility, allowing for continuation of intercellular communication even as the cells move in different directions (Veranic et al., 2008). At least one study has suggested that TnTs interface with gap junctions to connect cells and mediate intercellular cross-talk (Wang et al., 2010). Uniquely, TnTs serve as conduits for intercellular shuttling of cellular organelles and other cargo between connected, non-adjacent cells (Lou et al., 2012a,b). *In vitro* studies have shown that TnTs have the ability to directly mediate cell-to-cell communication by serving as long-range conduits between connected cells for intercellular transfer of proteins, mitochondria, Golgi vesicles, and even viruses (Koyanagi et al., 2005; Onfelt et al., 2005, 2006; Sherer et al., 2007; Davis and Sowinski, 2008; Sherer and Mothes, 2008; Plotnikov et al., 2010; Yasuda et al., 2010; He et al., 2011; Kadiu and Gendelman, 2011; Wang et al., 2011; Lou et al., 2012b) (For an example of time-lapse imaging we use in our work, please see **Movie S1** demonstrating intercellular transfer of mitochondria between mesothelioma cells connected via nanotube). The importance of intercellular transfer of genetic material is also a topic of growing interest. Our group recently demonstrated that TnTs can also transport oncogenic microRNAs between malignant cells, as well as between malignant and stromal cells, introducing a new aspect of tumor-stromal cross-talk that warrants further study (Thayanithy et al., 2014a).

TnTs have been studied in a wide variety of non-cancer cell types including dendritic cells and monocytes (Watkins and Salter, 2005; Salter and Watkins, 2006), mature macrophages (Eugenin et al., 2009; Hase et al., 2009), T cells (Sowinski et al., 2008, 2011; Rudnicka et al., 2009), B cells (Xu et al., 2009), neutrophils (Galkina et al., 2010), neuronal cells (Gousset et al., 2009), kidney cells (Gurke et al., 2008), endothelial progenitor cells (Yasuda et al., 2010), mesothelial cells (Ranzinger et al., 2011; Lou et al., 2012b), cardiomyocytes (Koyanagi et al., 2005), and mesenchymal stromal cells (Cselenyak et al., 2010; Plotnikov et al., 2010). Our group focuses on investigation of TnTs in the context of invasive forms of cancer (Lou et al., 2012a,b). To investigate TnTs as a physiologically relevant structure in human solid tumor malignancies, our initial work successfully visualized TnTs in solid tumors resected from patients with mesothelioma and lung adenocarcinomas (Lou et al., 2012b), providing the first evidence of the potential *in vivo* relevance of these cellular structures in cancer. We subsequently performed high-resolution microscopy and 3-dimensional reconstructions to confirm that nanotube structures are present in other invasive malignancies as well, including a murine model of osteosarcoma and human ovarian adenocarcinoma (Thayanithy et al., 2014a). In our *in vitro* work in mesothelioma, we used modified wound-healing assays and demonstrated TnT formation along the leading invasive edge of mesothelioma cells *in vitro*; time-lapse imaging revealed regular formation of TnTs by proliferating and migrating mesothelioma cells advancing to fill the gap (Lou et al., 2012b). This finding introduces the possibility that TnTs facilitate intercellular communication and the progression of malignancy at the leading edge of invasive mesothelioma tumors. More recently, we showed that exosomes and TnTs may work synergistically by demonstrating that exogenous tumor exosomes induced an increased rate of TnT formation (Thayanithy et al., 2014b). Electron microscopy revealed that exosomes were located at the base of TnTs and in the extracellular environment. Our subsequent studies identified enrichment of lipid rafts, small intra-cytoplasmic cholesterol microdomains, in mesothelioma cells connected via nanotubes (Thayanithy et al., 2014b). These findings implicate exosomes as potential chemotactic stimuli for TnT formation and lipid rafts as a potential biomarker for TnTs. The effects of TnT formation and TnT-mediated transport of cellular cargo on malignant cell behavior are currently unknown.

In the current study, we sought to further characterize the properties of TnTs in mesothelioma, including differences in formation of TnTs between malignant mesothelioma cells and non-malignant mesothelial cells; quantitative differences in TnT length in relation to cell proliferation; properties of TnT formation in clinically relevant models, such as between non-adherent cells, mimicking the scenario of mesothelioma cells floating in peritoneal or thoracic effusions as a hallmark of malignant progression; and structural components of TnTs in mesothelioma cells. Finally, we also sought to develop new approaches to 3-dimensional *in vitro* and *in vivo* modeling for the study of TnTs in tumor propagation and resistance to therapy.

MATERIALS AND METHODS

CELL LINES AND CULTURE MEDIA

MSTO-211H cells were derived from a patient with biphasic mesothelioma (ATCC no. CRL-2081); VAMT is a sarcomatoid mesothelioma cell line; and H2052 is a mesothelioma cell line of epithelioid histology. All three mesothelioma cell lines (MSTO-211H, VAMT, and H2052) were passaged using 10% fetal bovine serum (FBS) in RPMI-1640 with 25 mM glucose, supplemented with 1% penicillin-streptomycin (P-S) and 2% L-glutamine, at normal pH (7.6). The normal immortalized human mesothelium cell line MeT5A was passaged in 10% FBS in M199/MCDB105 (1:1) with 100 U/ml penicillin-streptomycin and 2% L-glutamine. All cell lines used in this study were authenticated by the Core Fragment Analysis Facility at Johns Hopkins University using short tandem repeat profiling. Cells were passaged in 75 cm^2 tissue culture flasks (Falcon, Becton Dickson, Oxnard, CA) at 37°C in 5% CO_2. Nanotube formation was stimulated by growing cells in 2.5% FBS in RPMI-1640 containing 50 mM glucose, supplemented with 1% P-S and 2% L-glutamine as described previously (Lou et al., 2012b); we refer to this combination throughout the text as "TnT medium." For 3-dimensional *in vitro* modeling, we mixed MSTO-211H cells in 5% FBS in RPMI medium containing 100 mM glucose in a 1:1 ratio with 2% agarose to compose a final medium composed of 1% agarose and TnT medium for further culture of cells. These cells were then added to 6-well culture plates for microscopic examination.

QUANTIFICATION OF TnTs PER CELL

Three MPM cell lines (H2052, VAMT, and MSTO-211H) and one benign mesothelial cell line (MeT5A) were plated at a density of 6×10^4 cells/well in 6-well adherent tissue culture plates (Fisher Scientific, Pittsburgh, PA) at 37°C in 5% CO_2 with TnT-inducing medium (described above). TnTs were identified using the parameters described by Rustom et al. (2004) as well as in our previous publications (Lou et al., 2012b; Thayanithy et al., 2014b). Briefly, these parameters included (i) lack of adherence to the substratum of tissue culture plates, including visualization of TnTs passing over adherent cells; (ii) TnTs connecting two cells or extending from one cell were counted if the width of the extension was appropriately narrow and estimated to be <1000 nm in width; and (iii) a narrow base at the site of extrusion from the plasma membrane. Cellular extensions not clearly consistent with the above parameters were not included in the final count. An Olympus IX70 inverted microscope (Olympus Corporation) with 20× objective lens was used to count the number of TnTs and cells in 10 randomly chosen fields of each 6-well plate at 24, 48, and 72 h. A single representative image was taken at all time points for each well for analysis of TnT length. Experiments were performed in duplicate for each cell line. The number of TnTs per cell (TnTs/cell) was counted to exclude the possibility that increases in TnTs were due to increased cell proliferation. Means were calculated and compared using two-sided, two-tailed *t*-tests assuming unequal variances. *P*-values <0.05 were considered statistically significant.

QUANTIFICATION OF TnT LENGTH

Representative images taken from the previous experiment were analyzed using ImageJ software. TnT length was measured by normalizing the 200 micron scale bar from the images to the number of pixels. The length of TnTs from each cancer cell line was measured at 24, 48, and 72 h. TnT lengths were not normally distributed; therefore, Wilcoxon Rank Sum tests were used to compare TnT lengths for each combination of time measurements within each cell line. *P*-values <0.05 were considered statistically significant.

TnT TETHERING ASSAYS

Pleural effusion or ascites specimens from cancer patients with MPM and lung adenocarcinoma were obtained via a Memorial Sloan-Kettering Cancer Center (MSKCC) Institutional Review Board (IRB)-approved protocol. Informed written consent was obtained from all patients, and patient identifiers were removed to ensure anonymity. Malignant cells were histologically confirmed by an experienced MSKCC pathologist and seeded in standard tissue culture-treated plates using a clonal dilution assay. Cells were seeded in 24-well non-adherent culture (Nunc Non-Treated Multidishes) and adherent treated tissue culture plates (Fisher Scientific, Pittsburgh, PA) using 10% FBS RPMI. Microscopic imaging was used to confirm the presence of single cells per well, and these wells were marked and monitored daily by microscopic imaging. We additionally performed similar experiments with mesothelioma cell lines VAMT, H2052, and MSTO-211H using an identical approach.

FIXATION AND SAMPLE PREPARATION

To prepare cells for IF staining, cells were cultured in one- or two-well sterile tissue culture-treated chamber slides (Lab-Tek II Chamber Slide™ system, Nunc, Rochester, NY) or on sterile poly-L-lysine (1 mg/ml; Sigma) coated glass coverslips (VWR VistaVision, catalog no. 16004-312) for 48–72 h using TnT medium to stimulate TnT formation. As TnTs are highly sensitive to movement and to light, we have modified existing protocols for cell fixation and analysis. To perform fixation and prevent disruption of existing nanotubes, 16% w/v paraformaldehyde (PFA) (Alfa Aesar, Ward Hill, MA) was added along the sides of the chambers or the dishes with glass coverslips, keeping the overlying culture medium intact to a final w/v concentration of 4%, After incubation at 4°C for 1–2 h, the fixative and chambers were removed, and slides were allowed to air dry. We have found this combination provides optimal preservation of intact cells with TnTs to allow for more accurate study of these thin

structures. Immunofluorescent staining was then performed to detect expression of the noted proteins.

IMMUNOFLUORESCENT STAINING

The primary antibodies and their working concentrations are as follows: cdc42 (Santa Cruz Biotech, 200 ug/ml, rabbit polyclonal IgG; catalog no. SC-87); NF2/merlin (Santa Cruz Biotech, 200 ug/ml, rabbit polyclonal IgG; catalog no. SC-332), p-selectin (CD62P) (BD Biosciences, 5 μg/ml; catalog no. 556087), beta-tubulin (Sigma–Aldrich, monoclonal anti-acetylated tubulin, clone 6-11B-1; catalog no. T6793-0.2ML); monoclonal anti-β-Tubulin IV (Sigma–Aldrich, catalog no. T7941, clone ONS.1A6); vimentin Alexa Fluor 488 (BD Pharmingen, human IgG; catalog no. 562338), Akt (Sigma–Aldrich, rabbit polyclonal IgG; catalog no. AAB4300259-100UG). Slides were first blocked with blocking solution (10% normal goat serum/2% BSA in PBS) or mouse IgG blocking agent from Vector Labs (catalog no. MKB-2213) for 30 min. Primary antibody incubation lasted 3–7 h at room temperature, followed by 30 min incubation with biotinylated secondary antibodies (Vector Labs, MOM Kit BMK-2202; 1:200 dilution). Detection was performed with Streptavidin-HRP D (Ventana Medical Systems) followed by Tyramide-Alexa Fluor 488 (Invitrogen, catalog no. T20922).

DRUG TREATMENT OF CELLS WITH MIGRASTATIN

Migrastatin core ether is a synthetic analog of migrastatin obtained courtesy of Dr. Samuel Danishefsky; it was used at 100 nM. MSTO-211H cells were prepared as above (i.e., 1×10^5 cells per well in 24-well tissue culture plates). The number of TnTs was counted in 10 fields per medium condition, at regular time intervals (0, 24, 48, and 72 h) using a 20× objective lens on a Nikon Eclipse Ti inverted microscope (Nikon Instruments, Inc.). Experiments were performed in duplicate. Means were calculated and compared using two-sided, two-tailed *t*-tests assuming unequal variances. *P*-values <0.05 were considered statistically significant.

TREATMENT OF CELLS WITH OTHER DRUGS (TUNICAMYCIN, DEXTRAN SULFATE, 4-METHYLUMBELLIFERONE) TO ASSESS POTENTIAL ASSOCIATION OF HYALURONAN WITH TnTS

Tunicamycin (Sigma, catalog no. T7765-1MG, lot no. CAS 11089-659) was used at a final concentration of 5 μg/ml; Poly I:C (Polyinosinic–polycytidylic acid sodium salt; Sigma, catalog no. P0913-10MG, lot no. CAS 42424-50-0) was used at a final concentration of 10 μg/ml; dextran sulfate (Sigma, catalog no. D8906-5G) stock solution was made by first dissolving in 2% FBS in phosphate-buffered saline (PBS) to create a stock solution of 100 μg/ml, which was then added to culture medium to final concentration 10 μg/ml; 4-methylumbelliferone (4-MU; Sigma, catalog no. M 1381) was prepared as a stock solution 20 mg/ml concentration in DMSO, then added to culture medium to final concentration 1.0 mM; Hyaluronidase (Sigma, H3884) was prepared as a stock solution of 10 mg/ml and used at a final concentration of 13 μM. For preparation of each drug, stock solution was added to 10% FBS RPMI-1640 medium to obtain final concentrations as listed; this medium was used in cell culture by adding to 1×10^4 MSTO-211H cells per well of 6-well tissue-culture treated plates (Fisher Scientific, Pittsburgh, PA). Following 48 h of incubation at 37°C (5% CO_2), exclusion assays were performing by adding either U937 mononuclear cells at 4°C for 1 h or red blood cells (erythrocytes) as noted in the Results Section and per standard protocols (DiCorleto and de la Motte, 1985; Rilla et al., 2008), followed by microscopic imaging. For fluorescent imaging, MSTO-211H cells transfected with a lentivirus expressing green fluorescent protein (GFP) were used along with U937 cells transfected with a lentivirus expressing Tomato Red.

IN VIVO GROWTH OF MESOTHELIOMA CELLS PRECONDITIONED WITH TnT MEDIUM

GFP-luciferase expressing MSTO cells were grown in either of two conditions: normal RPMI (10% FBS RPMI, 25 mM glucose) or TnT-inducing medium, which consists of low serum and high glucose RPMI (2.5% FBS RPMI, 50 mM glucose), for 7 days. Both sets of media were supplemented with 1% penicillin/streptoymycin and 2% L-glutamine. All cells were cultured in 6-well adherent tissue culture plates (Fisher Scientific, Pittsburgh, PA) at 37°C in 5% CO_2. Cells (2.9×10^5) were then suspended in 100 μL of RPMI and injected into the peritoneum of each mouse. Ten NOG (NOD/Shi-scid/IL-2Rγ^{null}) immunodeficient mice were used for each group. Each mouse was concurrently injected intraperitoneally with 1 ml of thioglycolate as a co-stimulatory inflammatory agent; the rationale for this is that inflammation is known to elicit formation of nanotubes in *in vivo* animal models (Seyed-Razavi et al., 2013). On days 7, 14, 21, and 31 post-tumor inoculation, mice were anesthetized with isoflurane and injected intraperitoneally with 150 μL of luciferin (15 mg/mL). Mice were then imaged with an Ivis 200 optical imaging system (Caliper Life Sciences, Hopkinton, MA) 5 min after injection. Capture time was 40 s. Living Image software version 2.5 was used to quantify average radiance (p/s/cm2/sr). Means were calculated and compared using two-sided, two-tailed *t*-tests assuming unequal variances. Overall survival (OS) of the mice was calculated from date of tumor inoculation to date of death, or censored at 40 days for those still alive at the end of the experiment. OS was summarized using a Kaplan-Meier curve and a comparison between groups was made using a Log-Rank test. *P*-values <0.05 were considered statistically significant.

SECTIONING, STAINING, AND IMAGING HUMAN TUMOR SAMPLES

Tumor specimens from patients with MPM were obtained via a MSKCC IRB-approved protocol. Informed written consent was obtained from all patients, and patient identifiers were removed to ensure anonymity. Resected intact tumor specimens were placed in PBS. Vibratome sections (100–300 mm thick) were cut and stained using Hoechst 33342 (10 mg/ml) and MitoTracker Red dyes (500 nM) using protocols we developed and have described previously (Lou et al., 2012b). Stained sections were mounted between two glass coverslips and imaged on a confocal microscope.

OPTICAL IMAGING OF HUMAN TUMOR SAMPLES AND IMAGE PROCESSING

Confocal imaging of samples was performed using Zeiss LSM 5Live line-scanning or Leica SP2 point-scanning microscopes

using Zeiss oil 406/1.3NA Plan-Neoflur, Zeiss oil 636/1.4NA Plan-Apochromat or Leica water 636/1.2NA HCX PL APO CS objectives. Serial z-stack images were obtained at optimal step size and maximum intensity projection images were produced. The Imaris Viewer program (Bitplane Scientific Software, Inc.) was used to construct and visualize 3-dimensional images of tumor samples. Metamorph (Molecular Devices) image analysis software was used to create still images and movies.

ELECTRON-MICROSCOPIC IMAGING OF NANOTUBES

To perform scanning and transmission EM, 1–3 $\times$ 10^6 MSTO-211H cells were cultured on Thermanox plastic tissue culture 25 mm cover slips (Lux Scientific Corporation). The fixative—2.5% glutaraldehyde/2% paraformaldehyde in 0.075 M sodium cacodylate buffer (pH 7.5; 10 ml, Electron Microscopy Sciences, Hatfield, PA)—was added directly to the overlying medium.

CELL CULTURE AND RNA ISOLATION

MSTO-211H cells (8×10^5) were seeded in 150 cm^2 flasks and grown for 7 days using passage medium or TnT medium at 37°C in a standard humidified chamber with 5% CO2 as already described in the text. After 7 days, the cells were harvested separately following trypsinization and subjected to RNA isolation using mirVana™ total RNA isolation protocol following the protocol of the manufacturer (Life Technologies, Carlsbad, CA). RNA preparation was quantified on a Nanodrop spectrophotometer (Thermo Fisher, Wilmington, DE, USA), and RNA quality was confirmed by resolving on a denaturing 1.2% agarose gel following standard electrophoresis protocol.

cDNA SYNTHESIS AND qRT-PCR

RNA was subjected to first strand cDNA using miScript II Reverse Transcription kit (Qiagen, Valencia, CA). Total RNA was reverse transcribed for 2 h at 37°C, and reverse transcriptase was heat inactivated by boiling the reaction mix at 95°C for 5 min. cDNA (5.0 ng) was diluted and amplified with 10 µl of miScript SYBR green PCR mix following the protocol of the manufacturer using gene-specific forward and reverse primers. PCR primers were purchased from a commercial vendor (IDT, Coralville, IA). The nucleotide sequence of the primers used are listed in Supplementary Table 1. The samples were run in triplicate in a Roche Light Cycler II (Roche GmbH, Germany), and values were normalized to the endogenous expression of 18S rRNA. Fold gene expression was calculated by comparative C(T) method (Schmittgen and Livak, 2008) and mean fold expression values relative to expression in control medium were compared using two-sided two-sample *t*-tests assuming unequal variances. *P*-values <0.05 were considered statistically significant.

TIME-LAPSE IMAGING OF CELLS IN CULTURE

Time-lapse imaging experiments were performed on Perkin Elmer UltraView ERS spinning-disk confocal microscope or Zeiss LSM 5Live line-scanning confocal microscope. Both microscopes were enclosed in environmental chambers that were maintained at 37°C with 5% CO_2 level. Viable Staining of Cell Lines for time-lapse imaging was performed as we have described previously (Lou et al., 2012b). Briefly, in order to assess the ability of mitochondria to be transmitted between mesothelioma cells via TnTs, we used MitoTracker Red to stain MSTO-211H cells which were then cultured in hyperglycemic, low-serum ("TnT") medium. The cells were cultured in clear-bottomed delta-T culture dishes (Bioptechs Inc., Butler, PA). MitoTracker Red CMX Ros (Invitrogen, M-7512, 50 µg/vial) was used at 500 nM to stain mitochondria, per manufacturer's protocols. Stained cells were re-suspended and added to a non-confluent culture of adherent, unstained MSTO-211H cells grown in another dish. Incubation was performed in high glucose medium for 5 h to stimulate formation of TnTs prior to imaging.

RESULTS

MALIGNANT MESOTHELIOMA CELLS FORM MORE TnTs THAN BENIGN MESOTHELIAL CELLS

We propose that TnTs create intercellular networks with the capability of transmitting signals that stimulate proliferation of invasive cancers. To determine whether TnT formation occurs at a higher rate in malignant mesothelioma cells than in benign cells, we cultured the MPM cell lines H2052, VAMT, and MSTO-211H and the benign mesothelial cell line MeT5A. Cells were cultured in medium that we previously demonstrated induces TnT formation (Lou et al., 2012b). Equivalent numbers of cells were added to culture wells and visualized using inverted microscopy at 24, 48, and 72 h; representative images are shown in the accompanying figures (**Figure 1A**; also Supplemental Figure S1 for composite panel of representative images at 24, 48, and 72 h). At each time point, we randomly selected 10 fields of view using the 20× objective and counted the number of TnTs per field. We also counted the number of cells present in each selected field to control for cellular proliferation. For all three malignant mesothelioma cell lines, the average number of TnTs/cell was significantly higher than that seen for the benign mesothelial MeT5A cell line (**Figure 1B**). No evidence of TnT formation was evident in the mesothelial cell line (MeT5A) at 24 h, and thus a ratio could not be reported. As expected, cell proliferation was higher in malignant mesothelioma cell lines as compared to normal MeT5A cells (**Figure 1C**); however, among malignant cells proliferation appeared to be inversely associated with the rate of TnT formation. The ratio of malignant:mesothelial TnTs/cell doubled or tripled from 48 to 72 h for all malignant cell lines (26.73–78.16 for H2052, 9.80–42.66 for VAMT, and 9.80–18.84 for MSTO) (**Figure 1D**). Taken together, these *in vitro* data show that TnTs formed at a markedly higher rate among malignant mesothelioma cell lines than among normal mesothelial cells in inverse proportion to the rate of cell proliferation, ranging from nearly 20-fold to 80-fold higher by 72 h of *in vitro* culture. Moreover, these data support the use of a "nanotube index" to quantitatively assess TnT formation in future studies of the biological role of TnTs in aggressive malignancies. This markedly higher rate of TnT formation in mesothelioma, and likely in other cancers as well, provides evidence to support TnTs as a potential novel target for selective therapy of such cancers.

OVERALL TnT LENGTH DECREASES WITH TIME AND WITH PROLIFERATION OF MESOTHELIOMA CELLS

In the context of a heterogeneous tumor matrix, TnTs may play an important role in long-distance cellular communication.

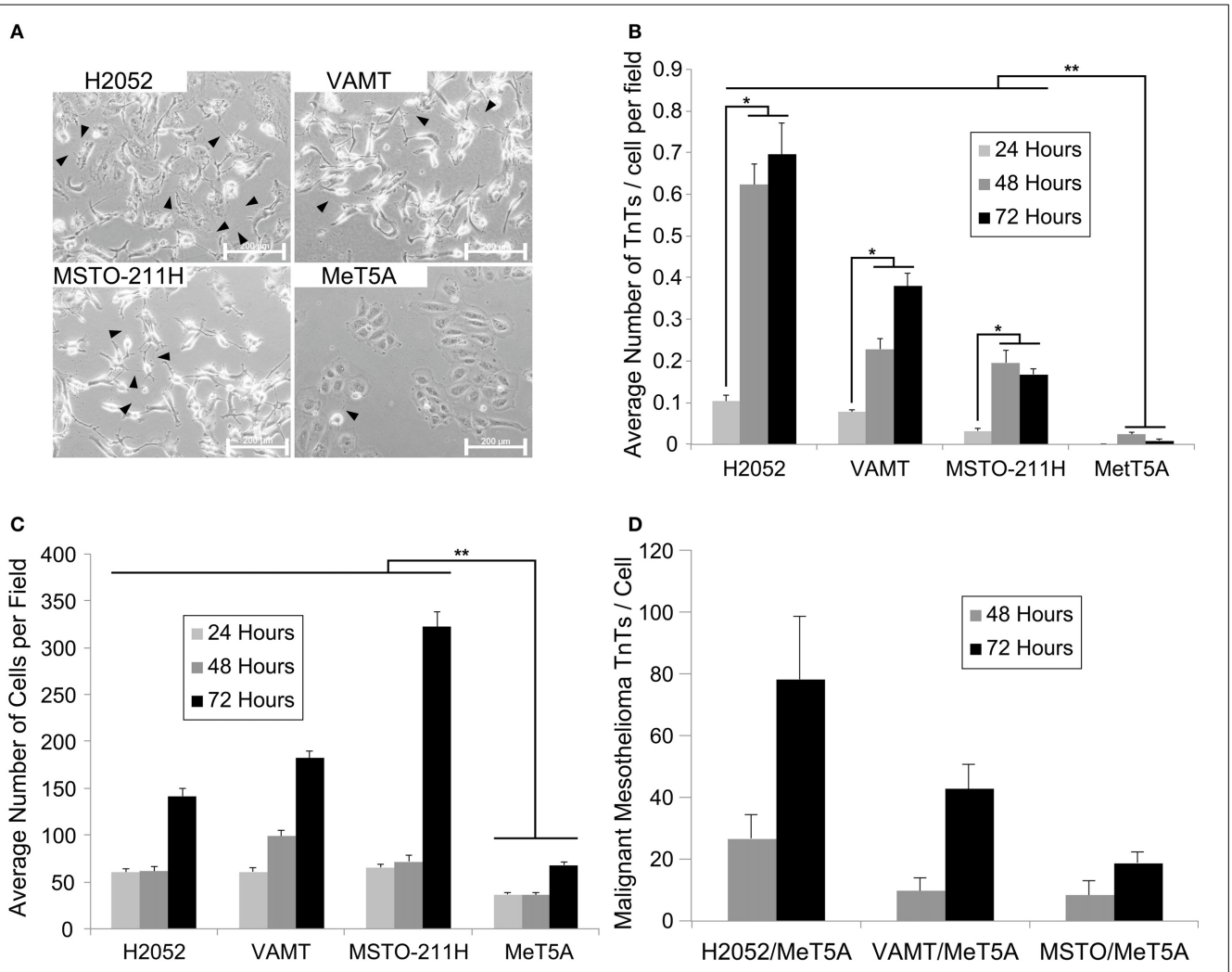

FIGURE 1 | Malignant mesothelioma cells form more TnTs than benign mesothelial cells. An Olympus IX70 inverted microscope with 20× objective lens was used to count the number of TnTs and cells in 10 randomly chosen fields at 24, 48, and 72 h. Representative images of TnTs of three malignant mesothelioma cell lines (H2052, VAMT, MSTO-211h) and a benign mesothelial cell line (MeT5A) were evaluated and are shown **(A)**. Arrowheads indicate nanotubes. The number of TnTs per cell (TnTs/cell) was counted **(B)** to exclude the possibility that increases in TnTs were due to increased cell proliferation **(C)**. Experiments were performed in duplicate for each cell line and results were averaged. Means ± standard errors are plotted. Double asterisks indicate statistically significant differences ($p < 0.05$) between each mesothelioma cell line compared to the mesothelial cell line; single asterisks indicate statistically significant differences between timepoints within each malignant mesothelioma cell line. Also shown is a ratio of TnTs per cell at 48 and 72 hours comparing individual malignant cell lines to MeT5A **(D)**.

To accomplish this, TnTs would need to extend to variable lengths depending on the distance of targeted cells. As more cells accumulate, this distance would become shorter. We hypothesized that TnT length would decrease as cells proliferate and accumulate over time in *in vitro* culture. We cultured the MPM cell lines H2052, VAMT, and MSTO-211H and the mesothelial cell line MeT5A. TnT length decreased over time among all malignant cell lines (**Figure 2**); these changes were statistically significant at most time points (**Table 1**). TnT length decreased slightly from day 2 to day 3 among the non-malignant MeT5A cells (**Figure 2**); however, this change was not statistically significant. We depict the data in the form of box plots in order to demonstrate the median and the wide range of lengths we observed in the malignant mesothelioma cell lines (**Figure 2**). Since TnT formation between MeT5A cells was rare, it was not possible to construct box plots for the distribution of TnT length over the three-day period for this non-malignant cell line. The decrease in TnT length observed among malignant cells was most noticeable for H2052 and VAMT cells, but was less dramatic for MSTO cells. This difference could be due to the relatively steady rate of proliferation of H2052 and VAMT cells and high proliferation rate of MSTO cells (**Figure 1C**). In addition, this finding is consistent with our prior study showing that TnTs are most prominent in sub-confluent cultures; in fully confluent cultures, cells are in close proximity, making it either difficult to discern any present TnTs and/or decreasing the number of TnTs that form

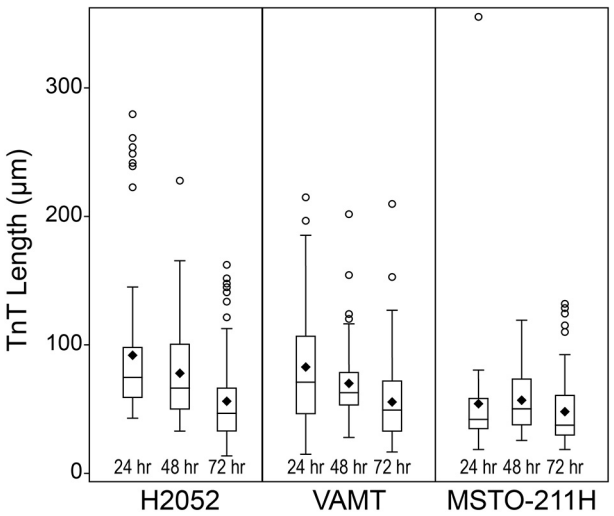

FIGURE 2 | TnT length decreases with time and with proliferation of mesothelioma cells. Microscopy images were taken of cells forming TnTs at 24, 48, and 72 h. Images were representative of the 10 randomly chosen fields from **Figure 1**. Average TnT length was estimated through measurement of image pixels. Box plot depicts distribution of lengths of TnTs in the malignant mesothelioma cell lines. Symbols on the boxplot are as follows: Box, 1st to 3rd (Q1–Q3) Quartiles; Diamond, Mean; Line inside box, Median; Circle, Outlier.

Table 1 | *P*-values from comparisons of TnTs Length in mesothelioma cells by cell line and time.

Cell lines:		H2052	VAMT	MSTO-211H
Time (hours)	24 vs. 48	$P = 0.112$	$P = 0.314$	$P = 0.075$
	24 vs. 72	$P < 0.0001$	$P < 0.0001$	$P = 0.386$
	48 vs. 72	$P < 0.0001$	$P < 0.0001$	$P = 0.002$

P-value ≤ 0.05 was considered significant.

in conditions that do not require long-distance connections (Lou et al., 2012b).

TnT TETHERING OF MESOTHELIOMA CELLS IN *IN VITRO* MODEL OF PLEURAL EFFUSIONS

Advanced thoracic malignancy is frequently associated with accumulation of malignant fluid in the pleural or peritoneal cavities. These effusions often contain detached, free-floating suspended malignant cells that are capable of undergoing epithelial-to-mesenchymal transition (EMT), thus increasing their invasive capability in some cancer types, such as lung adenocarcinoma (Chen et al., 2013; Chunhacha et al., 2013). In our prior study, we demonstrated that EMT effectively stimulates TnT formation in mesothelioma (Lou et al., 2012b). We hypothesized that non-adherent viable cells in culture in essence behave similarly to suspended effusion cells in mesothelioma patients. We thus next obtained pleural effusion specimens from 5 patients diagnosed with MPM or lung adenocarcinoma. After isolating malignant cells via centrifugation of pleural effusions, we confirmed the presence of malignant cells by morphology and TnT formation

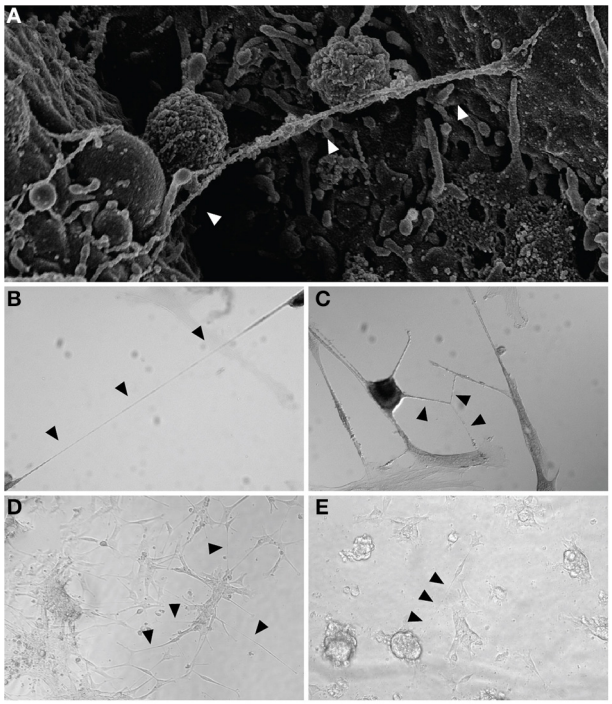

FIGURE 3 | TnT tethering of mesothelioma cells in *in vitro* models of pleural effusions. (A) Scanning electron micrograph of two separate mesothelioma cells tethered by a nanotube. **(B,C)** TnTs connecting primary malignant cells from pleural effusions. 40× magnification. **(D,E)** Clonal dilution assay using VAMT (sarcomatoid mesothelioma) cells grown in a low-adherence culture plate using 10% FCS RPMI medium; cells are shown on day 24 of culture in separate wells from the same plate. Arrowheads indicate nanotubes.

among these cells by inverted as well as by scanning electron microscopy (**Figure 3A**). We then cultured cells *in vitro* in standard tissue culture-treated plates and confirmed formation of TnTs connecting these patient-derived, primary malignant cells (**Figures 3B,C**).

We noted that malignant cells presented in effusions as dispersed single cells or as spheroid aggregates that could be disassembled into single cells through trypsinization or by physical separation with vigorous pipetting. We hypothesized that clusters of cells derived from a single parent cell could form TnTs in suspension and without full cell adherence to the substratum of the culture plate. To investigate this possibility, we performed separate clonal dilution assays using VAMT and H2052 cell lines cultured in 24-well non-adherent culture plates. We visually confirmed the presence of single cells and marked these wells for further daily follow-up. We performed daily microscopic imaging and reproducibly detected growth of groups of cells derived from parent cells forming mesh-like syncytial networks of TnTs connecting daughter cells. Cell aggregates formed prominently under non-adherent culture conditions while maintaining extensive TnT connections; these aggregates were in many instances connected to each other by nanotube structures while remaining suspended in culture medium (**Figures 3D,E**; also Supplemental Figure S2). As TnTs are in essence 3-dimensional structures

(i.e., non-adherent to the substratum), they may "oscillate" upon movement of the culture plate. Other actin-based structures, such as invadopodia, do not demonstrate this trait. Using fine focus to evaluate TnTs in live cell culture also helps to differentiate TnTs from other cell extensions. The observation that primary malignant cells formed a syncytial "network" connected by TnTs indicates that these or other cytoplasmic extensions may play an unrecognized role in facilitating communication among suspended malignant cells and malignant/mesothelial cells adherent to the pleural lining of the thoracic cavity.

These data suggest that TnTs may play a role in tethering suspended, non-adherent cells. As development of pleural effusions or abdominal ascites is a hallmark of a number of aggressive solid tumor malignancies—most especially malignant pleural and peritoneal mesotheliomas, as well as lung adenocarcinomas—these results provide potential insight into the cellular behavior of malignant cells at the advanced stages of cellular invasion. They also build upon our work demonstrating TnT formation between primary malignant mesothelioma cells *in vitro* (Lou et al., 2012b) as well as similar work demonstrating TnTs between human peritoneal mesothelial cells in culture (Ranzinger et al., 2011). Further *in vivo* studies will be necessary to clarify whether such TnT connections occur among malignant pleural or peritoneal mesothelioma cells invading the mesothelial lining.

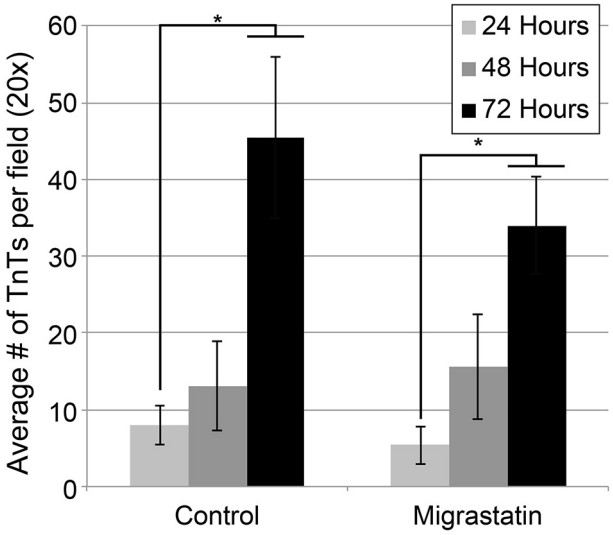

FIGURE 4 | Effect of Migrastatin on TnT formation in MSTO cells. Migrastatin was used at 100 nM. TnTs were counted in 10 fields per timepoint per condition using 20× objective lens, and the results averaged. Experiments were performed in duplicate. Comparisons between Migrastatin and the Control were statistically significant at 24 h ($p = 0.036$) and at 72 h ($p = 0.010$). Means ± standard deviations are presented. Asterisk indicates statistical significance ($p < 0.05$).

DRUG INHIBITION OF MESOTHELIOMA TnTs USING MIGRASTATIN, AN INHIBITOR OF FASCIN

We previously demonstrated that fascin localizes at the site of TnT extrusion from the plasma membrane at the leading edges of cells (Lou et al., 2012b). To determine whether fascin inhibition blocks TnT formation, we used migrastatin core ether (ME), a drug derived from migrastatin, a polyketide product initially derived from *Streptomyces* (Oskarsson et al., 2010). Synthetic analogs of migrastatin inhibit migration of cancer cells (Oskarsson et al., 2010) by targeting fascin and thereby blocking tumor progression (Chen et al., 2010). MSTO cells treated with ME exhibited a statistically significant difference with fewer TnTs, compared with the Control group without drug treatment, at 24 h ($p = 0.036$) and at 72 h ($p = 0.010$) (**Figure 4**). There was not significant difference at the 48-h timepoint.

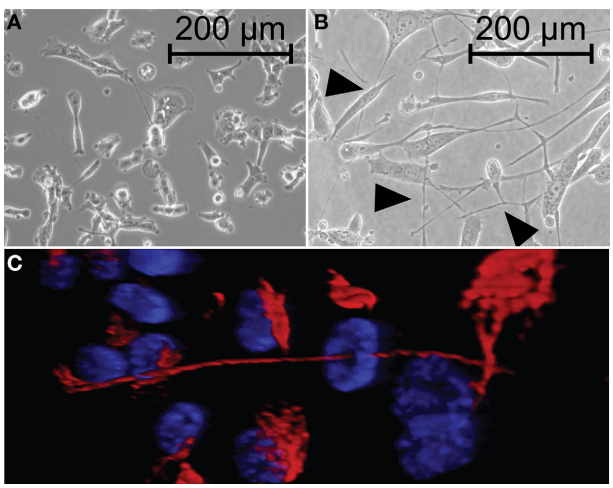

FIGURE 5 | 3-dimensional modeling of TnTs *in vitro*. (A) MSTO cells forming TnTs in regular tissue culture treated plate; **(B)** MSTO cells cultured in 1% agarose, forming TnTs vertically as well as horizontally within the agarose matrix. **(C)** 3-dimensional modeling of TnT connecting cells using confocal imaging with z-stacking (IF staining performed using fluorescent vimentin-specific antibody); also see **Movie S2**. Arrowheads indicate nanotubes.

THREE-DIMENSIONAL *IN VITRO* MODEL OF MESOTHELIOMA TUMOR MICROENVIRONMENT

Routine use of 3-dimensional modeling both *in vitro* and eventually *in vivo* will be critical to advancing the field of TnT biology, in cancer and in other diseases. To develop a 3-dimensional *in vitro* model of the tumor microenvironment, we used 1% agarose to culture mesothelioma cells to simulate suspension of cells within a 3-D viscous matrix. TnTs visualized in the 3D matrix were readily seen forming TnTs vertically and horizontally within the agarose matrix as compared to 2D tissue culture (standard tissue culture in **Figure 5A**; with TnT medium in 1% agarose, **Figure 5B**). Additionally, z-stacked confocal imaging of TnTs connecting cells stained with immunofluorescent antibodies can be used to visualize TnTs 3-dimensionally. Using this technology, we depicted a representative TnT stained with an immunofluorescent antibody to vimentin (**Figure 5C**; **Movie S2**, depicting rotating 3-dimensional model of this image). Immunofluorescence staining indicated the presence of vimentin along the length of TnTs.

In the case of solid tumor malignancies, including mesothelioma, standard and conventional evaluation of tumors involves histopathologic analysis of extremely thin 2-dimensional tumor

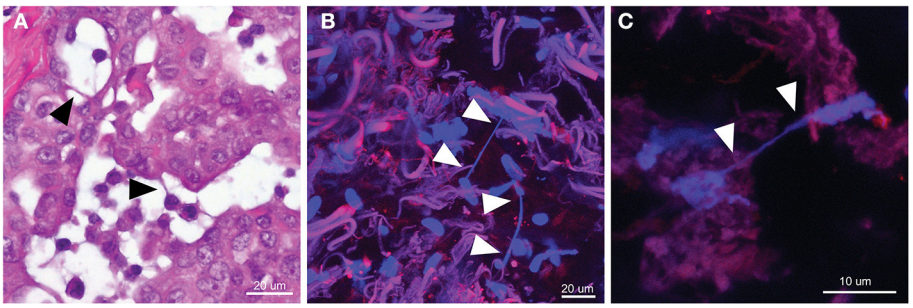

FIGURE 6 | Comparison of 2-dimensional histopathology section vs. 3-dimensional confocal imaging of primary human malignant mesothelioma tumors *ex vivo,* with specific examination for TnTs. (A) Hematoxylin and eosin (H&E) staining of sectioned primary human mesothelioma tumor; arrowheads indicate putative nanotube-like structures; **(B,C)** compiled confocal image produced by combining individual z-stacked images of representative portions of tumor tissue resected from a human patient. Tumors were stained with MitoTracker and Hoechst 334 dye; arrowheads indicate nanotube structures. Please also see **Movie S5**.

sections (**Figure 6A**). While slides prepared in this manner may potentially yield views of putative nanotube-like structures, advances in microscopic imaging are required to more effectively study 3-dimensional tumors. Advances in microscopic imaging that allow for layered z-stacked images of cells *in vitro* and methods we have developed to image *ex vivo* tumors provide an enhanced approach that allows for more advanced analysis of nanotubes connecting malignant cells in the stroma-rich tumor microenvironment (**Figures 6B,C**; Also see **Movie S5**). These visually detailed 3D images of mesothelioma cells provide further impetus for studying TnTs in this manner *in vitro*.

HYALURONIC ACID IS NOT ASSOCIATED WITH TnTs

Hyaluronic acid (HA), or hyaluronan, is a well-studied glycosaminoglycan that is secreted into the extracellular matrix; increased production of HA induces increased cell motility and an invasive phenotype in mesothelioma (Li and Heldin, 2001). Hyaluronan receptors are expressed preferentially on malignant mesothelioma cells but not on normal mesothelium (Asplund and Heldin, 1994). However, normal mesothelial cells and malignant cells derived from several organ sites synthesize relatively high quantities of hyaluronan, whose pericellular coat comprises bunches of short, adherent membranous protrusions consistent with actin-based stress fibers and microvilli (Kultti et al., 2006; Rilla et al., 2008). These coats create zones that have been well-described and are readily visualized microscopically using erythrocyte exclusion assays or the equivalent (McBride and Bard, 1979; Rilla et al., 2008). Conditions of cellular stress induced by either hyperglycemia, viral mimetic agent poly I:C, tunicamycin, or dextran sulfate, to name just several examples, have been shown to induce increased hyaluronan production and hyaluronan-based cellular "cables" that induce monocyte adhesion *in vitro* (Kultti et al., 2006); tunicamycin and dextran sulfate in particular induce endoplasmic reticulum-related metabolic stress that leads to increased production of hyaluronic acid, which in turn attracts and leads to increased adhesion of leukocytes via surface binding of CD44 (de La Motte et al., 1999; Majors et al., 2003; Wang and Hascall, 2004; Lauer et al., 2009). In our earliest studies examining what we later confirmed to be TnTs in mesothelioma, we performed standard exclusion assays using primary red blood cells (erythrocytes) or U937 lymphocyte (mononuclear) cells (Kultti et al., 2006; Rilla et al., 2008), but found no visual evidence of either pericellular zones or monocyte adhesion to TnT structures, indicating that TnTs were unlikely to harbor a significant amount of hyaluronan externally, also demonstrating that these entities are distinct from hyaluronan cables (**Figure 7**; Supplemental Figure S3). For fluorescent imaging and confirmation, we used MSTO-211H cells transfected with a lentivirus expressing GFP which we have used and described previously (Lou et al., 2012b) along with U937 cells transfected with a lentivirus expressing Tomato Red. To convincingly confirm that the extensions connecting cells were indeed TnTs, we performed time-lapse imaging that visibly demonstrated intercellular transfer of GFP (**Movies S3**, **S4**).

We also applied the HA-stimulating drug tunicamycin (final concentration 5 μg/ml) to MSTO cells in culture and examined these cells every 24 h up to 96 h. However, this led to no changes in TnT formation or morphology. Likewise, separate addition of dextran sulfate (10 μg/ml) to MSTO cells in culture led to cellular aggregation not unlike aggregates seen in patient effusion samples (Supplemental Figure S4). Poly I:C (10 μg/ml) induced a transformation of MSTO cells into a more mesenchymal, spindle-cell morphologic appearance without alteration of TnTs. This finding is consistent with similar effects of this drug on stimulating EMT in other cell types (Harada et al., 2009). We further treated MSTO cells with 4-methylumbelliferone (1.0 mM), an inhibitor of hyaluronan synthase and thus of hyaluronan cables (HAS) (Morohashi et al., 2006; Kultti et al., 2009); in separate wells we also assessed potential effects of the enzyme hyaluronidase (13 μM); neither drug had any effect on TnTs, consistent with the above data indicating HA does not play a notable role in TnT formation or maintenance (Supplemental Figure S4).

DECREASED TUMOR GROWTH IN MICE IMPLANTED WITH TnT-PRIMED MESOTHELIOMA CELLS ALSO CORRESPONDS WITH DECREASED SURVIVAL

Animal studies have identified nanotubes or similar structures *in vivo* in an inflammatory corneal mouse model (Chinnery et al., 2008; Seyed-Razavi et al., 2013) and *ex vivo* in adult mouse heart tissue (He et al., 2011), mouse alveoli (Islam et al., 2012),

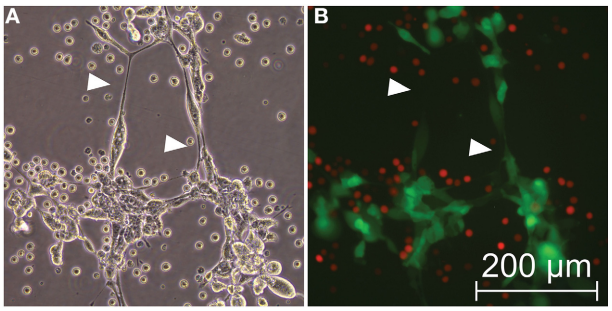

FIGURE 7 | Hyaluronic acid is not associated with TnTs. U937 mononuclear cells (expressing Tomato Red) were added to cell culture growing MSTO-211H cells (expressing GFP) with TnTs. **(A)** Brightfield and **(B)** Fluorescent views of the same field of view are shown. Arrowheads indicate nanotubes.

rabbit kidney parenchyma (Minuth and Denk, 2012), and mouse embryo non-neural ectoderm (Pyrgaki et al., 2010). Our group was the first to image TnTs in resected human tumor samples, initially on tumors from patients with MPM and lung adenocarcinoma (Lou et al., 2012b); we have been able to reproduce this finding using human mesothelioma tumors described in the current study (**Movie S5**). Our group has further extended demonstration of nanotube structures in malignant human ovarian tumors (Thayanithy et al., 2014a) as has another group (Pasquier et al., 2013). However, the technical difficulties of imaging nanotubes in the *in vivo* setting remain highly challenging. To assess effects of TnTs on *in vitro* cell proliferation, we used MSTO cells pre-conditioned in culture medium that we previously demonstrated increases the rate of TnT formation *in vitro* (Lou et al., 2012b). We conditioned MSTO cells in either low serum, hyperglycemic (2.5% FBS, 50 mM glucose) RPMI medium (referred to as "TnT medium") or control passage RPMI medium (10% FBS, 25 mM glucose) for 7 days. This experiment demonstrated that proliferation of MSTO cells in low-serum, hyperglycemic medium was approximately half that of cells cultured in passage medium by 72 h (**Figure 8A**). To next examine the effect of TnTs on tumor growth *in vivo*, we used a NOG xenograft mouse model of malignant mesothelioma. We conditioned MSTO cells transfected with a lentivirus expressing luciferase in either TnT medium or control passage RPMI medium (10% FBS, 25 mM glucose) for 7 days. We then injected these cells into the peritoneal cavity of NOG immunocompromised mice. Mice were bioimaged every 7 days up to 31 days and the average radiance was measured; interestingly, by 31 days the mice injected with cells pre-conditioned in low-serum, hyperglycemic medium had developed less tumor burden than mice injected with the same cell line pre-conditioned in passage medium (**Figure 8B**). Thus, this *in vivo* finding mirrored the *in vitro* studies that demonstrated that proliferation of MSTO cells in low-serum, hyperglycemic medium was approximately half that of cells cultured in passage medium. Moreover, none of the NOG mice injected with control medium ($n = 10$) had died by day 31, but 2 mice injected with cells pre-conditioned in low serum, hyperglycemic medium ($n = 10$) had died by day 31 and an additional one died just after imaging ($p = 0.067$, **Figure 8C**); in a separate experiment repeating this approach, 5 of 10 mice with injected cells pre-conditioned in TnT medium died by Day 31, whereas 0 of 10 died by that day (data not shown). Using weight as a surrogate measure for morbidity, mice injected with cells primed with TnT medium displayed a sharper drop in weight over time than did mice injected with cells cultured in passaged medium (data not shown). Bioimages demonstrating the visual differences between the two groups are shown (**Figure 8D**). These *in vivo* findings set the stage for further evaluation of the potential role for TnTs in solid tumor malignancies, possibly by increasing the locoregional but not distant invasive capability of mesothelioma cells, with a mechanism independent of cell proliferation.

GENE EXPRESSION PROFILING OF TnT-PRIMED MESOTHELIOMA CELLS

Due to the above findings, we next sought to determine relative differences in gene expression between MSTO cells conditioned in low serum, hyperglycemic (2.5 % FBS, 50 mM glucose) RPMI medium (i.e., "TnT medium") or control passage RPMI medium (10% FBS, 25 mM glucose). We first investigated RNA levels of M-Sec (which is also called TNFaip2, or tumor necrosis factor-α-induced protein 2) and leukocyte specific transcript 1 (LST1), two gene products that are known to be enriched in TnTs (Hase et al., 2009; Schiller et al., 2013). Both genes were significantly upregulated in MSTO cells cultured in TnT medium compared to control medium (**Figure 9A**). We then investigated whether TnT medium, which is significantly lower in essential nutrients and also includes low percent of added serum (2.5% FBS) relative to passage medium (10% FBS), affects genes that promote cell cycle progression (Bracken et al., 2004; Nalepa et al., 2013). RNA levels of E2F1, its downstream targets CCNA2 and CDC20, and CDKN3 were significantly lower in MSTO cells grown in TnT medium than in cells grown in control medium (**Figure 9B**). This finding is consistent with our observation that cells grown in TnT medium undergo a lower rate of cell division. We next studied whether key genes involved in cellular migration, invasion, and metastasis are altered in mesothelioma cells cultured in TnT medium (Scholler et al., 1999; Rittling and Chambers, 2004; Guttery et al., 2010; Al-Alwan et al., 2011; Servais et al., 2012; Pietras et al., 2014). Relative to the MTSO cells grown in normal medium, tenascin-C, CD44, osteopontin, fascin, and mesothelin were all significantly induced in MSTO cells grown in TnT medium (**Figure 9C**). Further studies will evaluate whether induction of these genes in cells grown in TnT medium induce an adaptive gene expression profile leading to TnT formation and a higher propensity to invade, migrate, and metastasize.

DISCUSSION

Intercellular communication between cancer cells is crucial to the progression of invasive cancers, but the mechanisms by which communication occurs between distant and proximal cells in a tumor matrix remains poorly understood. TnTs are a novel candidate to explain how this communication process occurs (Lou et al., 2012a). Our prior and current work have consistently demonstrated TnTs in malignant mesothelioma and lung adenocarcinoma tumors from human patients (Lou et al., 2012b). This observation is consistent with the finding of another group

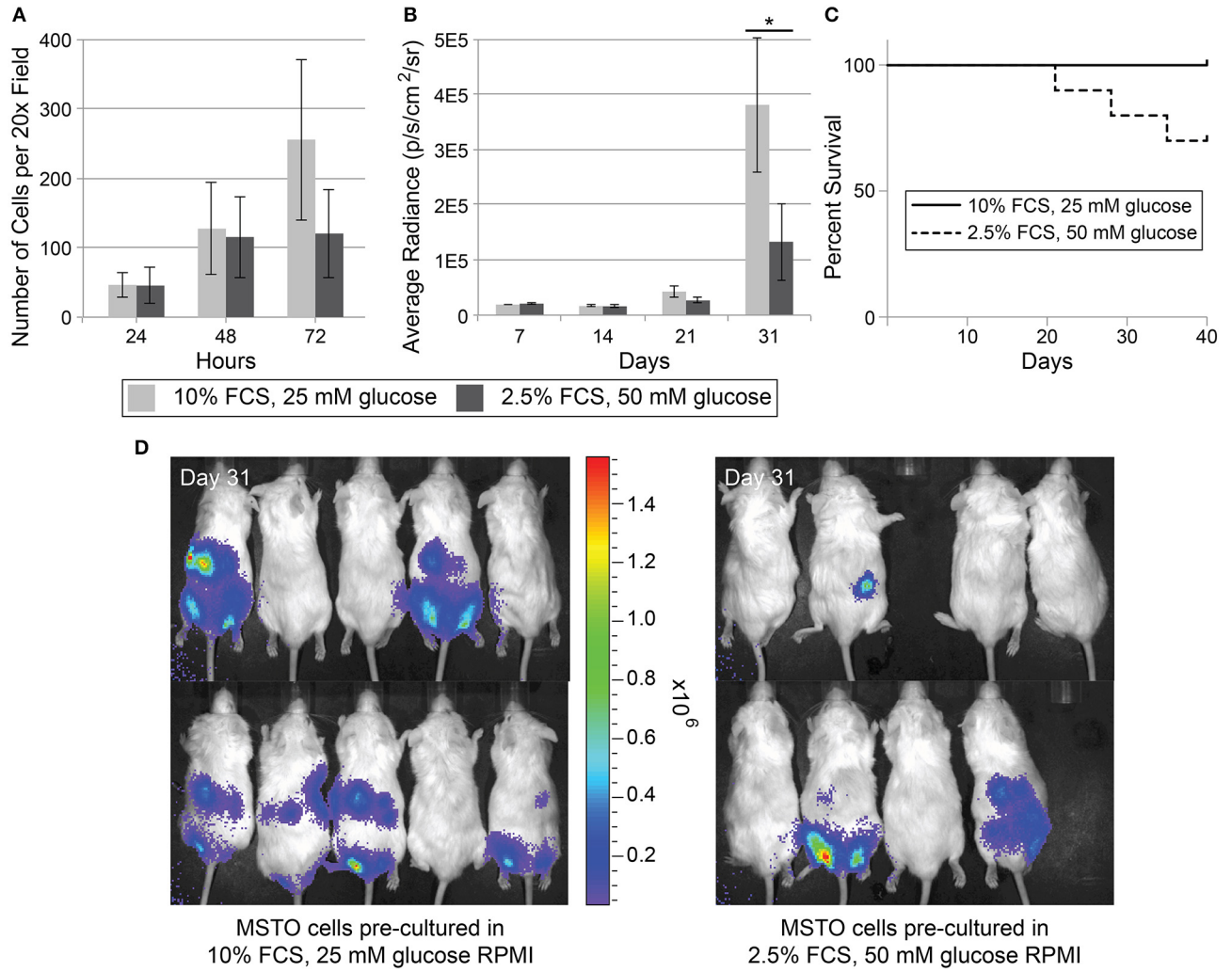

FIGURE 8 | Decreased tumor growth and survival of mice implanted with TnT-primed mesothelioma cells. (A) *In vitro* cellular proliferation rate of MSTO-211H cells cultured in passage medium (10% FCS, 25 mM glucose RPMI) vs. TnT medium (2.5% FCS, 50mM glucose RPMI); **(B)** Average radiance of tumor growth at 7,14,21, and 31 days following peritoneal implantation in immunodeficient NOG mice of MSTO-211H cells cultured for 7 days using either passage medium or TnT medium; *indicates statistically significant difference between the two groups ($p < 0.05$); **(C)** Kaplan–Meier curve of survival of injected NOG mice, 10 mice in each group; **(D)** Bioimaging of NOG mice from each cohort.

that successfully imaged membrane nanotubes *in vivo* using an inflammatory cornea animal model (Chinnery et al., 2008). We have further demonstrated that TnTs are not exclusive to malignant mesothelioma and lung adenocarcinoma, but can form between malignant cells from a wide variety of histologic cancers, including pancreatic cancer as one example (Lou et al., 2013). In the present study, we describe our approaches to studying the relevance of TnTs in invasive malignancies, specifically in the context of MPM.

TnT LENGTH AS A FUNCTION OF THE NEED FOR INTERCOMMUNICATION AMONG MESOTHELIOMA CELLS

When interpreting our findings of both cell proliferation rate and changes in TnT lengths, we take into account likely differences in natural biology and aggressiveness of the variable cell histologies (i.e., VAMT = sarcomatoid; H2052 = epithelioid, likely less aggressive; MSTO-211H = biphasic, encompassing features of both of VAMT and H2052). It is logical that as cells proliferate and are also motile, with less distance between cells over time, the average TnT length would decrease over time. The most aggressive cell line (VAMT, sarcomatoid) displayed the longest TnT length at 24 h (**Figure 2**), but not the highest proliferation rate by 72 h (**Figure 1C**); conversely, MSTO cells had the highest proliferation rate, but relatively shorter TnTs. Logically, this presents an interesting supposition: That cells proliferating at a low rate can be just as—if not more—aggressive, perhaps by forming longer TnTs and/or more TnTs. Knowing the clinical outcomes are worse with sarcomatoid variants than with other forms of mesothelioma, we postulate that this may hold true in the clinical setting. Further investigation is warranted based on these findings.

A key clinical manifestation of advanced thoracic malignancy (i.e., MPM and lung adenocarcinoma) is accumulation of pleural

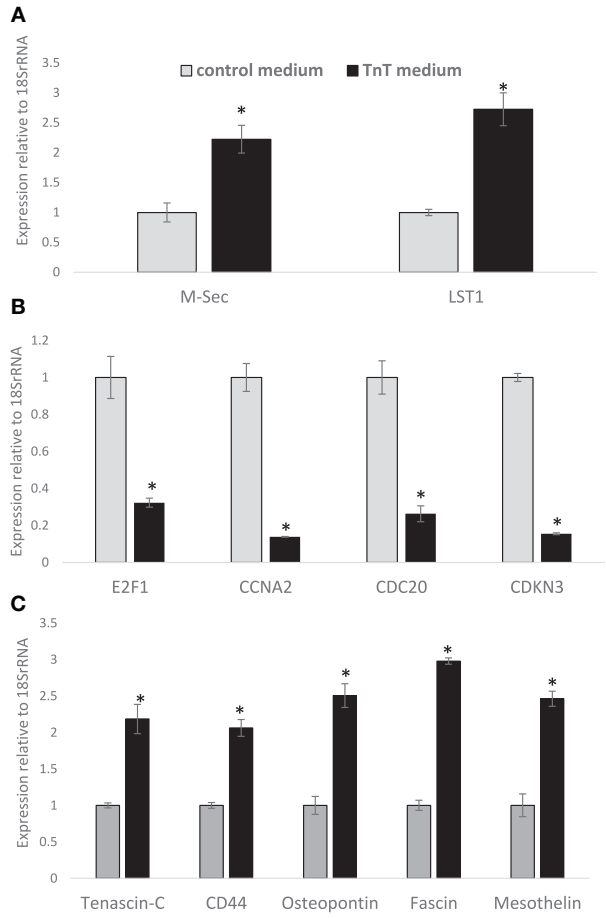

FIGURE 9 | Gene expression profiling of mesothelioma cells cultured in passage medium vs. TnT medium. Expression of selected genes in MSTO cells grown in TnT media; samples were run in triplicate and means ± standard deviations are presented. Gray columns = results from cells grown in Control medium; black columns = results from cells grown in TnT medium. Expression of genes specific to TnTs **(A)**, cell cycle regulation **(B)**, and genes attributed to invasion, migration and metastasis **(C)** relative to cells grown in control media are shown. Note the significant downregulation of genes that positively modulate cell cycle in cells grown in TnT media. Conversely, genes attributed to cellular invasion, migration and metastasis functions are upregulated (*indicate *p*-values <0.05).

fluid that marks development of pleural effusions. Ascites is a similar process marked by accumulation of fluid in the abdominal cavity or peritoneum. In advanced cancers such as pleural or peritoneal mesothelioma, the accumulation of malignant fluid is a diagnostic and prognostic hallmark of aggressive disease. These effusions often contain a significant number of free-floating or suspended malignant cells; diagnosis can be made following cytologic examination of extracted fluid. However, beyond examination as a mere diagnostic marker, little is known about the role this specific cell population plays in the propagation of mesothelioma and disease progression. This population of free-floating, suspended cells is capable of undergoing epithelial-to-mesenchymal transition (EMT), thus increasing their invasive capability. In our prior study, we demonstrated that EMT effectively stimulates TnT formation in mesothelioma, as does acidic pH (Lou et al., 2012b) in the context of low-serum, hyperglycemic medium. This is especially important as low pH of pleural fluid derived from malignant effusions, including those derived from malignant mesothelioma, is a poor prognostic factor associated with decreased overall patient survival (Sahn and Good, 1988; Gottehrer et al., 1991).

In the present study, we examined extra-cytoplasmic actin extension of TnTs. We found that as mesothelioma cells proliferated the average TnT length decreased over time, possibly as a result of the low cellular requirement for long-distance connections among confluent cultures. Further, our *in vitro* model of pleural/peritoneal effusions indicated that TnTs may function as tethers that link suspended, non-adherent malignant cells to other suspended cells or adherent cells of the pleural lining of the thoracic cavity. These findings indicate that non-adherent viable cells in culture behave similarly to suspended effusion cells from mesothelioma patients and that these cells are capable of forming TnTs. Relative differences in TnT length may be a function of chemotactic factors promoting their formation and guiding their extension; a precedent has been established for this in correlation of length of cytonemes (actin-based filopodial protrusions similar to TnTs) to length of chemotactic gradients of Hedgehog signals in Drosophila wing disc models (Bischoff et al., 2013).

DEVELOPING *IN VITRO* MODELS THAT SIMULATE POTENTIAL TnT ACTIVITY IN AN *IN VIVO* TUMOR MICROENVIRONMENT

To study the formation and function of TnTs, 3-dimensional *in vitro* models are needed to simulate the complex tumor microenvironment. A major challenge to 3-dimensional models of TnT signaling is the presence of other forms of external signaling that may confound study results. Exosomes, microvesicles, and other freely diffusible signals play an established role in intercellular signaling. Indeed, data recently published by our group demonstrated that tumor-derived exosomes stimulate TnT formation in mesothelioma cell culture (Thayanithy et al., 2014b). A previous report showed that other forms of external signaling could be excluded by culturing normal rat kidney cells in a viscous agarose matrix; this approach significantly decreased diffusion of extracellular signals, including from microvesicles or other free particles, while permitting TnT formation (Gurke et al., 2008). For the first time, in the current study we apply use of "TnT medium" (low-serum, hyperglycemic culture medium) to agarose in a relatively viscous microenvironment that not only remains permissive for, but also further induces, TnT formation in a manner that is reliable for further study. We propose using this approach for future studies that aim to minimize potential effect of exosomes and other diffusible factors that act as stimulatory signals and intercellular carriers of cargo, thus isolating examination of TnTs for specific analyses.

TnTs AS A THERAPEUTIC TARGET FOR MESOTHELIOMA AND OTHER TnT-FORMING MALIGNANCIES

TnTs are not exclusive to cancer and are a cellular entity in "normal," non-malignant cells. For the purposes of studying the potential role of TnTs in cancer, we developed a tool to

quantitatively assess TnT numbers that could be used as a "nanotube index" to study how increased "intercellular trafficking" of cellular cargo via TnTs is related to cell transformation and tumor formation. We adapted confocal microscopic techniques to visualize narrow nanotube structures. Quantitative assessment of TnTs/cell indicated that TnTs formed at a markedly higher rate among malignant mesothelioma cell lines than among normal mesothelial cells and in inverse proportion to the rate of cell proliferation. In fact, we found that the culture condition that most increased TnT numbers (low-serum, hyperglycemic medium, which we call "TnT medium") did not lead to a corresponding increase in cell number, but rather a notable decrease in cell proliferation by approximately half. We attribute this decreased cell proliferation to both elements, i.e., low serum concentration (2.5% FBS) as well as high glucose, which induces reductions in cell proliferation as well as increased cell apoptosis of pericytes *in vitro* (Beltramo et al., 2006). These data indicate that TnT formation and cell proliferation are distinct processes that may occur during specific stages of malignant growth.

We previously used several inhibitors of pathways that have been implicated in actin-based cell invasion, including latrunculin A, an actin-destabilizing agent that is commonly used in *in vitro* studies and that has been used in multiple TnT studies (Tavi et al., 2010; Lou et al., 2012b; Vallabhaneni et al., 2012). We previously investigated potential metabolic pathways essential for TnT formation in mesothelioma and effectively demonstrated suppression of TnT formation using drugs that are used in the clinical setting for other malignancies, such as an mTOR inhibitor and the widely available drug metformin (Lou et al., 2012b), which stimulates AMP-activated protein kinase (AMPK) and thus indirectly stimulates the mTOR pathway as well (Zhou et al., 2001). This is particularly important in context of our findings in the current study that effusion-derived mesothelioma cells (from both cell lines and from human patients) form aggregate spheroids that are tethered by TnTs. *In vitro* 3-D spheroid models of mesothelioma demonstrate increased resistance to drugs and apoptosis compared to 2-dimensional cultures, and this is at least in part mediated by mTOR; however, inhibitors of mTOR can overcome this acquired resistance (Barbone et al., 2008; Wilson et al., 2008). Considering susceptibility of TnTs to mTOR inhibition, TnTs may play an important role in mediating chemoresistance of spheroids.

In the current study, we demonstrate that an additional rational drug—migrastatin—suppresses TnT formation in mesothelioma. Migrastatin has been found to be potent in blocking migration and metastasis of lung cancer in separate studies (Lecomte et al., 2011), providing impetus for further exploration of this drug as a potential novel therapeutic agent for both lung adenocarcinoma and MPM.

ACCURATE *IN VIVO* ASSESSMENT OF TnT FUNCTIONS

In vivo examination of TnTs remains a major barrier to the study of the function of TnTs in cancer. *In vivo* studies of nanotubes have been limited to an inflammatory corneal model in mice (Chinnery et al., 2008; Seyed-Razavi et al., 2013), but successful intravital microscopy has been performed visualizing similar cellular extensions called cytonemes in Drosophila (Bischoff et al., 2013). We also developed specific protocols for imaging putative TnTs in human tumors, as our group's main research focus is cancer cell biology of highly invasive malignancies. In previous studies, we obtained 6 fresh intact tumor specimens from patients with either MPM or lung adenocarcinoma immediately following surgical resection. Using a Vibratome, we processed the specimens into thin cuts that were amenable to staining with Hoechst dye to visualize nuclei and MitoTracker Red to visualize the cell body and TnTs, which we had already demonstrated to work *in vitro* (Lou et al., 2012b). Of the six human patient-derived tumors, we detected TnTs in all six using confocal microscopy and 3-dimensional reconstruction using the Imaris software. TnTs have also been reported in ovarian tumor explants by our group and others (Pasquier et al., 2013; Thayanithy et al., 2014a). In the present study, cells primed in TnT medium had a lower proliferation rate *in vitro*; proliferation rate of these cells was similar when injected *in vivo*, as measured by lower detectable radiance. This is also supported by our finding that the level of genes involved in cell proliferation were also expressed at lower levels in cells that were primed in TnT medium compared to the cells primed with normal media (**Figure 9**). Although mice implanted with TnT-primed mesothelioma cells had lower overall disease burden, they also had poorer survival compared to mice implanted with mesothelioma cells pre-conditioned in control medium. Thus we postulate that a higher rate of formation of TnTs *in vivo* is associated with a higher level of local invasion of tumors, leading to lower survival in this animal model. Future work in our lab will follow up on these findings.This *in vivo* model will prove to be especially important to examining TnTs as a potential therapeutic target for treatment of cancer and subsequent studies for drug delivery via TnTs.

CONCLUSIONS

In Conclusion, the mechanisms by which cells communicate with one another in the tumor microenvironment are not well understood (Bissell and Radisky, 2001; Pietras and Ostman, 2010; Bissell and Hines, 2011). Our works challenges the current paradigm that gap junctions, exosomes, or cytokines and other diffusible chemical signals are exclusive modes by which cells mediate intercellular communication in mesothelioma. Tunneling nanotubes are a novel biologic conduit for intercellular signaling and transport of cellular cargo. At this time, there appear to be more questions than answers in terms of what the mechanisms, functions, and role of these nano-sized structures are in various cell types. TnTs have attracted the interest of researchers across a spectrum of fields including neuroscience, immunology, infectious diseases, and cancer as described here. What remains unknown is how these diseases use TnTs to coordinate "social networking" among connected cells, which characteristics of TnTs are universal across cell types (e.g., cancer vs. non-cancer cells), and which aspects may be unique to the cell type studied. Researchers with interest in cellular communication may adapt their approach to the study of TnTs according to their research objectives. In this paper, we describe our approach to studying the relevance of TnTs in cancer, specifically in the context of the solid tumor matrix of aggressive malignancies.

ACKNOWLEDGMENTS

We wish to thank Tao Tong, Sho Fujisawa, Ph.D, Yevgeniy Romin, Afsar Barlas, M.D., Sanghoon Oh, Ph.D. and Jiang-Cheng Wang, Ph.D. of the Molecular Cytology Core Facility at MSKCC for their helpful suggestions, expertise, and assistance with imaging and immunofluorescence; Mesruh Turkekul and Ning Fan for assistance with immunofluorescent staining; Nina Lampen for assistance with electron microscopy; Samuel Danishefsky, Ph.D for providing the migrastatin core ether compound; Valerie Rusch, M.D. of the Thoracic Surgery Service at MSKCC for providing primary pleural effusion and ascites specimens; and Ms. Katherine DeBeer for administrative assistance and support. We also thank Michael Franklin, M.S. for excellent editorial suggestions and critical review of the manuscript. This research was kindly funded and supported in part by the Baker Street Foundation, Minnesota Masonic Charities, Minnesota Medical Foundation, Institutional Research Grant #118198-IRG-58-001-52-IRG94 from the American Cancer Society, the Deborah Powell Center for Women's Health at the University of Minnesota, the National Pancreas Foundation, and the UMN Clinical and Translational Science Institute KL2 Scholar Award (to Emil Lou, grant number 5KL2TR113). Additional funding was provided by the National Center for Advancing Translational Sciences of the National Institutes of Health Award Number UL1TR000114. The content is solely the responsibility of the authors and does not necessarily represent the official views of the National Institutes of Health.

SUPPLEMENTARY MATERIAL

The Supplementary Material for this article can be found online at: http://www.frontiersin.org/journal/10.3389/fphys.2014.00400/abstract

Movie S1 | Time-lapse microscopy imaging of intercellular transfer of mitochondria between mesothelioma cells connected via a TnT. We used MitoTracker Red to stain MSTO-211H cells which were then cultured in hyperglycemic, low-serum ("TnT") medium. Cells were allowed to adhere and form TnTs, which were then identified for analysis. Images were taken every 20 min for 24 h using a Perkin–Elmer spinning-disk confocal microscope.

Movie S2 | 3-dimensional modeling of a nanotube. Cells were stained with vimentin (red) and nuclear staining with Hoechst 33342 dye (blue) as described. Images were were taken as a z-stack at 40× and compiled using Imaris Viewer software.

Movie S3 | Intercellular transfer of GFP between mesothelioma cells connected via TnTs. GFP-expressing (green) MSTO-211H cells were co-cultured with MSTO cells stained with the lipophilic dye DiI (red) as we have reported previously (Lou et al., 2012b) and cultured in 37°C, 5% CO_2 for time-lapse imaging. Images were taken every 15 min for 5 h. In this sequence, the middle cell (green) is connected to two cells simultaneously via TnTs, which facilitate transfer of GFP both to and from that cell.

Movie S4 | Intercellular transfer of GFP via TnT connecting two MSTO-211H cells. Higher-magnification view and time-lapse microscopy demonstrating bidirectional transfer of GFP between connected cells.

Movie S5 | 3-dimensional reconstruction of a tumor surgically resected from a human patient with malignant pleural mesothelioma. 3-dimensional imaging was performed using the Imaris Viewer.

REFERENCES

Al-Alwan, M., Olabi, S., Ghebeh, H., Barhoush, E., Tulbah, A., Al-Tweigeri, T., et al. (2011). Fascin is a key regulator of breast cancer invasion that acts via the modification of metastasis-associated molecules. *PLoS ONE* 6:e27339. doi: 10.1371/journal.pone.0027339

Asplund, T., and Heldin, P. (1994). Hyaluronan receptors are expressed on human malignant mesothelioma cells but not on normal mesothelial cells. *Cancer Res.* 54, 4516–4523.

Axelrod, R., Axelrod, D. E., and Pienta, K. J. (2006). Evolution of cooperation among tumor cells. *Proc. Natl. Acad. Sci. U.S.A.* 103, 13474–13479. doi: 10.1073/pnas.0606053103

Barbone, D., Yang, T. M., Morgan, J. R., Gaudino, G., and Broaddus, V. C. (2008). Mammalian target of rapamycin contributes to the acquired apoptotic resistance of human mesothelioma multicellular spheroids. *J. Biol. Chem.* 283, 13021–13030. doi: 10.1074/jbc.M709698200

Beltramo, E., Berrone, E., Giunti, S., Gruden, G., Perin, P. C., and Porta, M. (2006). Effects of mechanical stress and high glucose on pericyte proliferation, apoptosis and contractile phenotype. *Exp. Eye Res.* 83, 989–994. doi: 10.1016/j.exer.2006.05.008

Bischoff, M., Gradilla, A. C., Seijo, I., Andres, G., Rodriguez-Navas, C., Gonzalez-Mendez, L., et al. (2013). Cytonemes are required for the establishment of a normal Hedgehog morphogen gradient in Drosophila epithelia. *Nat. Cell Biol.* 15, 1269–1281. doi: 10.1038/ncb2856

Bissell, M. J., and Hines, W. C. (2011). Why don't we get more cancer? A proposed role of the microenvironment in restraining cancer progression. *Nat. Med.* 17, 320–329. doi: 10.1038/nm.2328

Bissell, M. J., and Radisky, D. (2001). Putting tumours in context. *Nat. Rev. Cancer* 1, 46–54. doi: 10.1038/35094059

Bobrie, A., Colombo, M., Raposo, G., and Thery, C. (2011). Exosome secretion: molecular mechanisms and roles in immune responses. *Traffic* 12, 1659–1668. doi: 10.1111/j.1600-0854.2011.01225.x

Bracken, A. P., Ciro, M., Cocito, A., and Helin, K. (2004). E2F target genes: unraveling the biology. *Trends Biochem. Sci.* 29, 409–417. doi: 10.1016/j.tibs.2004.06.006

Cerruto, C. A., Brun, E. A., Chang, D., and Sugarbaker, P. H. (2006). Prognostic significance of histomorphologic parameters in diffuse malignant peritoneal mesothelioma. *Arch. Pathol. Lab. Med.* 130, 1654–1661. doi: 10.1043/1543-2165(2006)130[1654:PSOHPI]2.0.CO;2

Chen, L., Yang, S., Jakoncic, J., Zhang, J. J., and Huang, X. Y. (2010). Migrastatin analogues target fascin to block tumour metastasis. *Nature* 464, 1062–1066. doi: 10.1038/nature08978

Chen, S. F., Lin, Y. S., Jao, S. W., Chang, Y. C., Liu, C. L., Lin, Y. J., et al. (2013). Pulmonary adenocarcinoma in malignant pleural effusion enriches cancer stem cell properties during metastatic cascade. *PLoS ONE* 8:e54659. doi: 10.1371/journal.pone.0054659

Chinnery, H. R., Pearlman, E., and McMenamin, P. G. (2008). Cutting edge: Membrane nanotubes *in vivo*: a feature of MHC class II+ cells in the mouse cornea. *J. Immunol.* 180, 5779–5783. doi: 10.4049/jimmunol.180.9.5779

Chunhacha, P., Sriuranpong, V., and Chanvorachote, P. (2013). Epithelial-mesenchymal transition mediates anoikis resistance and enhances invasion in pleural effusion-derived human lung cancer cells. *Oncol. Lett.* 5, 1043–1047. doi: 10.3892/ol.2013.1108

Cottin, S., Ghani, K., de Campos-Lima, P. O., and Caruso, M. (2010). Gemcitabine intercellular diffusion mediated by gap junctions: new implications for cancer therapy. *Mol. Cancer* 9:141. doi: 10.1186/1476-4598-9-141

Cselenyak, A., Pankotai, E., Horvath, E. M., Kiss, L., and Lacza, Z. (2010). Mesenchymal stem cells rescue cardiomyoblasts from cell death in an *in vitro* ischemia model via direct cell-to-cell connections. *BMC Cell Biol.* 11:29. doi: 10.1186/1471-2121-11-29

Davis, D. M., and Sowinski, S. (2008). Membrane nanotubes: dynamic long-distance connections between animal cells. *Nat. Rev. Mol. Cell Biol.* 9, 431–436. doi: 10.1038/nrm2399

de La Motte, C. A., Hascall, V. C., Calabro, A., Yen-Lieberman, B., and Strong, S. A. (1999). Mononuclear leukocytes preferentially bind via CD44 to hyaluronan on human intestinal mucosal smooth muscle cells after virus infection or treatment with poly(I.C). *J. Biol. Chem.* 274, 30747–30755. doi: 10.1074/jbc.274.43.30747

DiCorleto, P. E., and de la Motte, C. A. (1985). Characterization of the adhesion of the human monocytic cell line U937 to cultured endothelial cells. *J. Clin. Invest.* 75, 1153–1161. doi: 10.1172/JCI111810

Eugenin, E. A., Gaskill, P. J., and Berman, J. W. (2009). Tunneling nanotubes (TNT) are induced by HIV-infection of macrophages: a potential mechanism for intercellular HIV trafficking. *Cell. Immunol.* 254, 142–148. doi: 10.1016/j.cellimm.2008.08.005

Galkina, S. I., Stadnichuk, V. I., Molotkovsky, J. G., Romanova, J. M., Sud'ina, G. F., and Klein, T. (2010). Microbial alkaloid staurosporine induces formation of nanometer-wide membrane tubular extensions (cytonemes, membrane tethers) in human neutrophils. *Cell Adh. Migr.* 4, 32–38. doi: 10.4161/cam.4.1.10314

Gottehrer, A., Taryle, D. A., Reed, C. E., and Sahn, S. A. (1991). Pleural fluid analysis in malignant mesothelioma. Prognostic implications. *Chest* 100, 1003–1006. doi: 10.1378/chest.100.4.1003

Gousset, K., Schiff, E., Langevin, C., Marijanovic, Z., Caputo, A., Browman, D. T., et al. (2009). Prions hijack tunnelling nanotubes for intercellular spread. *Nat. Cell Biol.* 11, 328–336. doi: 10.1038/ncb1841

Gurke, S., Barroso, J. F., Hodneland, E., Bukoreshtliev, N. V., Schlicker, O., and Gerdes, H. H. (2008). Tunneling nanotube (TNT)-like structures facilitate a constitutive, actomyosin-dependent exchange of endocytic organelles between normal rat kidney cells. *Exp. Cell Res.* 314, 3669–3683. doi: 10.1016/j.yexcr.2008.08.022

Guttery, D. S., Hancox, R. A., Mulligan, K. T., Hughes, S., Lambe, S. M., Pringle, J. H., et al. (2010). Association of invasion-promoting tenascin-C additional domains with breast cancers in young women. *Breast Cancer Res.* 12:R57. doi: 10.1186/bcr2618

Harada, K., Sato, Y., Ikeda, H., Isse, K., Ozaki, S., Enomae, M., et al. (2009). Epithelial-mesenchymal transition induced by biliary innate immunity contributes to the sclerosing cholangiopathy of biliary atresia. *J. Pathol.* 217, 654–664. doi: 10.1002/path.2488

Hase, K., Kimura, S., Takatsu, H., Ohmae, M., Kawano, S., Kitamura, H., et al. (2009). M-Sec promotes membrane nanotube formation by interacting with Ral and the exocyst complex. *Nat. Cell Biol.* 11, 1427–1432. doi: 10.1038/ncb1990

He, K., Shi, X., Zhang, X., Dang, S., Ma, X., Liu, F., et al. (2011). Long-distance intercellular connectivity between cardiomyocytes and cardiofibroblasts mediated by membrane nanotubes. *Cardiovasc. Res.* 92, 39–47. doi: 10.1093/cvr/cvr189

Hegmans, J. P., Bard, M. P., Hemmes, A., Luider, T. M., Kleijmeer, M. J., Prins, J. B., et al. (2004). Proteomic analysis of exosomes secreted by human mesothelioma cells. *Am. J. Pathol.* 164, 1807–1815. doi: 10.1016/S0002-9440(10)63739-X

Huber, M. A., Kraut, N., and Beug, H. (2005). Molecular requirements for epithelial-mesenchymal transition during tumor progression. *Curr. Opin. Cell Biol.* 17, 548–558. doi: 10.1016/j.ceb.2005.08.001

Islam, M. N., Das, S. R., Emin, M. T., Wei, M., Sun, L., Westphalen, K., et al. (2012). Mitochondrial transfer from bone-marrow-derived stromal cells to pulmonary alveoli protects against acute lung injury. *Nat. Med.* 18, 759–765. doi: 10.1038/nm.2736

Kadiu, I., and Gendelman, H. E. (2011). Human immunodeficiency virus type 1 endocytic trafficking through macrophage bridging conduits facilitates spread of infection. *J. Neuroimmune Pharmacol.* 6, 658–675. doi: 10.1007/s11481-011-9298-z

Kenny, P. A., Lee, G. Y., and Bissell, M. J. (2007). Targeting the tumor microenvironment. *Front. Biosci.* 12, 3468–3474. doi: 10.2741/2327

Koyanagi, M., Brandes, R. P., Haendeler, J., Zeiher, A. M., and Dimmeler, S. (2005). Cell-to-cell connection of endothelial progenitor cells with cardiac myocytes by nanotubes: a novel mechanism for cell fate changes? *Circ. Res.* 96, 1039–1041. doi: 10.1161/01.RES.0000168650.23479.0c

Kultti, A., Pasonen-Seppanen, S., Jauhiainen, M., Rilla, K. J., Karna, R., Pyoria, E., et al. (2009). 4-Methylumbelliferone inhibits hyaluronan synthesis by depletion of cellular UDP-glucuronic acid and downregulation of hyaluronan synthase 2 and 3. *Exp. Cell Res.* 315, 1914–1923. doi: 10.1016/j.yexcr.2009.03.002

Kultti, A., Rilla, K., Tiihonen, R., Spicer, A. P., Tammi, R. H., and Tammi, M. I. (2006). Hyaluronan synthesis induces microvillus-like cell surface protrusions. *J. Biol. Chem.* 281, 15821–15828. doi: 10.1074/jbc.M512840200

Lamorte, L., Royal, I., Naujokas, M., and Park, M. (2002). Crk adapter proteins promote an epithelial-mesenchymal-like transition and are required for HGF-mediated cell spreading and breakdown of epithelial adherens junctions. *Mol. Biol. Cell* 13, 1449–1461. doi: 10.1091/mbc.01-10-0477

Lauer, M. E., Mukhopadhyay, D., Fulop, C., de la Motte, C. A., Majors, A. K., and Hascall, V. C. (2009). Primary murine airway smooth muscle cells exposed to poly(I,C) or tunicamycin synthesize a leukocyte-adhesive hyaluronan matrix. *J. Biol. Chem.* 284, 5299–5312. doi: 10.1074/jbc.M807965200

Lecomte, N., Njardarson, J. T., Nagorny, P., Yang, G., Downey, R., Ouerfelli, O., et al. (2011). Emergence of potent inhibitors of metastasis in lung cancer via syntheses based on migrastatin. *Proc. Natl. Acad. Sci. U.S.A.* 108, 15074–15078. doi: 10.1073/pnas.1015247108

Li, Y., and Heldin, P. (2001). Hyaluronan production increases the malignant properties of mesothelioma cells. *Br. J. Cancer* 85, 600–607. doi: 10.1054/bjoc.2001.1922

Lou, E., Fujisawa, S., Barlas, A., Romin, Y., Manova-Todorova, K., Moore, M. A., et al. (2012a). Tunneling nanotubes: a new paradigm for studying intercellular communication and therapeutics in cancer. *Commun. Integr. Biol.* 5, 399–403. doi: 10.4161/cib.20569

Lou, E., Fujisawa, S., Morozov, A., Barlas, A., Romin, Y., Dogan, Y., et al. (2012b). Tunneling nanotubes provide a unique conduit for intercellular transfer of cellular contents in human malignant pleural mesothelioma. *PLoS ONE* 7:e33093. doi: 10.1371/journal.pone.0033093

Lou, E., Subramanian, S., and Steer, C. J. (2013). Pancreatic cancer: modulation of KRAS, MicroRNAs, and intercellular communication in the setting of tumor heterogeneity. *Pancreas* 42, 1218–1226. doi: 10.1097/MPA.0000000000000007

Majors, A. K., Austin, R. C., de la Motte, C. A., Pyeritz, R. E., Hascall, V. C., Kessler, S. P., et al. (2003). Endoplasmic reticulum stress induces hyaluronan deposition and leukocyte adhesion. *J. Biol. Chem.* 278, 47223–47231. doi: 10.1074/jbc.M304871200

McBride, W. H., and Bard, J. B. (1979). Hyaluronidase-sensitive halos around adherent cells. Their role in blocking lymphocyte-mediated cytolysis. *J. Exp. Med.* 149, 507–515. doi: 10.1084/jem.149.2.507

Minuth, W. W., and Denk, L. (2012). Cell projections and extracellular matrix cross the interstitial interface within the renal stem/progenitor cell niche: accidental, structural or functional cues? *Nephron Exp. Nephrol.* 122, 131–140. doi: 10.1159/000351129

Morohashi, H., Kon, A., Nakai, M., Yamaguchi, M., Kakizaki, I., Yoshihara, S., et al. (2006). Study of hyaluronan synthase inhibitor, 4-methylumbelliferone derivatives on human pancreatic cancer cell (KP1-NL). *Biochem. Biophys. Res. Commun.* 345, 1454–1459. doi: 10.1016/j.bbrc.2006.05.037

Motta, A. B., Pinheiro, G., Antonângelo, L., Parra, E. R., Monteiro, M. M., Pereira, J. C. D. N., et al. (2006). Marcadores morfológicos de prognóstico no mesotelioma maligno: um estudo de 58 casos. *J. Bras. Pneumol.* 32, 322–332. doi: 10.1590/S1806-37132006000400011

Mueller, M. M., and Fusenig, N. E. (2004). Friends or foes–bipolar effects of the tumour stroma in cancer. *Nat. Rev. Cancer* 4, 839–849. doi: 10.1038/nrc1477

Nalepa, G., Barnholtz-Sloan, J., Enzor, R., Dey, D., He, Y., Gehlhausen, J. R., et al. (2013). The tumor suppressor CDKN3 controls mitosis. *J. Cell Biol.* 201, 997–1012. doi: 10.1083/jcb.201205125

Naus, C. C., and Laird, D. W. (2010). Implications and challenges of connexin connections to cancer. *Nat. Rev. Cancer* 10, 435–441. doi: 10.1038/nrc2841

Onfelt, B., Nedvetzki, S., Benninger, R. K., Purbhoo, M. A., Sowinski, S., Hume, A. N., et al. (2006). Structurally distinct membrane nanotubes between human macrophages support long-distance vesicular traffic or surfing of bacteria. *J. Immunol.* 177, 8476–8483. doi: 10.4049/jimmunol.177.12.8476

Onfelt, B., Purbhoo, M. A., Nedvetzki, S., Sowinski, S., and Davis, D. M. (2005). Long-distance calls between cells connected by tunneling nanotubules. *Sci. STKE* 2005:pe55. doi: 10.1126/stke.3132005pe55

Oskarsson, T., Nagorny, P., Krauss, I. J., Perez, L., Mandal, M., Yang, G., et al. (2010). Diverted total synthesis leads to the generation of promising cell-migration inhibitors for treatment of tumor metastasis: *in vivo* and mechanistic studies on the migrastatin core ether analog. *J. Am. Chem. Soc.* 132, 3224–3228. doi: 10.1021/ja9101503

Pap, E., Pallinger, E., and Falus, A. (2011). The role of membrane vesicles in tumorigenesis. *Crit. Rev. Oncol. Hematol.* 79, 213–223. doi: 10.1016/j.critrevonc.2010.07.015

Pasquier, J., Guerrouahen, B. S., Al Thawadi, H., Ghiabi, P., Maleki, M., Abu-Kaoud, N., et al. (2013). Preferential transfer of mitochondria from endothelial to cancer cells through tunneling nanotubes modulates chemoresistance. *J. Transl. Med.* 11:94. doi: 10.1186/1479-5876-11-94

Pietras, A., Katz, A. M., Ekstrom, E. J., Wee, B., Halliday, J. J., Pitter, K. L., et al. (2014). Osteopontin-CD44 signaling in the glioma perivascular niche enhances cancer stem cell phenotypes and promotes aggressive tumor growth. *Cell Stem Cell* 14, 357–369. doi: 10.1016/j.stem.2014.01.005

Pietras, K., and Ostman, A. (2010). Hallmarks of cancer: interactions with the tumor stroma. *Exp. Cell Res.* 316, 1324–1331. doi: 10.1016/j.yexcr.2010.02.045

Plotnikov, E. Y., Khryapenkova, T. G., Galkina, S. I., Sukhikh, G. T., and Zorov, D. B. (2010). Cytoplasm and organelle transfer between mesenchymal multipotent stromal cells and renal tubular cells in co-culture. *Exp. Cell Res.* 316, 2447–2455. doi: 10.1016/j.yexcr.2010.06.009

Pyrgaki, C., Trainor, P., Hadjantonakis, A. K., and Niswander, L. (2010). Dynamic imaging of mammalian neural tube closure. *Dev. Biol.* 344, 941–947. doi: 10.1016/j.ydbio.2010.06.010

Ranzinger, J., Rustom, A., Abel, M., Leyh, J., Kihm, L., Witkowski, M., et al. (2011). Nanotube action between human mesothelial cells reveals novel aspects of inflammatory responses. *PLoS ONE* 6:e29537. doi: 10.1371/journal.pone.0029537

Rilla, K., Tiihonen, R., Kultti, A., Tammi, M., and Tammi, R. (2008). Pericellular hyaluronan coat visualized in live cells with a fluorescent probe is scaffolded by plasma membrane protrusions. *J. Histochem. Cytochem.* 56, 901–910. doi: 10.1369/jhc.2008.951665

Rittling, S. R., and Chambers, A. F. (2004). Role of osteopontin in tumour progression. *Br. J. Cancer* 90, 1877–1881. doi: 10.1038/sj.bjc.6601839

Ruckert, F., Grutzmann, R., and Pilarsky, C. (2012). Feedback within the intercellular communication and tumorigenesis in carcinomas. *PLoS ONE* 7:e36719. doi: 10.1371/journal.pone.0036719

Rudnicka, D., Feldmann, J., Porrot, F., Wietgrefe, S., Guadagnini, S., Prevost, M. C., et al. (2009). Simultaneous cell-to-cell transmission of human immunodeficiency virus to multiple targets through polysynapses. *J. Virol.* 83, 6234–6246. doi: 10.1128/JVI.00282-09

Rustom, A., Saffrich, R., Markovic, I., Walther, P., and Gerdes, H. H. (2004). Nanotubular highways for intercellular organelle transport. *Science* 303, 1007–1010. doi: 10.1126/science.1093133

Sahn, S. A., and Good, J. T. Jr. (1988). Pleural fluid pH in malignant effusions. Diagnostic, prognostic, and therapeutic implications. *Ann. Intern. Med.* 108, 345–349 doi: 10.7326/0003-4819-108-3-345

Salter, R. D., and Watkins, S. C. (2006). Dynamic properties of antigen uptake and communication between dendritic cells. *Immunol. Res.* 36, 211–220. doi: 10.1385/IR:36:1:211

Schiller, C., Diakopoulos, K. N., Rohwedder, I., Kremmer, E., von Toerne, C., Ueffing, M., et al. (2013). LST1 promotes the assembly of a molecular machinery responsible for tunneling nanotube formation. *J. Cell Sci.* 126(Pt 3), 767–777. doi: 10.1242/jcs.114033

Schmittgen, T. D., and Livak, K. J. (2008). Analyzing real-time PCR data by the comparative C(T) method. *Nat. Protoc.* 3, 1101–1108. doi: 10.1038/nprot.2008.73

Scholler, N., Fu, N., Yang, Y., Ye, Z., Goodman, G. E., Hellstrom, K. E., et al. (1999). Soluble member(s) of the mesothelin/megakaryocyte potentiating factor family are detectable in sera from patients with ovarian carcinoma. *Proc. Natl. Acad. Sci. U.S.A.* 96, 11531–11536. doi: 10.1073/pnas.96.20.11531

Servais, E. L., Colovos, C., Rodriguez, L., Bograd, A. J., Nitadori, J., Sima, C., et al. (2012). Mesothelin overexpression promotes mesothelioma cell invasion and MMP-9 secretion in an orthotopic mouse model and in epithelioid pleural mesothelioma patients. *Clin. Cancer Res.* 18, 2478–2489. doi: 10.1158/1078-0432.CCR-11-2614

Seyed-Razavi, Y., Hickey, M. J., Kuffova, L., McMenamin, P. G., and Chinnery, H. R. (2013). Membrane nanotubes in myeloid cells in the adult mouse cornea represent a novel mode of immune cell interaction. *Immunol. Cell Biol.* 91, 89–95. doi: 10.1038/icb.2012.52

Sherer, N. M., and Mothes, W. (2008). Cytonemes and tunneling nanotubules in cell-cell communication and viral pathogenesis. *Trends Cell Biol.* 18, 414–420. doi: 10.1016/j.tcb.2008.07.003

Sherer, N. M., Lehmann, M. J., Jimenez-Soto, L. F., Horensavitz, C., Pypaert, M., and Mothes, W. (2007). Retroviruses can establish filopodial bridges for efficient cell-to-cell transmission. *Nat. Cell Biol.* 9, 310–315. doi: 10.1038/ncb1544

Sowinski, S., Alakoskela, J. M., Jolly, C., and Davis, D. M. (2011). Optimized methods for imaging membrane nanotubes between T cells and trafficking of HIV-1. *Methods* 53, 27–33. doi: 10.1016/j.ymeth.2010.04.002

Sowinski, S., Jolly, C., Berninghausen, O., Purbhoo, M. A., Chauveau, A., Kohler, K., et al. (2008). Membrane nanotubes physically connect T cells over long distances presenting a novel route for HIV-1 transmission. *Nat. Cell Biol.* 10, 211–219. doi: 10.1038/ncb1682

Strassburg, S., Hodson, N. W., Hill, P. I., Richardson, S. M., and Hoyland, J. A. (2012). Bi-directional exchange of membrane components occurs during co-culture of mesenchymal stem cells and nucleus pulposus cells. *PLoS ONE* 7:e33739. doi: 10.1371/journal.pone.0033739

Tavi, P., Korhonen, T., Hanninen, S. L., Bruton, J. D., Loof, S., Simon, A., et al. (2010). Myogenic skeletal muscle satellite cells communicate by tunnelling nanotubes. *J. Cell. Physiol.* 223, 376–383.

Thayanithy, V., Babatunde, V., Dickson, E. L., Wong, P., Oh, S., Ke, X., et al. (2014b). Tumor exosomes induce tunneling nanotubes in lipid raft-enriched regions of human mesothelioma cells. *Exp. Cell Res.* 323, 178–188. doi: 10.1016/j.yexcr.2014.01.014

Thayanithy, V., Dickson, E. L., Steer, C., Subramanian, S., and Lou, E. (2014a). Tumor-stromal cross talk: direct cell-to-cell transfer of oncogenic microRNAs via tunneling nanotubes. *Transl. Res.* doi: 10.1016/j.trsl.2014.05.011. [Epub ahead of print].

Tlsty, T. D., and Coussens, L. M. (2006). Tumor stroma and regulation of cancer development. *Annu. Rev. Pathol.* 1, 119–150. doi: 10.1146/annurev.pathol.1.110304.100224

Vallabhaneni, K. C., Haller, H., and Dumler, I. (2012). Vascular Smooth Muscle Cells Initiate Proliferation of Mesenchymal Stem Cells by Mitochondrial Transfer via Tunneling Nanotubes. *Stem Cells Dev.* 21, 3104–3113. doi: 10.1089/scd.2011.0691

Veranic, P., Lokar, M., Schutz, G. J., Weghuber, J., Wieser, S., Hagerstrand, H., et al. (2008). Different types of cell-to-cell connections mediated by nanotubular structures. *Biophys. J.* 95, 4416–4425. doi: 10.1529/biophysj.108.131375

Wang, A., and Hascall, V. C. (2004). Hyaluronan structures synthesized by rat mesangial cells in response to hyperglycemia induce monocyte adhesion. *J. Biol. Chem.* 279, 10279–10285. doi: 10.1074/jbc.M312045200

Wang, X., Veruki, M. L., Bukoreshtliev, N. V., Hartveit, E., and Gerdes, H. H. (2010). Animal cells connected by nanotubes can be electrically coupled through interposed gap-junction channels. *Proc. Natl. Acad. Sci. U.S.A.* 107, 17194–17199. doi: 10.1073/pnas.1006785107

Wang, Y., Cui, J., Sun, X., and Zhang, Y. (2011). Tunneling-nanotube development in astrocytes depends on p53 activation. *Cell Death Differ.* 18, 732–742. doi: 10.1038/cdd.2010.147

Watkins, S. C., and Salter, R. D. (2005). Functional connectivity between immune cells mediated by tunneling nanotubules. *Immunity* 23, 309–318. doi: 10.1016/j.immuni.2005.08.009

Wilson, S. M., Barbone, D., Yang, T. M., Jablons, D. M., Bueno, R., Sugarbaker, D. J., et al. (2008). mTOR mediates survival signals in malignant mesothelioma grown as tumor fragment spheroids. *Am. J. Respir. Cell Mol. Biol.* 39, 576–583. doi: 10.1165/rcmb.2007-0460OC

Xu, W., Santini, P. A., Sullivan, J. S., He, B., Shan, M., Ball, S. C., et al. (2009). HIV-1 evades virus-specific IgG2 and IgA responses by targeting systemic and intestinal B cells via long-range intercellular conduits. *Nat. Immunol.* 10, 1008–1017. doi: 10.1038/ni.1753

Yasuda, K., Park, H. C., Ratliff, B., Addabbo, F., Hatzopoulos, A. K., Chander, P., et al. (2010). Adriamycin nephropathy: a failure of endothelial progenitor cell-induced repair. *Am. J. Pathol.* 176, 1685–1695. doi: 10.2353/ajpath.2010.091071

Zhou, G., Myers, R., Li, Y., Chen, Y., Shen, X., Fenyk-Melody, J., et al. (2001). Role of AMP-activated protein kinase in mechanism of metformin action. *J. Clin. Invest.* 108, 1167–1174. doi: 10.1172/JCI13505

Conflict of Interest Statement: The authors declare that the research was conducted in the absence of any commercial or financial relationships that could be construed as a potential conflict of interest.

Received: 31 May 2014; accepted: 26 September 2014; published online: 31 October 2014.

Citation: Ady JW, Desir S, Thayanithy V, Vogel RI, Moreira AL, Downey RJ, Fong Y, Manova-Todorova K, Moore MAS and Lou E (2014) Intercellular communication in malignant pleural mesothelioma: properties of tunneling nanotubes. Front. Physiol. ***5****:400. doi: 10.3389/fphys.2014.00400*

This article was submitted to Membrane Physiology and Membrane Biophysics, a section of the journal Frontiers in Physiology.

frontiers in
PHYSIOLOGY

MINI REVIEW ARTICLE
published: 24 October 2014
doi: 10.3389/fphys.2014.00412

Membrane nanotubes between peritoneal mesothelial cells: functional connectivity and crucial participation during inflammatory reactions

Julia Ranzinger[1]*, Amin Rustom[2] and Vedat Schwenger[1]

[1] *Department of Nephrology, University of Heidelberg, Heidelberg, Germany*
[2] *Department of New Materials and Biosystems, Max Planck Institute for Intelligent Systems, Stuttgart, Germany*

Edited by:
Sotirios G. Zarogiannis, University of Thessaly, Greece

Reviewed by:
Martyn P. Mahaut-Smith, University of Leicester, UK
Abelardo I. Aguilera, Hospital Universitario de la Princesa, Spain

***Correspondence:**
Julia Ranzinger, Department of Nephrology, University of Heidelberg, Im Neuenheimer Feld 162, Heidelberg, 69120, Germany
e-mail: julia.ranzinger@med.uni-heidelberg.de

Peritoneal dialysis (PD) has attained increased relevance as continuous renal replacement therapy over the past years. During this treatment, the peritoneum functions as dialysis membrane to eliminate diffusible waste products from the blood-stream. Success and efficacy of this treatment is dependent on the integrity of the peritoneal membrane. Chronic inflammatory conditions within the peritoneal cavity coincide with elevated levels of proinflammatory cytokines leading to the impairment of tissue integrity. High glucose concentrations and glucose metabolites in PD solutions contribute to structural and functional reorganization processes of the peritoneal membrane during long-term PD. The subsequent loss of ultrafiltration is causal for the treatment failure over time. It was shown that peritoneal mesothelial cells are functionally connected via Nanotubes (NTs) and that a correlation of NT-occurrence and defined pathophysiological conditions exists. Additionally, an important participation of NTs during inflammatory reactions was shown. Here, we will summarize recent developments of NT-related research and provide new insights into NT-mediated cellular interactions under physiological as well as pathophysiological conditions.

Keywords: peritoneal dialysis, peritoneal mesothelial cells, inflammation, nanotubes, oxidative stress

SECTION

Peritoneal dialysis (PD) is an accepted alternative to hemodialysis in the treatment of end-stage renal disease. However, when compared internationally, PD-treatment is still underrepresented in Germany (Lameire and Van Biesen, 2010). In this treatment, the peritoneal membrane functions as semipermeable membrane allowing for ultrafiltration and diffusion (Krediet, 1999). In order to produce osmotically induced ultrafiltration, heat sterilized glucose containing dialysis solutions are used to ensure hyperosmolarity. The heat sterilization leads to the formation of glucose degradation products (GDPs) (Wieslander et al., 1995) which mainly contribute to the formation of advanced glycation end-products (AGEs) including methylglyoxal (MG) (Nakayama et al., 1997; Muller-Krebs et al., 2008). The implantation and presence of an indwelling catheter, high glucose concentrations, and GDPs in the dialysis solutions as well as peritonitis - a known complication of PD - coincide with high levels of proinflammatory cytokines within the peritoneal cavity and subsequent induce chronic inflammatory conditions leading to structural and functional changes of the peritoneal membrane (Witowski et al., 2000; Flessner et al., 2007, 2010).

Moreover, a strong induction of the expression of the receptor for advanced glycation end-products (RAGE) in the peritoneal membrane of uremic patients was demonstrated which further increased after PD treatment (Kihm et al., 2008), showing AGE-RAGE interactions being crucial in peritoneal damage due to inflammatory conditions, uremia, and PD. The resulting loss of ultrafiltration, as well as progressive fibrosis, angiogenesis, and vascular degeneration limit long-term PD-treatment (Margetts and Churchill, 2002; Devuyst et al., 2010).

It is now clear that peritoneal mesothelial cells, specialized epithelial cells that line the peritoneal cavity, not only function as non-adhesive surface to facilitate intracoelomic movement. These cells are crucial for the maintenance of peritoneal homeostasis, transport processes across the peritoneal membrane and tissue repair (Mutsaers, 2004; Yung and Chan, 2007). Furthermore, they provide defense against bacterial insult and are essentially exposed to the bioincompatible dialysis solutions during PD-treatment. In response to Tumor-Necrosis-Factor (TNF) and Interleukin-1 (IL-1) secreted by peritoneal macrophages, peritoneal mesothelial cells synthesize various cytokines, including IL-1, IL-6, and IL-8, thus enhance the inflammatory signal and recruit leukocytes in the peritoneal cavity (Douvdevani et al., 1994; Topley, 1995; Li et al., 1998). In the immune system, peritoneal mesothelial cells bear an effective antigen-presenting function for T cells and thereby play a relevant role during the immune response in the peritoneal cavity e.g., during peritonitis (Valle et al., 1995; Hausmann et al., 2000). However, with increasing PD-treatment, peritoneal mesothelial cells undergo a progressive loss of their epithelial phenotype toward a myofibroblast-like phenotype (Yanez-Mo et al., 2003). Thereby, a loss of characteristic cell-cell junctions, apical-basal polarity as well as reorganization

of the cytoskeleton and reprogramming of the gene expression take place (Lamouille et al., 2014). This differentiation process, known as epithelial-mesenchymal transition (EMT), reflects the enormous plasticity of mesothelial cells (Yung and Chan, 2012).

In the context of inflammatory immune reactions, intercellular communication plays a crucial role. In 2004, the discovery of Nanotubes (NTs) mediating membrane continuity has extended the understanding of cell-to-cell communication (Rustom et al., 2004). These NTs were initially characterized as thin intercellular membrane channels, formed between cultivated pheochromocytoma (PC12) cells at their nearest distance and without contact to the substratum (**Figure 1A**), displaying diameters from 50 to 200 nm and lengths of up to several cell diameters (Rustom et al., 2004). NTs contain F-actin and/or microtubule backbones and facilitate the intercellular transmission of various cellular components, including organelles as well as plasma membrane constituents or the transfer of electric signals (Hurtig et al., 2010; Wang et al., 2010; Wang and Gerdes, 2012). Meanwhile, NTs have been found to be present in cultures of different cell types including for example mesothelial (**Figure 1B**) and epithelial cells, fibroblasts, immune cells, and neurons (Vidulescu et al., 2004; Castro et al., 2005; Watkins and Salter, 2005; Davis and Sowinski, 2008; Gerdes and Carvalho, 2008; Pontes et al., 2008; Ranzinger et al., 2011). Moreover, recent research demonstrates the existence of NTs in human primary tumors (Lou et al., 2012).

During the last 10 years, a lot of knowledge concerning formation, function, and biological implications of NTs in health and disease has been gained. Aside from mediating functional connectivity between various cell types, it is now clear that NTs participate in several pathological processes of substantial medical interest. NTs were proposed to be involved in the intercellular spread of prion proteins (Gousset and Zurzolo, 2009; Dunning et al., 2012) and viral proteins, e.g., during HIV infections (Eugenin et al., 2009; Kadiu and Gendelman, 2011; Sowinski et al., 2011), the transfer of drug resistance between cancer cells (Pasquier et al., 2012) or the transfer of Aβ peptides in the context of Alzheimer's disease (Wang et al., 2011). Moreover, it could be demonstrated that the number of NTs in humans is dependent on the individual donor background (Ranzinger et al., 2011) and correlates with defined pathophysiological conditions. In *in vitro* experiments, in which cells were stimulated with TNF, the number of NTs is significantly increased and associated with a remodeling of the actin cytoskeleton. This finding could be confirmed when NT-numbers were investigated between cells from PD-patients (Ranzinger et al., 2011) pointing to an important participation of NTs during inflammatory reactions.

Additionally, a strong correlation of NT occurrence with cellular cholesterol contents and its distribution throughout the cell could be demonstrated. Experiments, in which cellular cholesterol homeostasis in HPMCs was affected by cholesterol depletion via methyl-β-cyclodextrin (MβCyc), revealed that gradual cholesterol depletion results in a strong, non-linear modulation of NT-numbers and lengths with significant peaks at given MβCyc concentrations, pointing to narrow windows of defined

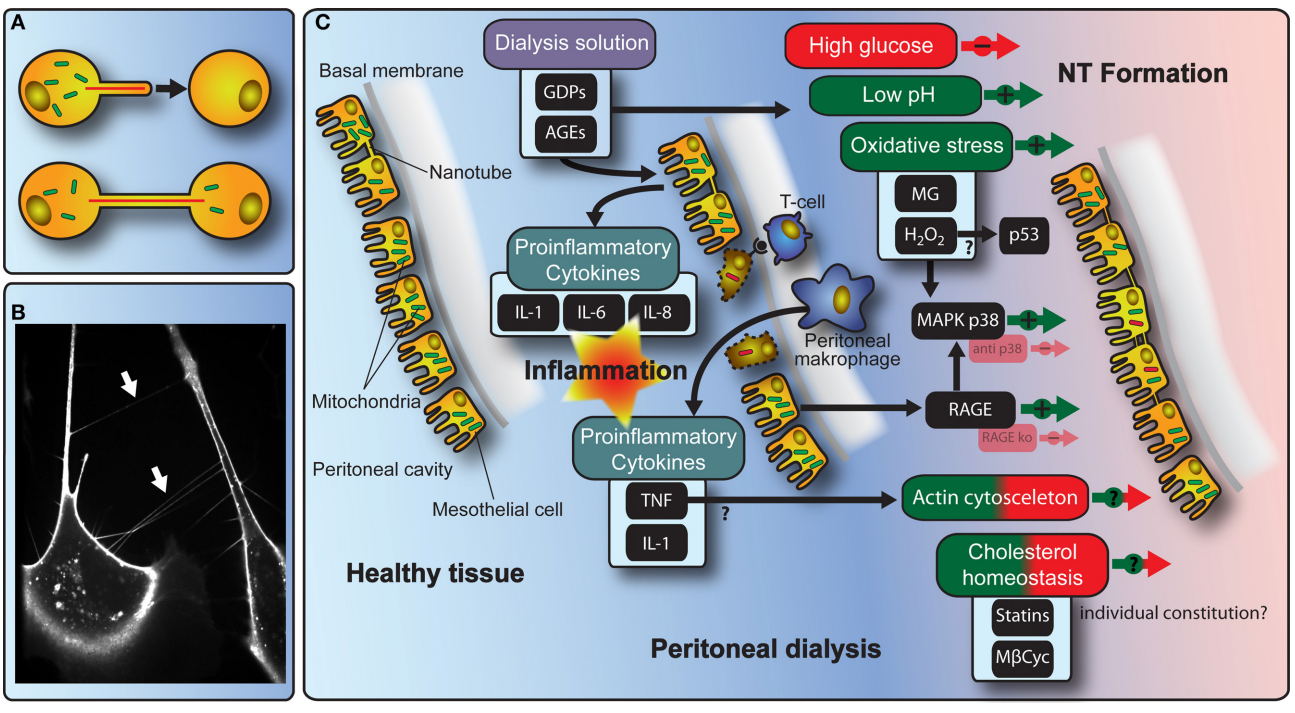

FIGURE 1 | Schematic model of molecular mechanisms with implications for NT-mediated cellular interactions during PD. (A) The cartoon depicts the principle of NT-formation and NT-mediated transfer of organelles between cells. **(B)** The fluorescence microscopy picture shows NTs (arrows) spanned between primary human peritoneal mesothelial cells. **(C)** Illustration of the interdependence of NT-formation and communication in the context of PD-treatment including stimulating/inhibiting factors.

cholesterol contents being beneficial or detrimental, e.g., by affecting NT tensile strength or by influencing the formation process (Ranzinger et al., 2011). The finding that statin-treatment of HPMCs resulted in significantly increased NT-numbers coincides with comparably high numbers of NTs found between cells from a patient undergoing statin treatment (Ranzinger et al., 2013). In a recent study, Thayanithy et al. (2014) explored exosomes and lipid rafts as mediators of NT-formation in mesothelioma cells. Their results provide evidence for exosomes as chemotactic stimuli for NT-formation and lipid raft formation as potential biomarker for NT-forming cells.

To date, aside from inflammatory conditions, several factors are known that lead to the induction of NT-formation, among these oxidative stress as well as several receptor-ligand interactions (Martinez et al., 2002; Zhu et al., 2005; Chinnery et al., 2008; Ranzinger et al., 2011; Wang et al., 2011; Sun et al., 2012). In the context of PD-treatment, the use of dialysis solutions lead to a significant reduction in NT-numbers between peritoneal mesothelial cells (Ranzinger et al., 2011). Observed more closely, oxidative stress caused by both methyglyoxal (MG) and acidified pH-value results in higher NT-numbers whereas alterations in cellular osmolarity due to enhanced glucose concentrations lead to a strong decrease in NT-numbers between the cells (Ranzinger et al., 2014). In this context, by blocking of RAGE, whose expression is upregulated during PD-treatment, it could be shown that this receptor is a strong regulator in NT-formation processes between murine and human peritoneal mesothelial cells *in vitro* and *in vivo* (Ranzinger et al., 2014).

Respective underlying molecular mechanisms involved in the formation of NTs are controversially discussed. Studies from Wang et al. (2011) showed that NT-formation in primary rat hippocampal astrocytes and neurons is dependent on the activation of the tumor suppressor protein p53 through hydrogen peroxide induced cellular stress. Andresen et al. (2013) however showed that p53 is dispensable for NT-formation in SAOS-2 cells and dKO-MSCs. The results of these studies demonstrate that signaling pathways and involved proteins having an impact on the formation of NTs act strongly cell-type dependent. A previous study from Zhu et al. (2005) showed that oxidative stress induced by H_2O_2 increases the formation of NTs in astrocytes through activation of the p38 mitogen-activated protein kinase (MAPK) pathway. In the context of RAGE being involved in the formation of NTs between peritoneal mesothelial cells, the MAPK signaling cascade, which is addressed upon RAGE activation, was investigated in a recent study from Ranzinger et al. (2014). It could be demonstrated that oxidative stress induced by MG not only induces NT-formation but also increases phosphorylated p38 protein levels. Subsequently, blocking of p38 resulted in reduced NT-numbers between the cells arguing that the action of p38 regulates NT-formation in peritoneal mesothelial cells.

The existence of NTs *in vivo* has been supported by an increasing number of publications (Eugenin et al., 2009; Pyrgaki et al., 2010; Caneparo et al., 2011; Ranzinger et al., 2014). However, their occurrence, architecture, and function in the body is still a matter of considerable debate and may vary in accordance to the respective species, tissue, developmental stage, age, genetic background, and pathophysiological variations. One possible function could be a NT-mediated rescue for cells and/or organs under pathophysiological conditions like oxidative stress (**Figure 1C**).

In this view, several studies showed e.g., the transfer of mitochondria via NTs (Koyanagi et al., 2005; Domhan et al., 2011; Wang et al., 2011). A study from Vallabhaneni et al. (2012) showed that vascular smooth muscle cells initiate proliferation of mesenchymal stem cells through the exchange of mitochondria in co-cultures. Pasquier et al. (2013) demonstrated that cancer cells acquiring mitochondria from endothelial cells display significant chemoresistance. Furthermore, work from Spees et al. (2006) could demonstrate that aerobic respiration in cells with dysfunctional mitochondria could be rescued by mitochondrial transfer. More recently, concerning ischemia/reperfusion (I/R)-induced injury of the kidney, in a RAGE knockout mouse model, it could be shown that under conditions where RAGE is absent, NT-numbers are increased and kidney tissue morphology is improved compared to kidneys from wild-type mice (Ranzinger et al., 2014). Interestingly, when RAGE is blocked and dialysis solution as secondary stimulus has been applied, increased NT-numbers could also be demonstrated in peritoneal mesothelial cells (Ranzinger et al., 2014). In these cases, one could speculate that a protective effect for the respective organ/tissue might be attributed to an increased NT-formation accompanied by frequent exchanges of for example mitochondria.

In the future, further investigations are needed to investigate NT-mediated transport mechanisms within the peritoneal cavity in greater detail. This will have significant impact on the understanding of a variety of processes, such as inflammatory immune reactions. Potentially, this knowledge will allow for the development of improved treatment options during peritoneal infection.

REFERENCES

Andresen, V., Wang, X., Ghimire, S., Omsland, M., Gjertsen, B. T., and Gerdes, H. H. (2013). Tunneling nanotube (TNT) formation is independent of p53 expression. *Cell Death Differ.* 20, 1124. doi: 10.1038/cdd.2013.61

Caneparo, L., Pantazis, P., Dempsey, W., and Fraser, S. E. (2011). Intercellular bridges in vertebrate gastrulation. *PLoS ONE* 6:e20230. doi: 10.1371/journal.pone.0020230

Castro, M. A., Grieneisen, V. A., and De Almeida, R. M. (2005). Disruption and de novo formation of nanotubular membrane extensions in SW620 colon carcinoma cell line during cell division. *Cell Biol. Int.* 29, 929–931. doi: 10.1016/j.cellbi.2005.05.013

Chinnery, H. R., Pearlman, E., and McMenamin, P. G. (2008). Cutting edge: membrane nanotubes *in vivo*: a feature of MHC class II+ cells in the mouse cornea. *J. Immunol.* 180, 5779–5783. doi: 10.4049/jimmunol.180.9.5779

Davis, D. M., and Sowinski, S. (2008). Membrane nanotubes: dynamic long-distance connections between animal cells. *Nat. Rev. Mol. Cell Biol.* 9, 431–436. doi: 10.1038/nrm2399

Devuyst, O., Margetts, P. J., and Topley, N. (2010). The pathophysiology of the peritoneal membrane. *J. Am. Soc. Nephrol.* 21, 1077–1085. doi: 10.1681/ASN.2009070694

Domhan, S., Ma, L., Tai, A., Anaya, Z., Beheshti, A., Zeier, M., et al. (2011). Intercellular communication by exchange of cytoplasmic material via tunneling nano-tube like structures in primary human renal epithelial cells. *PLoS ONE* 6:e21283. doi: 10.1371/journal.pone.0021283

Douvdevani, A., Rapoport, J., Konforty, A., Argov, S., Ovnat, A., and Chaimovitz, C. (1994). Human peritoneal mesothelial cells synthesize IL-1 alpha and beta. *Kidney Int.* 46, 993–1001. doi: 10.1038/ki.1994.359

Dunning, C. J., Reyes, J. F., Steiner, J. A., and Brundin, P. (2012). Can Parkinson's disease pathology be propagated from one neuron to another? *Prog. Neurobiol.* 97, 205–219. doi: 10.1016/j.pneurobio.2011.11.003

Eugenin, E. A., Gaskill, P. J., and Berman, J. W. (2009). Tunneling nanotubes (TNT): a potential mechanism for intercellular HIV trafficking. *Commun. Integr. Biol.* 2, 243–244. doi: 10.4161/cib.2.3.8165

Flessner, M. F., Credit, K., Henderson, K., Vanpelt, H. M., Potter, R., He, Z., et al. (2007). Peritoneal changes after exposure to sterile solutions by catheter. *J. Am. Soc. Nephrol.* 18, 2294–2302. doi: 10.1681/ASN.2006121417

Flessner, M. F., Credit, K., Richardson, K., Potter, R., Li, X., He, Z., et al. (2010). Peritoneal inflammation after twenty-week exposure to dialysis solution: effect of solution versus catheter-foreign body reaction. *Perit. Dial. Int.* 30, 284–293. doi: 10.3747/pdi.2009.00100

Gerdes, H. H., and Carvalho, R. N. (2008). Intercellular transfer mediated by tunneling nanotubes. *Curr. Opin. Cell Biol.* 20, 470–475. doi: 10.1016/j.ceb.2008.03.005

Gousset, K., and Zurzolo, C. (2009). Tunnelling nanotubes: a highway for prion spreading? *Prion* 3, 94–98. doi: 10.4161/pri.3.2.8917

Hausmann, M. J., Rogachev, B., Weiler, M., Chaimovitz, C., and Douvdevani, A. (2000). Accessory role of human peritoneal mesothelial cells in antigen presentation and T-cell growth. *Kidney Int.* 57, 476–486. doi: 10.1046/j.1523-1755.2000.00867.x

Hurtig, J., Chiu, D. T., and Onfelt, B. (2010). Intercellular nanotubes: insights from imaging studies and beyond. *Wiley Interdiscip. Rev. Nanomed. Nanobiotechnol.* 2, 260–276. doi: 10.1002/wnan.80

Kadiu, I., and Gendelman, H. E. (2011). Human immunodeficiency virus type 1 endocytic trafficking through macrophage bridging conduits facilitates spread of infection. *J. Neuroimmune Pharmacol.* 6, 658–675. doi: 10.1007/s11481-011-9298-z

Kihm, L. P., Wibisono, D., Muller-Krebs, S., Pfisterer, F., Morath, C., Gross, M. L., et al. (2008). RAGE expression in the human peritoneal membrane. *Nephrol. Dial. Transplant* 23, 3302–3306. doi: 10.1093/ndt/gfn272

Koyanagi, M., Brandes, R. P., Haendeler, J., Zeiher, A. M., and Dimmeler, S. (2005). Cell-to-cell connection of endothelial progenitor cells with cardiac myocytes by nanotubes: a novel mechanism for cell fate changes? *Circ. Res.* 96, 1039–1041. doi: 10.1161/01.RES.0000168650.23479.0c

Krediet, R. T. (1999). The peritoneal membrane in chronic peritoneal dialysis. *Kidney Int.* 55, 341–356. doi: 10.1046/j.1523-1755.1999.00264.x

Lameire, N., and Van Biesen, W. (2010). Epidemiology of peritoneal dialysis: a story of believers and nonbelievers. *Nat. Rev. Nephrol.* 6, 75–82. doi: 10.1038/nrneph.2009.210

Lamouille, S., Xu, J., and Derynck, R. (2014). Molecular mechanisms of epithelial-mesenchymal transition. *Nat. Rev. Mol. Cell Biol.* 15, 178–196. doi: 10.1038/nrm3758

Li, F. K., Davenport, A., Robson, R. L., Loetscher, P., Rothlein, R., Williams, J. D., et al. (1998). Leukocyte migration across human peritoneal mesothelial cells is dependent on directed chemokine secretion and ICAM-1 expression. *Kidney Int.* 54, 2170–2183. doi: 10.1046/j.1523-1755.1998.00174.x

Lou, E., Fujisawa, S., Morozov, A., Barlas, A., Romin, Y., Dogan, Y., et al. (2012). Tunneling nanotubes provide a unique conduit for intercellular transfer of cellular contents in human malignant pleural mesothelioma. *PLoS ONE* 7:e33093. doi: 10.1371/journal.pone.0033093

Margetts, P. J., and Churchill, D. N. (2002). Acquired ultrafiltration dysfunction in peritoneal dialysis patients. *J. Am. Soc. Nephrol.* 13, 2787–2794.

Martinez, A. D., Hayrapetyan, V., Moreno, A. P., and Beyer, E. C. (2002). Connexin43 and connexin45 form heteromeric gap junction channels in which individual components determine permeability and regulation. *Circ. Res.* 90, 1100–1107. doi: 10.1161/01.RES.0000019580.64013.31

Muller-Krebs, S., Kihm, L. P., Zeier, B., Gross, M. L., Deppisch, R., Wieslander, A., et al. (2008). Renal toxicity mediated by glucose degradation products in a rat model of advanced renal failure. *Eur. J. Clin. Invest.* 38, 296–305. doi: 10.1111/j.1365-2362.2008.01945.x

Mutsaers, S. E. (2004). The mesothelial cell. *Int. J. Biochem. Cell Biol.* 36, 9–16. doi: 10.1016/S1357-2725(03)00242-5

Nakayama, M., Kawaguchi, Y., Yamada, K., Hasegawa, T., Takazoe, K., Katoh, N., et al. (1997). Immunohistochemical detection of advanced glycosylation end-products in the peritoneum and its possible pathophysiological role in CAPD. *Kidney Int.* 51, 182–186. doi: 10.1038/ki.1997.22

Pasquier, J., Galas, L., Boulange-Lecomte, C., Rioult, D., Bultelle, F., Magal, P., et al. (2012). Different modalities of intercellular membrane exchanges mediate cell-to-cell p-glycoprotein transfers in MCF-7 breast cancer cells. *J. Biol. Chem.* 287, 7374–7387. doi: 10.1074/jbc.M111.312157

Pasquier, J., Guerrouahen, B. S., Al Thawadi, H., Ghiabi, P., Maleki, M., Abu-Kaoud, N., et al. (2013). Preferential transfer of mitochondria from endothelial to cancer cells through tunneling nanotubes modulates chemoresistance. *J. Transl. Med.* 11:94. doi: 10.1186/1479-5876-11-94

Pontes, B., Viana, N. B., Campanati, L., Farina, M., Neto, V. M., and Nussenzveig, H. M. (2008). Structure and elastic properties of tunneling nanotubes. *Eur. Biophys. J.* 37, 121–129. doi: 10.1007/s00249-007-0184-9

Pyrgaki, C., Trainor, P., Hadjantonakis, A. K., and Niswander, L. (2010). Dynamic imaging of mammalian neural tube closure. *Dev. Biol.* 344, 941–947. doi: 10.1016/j.ydbio.2010.06.010

Ranzinger, J., Rustom, A., Abel, M., Leyh, J., Kihm, L., Witkowski, M., et al. (2011). Nanotube action between human mesothelial cells reveals novel aspects of inflammatory responses. *PLoS ONE* 6:e29537. doi: 10.1371/journal.pone.0029537

Ranzinger, J., Rustom, A., Heide, D., Morath, C., Schemmer, P., Nawroth, P. P., et al. (2014). The receptor for advanced glycation end-products (RAGE) plays a key role in the formation of nanotubes (NTs) between peritoneal mesothelial cells and in murine kidneys. *Cell Tissue Res.* 357, 667–679. doi: 10.1007/s00441-014-1904-y

Ranzinger, J., Rustom, A., and Schwenger, V. (2013). Potential role of nanotubes in context of clinical treatments? *Commun. Integr. Biol.* 6:e22686. doi: 10.4161/cib.22686

Rustom, A., Saffrich, R., Markovic, I., Walther, P., and Gerdes, H. H. (2004). Nanotubular highways for intercellular organelle transport. *Science* 303, 1007–1010. doi: 10.1126/science.1093133

Sowinski, S., Alakoskela, J. M., Jolly, C., and Davis, D. M. (2011). Optimized methods for imaging membrane nanotubes between T cells and trafficking of HIV-1. *Methods* 53, 27–33. doi: 10.1016/j.ymeth.2010.04.002

Spees, J. L., Olson, S. D., Whitney, M. J., and Prockop, D. J. (2006). Mitochondrial transfer between cells can rescue aerobic respiration. *Proc. Natl. Acad. Sci. U.S.A.* 103, 1283–1288. doi: 10.1073/pnas.0510511103

Sun, X., Wang, Y., Zhang, J., Tu, J., Wang, X. J., Su, X. D., et al. (2012). Tunneling-nanotube direction determination in neurons and astrocytes. *Cell Death Dis.* 3, e438. doi: 10.1038/cddis.2012.177

Thayanithy, V., Babatunde, V., Dickson, E. L., Wong, P., Oh, S., Ke, X., et al. (2014). Tumor exosomes induce tunneling nanotubes in lipid raft-enriched regions of human mesothelioma cells. *Exp. Cell Res.* 323, 178–188. doi: 10.1016/j.yexcr.2014.01.014

Topley, N. (1995). The cytokine network controlling peritoneal inflammation. *Perit. Dial. Int.* 15, S35–S39. discussion: S39–S40.

Vallabhaneni, K. C., Haller, H., and Dumler, I. (2012). Vascular smooth muscle cells initiate proliferation of mesenchymal stem cells by mitochondrial transfer via tunneling nanotubes. *Stem Cells Dev.* 21, 3104–3113. doi: 10.1089/scd.2011.0691

Valle, M. T., Degl'innocenti, M. L., Bertelli, R., Facchetti, P., Perfumo, F., Fenoglio, D., et al. (1995). Antigen-presenting function of human peritoneum mesothelial cells. *Clin. Exp. Immunol.* 101, 172–176. doi: 10.1111/j.1365-2249.1995.tb02294.x

Vidulescu, C., Clejan, S., and O'connor, K. C. (2004). Vesicle traffic through intercellular bridges in DU 145 human prostate cancer cells. *J. Cell. Mol. Med.* 8, 388–396. doi: 10.1111/j.1582-4934.2004.tb00328.x

Wang, X., and Gerdes, H. H. (2012). Long-distance electrical coupling via tunneling nanotubes. *Biochim. Biophys. Acta* 1818, 2082–2086. doi: 10.1016/j.bbamem.2011.09.002

Wang, X., Veruki, M. L., Bukoreshtliev, N. V., Hartveit, E., and Gerdes, H. H. (2010). Animal cells connected by nanotubes can be electrically coupled through interposed gap-junction channels. *Proc. Natl. Acad. Sci. U.S.A.* 107, 17194–17199. doi: 10.1073/pnas.1006785107

Wang, Y., Cui, J., Sun, X., and Zhang, Y. (2011). Tunneling-nanotube development in astrocytes depends on p53 activation. *Cell Death Differ.* 18, 732–742. doi: 10.1038/cdd.2010.147

Watkins, S. C., and Salter, R. D. (2005). Functional connectivity between immune cells mediated by tunneling nanotubules. *Immunity* 23, 309–318. doi: 10.1016/j.immuni.2005.08.009

Wieslander, A. P., Kjellstrand, P. T., and Rippe, B. (1995). Heat sterilization of glucose-containing fluids for peritoneal dialysis: biological consequences of chemical alterations. *Perit. Dial. Int.* 15, S52–S59. discussion: S59–S60.

Witowski, J., Korybalska, K., Wisniewska, J., Breborowicz, A., Gahl, G. M., Frei, U., et al. (2000). Effect of glucose degradation products on human peritoneal mesothelial cell function. *J. Am. Soc. Nephrol.* 11, 729–739.

Yanez-Mo, M., Lara-Pezzi, E., Selgas, R., Ramirez-Huesca, M., Dominguez-Jimenez, C., Jimenez-Heffernan, J. A., et al. (2003). Peritoneal dialysis and epithelial-to-mesenchymal transition of mesothelial cells. *N. Engl. J. Med.* 348, 403–413. doi: 10.1056/NEJMoa020809

Yung, S., and Chan, T. M. (2007). Mesothelial cells. *Perit. Dial. Int.* 27 Suppl. 2, S110–S115.

Yung, S., and Chan, T. M. (2012). Pathophysiological changes to the peritoneal membrane during PD-related peritonitis: the role of mesothelial cells. *Mediators Inflamm.* 2012:484167. doi: 10.1155/2012/484167

Zhu, D., Tan, K. S., Zhang, X., Sun, A. Y., Sun, G. Y., and Lee, J. C. (2005). Hydrogen peroxide alters membrane and cytoskeleton properties and increases intercellular connections in astrocytes. *J. Cell Sci.* 118, 3695–3703. doi: 10.1242/jcs.02507

Conflict of Interest Statement: The authors declare that the research was conducted in the absence of any commercial or financial relationships that could be construed as a potential conflict of interest.

Received: 26 August 2014; accepted: 03 October 2014; published online: 24 October 2014.

Citation: Ranzinger J, Rustom A and Schwenger V (2014) Membrane nanotubes between peritoneal mesothelial cells: functional connectivity and crucial participation during inflammatory reactions. Front. Physiol. ***5****:412. doi: 10.3389/fphys.2014.00412*

This article was submitted to Membrane Physiology and Membrane Biophysics, a section of the journal Frontiers in Physiology.

frontiers in
PHYSIOLOGY

PERSPECTIVE ARTICLE
published: 01 August 2014
doi: 10.3389/fphys.2014.00284

The pleural mesothelium in development and disease

Hitesh Batra* and Veena B. Antony

Division of Pulmonary, Allergy and Critical Care Medicine, Department of Medicine, University of Alabama at Birmingham, Birmingham, AL, USA

Edited by:
Sotirios G. Zarogiannis, University of Thessaly, Greece

Reviewed by:
Vassilios Liakopoulos, Aristotle University of Thessaloniki, Greece
K. Onuma, Juntendo University, Japan

****Correspondence:***
Hitesh Batra, Division of Pulmonary, Allergy and Critical Care Medicine, Department of Medicine, University of Alabama at Birmingham, 1900 University Blvd., THT 422, Birmingham, AL 35294-0006, USA
e-mail: hiteshbatra921@gmail.com

The pleural mesothelium, derived from the embryonic mesoderm, is formed by a metabolically active monolayer of cells that blanket the chest wall and lungs on the parietal and visceral surfaces, respectively. The pleura and lungs are formed as a result of an intricate relationship between the mesoderm and the endoderm during development. Mesenchymal signaling pathways such as Wnt/B-catenin, Bmp4, and sonic hedgehog appear to be quintessential for lung development. Pleural Mesothelial Cells (PMCs) are known to express Wilms tumor-1 (Wt1) gene and in lineage labeling studies of the developing embryo, PMCs were found to track into the lung parenchyma and undergo mesothelial-mesenchymal transition (MMT) to form α-smooth muscle actin (α-SMA)-positive cells of the mesenchyme and vasculature. There is definite evidence that mesothelial cells can differentiate and this seems to play an important role in pleural and parenchymal pathologies. Mesothelial cells can differentiate into adipocytes, chondrocytes, and osteoblasts; and have been shown to clonally generate fibroblasts and smooth muscle cells in murine models. This supports the possibility that they may also modulate lung injury-repair by re-activation of developmental programs in the adult reflecting an altered recapitulation of development, with implications for regenerative biology of the lung. In a mouse model of lung fibrosis using lineage-tracing studies, PMCs lost their polarity and cell-cell junctional complexes, migrated into lung parenchyma, and underwent phenotypic transition into myofibroblasts in response to the pro-fibrotic mediator, transforming growth factor-β1 (TGF-β1). However, intra-pleural heme-oxygenase-1 (HO-1) induction inhibited PMC migration after intra-tracheal fibrogenic injury. Intra-pleural fluorescein isothiocyanate labeled nanoparticles decorated with a surface antibody to mesothelin, a surface marker of mesothelial cells, migrate into the lung parenchyma with PMCs supporting a potential role for pleural based therapies to modulate pleural mesothelial activation and parenchymal disease progression.

Keywords: pleural mesothelium, pleural mesothelial cells, idiopathic pulmonary fibrosis (IPF), Wilms tumor-1 (WT1), epithelial-mesenchymal transition (EMT)

INTRODUCTION

The lung is a complex, integrated structure of airways, vasculature and interstitium, surrounded by the pleural mesothelium (Jantz and Antony, 2006). The pleural mesothelium, derived from the embryonic mesoderm, is formed by a layer of cells that blanket the chest wall and lungs on the parietal and visceral surfaces, respectively. A complex interplay of signaling pathways such as Wnt/β-catenin, Bone morphogenetic protein 4 (Bmp4), sonic hedgehog, and Fibroblast growth factor 10 (Fgf10) between the developing endoderm and mesoderm is essential for development.

Wilms tumor-1 (Wt1), a zinc finger transcription factor (Haber et al., 1990), is expressed in certain mesoderm-derived tissues including the pleura (Park et al., 1993) and is known to regulate many functional properties of the developing mesothelium (Ito et al., 2006; Jomgeow et al., 2006). It also regulates pleural mesothelial cell (PMC) plasticity. Wt1 expressing PMCs have been shown to migrate into the lung parenchyma and differentiate into subpopulations of bronchial smooth muscle cells, vascular smooth muscle cells and fibroblasts (Colvin et al., 2001; Dixit et al., 2013).

The presence of Wt1-expressing PMCs on both the pleural surface and in the lung parenchyma of patients with IPF suggests a role for crosstalk between the parenchymal lung injury and activation of the pleural mesothelium in the pathogenesis of IPF. PMCs migrate into the pulmonary parenchyma in IPF and transition into myofibroblasts suggesting the novel hypothesis that IPF is an altered, recapitulation of development, with implications for regenerative biology of the lung.

PMCs could represent a new cellular therapeutic target in a disease where we currently lack treatment modalities. Intra-pleural delivery of compounds is a lung targeted, innovative

Abbreviations: PMCs, Pleural Mesothelial Cells (PMCs); Wt1, Wilms tumor-1 (Wt1); MMT, Mesothelial-mesenchymal transition (MMT); α-SMA, α-smooth muscle actin; Bmp4, Bone morphogenetic protein 4; Shh, Sonic hedgehog; Fgf10, Fibroblast growth factor 10; IPF, Idiopathic Pulmonary Fibrosis; TGF-β1, Transforming growth factor-β1; HO-1, Heme-oxygenase-1 (HO-1); EMT, Epithelial-mesenchymal transition; NOX-4, NADPH oxidase-4; UIP, Usual interstitial pneumonia; RNA, Ribonucleic acid; BAL, Bronchoalveolar lavage; NP, Nanoparticle; FITC, Fluorescein isothiocyanate; PLGA, Poly-lactic-co-glycolic acid.

therapeutic modality that can be refined to deliver drugs, minimizing systemic toxicity.

DEVELOPMENT

The lungs arise from the anterior foregut endoderm via a complex and highly regulated process comprising of the embryonic stage, pseudo-glandular stage, branching morphogenesis, canalicular stage, saccular stage, and the alveolarization stage. During all stages of endodermal development, the lung mesoderm interacts with the lung endoderm to generate the various lineages within the lung (Herriges and Morrisey, 2014) and plays a central role in regulating morphogenesis of the lung, including branching, lung size, and vascular development (Que et al., 2008).

ROLE OF MESODERM DURING DEVELOPMENT

The lung mesoderm is an important source of paracrine signals such as Fgf10 and Wnt2 (Bellusci et al., 1997; Sekine et al., 1999; Weaver et al., 2000; Goss et al., 2009), which are essential for multiple processes during lung development, including the patterning of early endoderm progenitors, epithelial proliferation, and differentiation. The mature lung contains many mesodermal derivatives, including airway smooth muscle, vascular smooth muscle, endothelial and mesothelial cells, as well as multiple less well-understood cell types, such as pericytes, alveolar fibroblasts, and lipofibroblasts (Herriges and Morrisey, 2014). In lineage labeling studies of the developing embryo, PMCs were found to track into the lung parenchyma and undergo mesothelial-mesenchymal transition (MMT) to form α-smooth muscle actin (α-SMA)-positive cells of the mesenchyme and vasculature (Que et al., 2008).

SIGNALING PATHWAYS

During development, Wnt/β-catenin signaling is responsible for specifying Nkx2.1+ respiratory endoderm progenitors, which mark the specification of the respiratory system in the anterior foregut endoderm (Herriges and Morrisey, 2014). This, in turn, is dependent upon active Bmp signaling that represses the transcription factor Sox2, thereby allowing for expression of Nkx2.1. Loss of Bmp signaling through inactivation of the Bmp receptors, Bmpr1a and Bmpr1b, leads to tracheal agenesis with retention of the branching region of the lungs (Domyan et al., 2011). Moreover, signaling between the developing endoderm and mesoderm appears to be essential for branching morphogenesis and the loss of Fgf10 signaling to Fgfr2 in the developing endoderm leads to disruption of branching (Sekine et al., 1999; Ohuchi et al., 2000). Fgf10 expression is regulated by several signaling pathways such as Bmp4 and sonic hedgehog (Shh), suggesting a complex interplay of signaling molecules during development (Bellusci et al., 1997; Pepicelli et al., 1998; Weaver et al., 2000).

Wt1

The Wt1 gene encodes a 49–52 kDa protein with an N-terminal domain that is involved in protein-RNA interactions critical for its transcriptional regulatory function (Call et al., 1990).

Wt1 IN PRENATAL DEVELOPMENT

PMCs are known to express Wt1 gene and migrate into the lung parenchyma to form smooth muscle cells of the vascular wall, as well as other cells of the lung mesenchyme during development (Que et al., 2008; Zhou et al., 2010, 2011).

Recent cell lineage labeling studies in the developing heart provide evidence that the surface epicardial mesothelium undergoes epithelial-mesenchymal transition (EMT) and migrates into the myocardium where it differentiates into various cell types, including endothelium, smooth muscle cells, and cardiomyocytes (Mikawa and Gourdie, 1996; Dettman et al., 1998; Cai et al., 2008; Zhou et al., 2010). In addition, lineage tracing and other studies show that the serosal mesothelium of the gut also contributes the majority of vascular smooth muscle cells (Wilm et al., 2005; Kawaguchi et al., 2007). A major role of Wt1 and PMCs in mesenchymal differentiation and development was demonstrated by lineage tracing studies in the embryonic mouse (Colvin et al., 2001). PMCs were shown to readily migrate into the lung parenchyma and express α-SMA. Another recent study employing $Wt1^{CreERT2/+}$ mice visualized Wt1+ mesothelial cell entry into the lung by live imaging, identified their progenies in subpopulations of bronchial smooth muscle cells, vascular smooth muscle cells, and desmin+ fibroblasts by lineage tagging; and demonstrated that mesothelial cell movement into the lung requires the direct action of sonic hedgehog (shh) signaling (Dixit et al., 2013). Together, these studies demonstrate that the mesothelium lining of serosal surfaces of multiple organ systems plays a critical role during development and organogenesis, supporting the possibility that they may also modulate lung injury-repair by re-activation of developmental programs in the adult.

Wt1 IN POSTNATAL DISEASE

Wt1 can induce a morphological transition from an epithelial phenotype to a mesenchymal phenotype (Burwell et al., 2007). It is a potent transcription factor that can function as a tumor suppressor (Zhang et al., 2003), or as an oncogene depending on the cell type (Loeb et al., 2001; Oji et al., 2002; Ueda et al., 2003). It was in fact initially discovered as a tumor suppressor gene in Wilms tumor of the kidney (Haber et al., 1990). Wt1 demonstrates tissue specific responses and is recognized to regulate TGF-β1 in the kidney. In other cell types such as hematological cells it is reported to confer oncogenic properties (Licciulli and Kissil, 2010). Wt1 is expressed in normal pleural mesothelium, and is over-expressed in malignant mesothelioma (Amin et al., 1995). However, there is limited information of the role of Wt1 in non-malignant lung diseases.

Wt1 IN IDIOPATHIC PULMONARY FIBROSIS (IPF)

Several studies support a role for Wt1 in mesothelial-to-mesenchymal transition (MMT) (Burwell et al., 2007; Bax et al., 2011a,b). Hecker et al. have evaluated the responses of PMCs to TGF-β1, their expression of MMT markers such as e-cadherin, α-SMA, vimentin; their contractile ability using a collagen gel contraction assay (Hecker et al., 2009); and also biological functional assays such as migration and proliferation (Hecker et al., 2009). Studies indicate a role for TGF-β1 in mediating MMT (Nasreen et al., 2009). For example, treatment of mouse

PMCs with TGF-β1 increased expression of the myofibroblast markers α-SMA and NADPH oxidase-4 (NOX-4) (Zolak et al., 2013). Wt1-expressing PMCs are present both on the pleural surface and in the lung parenchyma of patients with IPF suggesting their role in the pathogenesis of IPF. However, the precise relationship between Wt1 and TGF-β1 remains unclear. Also, the role of Wt1 in regulating PMC plasticity needs to be analyzed.

PLURIPOTENCY OF MESOTHELIAL CELLS

Although mesenchymal in origin, mesothelial cells exhibit characteristics such as a polygonal cell shape, expression of surface microvilli, epithelial cytokeratins, and tight junctions, which are typical of epithelial cells (Mutsaers, 2002). During development, endothelium and vascular smooth muscle cells of the vascular system, heart, liver and gut are derived from the differentiation of mesothelium via a process of epithelial-to-mesenchymal transition (EMT) (Munoz-Chapuli et al., 1999; Perez-Pomares et al., 2002, 2004). Increasing evidence suggests existence of a population of progenitor-like mesothelial cells with the capacity to differentiate into cells of different phenotypes (Herrick and Mutsaers, 2004). By targeting mesothelin and using a genetic lineage tracing approach, Rinkevich et al. demonstrated that embryonic and adult mesothelium represents a common lineage to trunk fibroblasts, smooth muscle cells, and vasculature (Rinkevich et al., 2012).

Recently, primary rat and human mesothelial cells, when maintained in osteogenic or adipogenic media, were shown to differentiate into osteoblast- and adipocyte-like cells via epithelial-to-mesenchymal transition as suggested by the changes in mRNA expression of these cells. This supports mesothelial cell differentiation as the potential source of different tissue types in malignant mesothelioma and other serosal pathologies (Lansley et al., 2011). The term *mesodermoma* was introduced by Donna and Betta to define neoplasms arising from undifferentiated and multipotential mesoderm (Donna and Betta, 1981).

Mesothelial cells appear to retain the ability to produce mesenchyme, including smooth muscle cells, in response to transforming growth factor-β_1 (TGF-β_1) and platelet derived growth factor (Wada et al., 2003; Kawaguchi et al., 2007). Moreover, mesothelial cells have been shown to adopt a myofibroblast phenotype *in vitro*, in response to TGF-β_1 (Yang et al., 2003). Transfection of the peritoneum and pleura of rats with an adenovirus expressing TGF-β_1 induced mesothelial cells to undergo EMT with subsequent fibrotic changes (Margetts et al., 2005; Decologne et al., 2007).

The significance of EMT in malignant pleural mesothelioma (MPM) was demonstrated by Schramm et al. in their study of a retrospective cohort of 352 patients. Immunohistochemistry of a tissue microarray showed that the activation of periostin-triggered EMT is associated with the sarcomatoid histotype of malignant mesothelioma and has an impact on shorter survival of patients (Schramm et al., 2010). Periostin secretion by MPM cells has in turn been shown to be upregulated by CD26 (Komiya et al., 2014), the expression of which is increased in various cancers (Havre et al., 2008).

IDIOPATHIC PULMONARY FIBROSIS (IPF)

SUB-PLEURAL DISTRIBUTION

IPF is a progressive lung disease process that appears to begin in the sub-pleural regions, and then extend centrally. This sub-pleural and basilar distribution, which is the defining feature of idiopathic pulmonary fibrosis (IPF) has not been adequately explained (King et al., 2011). However, this pattern of distribution suggests pleural involvement in the disease process.

MYOFIBROBLASTS AND FIBROBLASTIC FOCI

The presence of myofibroblasts in fibrobastic foci in lungs of patients with IPF is well-established. The fibroblast and myofibroblast foci secrete excessive amounts of extracellular matrix, mainly collagens, resulting in scarring and destruction of the lung architecture. The profusion of fibroblastic foci is predictive of survival in IPF patients (King et al., 2001a,b). A recent study has shown that the hallmark lesion in usual interstitial pneumonia (UIP), fibroblastic foci, on three-dimensional histo-pathological reconstruction are part of a complex and highly interconnected reticulum of fibrous tissue that extends from the pleura into the lung parenchyma (Cool et al., 2006). Neither the origin of these myofibroblasts nor the molecular mechanisms involved in the formation of fibroblastic foci have been well-defined (Phan, 2008).

While a number of cellular source(s) and progenitors of tissue myofibroblasts have been proposed, none of these hypotheses provide a indisputable explanation for the histo-pathological pattern of usual interstitial pneumonia (UIP) and its peripheral localization (Raghu et al., 2011). However, evidence suggests that abnormal recapitulation of developmental pathways and epigenetic changes may play a role in the pathogenesis of IPF (King et al., 2011). IPF is a devastating disease with an inexorable course and its pathogenesis remains unclear. There are no therapies that directly impact the disease progression or mortality, and we urgently need innovative new ideas that will impact therapeutics in this disease (King et al., 2011; Raghu et al., 2011). PMCs serve as myofibroblast progenitors in animal models of fibrosis, and therapeutic targeting of these cells may be effective as an anti-fibrotic approach (Que et al., 2008).

PLEURAL MESOTHELIAL CELLS IN IPF

PMCs are metabolically active cells (Antony, 2003; Mohammed et al., 2007), responsive to their microenvironment (Antony, 2003), and are recognized to demonstrate plasticity of their phenotype (Nasreen et al., 2009).The presence of calretinin and mesothelin (markers of mesothelial cells) (Mubarak et al., 2012) and Wt-1 expressing PMCs (Zolak et al., 2013) was recently demonstrated in parenchymal cells of explanted lung tissues from 16 patients with IPF supporting a role for PMC differentiation and their trafficking into the lung as contributors to the myofibroblast population in lung fibrosis. It is not known if the number or profusion of PMCs may be predictive of the severity and/or progression of IPF.

The Ashcroft score is a score for histo-pathological grading of pulmonary fibrosis (Hagiwara et al., 2000; Matsuoka et al., 2002; Simler et al., 2002; Murakami et al., 2006). There exists a correlation between the number of calretinin-positive cells and the

degree of fibrotic change in the parenchyma, as measured by the Ashcroft score. Whether the number of calretinin-positive cells was measured as a raw number, or as percentage of the total nucleated cells seen in a photomicrograph, the correlation with the degree of fibrosis was highly significant (Mubarak et al., 2012). These studies suggest that PMCs may represent a novel cellular biomarker of disease activity, and more importantly, play a role in the tissue remodeling responses seen in patients with IPF.

Recent studies demonstrate that PMCs cells lose their polarity and cell-cell junctional complexes, migrate into lung parenchyma, and undergo phenotypic transition into myofibroblasts in response to the pro-fibrotic mediator, TGF-β1 (Nasreen et al., 2009; Mubarak et al., 2012). The transition of PMC to myofibroblasts is dependent on smad-2 signaling and knockdown of smad-2 gene by silencing small interfering RNA significantly suppresses the transition of PMCs to myofibroblasts and inhibits PMC haptotaxis (Nasreen et al., 2009). We have demonstrated in a murine model, that TGF-β1 induces PMC trafficking into the lung and differentiation into myofibroblasts. Moreover, carbon monoxide or the induction of heme oxygenase-1 (HO-1) inhibits the expression of myofibroblast markers, contractility, and haptotaxis in PMCs treated with TGF-β1. These findings support a potential role for pleural-based therapies to modulate pleural mesothelial activation and parenchymal fibrosis progression (Zolak et al., 2013).

PLEURAL MESOTHELIAL CELLS AS A POTENTIAL THERAPEUTIC TARGET

PMCs migrate into the pulmonary parenchyma in IPF and transition into myofibroblasts. This invokes a novel, alternative hypothesis for the origin and source of the myofibroblasts in the lungs of patients with IPF, and provides a rational explanation for the spatio-temporal distribution of fibrosis in IPF. PMCs could represent a new cellular therapeutic target in a disease where we currently lack treatment options. Intra-pleural delivery of compounds is a lung targeted, innovative therapeutic modality that can be refined to deliver drugs, minimizing systemic toxicity.

Direct delivery of the small molecule inhibitors to the pleura could potentially have several advantages: (Jantz and Antony, 2006) It can potentially provide a direct, high concentration of the compound to target the pro-fibrogenic activities of PMCs; (Haber et al., 1990) Intra-pleural delivery might delay systemic absorption, protecting against systemic toxicity while increasing efficacy; (Park et al., 1993) Intra-pleural delivery may result in higher, sustained levels in the Bronchoalveolar lavage (BAL) when compared with serum levels (Mubarak et al., 2012); and (Jomgeow et al., 2006) innovative, less invasive methods of accessing the pleural space such as tunneled pleural catheters could make intra-pleural delivery a viable option in patients.

There are several methods that can be utilized for site-directed delivery of therapeutic agents. These include liposomal drug delivery, nanoparticle (NP) delivery of proteins, and gene therapy (Watanabe et al., 2010). Several of these methods have been utilized to target the pleura (Perez-Soler et al., 1997; Liu et al., 2006; Watanabe et al., 2010). We have demonstrated that PMCs migrate into the parenchyma (Zolak et al., 2013). Biodegradable fluorescein isothiocyanate (FITC) labeled PLGA (poly-lactic-co-glycolic acid) nanoparticles (which can carry therapeutic compounds conjugated to PLGA) decorated with antibody targeted to mesothelin (a PMC marker) localize to the pleural surface in control mice, but diffuse into the lung parenchyma in mice given intra-tracheal bleomycin (**Figure 1**). It appears that intra-pleural delivery of molecules to the lung is feasible, albeit, with the recognition that refinement of techniques for minimal lung injury will be required.

CONCLUSION

The pleural mesothelium is a derivative of the embryonic mesoderm. Several complex pathways of interplay between the mesoderm and endoderm lead to the development of the lungs and pleura. Lineage labeling and other studies have shown the ability of the PMCs to undergo MMT to form other mesenchymal structures and have therefore established their pluripotency during development. Moreover, recent studies have shown that the plasticity of mesothelial cells is retained postnatally and gives them the ability to migrate and differentiate into other cell types. This supports the possibility that PMCs may modulate lung injury-repair by reactivation of developmental programs in the adult, reflecting an altered recapitulation of development with implications for regenerative biology of the lung. We have shown that PMCs are present in the lung parenchyma in lungs with IPF. Also, PMC migration into lung parenchyma and phenotypic transition into myofibroblasts can be induced by the pro-fibrotic mediator, TGF-β1 and is inhibited by intra-pleural heme-oxygenase-1 (HO-1). The possible role of PMCs in disease pathogenesis and/or progression of IPF makes them an attractive cellular target for potential therapeutic interventions in a disease where we currently lack treatment modalities. Intra-pleural delivery of compounds is a lung targeted, innovative therapeutic modality that can be refined to deliver drugs, thereby minimizing systemic toxicity. Intra-pleural fluorescein isothiocyanate labeled nanoparticles decorated with a surface antibody to mesothelin, a surface marker of mesothelial cells, migrate into the lung parenchyma with PMCs supporting a potential role for pleural based therapies to modulate pleural mesothelial activation and parenchymal disease progression. However, further studies are

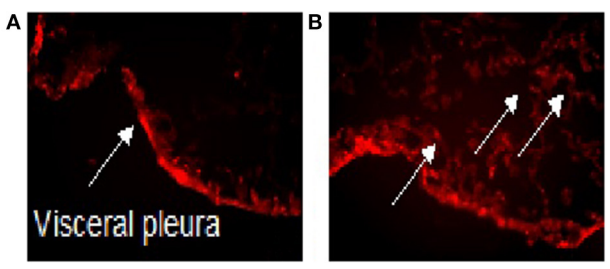

FIGURE 1 | Intra-pleural delivery of PLGA NP. Biodegradable FITC labeled PLGA nanoparticles (which can carry therapeutic compounds conjugated to PLGA) decorated with antibody targeted to mesothelin (a PMC marker) localize to the pleural surface in control mice treated with saline **(A)**, but diffuse into the lung parenchyma in mice given intra-tracheal bleomycin **(B)**. The arrow point to FITC labeled PLGA nanoparticles. PLGA, Poly Lactic-co-Glycolic Acid; NP, Nanoparticles; FITC, Fluorescein isothiocyanate.

needed to develop such therapies and effective pleural-based drug delivery systems.

REFERENCES

Amin, K. M., Litzky, L. A., Smythe, W. R., Mooney, A. M., Morris, J. M., Mews, D. J., et al. (1995). Wilms' tumor 1 susceptibility (WT1) gene products are selectively expressed in malignant mesothelioma. *Am. J. Pathol.* 146, 344–356.

Antony, V. B. (2003). Immunological mechanisms in pleural disease. *Eur Respir. J.* 21, 539–544. doi: 10.1183/09031936.03.00403902

Bax, N. A., Pijnappels, D. A., van Oorschot, A. A., Winter, E. M., de Vries, A. A., van Tuyn, J., et al. (2011a). Epithelial-to-mesenchymal transformation alters electrical conductivity of human epicardial cells. *J. Cell. Mol. Med.* 15, 2675–2683. doi: 10.1111/j.1582-4934.2011.01266.x

Bax, N. A., van Oorschot, A. A., Maas, S., Braun, J., van Tuyn, J., de Vries, A. A., et al. (2011b). *In vitro* epithelial-to-mesenchymal transformation in human adult epicardial cells is regulated by TGFbeta-signaling and WT1. *Basic Res. Cardiol.* 106, 829–847. doi: 10.1007/s00395-011-0181-0

Bellusci, S., Furuta, Y., Rush, M. G., Henderson, R., Winnier, G., and Hogan, B. L. (1997). Involvement of Sonic hedgehog (Shh) in mouse embryonic lung growth and morphogenesis. *Development* 124, 53–63.

Burwell, E. A., McCarty, G. P., Simpson, L. A., Thompson, K. A., and Loeb, D. M. (2007). Isoforms of Wilms' tumor suppressor gene (WT1) have distinct effects on mammary epithelial cells. *Oncogene* 26, 3423–3430. doi: 10.1038/sj.onc.1210127

Cai, C. L., Martin, J. C., Sun, Y., Cui, L., Wang, L., Ouyang, K., et al. (2008). A myocardial lineage derives from Tbx18 epicardial cells. *Nature* 454, 104–108. doi: 10.1038/nature06969

Call, K. M., Glaser, T., Ito, C. Y., Buckler, A. J., Pelletier, J., Haber, D. A., et al. (1990). Isolation and characterization of a zinc finger polypeptide gene at the human chromosome 11 Wilms' tumor locus. *Cell* 60, 509–520. doi: 10.1016/0092-8674(90)90601-A

Colvin, J. S., White, A. C., Pratt, S. J., and Ornitz, D. M. (2001). Lung hypoplasia and neonatal death in Fgf9-null mice identify this gene as an essential regulator of lung mesenchyme. *Development* 128, 2095–2106.

Cool, C. D., Groshong, S. D., Rai, P. R., Henson, P. M., Stewart, J. S., and Brown, K. K. (2006). Fibroblast foci are not discrete sites of lung injury or repair: the fibroblast reticulum. *Am. J. Respir. Crit. Care Med.* 174, 654–658. doi: 10.1164/rccm.200602-205OC

Decologne, N., Kolb, M., Margetts, P. J., Menetrier, F., Artur, Y., Garrido, C., et al. (2007). TGF-beta1 induces progressive pleural scarring and subpleural fibrosis. *J. Immunol.* 179, 6043–6051. doi: 10.4049/jimmunol.179.9.6043

Dettman, R. W., Denetclaw, W. Jr., Ordahl, C. P., and Bristow, J. (1998). Common epicardial origin of coronary vascular smooth muscle, perivascular fibroblasts, and intermyocardial fibroblasts in the avian heart. *Dev. Biol.* 193, 169–181. doi: 10.1006/dbio.1997.8801

Dixit, R., Ai, X., and Fine, A. (2013). Derivation of lung mesenchymal lineages from the fetal mesothelium requires hedgehog signaling for mesothelial cell entry. *Development* 140, 4398–4406. doi: 10.1242/dev.098079

Domyan, E. T., Ferretti, E., Throckmorton, K., Mishina, Y., Nicolis, S. K., and Sun, X. (2011). Signaling through BMP receptors promotes respiratory identity in the foregut via repression of Sox2. *Development* 138, 971–981. doi: 10.1242/dev.053694

Donna, A., and Betta, P. G. (1981). Mesodermomas: a new embryological approach to primary tumours of coelomic surfaces. *Histopathology*. 5, 31–44. doi: 10.1111/j.1365-2559.1981.tb01764.x

Goss, A. M., Tian, Y., Tsukiyama, T., Cohen, E. D., Zhou, D., Lu, M. M., et al. (2009). Wnt2/2b and beta-catenin signaling are necessary and sufficient to specify lung progenitors in the foregut. *Dev. Cell* 17, 290–298. doi: 10.1016/j.devcel.2009.06.005

Haber, D. A., Buckler, A. J., Glaser, T., Call, K. M., Pelletier, J., Sohn, R. L., et al. (1990). An internal deletion within an 11p13 zinc finger gene contributes to the development of Wilms' tumor. *Cell* 61, 1257–1269. doi: 10.1016/0092-8674(90)90690-G

Hagiwara, S. I., Ishii, Y., and Kitamura, S. (2000). Aerosolized administration of N-acetylcysteine attenuates lung fibrosis induced by bleomycin in mice. *Am. J. Respir. Crit. Care Med.* 162, 225–231. doi: 10.1164/ajrccm.162.1.9903129

Havre, P. A., Abe, M., Urasaki, Y., Ohnuma, K., Morimoto, C., and Dang, N. H. (2008). The role of CD26/dipeptidyl peptidase IV in cancer. *Front. Biosci.* 13, 1634–1645. doi: 10.2741/2787

Hecker, L., Vittal, R., Jones, T., Jagirdar, R., Luckhardt, T. R., Horowitz, J. C., et al. (2009). NADPH oxidase-4 mediates myofibroblast activation and fibrogenic responses to lung injury. *Nat. Med.* 15, 1077–1081. doi: 10.1038/nm.2005

Herrick, S. E., and Mutsaers, S. E. (2004). Mesothelial progenitor cells and their potential in tissue engineering. *Int. J. Biochem. Cell Biol.* 36, 621–642. doi: 10.1016/j.biocel.2003.11.002

Herriges, M., and Morrisey, E. E. (2014). Lung development: orchestrating the generation and regeneration of a complex organ. *Development* 141, 502–513. doi: 10.1242/dev.098186

Ito, K., Oji, Y., Tatsumi, N., Shimizu, S., Kanai, Y., Nakazawa, T., et al. (2006). Antiapoptotic function of 17AA(+)WT1 (Wilms' tumor gene) isoforms on the intrinsic apoptosis pathway. *Oncogene* 25, 4217–4229. doi: 10.1038/sj.onc.1209455

Jantz, M. A., and Antony, V. B. (2006). Pleural fibrosis. *Clin. Chest Med.* 27, 181–191. doi: 10.1016/j.ccm.2005.12.003

Jomgeow, T., Oji, Y., Tsuji, N., Ikeda, Y., Ito, K., Tsuda, A., et al. (2006). Wilms' tumor gene WT1 17AA(-)/KTS(-) isoform induces morphological changes and promotes cell migration and invasion *in vitro*. *Cancer Sci.* 97, 259–270. doi: 10.1111/j.1349-7006.2006.00169.x

Kawaguchi, M., Bader, D. M., and Wilm, B. (2007). Serosal mesothelium retains vasculogenic potential. *Dev. Dyn.* 236, 2973–2979. doi: 10.1002/dvdy.21334

King, T. E. Jr., Pardo, A., and Selman, M. (2011). Idiopathic pulmonary fibrosis. *Lancet* 378, 1949–1961. doi: 10.1016/S0140-6736(11)60052-4

King, T. E. Jr., Schwarz, M. I., Brown, K., Tooze, J. A., Colby, T. V., Waldron, J. A. Jr., et al. (2001a). Idiopathic pulmonary fibrosis: relationship between histopathologic features and mortality. *Am. J. Respir. Crit. Care Med.* 164, 1025–1032. doi: 10.1164/ajrccm.164.6.2001056

King, T. E. Jr., Tooze, J. A., Schwarz, M. I., Brown, K. R., and Cherniack, R. M. (2001b). Predicting survival in idiopathic pulmonary fibrosis: scoring system and survival model. *Am. J. Respir. Crit. Care Med.* 164, 1171–1181. doi: 10.1164/ajrccm.164.7.2003140

Komiya, E., Ohnuma, K., Yamazaki, H., Hatano, R., Iwata, S., Okamoto, T., et al. (2014). CD26-mediated regulation of periostin expression contributes to migration and invasion of malignant pleural mesothelioma cells. *Biochem. Biophys. Res. Commun.* 447, 609–615. doi: 10.1016/j.bbrc.2014.04.037

Lansley, S. M., Searles, R. G., Hoi, A., Thomas, C., Moneta, H., Herrick, S. E., et al. (2011). Mesothelial cell differentiation into osteoblast- and adipocyte-like cells. *J. Cell. Mol. Med.* 15, 2095–2105. doi: 10.1111/j.1582-4934.2010.01212.x

Licciulli, S., and Kissil, J. L. (2010). WT1: a weak spot in KRAS-induced transformation. *J. Clin. Invest.* 120, 3804–3807. doi: 10.1172/JCI44901

Liu, J., Wong, H. L., Moselhy, J., Bowen, B., Wu, X. Y., and Johnston, M. R. (2006). Targeting colloidal particulates to thoracic lymph nodes. *Lung Cancer* 51, 377–386. doi: 10.1016/j.lungcan.2005.11.006

Loeb, D. M., Evron, E., Patel, C. B., Sharma, P. M., Niranjan, B., Buluwela, L., et al. (2001). Wilms' tumor suppressor gene (WT1) is expressed in primary breast tumors despite tumor-specific promoter methylation. *Cancer Res.* 61, 921–925.

Margetts, P. J., Bonniaud, P., Liu, L., Hoff, C. M., Holmes, C. J., West-Mays, J. A., et al. (2005). Transient overexpression of TGF-{beta}1 induces epithelial mesenchymal transition in the rodent peritoneum. *J. Am. Soc. Nephrol.* 16, 425–436. doi: 10.1681/ASN.2004060436

Matsuoka, H., Arai, T., Mori, M., Goya, S., Kida, H., Morishita, H., et al. (2002). A p38 MAPK inhibitor, FR-167653, ameliorates murine bleomycin-induced pulmonary fibrosis. *Am. J. Physiol. Lung Cell. Mol. Physiol.* 283, L103–L112.

Mikawa, T., and Gourdie, R. G. (1996). Pericardial mesoderm generates a population of coronary smooth muscle cells migrating into the heart along with ingrowth of the epicardial organ. *Dev. Biol.* 174, 221–232. doi: 10.1006/dbio.1996.0068

Mohammed, K. A., Nasreen, N., and Antony, V. B. (2007). Bacterial induction of early response genes and activation of proapoptotic factors in pleural mesothelial cells. *Lung* 185, 355–365. doi: 10.1007/s00408-007-9046-6

Mubarak, K. K., Montes-Worboys, A., Regev, D., Nasreen, N., Mohammed, K. A., Faruqi, I., et al. (2012). Parenchymal trafficking of pleural mesothelial cells in idiopathic pulmonary fibrosis. *Eur. Respir. J.* 39, 133–140. doi: 10.1183/09031936.00141010

Munoz-Chapuli, R., Perez-Pomares, J. M., Macias, D., Garcia-Garrido, L., Carmona, R., and Gonzalez, M. (1999). Differentiation of hemangioblasts

from embryonic mesothelial cells? A model on the origin of the vertebrate cardiovascular system. *Differentiation* 64, 133–141. doi: 10.1007/s0025800 50268

Murakami, S., Nagaya, N., Itoh, T., Kataoka, M., Iwase, T., Horio, T., et al. (2006). Prostacyclin agonist with thromboxane synthase inhibitory activity (ONO-1301) attenuates bleomycin-induced pulmonary fibrosis in mice. *Am. J. Physiol. Lung Cell. Mol. Physiol.* 290, L59–L65. doi: 10.1152/ajplung.00042.2005

Mutsaers, S. E. (2002). Mesothelial cells: their structure, function and role in serosal repair. *Respirology* 7, 171–191. doi: 10.1046/j.1440-1843.2002.00404.x

Nasreen, N., Mohammed, K. A., Mubarak, K. K., Baz, M. A., Akindipe, O. A., Fernandez-Bussy, S., et al. (2009). Pleural mesothelial cell transformation into myofibroblasts and haptotactic migration in response to TGF-beta1 *in vitro*. *Am. J. Physiol. Lung Cell. Mol. Physiol.* 297, L115–L124. doi: 10.1152/ajplung.90587.2008

Ohuchi, H., Hori, Y., Yamasaki, M., Harada, H., Sekine, K., Kato, S., et al. (2000). FGF10 acts as a major ligand for FGF receptor 2 IIIb in mouse multi-organ development. *Biochem. Biophys. Res. Commun.* 277, 643–649. doi: 10.1006/bbrc.2000.3721

Oji, Y., Miyoshi, S., Maeda, H., Hayashi, S., Tamaki, H., Nakatsuka, S., et al. (2002). Overexpression of the Wilms' tumor gene WT1 in de novo lung cancers. *Int. J. Cancer* 100, 297–303. doi: 10.1002/ijc.10476

Park, S., Schalling, M., Bernard, A., Maheswaran, S., Shipley, G. C., Roberts, D., et al. (1993). The Wilms tumour gene WT1 is expressed in murine mesoderm-derived tissues and mutated in a human mesothelioma. *Nat. Genet.* 4, 415–420. doi: 10.1038/ng0893-415

Pepicelli, C. V., Lewis, P. M., and McMahon, A. P. (1998). Sonic hedgehog regulates branching morphogenesis in the mammalian lung. *Curr. biol.* 8, 1083–1086. doi: 10.1016/S0960-9822(98)70446-4

Perez-Pomares, J. M., Carmona, R., Gonzalez-Iriarte, M., Atencia, G., Wessels, A., and Munoz-Chapuli, R. (2002). Origin of coronary endothelial cells from epicardial mesothelium in avian embryos. *Int. J. Dev. Biol.* 46, 1005–1013.

Perez-Pomares, J. M., Carmona, R., Gonzalez-Iriarte, M., Macias, D., Guadix, J. A., and Munoz-Chapuli, R. (2004). Contribution of mesothelium-derived cells to liver sinusoids in avian embryos. *Dev. Dyn* 229, 465–474. doi: 10.1002/dvdy.10455

Perez-Soler, R., Shin, D. M., Siddik, Z. H., Murphy, W. K., Huber, M., Lee, S. J., et al. (1997). Phase I clinical and pharmacological study of liposome-entrapped NDDP administered intrapleurally in patients with malignant pleural effusions. *Clin. Cancer Res.* 3, 373–379.

Phan, S. H. (2008). Biology of fibroblasts and myofibroblasts. *Proc. Am. Thorac. Soc.* 5, 334–337. doi: 10.1513/pats.200708-146DR

Que, J., Wilm, B., Hasegawa, H., Wang, F., Bader, D., and Hogan, B. L. (2008). Mesothelium contributes to vascular smooth muscle and mesenchyme during lung development. *Proc. Natl. Acad. Sci. U.S.A.* 105, 16626–16630. doi: 10.1073/pnas.0808649105

Raghu, G., Collard, H. R., Egan, J. J., Martinez, F. J., Behr, J., Brown, K. K., et al. (2011). An official ATS/ERS/JRS/ALAT statement: idiopathic pulmonary fibrosis: evidence-based guidelines for diagnosis and management. *Am. J. Respir. Crit. Care Med.* 183, 788–824. doi: 10.1164/rccm.2009-040GL

Rinkevich, Y., Mori, T., Sahoo, D., Xu, P. X., Bermingham, J. R. Jr., and Weissman, I. L. (2012). Identification and prospective isolation of a mesothelial precursor lineage giving rise to smooth muscle cells and fibroblasts for mammalian internal organs, and their vasculature. *Nat. Cell Biol.* 14, 1251–1260. doi: 10.1038/ncb2610

Schramm, A., Opitz, I., Thies, S., Seifert, B., Moch, H., Weder, W., et al. (2010). Prognostic significance of epithelial-mesenchymal transition in malignant pleural mesothelioma. *Eur. J. Cardiothorac. Surg.* 37, 566–572. doi: 10.1016/j.ejcts.2009.08.027

Sekine, K., Ohuchi, H., Fujiwara, M., Yamasaki, M., Yoshizawa, T., Sato, T., et al. (1999). Fgf10 is essential for limb and lung formation. *Nat. Genet.* 21, 138–141. doi: 10.1038/5096

Simler, N. R., Howell, D. C., Marshall, R. P., Goldsack, N. R., Hasleton, P. S., Laurent, G. J., et al. (2002). The rapamycin analogue SDZ RAD attenuates bleomycin-induced pulmonary fibrosis in rats. *Eur Respir. J.* 19, 1124–1127. doi: 10.1183/09031936.02.00281602

Ueda, T., Oji, Y., Naka, N., Nakano, Y., Takahashi, E., Koga, S., et al. (2003). Overexpression of the Wilms' tumor gene WT1 in human bone and soft-tissue sarcomas. *Cancer Sci.* 94, 271–276. doi: 10.1111/j.1349-7006.2003.tb01432.x

Wada, A. M., Smith, T. K., Osler, M. E., Reese, D. E., and Bader, D. M. (2003). Epicardial/Mesothelial cell line retains vasculogenic potential of embryonic epicardium. *Circ. Res.* 92, 525–531. doi: 10.1161/01.RES.0000060484.11032.0B

Watanabe, M., Boyer, J. L., and Crystal, R. G. (2010). AAVrh.10-mediated genetic delivery of bevacizumab to the pleura to provide local anti-VEGF to suppress growth of metastatic lung tumors. *Gene Ther.* 17, 1042–1051. doi: 10.1038/gt.2010.87

Weaver, M., Dunn, N. R., and Hogan, B. L. (2000). Bmp4 and Fgf10 play opposing roles during lung bud morphogenesis. *Development* 127, 2695–2704.

Wilm, B., Ipenberg, A., Hastie, N. D., Burch, J. B., and Bader, D. M. (2005). The serosal mesothelium is a major source of smooth muscle cells of the gut vasculature. *Development* 132, 5317–5328. doi: 10.1242/dev.02141

Yang, A. H., Chen, J. Y., and Lin, J. K. (2003). Myofibroblastic conversion of mesothelial cells. *Kidney Int.* 63, 1530–1539. doi: 10.1046/j.1523-1755.2003.00861.x

Zhang, T. F., Yu, S. Q., Guan, L. S., and Wang, Z. Y. (2003). Inhibition of breast cancer cell growth by the Wilms' tumor suppressor WT1 is associated with a destabilization of beta-catenin. *Anticancer Res.* 23, 3575–3584.

Zhou, B., Honor, L. B., He, H., Ma, Q., Oh, J. H., Butterfield, C., et al. (2011). Adult mouse epicardium modulates myocardial injury by secreting paracrine factors. *J. Clin. Invest.* 121, 1894–1904. doi: 10.1172/JCI45529

Zhou, B., von Gise, A., Ma, Q., Hu, Y. W., and Pu, W. T. (2010). Genetic fate mapping demonstrates contribution of epicardium-derived cells to the annulus fibrosis of the mammalian heart. *Dev. Biol.* 338, 251–261. doi: 10.1016/j.ydbio.2009.12.007

Zolak, J. S., Jagirdar, R., Surolia, R., Karki, S., Oliva, O., Hock, T., et al. (2013). Pleural mesothelial cell differentiation and invasion in fibrogenic lung injury. *Am. J. Pathol.* 182, 1239–1247. doi: 10.1016/j.ajpath.2012.12.030

Conflict of Interest Statement: The authors declare that the research was conducted in the absence of any commercial or financial relationships that could be construed as a potential conflict of interest.

Received: 27 May 2014; accepted: 10 July 2014; published online: 01 August 2014.
*Citation: Batra H and Antony VB (2014) The pleural mesothelium in development and disease. Front. Physiol. **5**:284. doi: 10.3389/fphys.2014.00284*
This article was submitted to Membrane Physiology and Membrane Biophysics, a section of the journal Frontiers in Physiology.

frontiers in PHYSIOLOGY

ORIGINAL RESEARCH ARTICLE
published: 30 June 2014
doi: 10.3389/fphys.2014.00232

Role of $[Ca^{2+}]_i$ and F-actin on mesothelial barrier function

Masayoshi Kuwahara*

Laboratory of Veterinary Pathophysiology and Animal Health, Department of Veterinary Medical Sciences, Graduate School of Agricultural and Life Sciences, The University of Tokyo, Tokyo, Japan

Edited by:
Sotirios G. Zarogiannis, University of Thessaly, Greece

Reviewed by:
Irena Levitan, University of Illinois at Chicago, USA
Huazhi Eric Han, University of Illinois at Chicago, USA
Kinji Asahina, University of Southern California, USA

****Correspondence:***
Masayoshi Kuwahara, Laboratory of Veterinary Pathophysiology and Animal Health, Department of Veterinary Medical Sciences, Graduate School of Agricultural and Life Sciences, The University of Tokyo, 1-1-1 Yayoi, Bunkyo-ku, Tokyo 113-8657, Japan
e-mail: akuwam@mail.ecc.u-tokyo.ac.jp

The mesothelial layer acts as a biological barrier between the organ and the enveloping serous cavity and may have functions of transport, equilibrium maintenance, and protection. However, the role of the mesothelial cells in regulation of pleural permeability remains essentially undefined. The present study was designed to clarify the effects of bradykinin, histamine, and thrombin on permeability in pleural mesothelial cells. Rat pleural mesothelial cells were cultured *in vitro*, and the permeability of mesothelial monolayers was evaluated by transmesothelial albumin diffusion and electrical resistance measurements. Furthermore, the temporal relationship between changes in the levels of $[Ca^{2+}]_i$ and the mesothelial permeability was examined. Bradykinin (10 μM), histamine (1 mM), and thrombin (10 U) caused albumin diffusion within 5 min. The electrical resistance of mesothelial monolayer began falling within 5 min of adding each agent. Time and concentration dependency of changes in electrical resistance were almost the same as that in albumin diffusion. Each agent also induced a biphasic elevation of $[Ca^{2+}]_i$ in pleural mesothelial cells. The concentration-dependency of the $[Ca^{2+}]_i$ responses were almost similar to that noted for each agent induced albumin diffusion and electrical resistance fall. The increase in permeability occurred with reorganization of F-actin cytoskeleton and increased actin polymerization. These results suggest that the Ca^{2+}- dependency of increases induced by these agents in mesothelial permeability have been related to the regulatory role of Ca^{2+} in the F-actin cytoskeletal reorganization in pleural mesothelial cells.

Keywords: actin cytoskeleton, bradykinin, cytosolic calcium, cytochalasin B, F-actin, histamine, pleura, thrombin

INTRODUCTION

The visceral and parietal pleura are lined by a unicellular layer of mesothelial cells that overlie a discontinuous basal lamina. This mesothelial layer acts as a biological barrier between the organ and the enveloping serous cavity and may have functions of transport, equilibrium maintenance, and protection (Wang, 1985). Changes in pleural permeability, the influx of phagocytic cells, and the leak of serum proteins into the pleural space lead to the development of an inflammatory exudate (Robbins and Kumar, 1987). However, the role of the mesothelial cells in regulation of pleural permeability remains essentially undefined.

We have shown that pleural and pericardial mesothelial cells can respond to histamine (Ito et al., 1995). Histamine elevates intracellular calcium concentration ($[Ca^{2+}]_i$) and induces F-actin cytoskeletal reorganization in mesothelial cells. Because F-actin-staining studies have shown the regulatory role of $[Ca^{2+}]_i$ in cytoskeleton assembly in mesothelial cells, we have suggested that changes in $[Ca^{2+}]_i$ may have relevance to the regulation of mesothelial permeability. Therefore, the present study was designed to clarify the effects of bradykinin, histamine, and thrombin on permeability in pleural mesothelial cells. For this purpose, rat pleural mesothelial cells were cultured *in vitro*, and the permeability of mesothelial monolayers was evaluated by transmesothelial albumin diffusion and electrical resistance measurements. Furthermore, the temporal relationship between changes in the levels of $[Ca^{2+}]_i$ and the mesothelial permeability was examined.

MATERIALS AND METHODS

REAGENTS, MEDIA, AND BUFFERS

For the Ca^{2+} measurements we used a N-2-hydroxyethylpiperazine-N′-2-ethanesulfonic acid (HEPES) buffer containing (in mM) 10 HEPES, 136.9 NaCl, 5.4 KCl, 1.0 $MgCl_2$, 1.5 $CaCl_2$, 0.001 EDTA, and 5.5 glucose (HEPES-buffered solution). Dulbecco's modified eagles medium (DMEM), Hanks' balanced salt solution (HBSS), fetal bovine serum (FBS), and trypsin-EDTA were purchased from GIBCO, Grand Island, NY. Bradykinin, thrombin, ionomycin, albumin, cytochalasin B and 1,2-bis(2-aminophenoxy) ethane-N,N,N',N'-tetraacetic acid (BAPTA) were purchased from Sigma Chemical Co., St. Louis, MO. Fura 2-acetoxymethyl ester (fura 2-AM) was obtained from Dojindo Laboratories, Kumamoto, Japan. Histamine was purchased from Wako, Tokyo, Japan. Other materials and chemicals were obtained from commercial sources.

RAT PLEURAL MESOTHELIAL CELL CULTURES

Rat pleural mesothelial cells were established and maintained, as described previously (Ito et al., 1995). Briefly, adult Wistar Kyoto rats were anesthetized with sodium pentobarbital (50 mg/kg ip)

and were immediately killed by exsanguination from a severed abdominal aorta. The complete thoracic wall was removed under sterile conditions and immersed in petri dish for 20 min in HBSS. The parietal pleural surface was scraped repeatedly with cell scrapers. The cells were then seeded into 55-cm^2 tissue-culture dishes (Corning, Wexford, PA) in DMEM with 10% FBS, 10^5 U/l penicillin, and 100 mg/l streptomycin. Subsequently, the mesothelial cell cultures were maintained for up to 15 passages at 37°C in a humidified environment containing 5% CO_2. The cultured cells exhibited the characteristic features of mesothelial cells: a polyhedral, cobblestone morphologic pattern and positive immunohistochemical staining for cytokeratin and vimentin (Kuwahara et al., 1991).

TRANSMESOTHELIAL ALBUMIN PERMEABILITY

The transmesothelial albumin flux across cultured monolayers of mesothelial cells was measured using an *in vitro* system as described by Rotrosen and Gallin (1986). Monolayers grown on membranes in Millicell-HA inserts (Millipore, Bedford, MA) were gently washed with HBSS and replaced in 24-well culture plates (Costar Cambridge, MA). The monolayers were covered immediately with DMEM containing a trypan blue-albumin complex [36 mg trypan blue and 800 mg bovine serum albumin were dissolved in 100 ml DMEM to yield a stable complex (trypan blue > 99% protein bound as determined by TCA precipitation) with absorption maximum at 590 nm]. To avoid hydrostatic pressure across the monolayer, the fluid levels inside and outside the culture well were equalized. The monolayers were then incubated during the defined time with stimulant at 37°C, 5% CO_2. At the end of the incubation the monolayer-inserts were carefully removed, and albumin diffusion across the monolayer was quantified by measuring absorbance at 590 nm of the bottom well fluid. Stimulated albumin diffusion was compared with simultaneous controls and expressed as:

% change vs. control = 100 × [Absorbance (test)-Absorbance (control)]/Absorbance (control).

To show the diffusion rate in control (without stimulant), % change albumin diffusion in control was calculated by dividing the absorbance at defined time point by starting (0 time) absorbance.

TRANSMESOTHELIAL ELECTRICAL RESISTANCE MEASUREMENTS

Transmesothelial electrical resistance was determined using a Millicell-ERS (Millipore, Bedford, MA). Pleural mesothelial cell monolayers grown on membranes in Millicell-HA inserts (Millipore, Bedford, MA) were gently washed with HBSS and replaced in 24-well culture plates (Costar Cambridge, MA). The monolayers were incubated with DMEM at 37°C, 5% CO_2 for at least 30 min before the start of each experiment. The initial transmesothelial electrical resistance was then determined, and the monolayers were incubated during the defined time with stimulant at 37°C, 5% CO_2. The resistance of each sample and blank (without monolayers) was measured using Ag/AgCl electrodes placed into both inside and outside Millicell insert. Transmesothelial electrical resistance (TER) was calculated as:

TER (Ohms × cm^2) = [Resistance (test)-Resistance (blank)]/Effective membrane area (in this study 0.6 cm^2).

MEASUREMENT OF $[CA^{2+}]_I$

Changes in $[Ca^{2+}]_i$ were determined as previously reported (Ito et al., 1995). Pleural mesothelial cells were incubated on 25-mm glass coverslips (Matsunami, Tokyo, Japan) in DMEM with 10% FBS. After reaching confluence, the cells were cultured further in serum-free culture medium for 12 h, and then the mesothelial cell monolayers were loaded with fura 2 by incubating them with 2 μM fura 2-AM for 30 min at 37°C in HEPES-buffered solution. Loaded cells were washed in HEPES-buffered solution and maintained in this solution for 20 min at room temperature to allow for complete hydrolysis of fura 2 to the acid form.

The glass coverslip was placed horizontally in a temperature-controlled (37°C) bath that was mounted on Intracellular Ion Analyzer (CAF-110, Japan Spectroscopic, Tokyo, Japan). Fluorescence excitation was obtained from a xenon high-pressure lamp (150 W). Ultraviolet light of alternating 340 and 380 nm (10 nm bandwidth) was obtained with a monochromator equipped with a chopping wheel (400 Hz) placed in front of the monochromator. Fura 2 fluorescence from the cells was imaged with a Nikon UV-Fluor objective lens (× 10). The dichroic mirror was used as a beam splitter to transmit emitted fluorescence (500 nm) into the photomultiplier. The fluorescence signals (340 and 380 nm) and their ratio (340:380 nm) were continuously recorded on a chart recorder. At the end of experimental run, background autofluorescence (the inherent fluorescence emitted from cells, coverslip, and bath at 340 and 380 nm) was obtained by the method of Hallam et al. (1988).

After autofluorescence was subtracted, the changes in $[Ca^{2+}]_i$ were determined quantitatively by using the following equation: $[Ca^{2+}]_i = K_d[(R\text{-}R_{min})/(R_{max}\text{-}R)](Sf_2/Sb_2)$ where the dissociation constant K_d has a value of 224 nM (Grynkiewicz et al., 1985), R is the fluorescence ratio within the cells, R_{max} is the maximal fluorescence ratio after addition of 40 μM ionomycin in the presence of 1.5 mM $CaCl_2$, R_{min} is the minimal ratio determined by the subsequent addition of 5 mM EGTA, and Sf_2/Sb_2 is the ratio of fluorescence values at 380-nm excitation determined at R_{min} and R_{max}, respectively.

F-ACTIN STAINING

Pleural mesothelial cells were fixed in 3% phosphate-buffered saline (PBS)-formalin for 10 min, and permeabilized with 1% Triton X-100 in PBS for 10 min at room temperature. After two washes with PBS, cells were stained with fluorescein isothiocyanate (FITC)-labeled phalloidin (5 unit/ml in PBS) to localize F-actin for 20 min in a dark room at room temperature. Cells were washed with PBS twice and maintained in PBS. Dishes were mounted on the stage of Leica TCS/NT confocal laser scanning microscope equipped with an Ar–Kr laser. The excitation and emission wavelengths for FITC-phalloidin were 490 and 525 nm. To standardize the fluorescence intensity measurements among experiments, the time of image capture, the image intensity gain, the image

enhancement, and the image black level in both channels were optimally adjusted at the outset and kept constant for all experiments.

QUANTIFICATION OF F-ACTIN CONTENT

Mesothelial cells were stained with nitrobenzoxadiazole (NBD)-phallacidin (Molecular Probes, Junction City, OR) and analyzed with a FACScan (Becton Dickinson Immunocytometry System, Mountain View, CA) (Howard and Oresajo, 1985) with following some modifications. In all cases a two-step stain procedure was used. Mesothelial cells suspensions (1×10^6 cells/ml) were incubated at the desired time in HBSS with and without agents; fixed with formalin (3.7% vol/vol) for 15 min at 25°C; and then exposed to a final concentration of 100 μg/ml lysophosphatidyl choline and 1.65×10^{-7} M NBD-phallacidin. Stained cells were analyzed by FACScan within 1 h of staining. In all instances the fluorescence histogram of cells yielded a normal distribution, and the fluorescence was recorded as the peak fluorescence channel number. The relative F-actin content is expressed as the ratio of the agents treated peak channel number to the control peak channel number.

Ca^{2+} CHELATION AND STABILIZATION OF THE ACTIN CYTOSKELETON

To show the role of Ca^{2+} and F-actin on the mesothelial permeability, effects of Ca^{2+} chelation by BAPTA (5 mM) and stabilization of the actin cytoskeleton by cytochalasin B (10 μg/ml) were determined for some experiments. The dose of cytochalasin B was selected according to previous study (Kuwahara et al., 1994).

STATISTICAL ANALYSIS

Results were expressed as means ± *SD*. Statistical comparisons were made with the use of the Student's *t*-test or analysis of variance. A value of $P < 0.05$ was considered significant.

RESULTS

CHANGES IN ALBUMIN DIFFUSION AND ELECTRICAL RESISTANCE

The effects of histamine (1 mM), bradykinin (10 μM), and thrombin (10 U) on time course of trypan blue-albumin diffusion across the mesothelial cell monolayers are shown in **Figure 1A**. All of these agents caused albumin diffusion within 5 min. Albumin diffusion was gradually increased after 5 min exposure. The magnitude of increase in bradykinin and thrombin to albumin diffusion was almost the same, but larger than that in histamine. Albumin diffusion was not induced in control group. The electrical resistance of mesothelial monolayer began falling within 5 min of adding each agent and leveled off after 30 min as shown in **Figure 1B**. Time dependency of changes in electrical resistance was almost similar to that in albumin diffusion. The effects of Ca^{2+} chelation by BAPTA and stabilization of the actin cytoskeleton by cytochalasin B on albumin diffusion across the mesothelial cell monolayers are shown in **Figure 1C**. The increase in agents induced albumin diffusion after 10 min incubation was significantly reduced by BAPTA and cytochalasin B treatments. Concentration dependency of changes in both albumin diffusion and electrical resistance of mesothelial monolayer after 30 min incubation is shown in **Figure 1D**. Each agent induced albumin diffusion and electrical resistance fall in a concentration-dependent manner.

CHANGES IN $[Ca^{2+}]_i$ IN MESOTHELIAL CELLS

As shown in **Figure 2A**, histamine (1 mM), bradykinin (10 μM), and thrombin (10 U) induced a biphasic elevation of $[Ca^{2+}]_i$ in pleural mesothelial cells that consisted of an initial transient component and a following sustained component in the presence of 1.5 mM extracellular Ca^{2+}. The peak of initial transient component was appeared within 30 s after stimulation and sustained component was followed. The characteristics of the response were similar for each agent. Each agent elicited the elevation of $[Ca^{2+}]_i$ in a dose-dependent manner. Concentration-response curves were obtained from the peak values of each initial component of the $[Ca^{2+}]_i$ response as shown in **Figure 2B**. These responses of $[Ca^{2+}]_i$ in the concentration-dependency were almost similar to that noted for each agent induced albumin diffusion and electrical resistance fall.

F-ACTIN CYTOSKELETAL ORGANIZATION

The F-actin cytoskeletal organization was studied after 5 min of histamine (1 mM), bradykinin (10 μM), and thrombin (10 U) challenge. The representative F-actin patterns are shown in **Figure 3**. In the control group, mesothelial cells formed a cobblestone mosaic pattern composed of polyhedral cells (**Figure 3A**). After 5 min of agent exposure, the cells became elongated compared with the control cells. The density of stress fibers spanning the cells increased in histamine (**Figure 3B**), bradykinin (**Figure 3C**), and thrombin (**Figure 3D**) exposure.

F-ACTIN CONTENT

Figure 4A shows the time course of change in relative F-actin content during 30 min after agent stimulation. During the first 1 min after stimulation there was a dramatic increase in relative F-actin content that was maximal at 3–5 min and reflects agents induced actin polymerization. After maximal F-actin content was observed there was a decline in relative F-actin content during the next 30 min. These agents induced actin polymerization after 5 min incubation were significantly inhibited by Ca^{2+} chelation or cytochalasin B treatment (**Figure 4B**).

DISCUSSION

The present study has demonstrated that bradykinin, histamine, and thrombin increased transmesothelial permeability in cultured pleural mesothelial cell monolayers. The magnitude of increase in mesothelial permeability in response to histamine was smaller than that to bradykinin and thrombin. The Ca^{2+}-dependency of the bradykinin-, histamine-, and thrombin-induced increases in mesothelial permeability have been related to the regulatory role of Ca^{2+} in the F-actin cytoskeletal reorganization in pleural mesothelial cells.

We have shown that the mesothelial cells respond to histamine and elevate $[Ca^{2+}]_i$ via H_1 receptors pathway (Ito et al., 1995). Hott et al. (1992) have reported that thrombin induces proliferation and chemotaxis of rat pleural mesothelial cells. Bradykinin has also induced $[Ca^{2+}]_i$ via BK_2 receptors pathway in human mesothelial cells (Andre et al., 1998), and bradykinin is generated

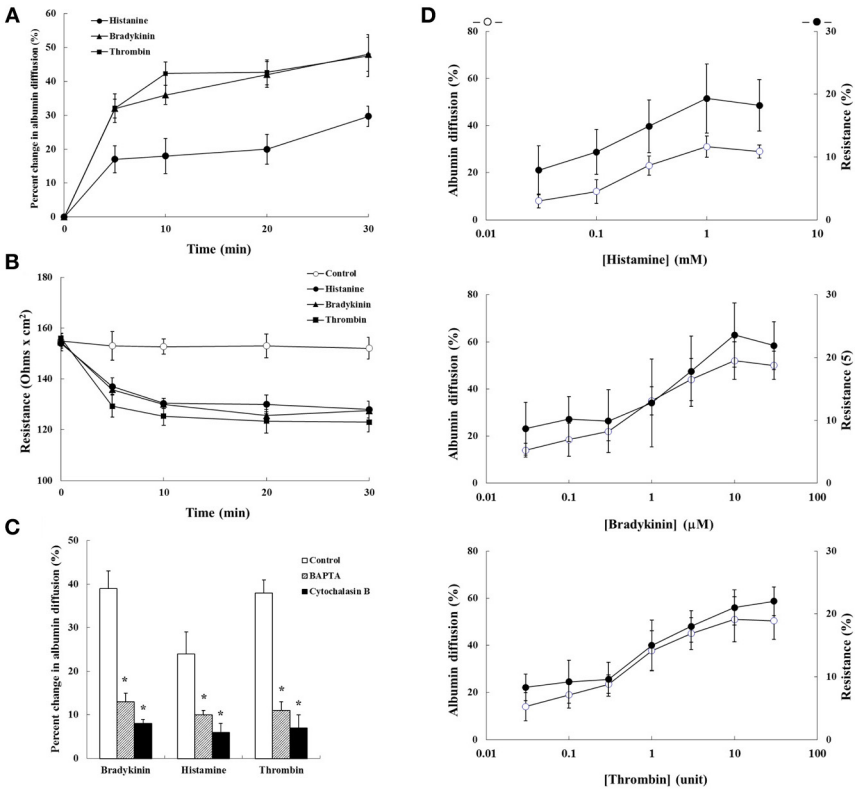

FIGURE 1 | The effects of bradykinin (10 μM), histamine (1 mM), and thrombin (10 U) on the permeability of mesothelial cell monolayers. (A) Time course of trypan blue-albumin diffusion across the mesothelial cell monolayers, **(B)** time course of transmesothelial electrical resistance of the mesothelial cell monolayers, and **(C)** effects of Ca^{2+} chelation by BAPTA (5 mM) and stabilization of the actin cytoskeleton by cytochalasin B (10 μg/ml). **(D)** Concentration dependency between trypan blue-albumin diffusion and transmesothelial electrical resistance. Values are means ± *SD* of 5 separate experiments. $^*P < 0.05$, significant difference from each control.

by the serine proteases, kallikreins, at sites of tissue injury and responds in a variety of tissues (Regoli and Barabe, 1980). Furthermore, these agents are known to be potent permeability-increasing agents for endothelial cells (Rotrosen and Gallin, 1986; Alexander et al., 1988; Lum et al., 1989, 1992). Therefore, we have chosen these agents to examine the effects on mesothelial permeability.

Bradykinin, histamine, and thrombin-induced increases in endothelial permeability may be dependent on $[Ca^{2+}]_i$ elevation and related to the regulatory role of Ca^{2+} in cytoskeleton assembly, structure, and contractility (Berridge, 1987). Rotrosen and Gallin (1986) have reported that concentrations of histamine required to augment monolayer permeability are of the same order of magnitude as those shown to elevate endothelial $[Ca^{2+}]_i$. Because responses of $[Ca^{2+}]_i$ in the concentration-dependency were almost similar to that noted for each agent induced mesothelial permeability, our results are in accordance with those observations in endothelial cells. However, because circulating physiological concentrations of these agents may be lower than experimental concentrations in this study, the local paracrine action of these agents in diseased states are more important than their systemic effects in healthy states.

Although the magnitude of the initial transient increase in $[Ca^{2+}]_i$ induced by higher dosage was almost the same among agents, the magnitude of increase in mesothelial permeability in response to histamine was smaller than that to bradykinin and thrombin. The signal transduction pathways to these agents in mesothelial cells are not fully understood. Three receptor subtypes (BK_1, BK_2, and BK_3) have been classified according to their affinities for bradykinin and to the relative potencies of their agonists and antagonists (Regoli and Barabe, 1980; Farmer et al., 1989; Steranka et al., 1989). Because only the activation of BK_2 receptors mediates the bradykinin-induced increase in $[Ca^{2+}]_i$ both endothelial (Morgan-Boyd et al., 1987) and mesothelial (Andre et al., 1998) cells, and phosphoinositide turnover in endothelial cells (Derian and Moskowitz, 1986), it seems that bradykinin-induced elevations of $[Ca^{2+}]_i$ and permeability in mesothelial cells are dependent on BK_2 receptors. It is generally thought H_1 receptor couples $G_{q/11}$ and mediated by protein kinase C. We suggest that angiotensin II-induced actin reorganization in pleural mesothelial cells is dependent on the angiotensin AT_1 receptor coupled with pertussis toxin-insensitive heterotrimeric G proteins, Rho GTPases and tyrosine phosphorylation pathways (Kuwahara and Kuwahara, 2002). Evidence has suggested G protein activation is a critical step in relaying signals from the receptors to the endothelial contractile machinery (Brock and Capasso, 1989; Voyno-Yasenetskaya et al., 1989; Garcia et al., 1991; Tkachuk and Voyno-Yasenetskaya, 1991).

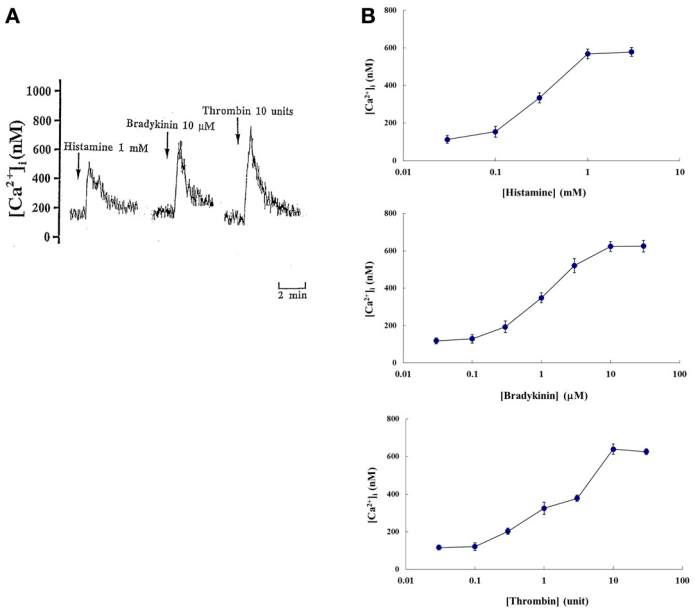

FIGURE 2 | (A) Tracings showing effects of histamine (1 mM), bradykinin (10 μM), and thrombin (10 U) on cytoplasmic Ca^{2+} concentration level ($[Ca^{2+}]_i$) of rat pleural mesothelial cells in the presence of 1.5 mM extracellular Ca^{2+}. Addition of each agent induced a biphasic elevation of $[Ca^{2+}]_i$: a large initial transient component followed by a sustained component in fura 2 loaded pleural mesothelial cells. Each tracing is a representative of 5 independent experiments. **(B)** Dose-response curves showing magnitude of initial transient increase in $[Ca^{2+}]_i$ in rat pleural mesothelial cells. Each point represent mean ± *SD* of 5∼7 separate experiments.

Therefore, one possible explanation of the differences in the magnitude of permeability is the contribution of specific G protein subtypes in activating mesothelial signaling pathways in response to these agents. Another possibility is that selective activation of protein kinase C isoforms or the presence of different degrees of negative feedback pathways may contribute these differences. However, further studies will be necessary to clarify the signal transduction pathways to these agents in mesothelial cells.

The bradykinin, histamine, and thrombin-induced increase of F-actin polymerization occurred at similar time points as that of the permeability increases. The majority of mesothelial cells showed an increased number of centralized actin stress fibers within 5 min of stimulation. Our results show that immediately after stimulation there is a rapid polymerization of actin (F-actin content) followed by a slower depolymerization of actin. Furthermore, agents-induced polymerization is inhibited by in the presence of BAPTA or cytochalasin B. The temporal relationship between cytoskeletal reorganization and permeability increase supports the hypothesis that reorganization of F-actin microfilament is involved in mediating the permeability increase. These findings have important implications for our understanding of the intracellular mechanisms that control the state of actin polymerization and permeability of the mesothelial cells.

Changes in pleural permeability, the influx of phagocytic cells, and the leak of serum proteins into the pleural space lead to the development of an inflammatory exudate. The pleural mesothelial cells produce chemoattractants for fibroblasts, fibronectin (Kuwahara et al., 1991), and for neutrophils, interleukin-8 (Boylan et al., 1992). Fibrinogen and fibrin may serve as chemotaxins (Sueishi et al., 1981), and promote fibroblast adherence, proliferation, and collagen production (Senior et al., 1986). Thrombin may participate in macrophage chemotaxis (Bar-Shavit et al., 1983). Therefore, these factors are also important to maintain the pleural space in healthy and diseased states.

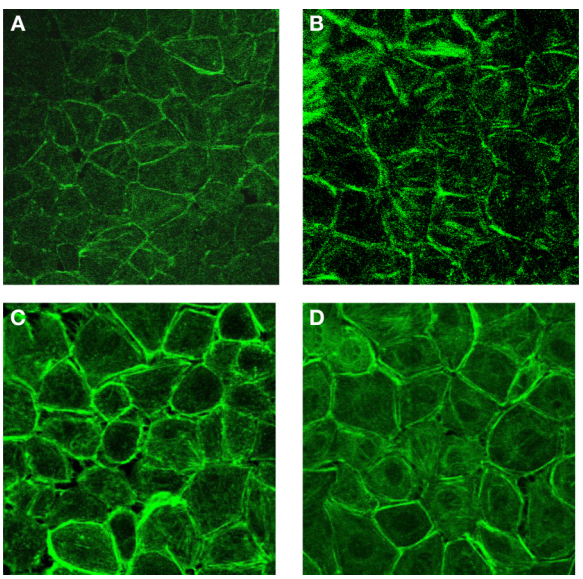

FIGURE 3 | The effects of histamine (1 mM), bradykinin (10 μM), and thrombin (10 U) on F-actin cytoplasmic distribution in rat pleural mesothelial cells. Control **(A)**, after 5 min exposure histamine **(B)**, bradykinin **(C)**, and thrombin **(D)**.

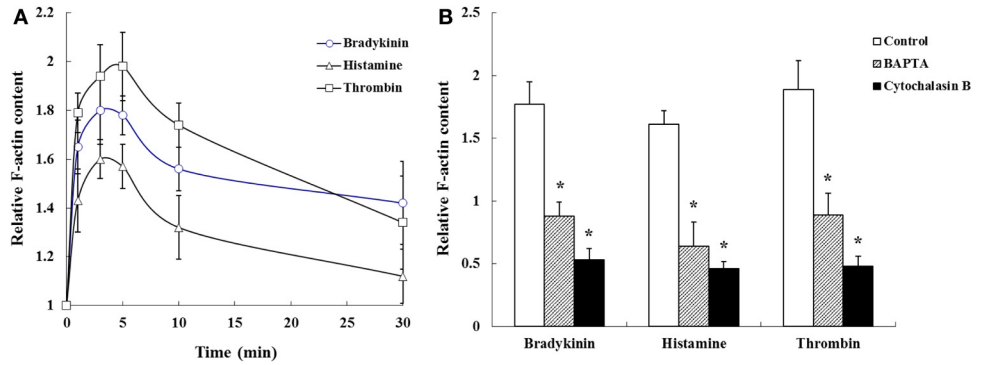

FIGURE 4 | (A) Time course of changes and **(B)** effects of Ca^{2+} chelation by BAPTA (5 mM) and stabilization of the actin cytoskeleton by cytochalasin B (10 μg/ml) on histamine (1 mM), bradykinin (10 μM), and thrombin (10 U) induced F-actin content. Values are means ± *SD* of 3 separate experiments. $^*P < 0.05$, significant difference from each control.

In summary, the effects of bradykinin, histamine and thrombin on permeability in mesothelial cells were studied. The Ca^{2+}-dependency of these agents-induced increases in mesothelial permeability have been related to the regulatory role of Ca^{2+} in the F-actin cytoskeletal reorganization in pleural mesothelial cells. This temporal relationship is consistent with the hypothesis that these agents-induced mobilization of Ca^{2+} signals increase in mesothelial permeability.

ACKNOWLEDGMENT

This work was supported in part by Grant-In-Aid from the Ministry of Education, Science, Sports and Culture, Japan.

REFERENCES

Alexander, J. S., Hechtman, H. B., and Shepro, D. (1988). Phalloidin enhances endothelial barrier function and reduces inflammatory permeability *in vitro*. *Microvasc. Res.* 35, 308–315. doi: 10.1016/0026-2862(88)90085-4

Andre, M., Rahimi, S., Schollmeyer, P., and Pavenstadt, H. (1998). Bradykinin stimulates the intracellular calcium activity in human mesothelial cells. *Nephrol. Dial. Transplant*. 13, 2047–2052. doi: 10.1093/ndt/13.8.2047

Bar-Shavit, R., Kahn, A., Wilner, G. D., and Fenton, J. W. II. (1983). Monocyte chemotaxis: stimulation by specific exosite region in thrombin. *Science* 220, 728–731. doi: 10.1126/science.6836310

Berridge, M. J. (1987). Inositol triphosphate and diacylglycerol: two interacting second messengers. *Annu. Rev. Biochem.* 56, 159–193. doi: 10.1146/annurev.bi.56.070187.001111

Boylan, A. M., Ruegg, C., Kim, K. J., Hebert, C. A., Hoeffel, J. M., Pytela, R., et al. (1992). Evidence for a role for mesothelial cell-derived interleukin-8 in the pathogenesis of asbestos-induced pleurisy in rabbits. *J. Clin. Invest.* 89, 1257–1267. doi: 10.1172/JCI115710

Brock, T. A., and Capasso, E. A. (1989). GTPγS increases thrombin-mediated inositol triphosphate accumulation in permeabilized human endothelial cells. *Am. Rev. Respir. Dis.* 140, 1121–1125. doi: 10.1164/ajrccm/140.4.1121

Derian, C. K., and Moskowitz, M. A. (1986). Polyphosphoinositide hydrolysis in endothelial cells and carotid artery segments. Bradykinin-2 receptor stimulation is calcium-dependent. *J. Biol. Chem.* 261, 3831–3837.

Farmer, S. G., Burch, R. M., Meeker, S. A., and Wilkins, D. E. (1989). Evidence for a pulmonary B_3 bradykinin receptor. *Mol. Pharmacol.* 36, 1–8.

Garcia, J. G. N., Dominez, J., and English, D. (1991). Sodium fluoride induces phosphoinositide hydrolysis, Ca^{2+} mobilization, and prostacyclin synthesis in cultured human endothelium: further evidence for regulation by a pertussis toxin-insensitive guanine nucleotide-binding protein. *Am. J. Respir. Cell Mol. Biol.* 5, 113–124. doi: 10.1165/ajrcmb/5.2.113

Grynkiewicz, G., Poenie, M., and Tsien, R. Y. (1985). A new generation of Ca^{2+} indicators with greatly improved fluorescence properties. *J. Biol. Chem.* 260, 3440–3450.

Hallam, T. J., Pearson, J. D., and Needham, L. A. (1988). Thrombin stimulated elevation of endothelial cell cytoplasmic free calcium concentration causes prostacyclin production. *Biochem. J.* 251, 243–249.

Hott, J. W., Sparks, J. A., Godbey, S. W., and Antony, V. B. (1992). Mesothelial cell response to pleural injury: thrombin-induced proliferation and chemotaxis of rat pleural mesothelial cells. *Am. J. Respir. Cell Mol. Biol.* 6, 421–425. doi: 10.1165/ajrcmb/6.4.421

Howard, T. H., and Oresajo, C. O. (1985). The kinetics of chemotactic peptide-induced change in F-actin content, F-actin distribution, and the shape of neutrophils. *J. Cell Biol.* 101, 1078–1085. doi: 10.1083/jcb.101.3.1078

Ito, K., Kuwahara, M., Sugano, S., and Kuwahara, M. (1995). Role of intra- and extracellular calcium stores in mesothelial cell response to histamine. *Am. J. Physiol.* 268, L63–L70.

Kuwahara, M., and Kuwahara, M. (2002). Involvement of Rho and tyrosine kinase in angiotensin II-induced actin reorganization in mesothelial cells. *Eur. J. Pharmacol.* 436, 15–21. doi: 10.1016/S0014-2999(01)01591-6

Kuwahara, M., Kuwahara, M., Bijwaard, K. E., Gersten, D. M., Diglio, C. A., and Kagan, E. (1991). Mesothelial cells produce a chemoattractant for lung fibroblasts: role of fibronectin. *Am. J. Respir. Cell Mol. Biol.* 5, 256–264. doi: 10.1165/ajrcmb/5.3.256

Kuwahara, M., Kuwahara, M., Verma, K., Ando, T., Hemenway, D. R., and Kagan, E. (1994). Asbestos exposure stimulates pleural mesothelial cells to secrete the fibroblast chemoattractant, fibronectin. *Am. J. Respir. Cell Mol. Biol.* 10, 167–176. doi: 10.1165/ajrcmb.10.2.8110473

Lum, H., Aschner, J. L., Phillips, P. G., Fletcher, P. W., and Malik, A. B. (1992). Time-course of thrombin-induced increase in endothelial permeability: relationship to Ca_i^{2+} and inositol polyphosphates. *Am. J. Physiol.* 263, L219–L225.

Lum, H., Del Vecchio, P. J., Schneider, A. S., Goligorsky, M. S., and Malik, A. B. (1989). Calcium dependence of the thrombin-induced increase in endothelial albumin permeability. *J. Appl. Physiol.* 66, 1471–1476.

Morgan-Boyd, R., Stewart, J. M., Vavrek, R. J., and Hassidd, A. (1987). Effects of bradykinin and angiotensin II on intracellular Ca^{2+} dynamics in endothelial cells. *Am. J. Physiol.* 253, C588–C598.

Regoli, D., and Barabe, J. (1980). Pharmacology of bradykinin and related kinins. *Pharmacol. Rev.* 32, 1–46.

Robbins, S. L., and Kumar, V. (1987). *Basic Pathology, 4th Edn.* Philadelphia, PA: W.B. Saunders Company.

Rotrosen, D., and Gallin, J. I. (1986). Histamine type 1 receptor occupancy increases endothelial cytosolic calcium, reduces F-actin and promotes albumin diffusion across cultured endothelial monolayers. *J. Cell Biol.* 103, 2379–2387. doi: 10.1083/jcb.103.6.2379

Senior, R. M., Skodgen, W. F., Griffen, G. L., and Wilner, G. D. (1986). Effects of fibrinogen derivatives upon the inflammatory response. *J. Clin. Invest.* 77, 1014–1019. doi: 10.1172/JCI112353

Steranka, L. R., Farmer, S. G., and Burch, R. M. (1989). Antagonists of B_2 bradykinin receptors. *FASEB J.* 3, 2019–2025.

Sueishi, K., Nanno, S., and Tanaka, K. (1981). Permeability enhancing and chemotactic activities of lower molecular weight degradation products of human fibrinogen. *Thromb. Haemost*. 45, 90–94.

Tkachuk, V. A., and Voyno-Yasenetskaya, T. A. (1991). Two types of G proteins involved in regulation of phosphoinositide turnover in pulmonary endothelial cells. *Am. J. Physiol.* 261, 118–122.

Voyno-Yasenetskaya, T. A., Tkachuk, V. A., Cheknyova, E. G., Panchenko, M. P., Grigorian, G. Y., Vavrek, R. J., et al. (1989). Guanine nucleotide-dependent, pertussis toxin-insensitive regulation of phosphoinositide turnover by bradykinin in bovine pulmonary artery endothelial cells. *FASEB J.* 3, 44–51.

Wang, N. S. (1985). "Mesothelial cells *in situ,*" in *The Pleura in Health and Disease,* eds J. Chretien, J. Bignon, and A. Hirsch (New York, NY: Dekker), 23–42.

Conflict of Interest Statement: The author declares that the research was conducted in the absence of any commercial or financial relationships that could be construed as a potential conflict of interest.

Received: 12 March 2014; accepted: 02 June 2014; published online: 30 June 2014.
Citation: Kuwahara M (2014) Role of $[Ca^{2+}]_i$ and F-actin on mesothelial barrier function. Front. Physiol. ***5****:232. doi: 10.3389/fphys.2014.00232*
This article was submitted to Membrane Physiology and Membrane Biophysics, a section of the journal Frontiers in Physiology.

frontiers in
PHYSIOLOGY

REVIEW ARTICLE
published: 24 June 2014
doi: 10.3389/fphys.2014.00221

Tight junction physiology of pleural mesothelium

Alexander G. Markov*[1] *and Salah Amasheh*[2]*

[1] *Department of General Physiology, St. Petersburg State University, St. Petersburg, Russia*
[2] *Department of Veterinary Medicine, Institute of Veterinary Physiology, Freie Universität Berlin, Berlin, Germany*

Edited by:
Sotirios G. Zarogiannis, University of Thessaly, Greece

Reviewed by:
Alexi Alekov, Medizinische Hochschule Hannover, Germany
Jose L. Reyes, National Polytechnic Institute, Mexico

****Correspondence:***
Salah Amasheh, Institute of Veterinary Physiology, Oertzenweg 19b, 14163 Berlin, Germany
e-mail: salah.amasheh@fu-berlin.de

Pleura consists of visceral and parietal cell layers, producing a fluid, which is necessary for lubrication of the pleural space. Function of both mesothelial cell layers is necessary for the regulation of a constant pleural fluid volume and composition to facilitate lung movement during breathing. Recent studies have demonstrated that pleural mesothelial cells show a distinct expression pattern of tight junction proteins which are known to ubiquitously determine paracellular permeability. Most tight junction proteins provide a sealing function to epithelia, but some have been shown to have a paracellular channel function or ambiguous properties. Here we provide an in-depth review of the current knowledge concerning specific functional contribution of these proteins determining transport and barrier function of pleural mesothelium.

Keywords: pleura, tissue barrier, mesothelial cells, tight junctions, claudins

INTRODUCTION

Pleura, peritoneum and pericardium are squamous epithelia of mesothelial origin, which line lungs, chest cavity, abdomen, and heart, respectively. Pleura can be divided in the pleura visceralis or pleura pulmonalis covering lungs, and pleura parietalis covering the ribs. Both are delimitated by a single layer of epithelial cells which attach to a lamina propria, and have different functions regarding transport and barrier properties. Between the two layers, the pleura cavity is located (**Figure 1**). The pleura provides a fluid layer for lung movement, and therefore is necessary for breathing This small volume of pleural liquid is a result of filtration and absorptive processes, and its volume and composition is tightly regulated (Zocchi, 2002). An imbalance of this regulation can result in an accumulation of fluid between the parietal and the visceral pleura, a condition defined as pleural effusion (Light, 1997).

The difference between hydrostatic and colloid-osmotic pressure of pleural liquid and capillary blood results in filtration of pleural liquid in the pleural cavity. In caudal parietal pleura, the elimination of liquid from a pleural cavity occurs through lymphatic vessels. In this context, further mechanisms related to mesothelial cell activity have been discussed to be more relevant, including a solute-coupled absorption of liquid from the pleural space (Zocchi, 2002). However, vectorial transport across epithelia depends on a concerted action of transcellular transport mechanisms in combination with paracellular channel and barrier functions, and several transcellular transport mechanisms have been identified to participate in the formation of pleural liquid. For analysis, electrophysiological measurements have been performed in different species including man (Hatzoglou et al., 2001; Sarkos et al., 2002; Kouritas et al., 2008; Markov et al., 2011). Moreover, the molecular correlate of paracellular channel and barrier function has been discovered in recent years, namely the tight junction (TJ) which shows a tissue specific expression of tight junction proteins determining the functional properties of the tissues (for review, see e.g., Amasheh et al., 2011; Rosenthal et al., 2012). Neighboring epithelial cells are linked together by these structures, which show a distinct strand pattern in freeze fracture electron micrographs (Staehelin, 1973). Typically tight junctions are located between the apical and the basolateral membrane of epithelial cells, providing not only a *gate* function describing the role for paracellular permeability, but also a *fence* function which is a prerequisite for polarity of the cells, as it delimits diffusion of basolateral and apically located integral membrane molecules to the opposite membrane compartment, respectively (Tsukita et al., 2001). Taken together, both transcellular and paracellular determinants of transport and barrier function can be regarded to contribute to the generation of different ionic composition of pleural fluid compared to plasma (**Table 1**).

Furthermore, inflammation was identified as one major mechanism perturbing barrier integrity, as shown previously in inflammatory bowel diseases (Amasheh et al., 2009a). In this context, also an effect of pleura inflammation on tight junction proteins was observed (Markov et al., 2011).

TRANSPORT AND BARRIER MECHANISMS IN PLEURA MESOTHELIUM

ELECTROPHYSIOLOGICAL PROPERTIES OF PLEURA MESOTHELIUM

In Ussing chambers, transmesothelial potential (V_m), and transmesothelial resistance (R_m) have been reported. The experiments revealed differences concerning absolute values, which might be attributed to different specimens and preparative protocols. However, these differences were rather marginal and in comparison with studies focusing on established epithelial models of kidney and intestine (Amasheh et al., 2002; Markov et al., 2010), these values indicated rather leaky properties of both, visceral and parietal pleura (**Table 2**).

The existence of electrophysiological parameters indicates transport and barrier mechanisms, as transmesothelial transport

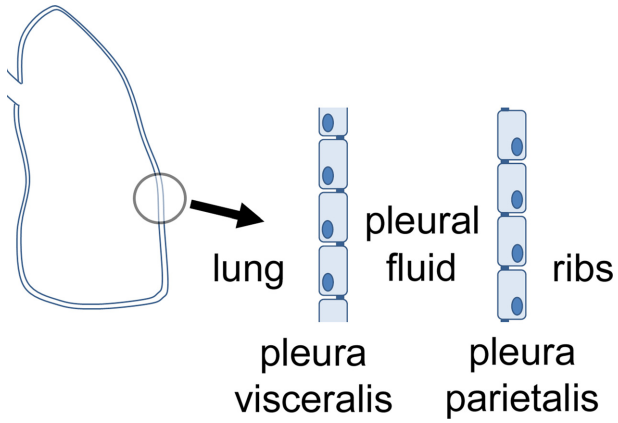

FIGURE 1 | Orientation of visceral and parietal pleura mesothelium.

Table 1 | Comparison of ionic composition of pleural fluid and plasma.

Ion	Pleural fluid	Plasma	Species	References
Na^+	139 (141*)	142 (151*)	Rabbit, anesthesia	Zocchi et al., 1991
	141	149	Rats, no anesthesia	Rolf and Travis, 1973
K^+	4.48	4.42	Rabbit, anesthesia	Zocchi et al., 1991
Cl^-	96 (98*)	93 (102*)	Rabbit anesthesia	Zocchi et al., 1991
	111	122	Rats, no anesthesia	Rolf and Travis, 1973
	109	113	Rabbit, no anesthesia	Sahn et al., 1979
HCO_3^-	29	26	Rabbit anesthesia	Zocchi et al., 1991

Corrected according to the concentration of electrolytes per liter of serum water or of pleural liquid water.

implies a transmesothelial barrier function to limit the paracellular pathway during active transport mechanisms, restricting back leak and therefore allowing vectorial transport and the generation of gradients, as e.g., also demonstrated in human gastrointestinal tract before (Amasheh et al., 2009b). This functional interplay of transport and barrier function can be identified by transmesothelial potential measurements; **Figure 2**.

There are specific regional functional differences in organs with large epithelial surface, as shown in detail for intestine and kidney (Markov et al., 2010; Amasheh et al., 2011). In intestine, this segment specific correlation of barrier properties was analyzed by a combination of electrophysiological and molecular analyses (Markov et al., 2010). In analogy the segmentation of different pleura areas may also be associated with differential barrier properties. Electrophysiological experiments employing paracellular flux markers of different masses, and protein expression profiles allow a detailed analysis of these variations. Currently,

Table 2 | Comparison of transmesothelial potential (V_m) and resistance (R_m) values measured in different species including human tissue specimens.

Species	Visceral pleura		Parietal pleura		References
	V_m (mV)	R_m ($\Omega \cdot cm^2$)	V_m (mV)	R_m ($\Omega \cdot cm^2$)	
Canine	0.06	20	0.03	22	Payne et al., 1988
Sheep	0.4	22	0.5	22	Hatzoglou et al., 2001
	–	21	–	20	Zarogiannis et al., 2006
	–	–	0.5	19 (costal)	Zarogiannis et al., 2007
	–	–	0.6	21 (diaphragmal)	Vogiatzidis et al., 2006
	–	–	–	38	Sarkos et al., 2002
Human	–	–	–	26 21 (Cranial, mediastinal) 18 (Caudal)	Sarkos et al., 2002 Kouritas et al., 2008
	1.6	14	1.3	18	Markov et al., 2011

– not provided.

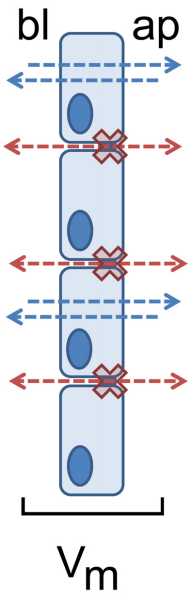

FIGURE 2 | Restricted paracellular permeability as a prerequisite for pleural transmesothelial potential. Transport routes are indicated as blue (transcellular) and red (paracellular) arrows between apical (ap) and basolateral (bl) compartments. The paracellular barrier is indicated as red crosses.

different electrophysiological properties are known concerning parts of parietal pleura, namely mediastinal, costal and diaphragmal pleura. In sheep, transmesothelial resistance of costal pleura showed a lower transmesothelial resistance than diaphragmal

pleura (Zarogiannis et al., 2007) whereas in human pleura, a higher resistance of cranial pleura compared to caudal pleura was reported (Kouritas et al., 2008; **Table 2**).

For analyses of pleural transport function, ouabain and amiloride have been employed. Whereas ouabain is a selective blocker of the—typically basolaterally located—Na^+/K^+-ATPase, application of amiloride inhibits the epithelial sodium channel (ENaC), typically located in the apical membrane. Application of ouabain and amiloride had different effects on human parietal pleura. Whereas in the caudal region, an increase of transmesothelial resistance was reported, in the cranial and mediastinal pleura no significant ouabain effect was observed (Kouritas et al., 2008). This apparent contradiction might indicate that there is no generally uniform mapping, as some studies refer to the cranial-caudal axis, and others referring to single rib areas (Kouritas et al., 2008).

PLEURAL TRANSMESOTHELIAL TRANSPORT SYSTEMS

Transport properties have been analyzed in pleura in detail by inducing a hydrothorax (Agostoni and Zocchi, 1990). This model includes an injection of Ringer solution into the pleural cavity to replace single ions, and the application of a variety of blockers including ouabain and amiloride. With this technique, a solute-coupled absorption of liquid from the pleural space was observed (Agostoni and Zocchi, 1990; Zocchi et al., 1991). Moreover, a general epithelial phenotype was identified, which included the expression of the Na^+/K^+-ATPase. Interestingly, the distinct localization of the Na^+/K^+-ATPase is not resolved yet: Western blots revealed an expression of the Na^+/K^+-ATPase a1 subunit in both, visceral and parietal pleura of rabbits, and mesothelial primary cell culture of rabbits (Sironi et al., 2007, 2008). Existence of this subunit is characteristic for epithelia and endothelium (Krenek et al., 2006; Gupta et al., 2012). Employing the hydrothorax model, injection of Ringer's solution with the Na^+/K^+-ATPase blocker ouabain resulted in a reduction of water absorption, and a decrease of ion absorption from the pleural cavity (Agostoni and Zocchi, 1990; Zocchi et al., 1991). These findings indicated that the Na^+/K^+-ATPase was located in the apical membrane of pleural mesothelium, but a discrimination between visceral and parietal pleura was approached only in later experiments employing the Ussing chamber technique. In these studies, analysis of transmesothelial resistance of different pleural specimens with ouabain revealed differences of Na^+/K^+ ATPase localization in visceral and parietal pleura (Hatzoglou et al., 2001), as ouabain induced an increase of transmesothelial resistance only in visceral pleura when added to the apical compartment, whereas in parietal pleura, an effect of ouabain on both, the apical and basolateral side of the epithelium, was observed.

Further evidence for the localization of Na^+/K^+-ATPase of parietal pleura was found in human tissue. In Ussing chamber experiments employing parietal pleura specimens, apical addition of ouabain showed an effect (Kouritas et al., 2008).

As until now no immunohistochemical detection of the localization has been published, these results cannot fully provide an evidence for localization of Na^+/K^+-ATPase in pleura mesothelium, though. This still makes it difficult to define the transcellular absorption from and secretion into the pleural cavity in detail. Another indicator of typical epithelial properties is provided by apical expression of the epithelial sodium channel (ENaC) and exchangers, which also contribute to vectorial transport. ENaC is the limiting factor for epithelial sodium absorption in a variety of tissues and organs, including the distal nephron and colon epithelium (Amasheh et al., 2000). For proper function in epithelia, functional co-regulation of the tight junction to limit paracellular back leak has been reported (Amasheh et al., 2009b).

Evidence of ENaC in parietal and visceral pleura was provided by the hydrothorax model employing amiloride injection, which decreased water absorption, and transport of Na^+ and Cl^- from the pleural cavity (Agostoni and Zocchi, 1990; Zocchi et al., 1991). Terbutaline, an activator of ENaC, as well as the specific ENaC inhibitor amiloride, were injected in mice pleural cavity, leading to an increase, and decrease of water absorption from the pleural cavity, respectively (Jiang et al., 2003).

Application of amiloride from the apical side of human and sheep parietal pleura increases transmesothelial resistance (Sarkos et al., 2002; Kouritas et al., 2008). In contrast, a different group reported that amiloride from the apical side of parietal pleura did not change transmesothelial resistance, but increased the value when added to the basolateral side (Hatzoglou et al., 2001).

This apparent contradiction could be resolved by Nie et al. (2009); when ENaC was apically detected in primary culture of human mesothelial cells and murine parietal pleura (Nie et al., 2009). Although these studies did not include a mapping of the expression in pleura as shown e.g., on functional level (Kouritas et al., 2008), they might become important for the understanding of pathophysiological regulatory mechanisms of transcellular pleural transport, shown for histamine and prostaglandins, recently (Kouritas et al., 2011, 2012).

In visceral pleura, Ussing chamber studies on sheep tissue specimens did not reveal effects of amiloride, when applied to the apical or basolateral side, indicating no functional ENaC expression at all (Hatzoglou et al., 2001). Therefore, it remains an open question if ENaC is localized in the apical membrane of visceral pleura.

In pleural fluid, concentration of glucose is comparable with blood levels. As glucose is present in the pleural space, a transport mechanism for glucose can be expected. In accordance, Western blotting experiments revealed expression of the sodium-glucose linked transporter-1 (SGLT1) in visceral and parietal pleura of rabbit and sheep, and human primary cells (Sironi et al., 2007, 2008). Functional properties were analyzed by experiments using the SGLT-blocker phloricin in the hydrothorax model, which reduced water absorption from the pleural space (Zocchi et al., 1996). Na^+-Glucose cotransport can be molecular candidate for solute-coupled absorption of liquid from the pleural space, indicating an epithelial phenotype as also found e.g., in intestine and kidney.

Taken together the analyses of transport function, a clear indication of a typical epithelial phenotype is not given. To discriminate an epithelial phenotype in more detail, a lateral diffusion of molecules has to be restricted by tight junctions, though. As epithelial cells typically show a tissue- and organ-specific

expression pattern of claudins, these proteins may provide more insight regarding the epithelial functions of pleura.

PHYSIOLOGICAL CONTRIBUTION OF TIGHT JUNCTION PROTEINS

The ignition of molecular tight junction protein research occurred in 1993, when the group of Shoichiro Tsukita described the first discovery of a molecular correlate of barrier function, namely occludin (Furuse et al., 1993). Before this time point, it was even not clear if the tight junction, which had been visualized in electron microscopic images for decades before, was of protein or lipoid origin. This finding soon catalyzed the establishment of a new research field, resulting in a broad variety of novel basic physiological as well as clinically related findings. Soon after Tsukita's pioneer work in the field of molecular tight junction analysis, a second landmark paper was published, this time presenting the first members of the family of claudins, namely claudin-1 and -2. Paralleled by the finding that occludin might not be the most crucial factor for barrier integrity, as the complete knock out did not show a perturbation of barrier properties (Furuse et al., 1998; Schulzke et al., 2005), a series of further publications highlighted the functional contribution of single claudins to major epithelial functions (Amasheh et al., 2011). These studies led to a classification of single members of the claudin family in barrier building (sealing), pore-forming (paracellular channel function) and intermediate claudins, which still is valid and can be regarded as a general outcome of tight junction research. Finally, a third type of tight junction protein was described, which led to a novel classification of non-claudin tight junction proteins as members of the TAMP family, namely tricellulin, MarvelD3, and occludin (Ikenouchi et al., 2005; Steed et al., 2009).

Among the variety of tetraspan TJ proteins that have been reported to be localized within TJ strands of different organs, occludin (Furuse et al., 1993) and claudins (Furuse et al., 1993) have been identified to primarily provide a barrier against the paracellular passage of ions. Although occludin was the first tetraspan membrane protein that was detected within TJ strands (Furuse et al., 1993), its contribution to barrier properties is still discussed, though (Schulzke et al., 2005). At least, ubiquitous detection in immunofluorescent stainings, established occludin as a general marker of TJ localization, which has been evaluated in many studies (Amasheh et al., 2002, 2005, 2009a,b; Dittmann et al., 2014; Markov et al., 2014). Moreover, occludin can also be visualized in pleura (**Figure 3**).

In contrast, members of the claudin family have been attributed to the organ-specific properties of epithelia, as e. g. shown in intestine, mammary gland, kidney and lungs (Kaarteenaho et al., 2010; Kirk et al., 2010; Markov et al., 2010, 2012). The single contribution of claudins to barrier properties varies, though. As e.g., claudin-1, -3, and -5, decrease tight junctional ion permeability, other claudins have been demonstrated to specifically mediate paracellular permeability, as it has been shown in detail for claudin-2 which forms a paracellular channel (Amasheh et al., 2002, 2005; Furuse et al., 2002; Milatz et al., 2010).

Information on the molecular correlate of barrier function in the pleura reaches back to the pre-molecular era of tight junction research, when desmosomes and TJs have been discovered as intercellular contacts by electron microscopy (Wang, 1974), and a final breakthrough was achieved by detection of claudins and the correlation with functional barrier properties (Markov et al., 2011).

Recently, for the first time a combined analysis of pleura mesothelial barrier function and expression of TJ proteins was performed. In this study, claudin-1, -3, -5, and -7, were detected in visceral pleura. In parietal pleura, the same TJ proteins were detected, except claudin-7 (Markov et al., 2011; **Figure 4**). Moreover, in inflamed pleura, claudin-2 was induced, indicating a typical pathophysiological mechanism (see paragraph 4).

According to the functional contribution to barrier properties, claudins can be divided in three groups, namely (i) sealing tight junction proteins, (ii) claudins mediating paracellular permeability and (iii) claudins with ambiguous function. Among the claudins detected in pleura mesothelium, claudin-1, -3, and -5 belong to the first group, whereas claudin-2 belongs to the second, and claudin-7 to the third group.

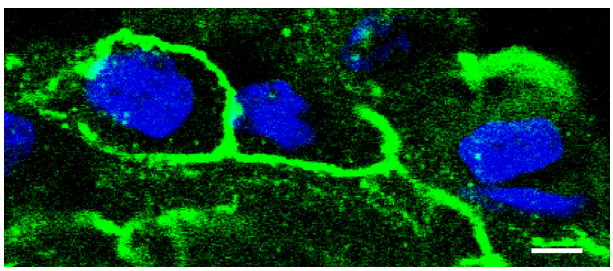

FIGURE 3 | Detection of tight junction proteins in pleural cells. Immunostaining of occludin with anti-occludin (green), detected by confocal laser scanning microscopy reveals a honeycomb-like distribution of tight junctions in pleural cells (visceral pleura, typical experiment, nuclei stained in blue, bar: 5 μm).

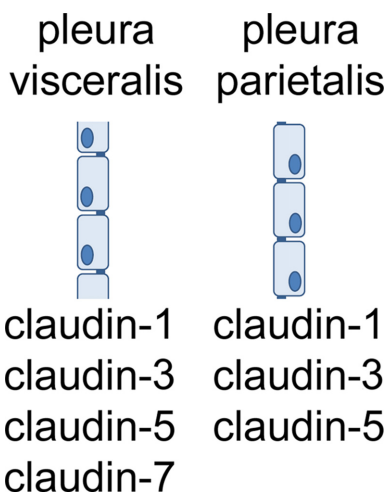

FIGURE 4 | Claudins of visceral and parietal pleura.

PLEURA PROTEINS WITH PORE FORMING, SEALING, AND AMBIGUOUS FUNCTION

Claudin-1-deficient mice die within hours after birth because of dehydration. These animals show a severe weight loss due to evaporation of water through the skin (Furuse et al., 2002). Therefore, claudin-1 is regarded as one major barrier-building TJ protein.

The functional contribution of claudin-3 has been analyzed in detail by analysis of stably transfected cells, recently (Milatz et al., 2010). This study demonstrates a strong sealing effect on the paracellular pathway regarding the passage of cations, anions, and uncharged solutes. These findings are in accordance with the literature, which reports a ubiquitous presence of claudin-3 in many epithelia including kidney and intestine (Kiuchi-Saishin et al., 2002; Markov et al., 2010).

Sealing properties of claudin-5 have been analyzed in detail in both knock out experiments, and stable transfection of epithelial cells (Nitta et al., 2003; Amasheh et al., 2005). Moreover, recent findings suggest that apart from a tightening of the paracellular barrier against the passage of ions, also the passage of uncharged molecules up to a size of 330 Da is restricted by claudin-5 (Dittmann et al., 2014). Taken together a combination of claudin-1, -3, and -5 can also be found in other epithelia with distinct barrier properties such as the gastrointestinal tract (Markov et al., 2010) and airway epithelium (Coyne et al., 2003).

In contrast to clearly defined claudin properties outlined above, the contribution of claudin-7 to barrier properties is still discussed, as cell type specific differences were observed concerning Cl^- and Na^+ permeability (Alexandre et al., 2005; Hou et al., 2006).

The obtained results indicate that barrier properties of both parietal and visceral pleura mesothelium participate in the formation and determination pleural liquid ionic composition, and different expression levels of occludin, claudin-3, -5, and -7, reflect different extent of functional contributions, respectively.

In contrast to the sealing properties provided by the majority of claudins, claudin-2 has been identified to form a paracellular channel selective for small cations and water (Amasheh et al., 2002; Rosenthal et al., 2010). As a TJ protein mediating paracellular permeability, increased claudin-2 expression is discussed to sustain and aggravate inflammation (Amasheh et al., 2009a,b).

PLEURAL TIGHT JUNCTIONS IN HEALTH AND DISEASE

The expression of claudin-1, -3, -5, and -7 in human pleura indicates an important role of specific barrier properties of the mesothelial cell layers (Markov et al., 2011). These findings are in accordance with previous studies, which have underlined specific contributions of single members of the tight junction protein family of claudins to barrier function of other leaky epithelia such as small intestine and proximal tubule (Markov et al., 2010; Amasheh et al., 2011).

Expression of claudins in pleura mesothelium has been shown to be altered in several pathophysiological conditions. These changes can be found in inflammatory events and in cancer. In previous studies, the paracellular channel claudin-2 has been reported to be induced by tumor necrosis factor α (TNFα), which explains e.g., the pathomechanism of inflammatory bowel diseases (Amasheh et al., 2009a, 2010). The two main forms of inflammatory bowel diseases, namely Crohn's disease and ulcerative colitis, as well as collagenous colitis and pouchitis, all typically show a perturbation of TJ protein expression and localization. This mechanism is regarded to be an important factor for the sustained and aggravated course of the diseases mediated by TNFα (Bürgel et al., 2002; Heller et al., 2005; Zeissig et al., 2007; Amasheh et al., 2009a).

In inflamed pleura, a general reduction of tightening TJ proteins and an increase of permeability mediating TJ proteins was reported, recently (Markov et al., 2011). Claudin-2 was reported to be elevated in inflamed pleura, which has also been shown for Crohn's disease, ulcerative colitis, and pouchitis (Heller et al., 2005; Zeissig et al., 2007; Amasheh et al., 2009a). Moreover, in inflamed pleura, a decrease of occludin, claudin-1, -3, -5, and -7 was detected, which also shows parallels with mechanisms reported in inflammatory bowel diseases (Heller et al., 2005; Zeissig et al., 2007; Amasheh et al., 2009a).

In accordance, pleural exudates showed a marked increase of TNFα levels in a mouse lung inflammation model (Mazzon and Cuzzocrea, 2007). Moreover, TNFα is also elevated in other lung pathologies, e.g., tuberculosis and cancer (Qian et al., 2012).

TNFα at higher levels was reported to induce a downregulation of the tight junction scaffolding protein zonula occludens protein 1 (ZO-1), and an opening of the paracellular barrier (Ma et al., 2004). As a prerequisite of the pathomechanism of TNFα altering tight junction protein expression in lungs, the TNFα receptor TNFR1 was identified (Mazzon and Cuzzocrea, 2007). If, apart from claudin-2, a number of tightening tight junction proteins are reduced due to a general perturbation of ZO-1, this results in a decrease of barrier properties despite reduction of the paracellular pore claudin-2 (Schneeberger and Lynch, 1992; Fink and Delude, 2005; Jacob et al., 2005), though. Taken together, whereas the increase of claudin-2 in pleural inflammation indicates a separate regulatory pathway which has been reported for inflammatory bowel diseases, the general reduction of tightening proteins in inflamed pleura also points at a mechanism reported in a mouse lung inflammation model, which is not even based on an increase of claudin-2, but a universal decrease of tight junction proteins which may less specifically perturb the epithelial barrier. Both regulatory pathways however appear to be primarily targeted by TNFα.

These alterations in claudin expression are in contrast to findings reported in analyses of pleura cancer and mesothelioma, which show an alteration of claudin-4. In this context, Claudin 4 was identified to be an important marker for carcinoma vs. mesothelioma diagnosis in pleural and peritoneal biopsies and effusions, as it is detected in metastatic tumor cells but not in benign forms of mesotheliomas (Facchetti et al., 2007; Lonardi et al., 2011).

CONCLUSIONS

Transport and barrier function of pleura mesothelium indicate typical epithelial characteristics. Expression of the major sealing tight junction proteins-1, -3, and -5 indicate a physiological role of the mesothelial barrier function for pleural liquid formation. Moreover, the effects observed in inflamed pleura, namely an induction of the paracellular pore claudin-2 and the decrease

of tightening tight junction proteins are in accordance with regulatory mechanisms observed in inflamed epithelia, as shown e.g., for inflammatory bowel diseases. These findings may contribute to future therapeutic and preventive approaches regarding mesothelia.

AUTHOR CONTRIBUTIONS

Alexander G. Markov and Salah Amasheh conceived the review, conducted literature survey and wrote the review.

ACKNOWLEDGMENTS

The study has been supported by the Deutsche Forschungsgemeinschaft (DFG), the Sonnenfeld-Stiftung Berlin, the Partnership Program FU Berlin—University St. Petersburg and the Grant of St. Petersburg State University, Grant No. 1.38.231.2014.

REFERENCES

Agostoni, E., and Zocchi, L. (1990). Solute-coupled liquid absorption from the pleural space. *Respir. Physiol.* 81, 19–28. doi: 10.1016/0034-5687(90)90066-8

Alexandre, M. D., Lu, Q., and Chen, Y. H. (2005). Overexpression of claudin-7 decreases the paracellular Cl^- conductance and increases the paracellular Na^+ conductance in LLC-PK1 cells. *J. Cell Sci.* 118, 2683–2693. doi: 10.1242/jcs.02406

Amasheh, M., Fromm, A., Krug, S. M., Amasheh, S., Andres, S., Zeitz, M., et al. (2010). TNFalpha-induced and berberine-antagonized tight junction barrier impairment via tyrosine kinase, Akt and NFkappaB signaling. *J Cell Sci.* 123, 4145–4155. doi: 10.1242/jcs.070896

Amasheh, S., Dullat, S., Fromm, M., Schulzke, J. D., Buhr, H. J., and Kroesen, A. J. (2009a). Inflamed pouch mucosa possesses altered tight junctions indicating recurrence of inflammatory bowel disease. *Int. J. Colorectal. Dis.* 24, 1149–1156. doi: 10.1007/s00384-009-0737-8

Amasheh, S., Epple, H. J., Mankertz, J., Detjen, K., Goltz, M., Schulzke, J. D., et al. (2000). Differential regulation of ENaC by aldosterone in rat early and late distal colon. *Ann. N. Y. Acad. Sci.* 915, 92–94. doi: 10.1111/j.1749-6632.2000.tb05227.x

Amasheh, S., Fromm, M., and Günzel, D. (2011). Claudins of intestine and nephron – a correlation of molecular tight junction structure and barrier function. *Acta Physiol.* 201, 133–140. doi: 10.1111/j.1748-1716.2010.02148.x

Amasheh, S., Meiri, N., Gitter, A. H., Schöneberg, T., Mankertz, J., Schulzke, J. D., et al. (2002). Claudin-2 expression induces cation-selective channels in tight junctions of epithelial cells. *J. Cell Sci.* 115, 4969–4976. doi: 10.1242/jcs.00165

Amasheh, S., Milatz, S., Krug, S. M., Bergs, M., Amasheh, M., Schulzke, J. D., et al. (2009b). Na^+ absorption defends from paracellular back-leakage by claudin-8 upregulation. *Biochem. Biophys. Res. Commun.* 378, 45–50. doi: 10.1016/j.bbrc.2008.10.164

Amasheh, S., Schmidt, T., Mahn, M., Florian, P., Mankertz, J., Tavalali, S., et al. (2005). Contribution of claudin-5 to barrier properties in tight junctions of epithelial cells. *Cell Tissue Res.* 321, 89–96. doi: 10.1007/s00441-005-1101-0

Bürgel, N., Bojarski, C., Mankertz, J., Zeitz, M., Fromm M., and Schulzke J. D. (2002). Mechanisms of diarrhea in collagenous colitis. *Gastroenterology* 123, 433–443. doi: 10.1053/gast.2002.34784

Coyne, C. B., Gambling, T. M., Boucher, R. C., Carson, J. L., and Johnson, L. G. (2003). Role of claudin interactions in airway tight junctional permeability. *Am. J. Physiol. Lung Cell. Mol. Physiol.* 285, L1166–L1178.

Dittmann, I., Amasheh, M., Krug, S., Markov, A. G., Fromm, M., and Amasheh, S. (2014). Laurate permeates the paracellular pathway for small molecules in the intestinal epithelial cell model HT-29/B6 via opening the tight junctions by reversible relocation of claudin-5. *Pharm Res.* doi: 10.1007/s11095-014-1350-2. [Epub ahead of print].

Facchetti, F., Lonardi, S., Gentili F., Bercich, L., Falchetti, M., Tardanico, R., et al. (2007). Claudin 4 identifies a wide spectrum of epithelial neoplasms and represents a very useful marker for carcinoma versus mesothelioma diagnosis in pleural and peritoneal biopsies and effusions. *Virchows Arch.* 451, 669–680. doi: 10.1007/s00428-007-0448-x

Fink, M. P., and Delude, R. L. (2005). Epithelial barrier dysfunction: a unifying theme to explain the pathogenesis of multiple organ dysfunction at the cellular level. *Crit. Care Clin.* 21, 177–196. doi: 10.1016/j.ccc.2005.01.005

Furuse, M., Fujita, K., Hiiragi, T., Fujimoto, K., and Tsukita S. (1998). Claudin-1 and -2: novel integral membrane proteins localizing at tight junctions with no sequence similarity to occludin. *J. Cell Biol.* 141, 1539–1550. doi: 10.1083/jcb.141.7.1539

Furuse, M., Hata, M., Furuse, K., Yoshida, Y., Haratake, A., Sugitani, Y., et al. (2002). Claudin-based tight junctions are crucial for the mammalian epidermal barrier: a lesson from claudin-1-deficient mice. *J. Cell Biol.* 156, 1099–1111. doi: 10.1083/jcb.200110122

Furuse, M., Hirase, T., Itoh, M., Nagafuchi, A., Yonemura, S., Tsukita, S., et al. (1993). Occludin: a novel integral membrane protein localizing at tight junctions. *J. Cell Biol.* 123, 1777–1788. doi: 10.1083/jcb.123.6.1777

Gupta, S., Yan, Y., Malhotra, D., Liu, J., Xie, Z., Najjar, S. M., et al. (2012). Ouabain and insulin induce sodium pump endocytosis in renal epithelium. *Hypertension* 59, 665–672. doi: 10.1161/HYPERTENSIONAHA.111.176727

Hatzoglou, C. H., Gourgoulianis, K. I., and Molyvdas, P. A. (2001). Effects of SNP, ouabain, and amiloride on electrical potential profile of isolated sheep pleura. *J. Appl. Physiol.* 90, 1565–1569.

Heller, F., Florian, P., Bojarski, C., Richter, J., Christ, M., Hillenbrand, B., et al. (2005). Interleukin-13 is the key effector Th2 cytokine in ulcerative colitis that affects epithelial tight junctions, apoptosis, and cell restitution. *Gastroenterology* 129, 550–564. doi: 10.1016/j.gastro.2005.05.002

Hou, J., Gomes, A. S., Paul, D. L., and Goodenough, D. A. (2006). Study of claudin function by RNA interference. *J. Biol. Chem.* 281, 36117–36123. doi: 10.1074/jbc.M608853200

Ikenouchi, J., Furuse, M., Furuse, K., Sasaki, H., Tsukita S., and Tsukita S. (2005). Tricellulin constitutes a novel barrier at tricellular contacts of epithelial cells. *J. Cell Biol.* 171, 939–945. doi: 10.1083/jcb.200510043

Jacob, C., Yang, P. C., Darmoul, D., Amadesi, S., Saito, T., Cottrell, G. S., et al. (2005). Mast cell tryptase controls paracellular permeability of the intestine. Role of protease-activated receptor 2 and beta-arrestins. *J. Biol. Chem.* 280, 31936–31948. doi: 10.1074/jbc.M506338200

Jiang, J., Hu, J., and Bai, C. (2003). Role of aquaporin and sodium channel in pleural water movement. *Respir. Physiol. Neurobiol.* 139, 83–88. doi: 10.1016/j.resp.2003.08.001

Kaarteenaho, R., Merikallio, H., Lehtonen, S., Harju, T., and Soini Y. (2010). Divergent expression of claudin-1, -3, -4, -5 and -7 in developing human lung. *Respir. Res.* 11, 59. doi: 10.1186/1465-9921-11-59

Kirk, A., Campbell, S., Bass, P., Mason, J., and Collins J. (2010). Differential expression of claudin tight junction proteins in the human cortical nephron. *Nephrol. Dial. Transplant.* 250, 2107–2119. doi: 10.1093/ndt/gfq006

Kiuchi-Saishin, Y., Gotoh, S., Furuse, M., Takasuga, A., Tano, Y., and Tsukita S. (2002). Differential expression patterns of claudins, tight junction membrane proteins, in mouse nephron segments. *J. Am. Soc. Nephrol.* 13, 875–886.

Kouritas, V. K., Hatzoglou, C., Foroulis, C. N., and Gourgoulianis, K. I. (2008). Human parietal pleura present electrophysiology variations according to location in pleural cavity. *Interact. Cardiovasc. Thorac. Surg.* 7, 544–547. doi: 10.1510/icvts.2007.172007

Kouritas, V. K., Tsantsaridou, A., Tepetes, K., Tsilimingas, N., Gourgoulianis, K. I., Molyvdas, P. A., et al. (2011) Effect of histamine on the electrophysiology of the human parietal pleura. *Mol. Cell. Endocrinol.* 332: 271–276. doi: 10.1016/j.mce.2010.11.003

Kouritas, V. K., Zisis, C., Bellenis, I., Gourgoulianis, K. I., Molyvdas, P. A., and Hatzoglou, C. (2012). Nonsteroidal anti-inflammatory drugs alter the human mesothelial pleural permeability via ion cellular transportation by inhibiting prostaglandin synthesis. *Respiration* 84, 62–68. doi: 10.1159/000336837

Krenek, P., Hamaide, M. C., Morel, N., and Wibo, M. (2006). A simple method for rapid separation of endothelial and smooth muscle mRNA reveals Na^+/K^+-ATPase alpha-subunit distribution in rat arteries. *J. Vasc. Res.* 43, 502–510. doi: 10.1159/000095963

Light, R. W. (1997). Diagnostic principles in pleural disease. *Eur. Respir. J.* 10, 476–481. doi: 10.1183/09031936.97.10020476

Lonardi, S., Manera, C., Marucci, R., Santoro, A., Lorenzi, L., and Facchetti F. (2011). Usefulness of Claudin 4 in the cytological diagnosis of serosal effusions. *Diagn. Cytopathol.* 39, 313–317. doi: 10.1002/dc.21380

Ma, T. Y., Iwamoto, G. K., Hoa, N. T., Akotia, V., Pedram, A., Boivin, M. A., et al. (2004). TNF-alpha-induced increase in intestinal epithelial tight junction permeability requires NF-kappa B activation. *Am. J. Physiol.* 286. G367–G376.

Markov, A. G., Falchuk, E. L., Kruglova, N. M., Rybalchenko, O. V., Fromm, M., and Amasheh, S. (2014). Comparative analysis of theophylline and cholera toxin in rat colon reveals an induction of sealing tight junction proteins. *Pflügers Arch.* doi: 10.1007/s00424-014-1460-z. [Epub ahead of print].

Markov, A. G., Kruglova, N. M., Fomina, Y. A., Fromm, M., and Amasheh, S. (2012). Altered expression of tight junction proteins in mammary epithelium after discontinued suckling in mice. *Pflügers Arch*. 463, 391–398. doi: 10.1007/s00424-011-1034-2

Markov, A. G., Veshnyakova, A., Amasheh, M., and Amasheh S. (2010). Segmental expression of claudin proteins correlates with tight junction barrier properties in rat intestine. *J. Comp. Physiol. B* 180, 591–598. doi: 10.1007/s00360-009-0440-7

Markov, A. G., Voronkova, M. A., Volgin, G. N., Yablonsky, P. K., Fromm, M., and Amasheh, S. (2011). Tight junction proteins contribute to barrier properties in human pleura. *Resp. Physiol. Neurobiol*. 175, 331–335. doi: 10.1016/j.resp.2010.12.012

Mazzon, E., and Cuzzocrea, S. (2007). Role of TNF-α in lung tight junction alteration in mouse model of acute lung inflammation. *Respir. Res*. 8, 75. doi: 10.1186/1465-9921-8-75

Milatz, S., Krug, S. M., Rosenthal, R., Günzel, D., Müller, D., Schulzke, J. D., et al. (2010). Claudin-3 acts as a sealing component of the tight junction for ions of either charge and uncharged solutes. *Biochim. Biophys. Acta Biomembr*. 1798, 2048–2057. doi: 10.1016/j.bbamem.2010.07.014

Nie, H. G., Tucker, T., Su, X. F., Na, T., Peng, J. B., Smith, P. R., et al. (2009). Expression and regulation of epithelial Na^+ channels by nucleotides in pleural mesothelial cells. *Am. J. Respir. Cell Mol. Biol*. 40, 543–554. doi: 10.1165/rcmb.2008-0166OC

Nitta, T., Hata, M., Gotoh, S., Seo, Y., Sasaki, H., Hashimoto, N., et al. (2003). Size-selective loosening of the blood–brain barrier in claudin-5-deficient mice. *J. Cell Biol*. 161, 653–660. doi: 10.1083/jcb.200302070

Payne, D. K., Kinasewitz, G. T., and Gonzalez, E. (1988). Comparative permeability of canine visceral and parietal pleura. *J. Appl. Physiol*. 65, 2558–2564

Qian, Q., Sun, W. K., Zhan, P., Zhang, Y., Song, Y., and Yu, L. K. (2012). Role of monocyte chemoattractant protein-1, tumor necrosis factor-alpha and interleukin-6 in the control of malignant pleural effusion and survival in patients with primary lung adenocarcinoma. *Int. J. Biol. Markers* 27, e118–e124. doi: 10.5301/JBM.2012.9197

Rolf, L. L., and Travis, D. M. (1973). Pleural fluid-plasma bicarbonate gradients in oxygen and normal rats. *Am. J. Physiol*. 224, 857–861

Rosenthal, R., Heydt, M. S., Amasheh, M., Stein, C., Fromm, M., and Amasheh, S. (2012). Analysis of absorption enhancers in epithelial cell models. *Ann. N. Y. Acad. Sci.* 1258, 86–92. doi: 10.1111/j.1749-6632.2012.06562.x

Rosenthal, R., Milatz, S., Krug, S. M., Oelrich, B., Schulzke, J. D., Amasheh, S., et al. (2010). Claudin-2, a component of the tight junction, forms a paracellular water channel. *J. Cell Sci*. 123, 1913–1921. doi: 10.1242/jcs.060665

Sahn, S.t. A., Willcox, M. L., Good, J. T., Potts, D. E., and Filley, G. F. (1979). Characteristics of normal rabbit pleural fluid: physiologic and biochemical implications. *Lung* 156, 63–69. doi: 10.1007/BF02713992

Sarkos, S., Hatzoglou, C. H., Dahabre, J., Gourgoulianis, K. I., and Molyvdas, P. A. (2002). Effect of amiloride in human and sheep parietal pleura. *Respir. Physiol. Neurobiol*. 132, 233–237. doi: 10.1016/S1569-9048(02)00077-0

Schneeberger, E. E., and Lynch, R. D. (1992). Structure, function, and regulation of cellular tight junctions. *Am. J. Physiol*. 262, L647–L661

Schulzke, J. D., Gitter, A. H., Mankertz, J., Spiegel, S., Seidler, U., Amasheh, S., et al. (2005). Epithelial transport and barrier function in occludin-deficient mice. *Biochim. Biophys. Acta Biomembr*. 1669, 34–42. doi: 10.1016/j.bbamem.2005.01.008

Sironi, C., Bodega, F., Porta, C., Monaco, A., Zocchi, L., and Agostoni, E. (2008). Na^+–glucose cotransporter is also expressed in mesothelium of species with thick visceral pleura. *Resp. Physiol. Neurobiol*. 161, 261–266. doi: 10.1016/j.resp.2008.02.013

Sironi, C., Bodega, F., Porta, C., Zocchi, L., and Agostoni, E. (2007). Expression of Na^+–glucose cotransporter (SGLT1) in visceral and parietal mesothelium of rabbit pleura. *Respir. Physiol. Neurobiol*. 159, 68–75. doi: 10.1016/j.resp.2007.05.012

Staehelin, L. A. (1973). Further observations on the fine structure of freeze-cleaved tight junctions. *J. Cell Sci.* 13: 763–786.

Steed, E., Rodrigues, N. T., Balda, M. S., and Matter, K. (2009). Identification of MarvelD3 as a tight junction-associated transmembrane protein of the occludin family. *BMC Cell Biol*. 10:95. doi: 10.1186/1471-2121-10-95

Tsukita, S., Furuse, M., and Itoh, M. (2001). Multifunctional strands in tight junctions. *Nat. Rev. Mol. Cell Biol.* 2, 285–293. doi: 10.1038/35067088

Vogiatzidis, K., Hatzoglou, C., Zarogiannis, S., Matafia, G., Gourgoulianis, K., and Molyvdas, P. A. (2006). mu-Opioid influence on transmesothelial resistance of isolated sheep pleura and parietal pericardium. *Eur. J. Pharmacol*. 530, 276–280. doi: 10.1016/j.ejphar.2005.11.050

Wang, N. S. (1974). The regional difference of pleural mesothelial cells in rabbits. *Am. Rev. Respir. Dis.* 110, 623–626.

Zarogiannis, S., Hatzoglou, C., Stefanidis, I., Ioannou, M., Paraskeva, E., Gourgoulianis, K., et al. (2007). Comparison of the electrophysiological properties of the sheep isolated costal and diaphragmatic parietal pleura. *Clin. Exp. Pharmacol. Physiol.* 34, 129–131. doi: 10.1111/j.1440-1681.2007.04549.x

Zarogiannis, S., Hatzoglou, C., Stefanidis, I., Matafia, G., Vogiatzidis, K., Gourgoulianis, K., et al. (2006). Effect of adrenaline on transmesothelial resistance of isolated sheep pleura. *Respir. Physiol. Neurobiol*. 150, 165–172. doi: 10.1016/j.resp.2005.04.006

Zeissig, S., Bürgel, N., Günzel, D., Richter, J., Mankertz, J., Wahnschaffe, U., et al. (2007). Changes in expression and distribution of claudin 2, 5 and 8 lead to discontinuous tight junctions and barrier dysfunction in active Crohn's disease. *Gut* 56, 61–72. doi: 10.1136/gut.2006.094375

Zocchi, L. (2002). Physiology and pathophysiology of pleural fluid turnover. *Eur. Respir. J*. 20, 1545–1558. doi: 10.1183/09031936.02.00062102

Zocchi, L., Agostoni, E., and Cremachi, D. (1991). Electrolyte transport across the pleura of rabbits. *Respir. Physiol*. 86, 125–138 doi: 10.1016/0034-5687(91)90044-J

Zocchi, L., Agostoni, E., and Raffaini, A. (1996). Effect of phloridzin on net rate of liquid absorption from the pleural space of rabbits. *Exp. Physiol*. 81, 957–967.

Conflict of Interest Statement: The authors declare that the research was conducted in the absence of any commercial or financial relationships that could be construed as a potential conflict of interest.

Received: 21 March 2014; accepted: 27 May 2014; published online: 24 June 2014.
*Citation: Markov AG and Amasheh S (2014) Tight junction physiology of pleural mesothelium. Front. Physiol. **5**:221. doi: 10.3389/fphys.2014.00221*
This article was submitted to Membrane Physiology and Membrane Biophysics, a section of the journal Frontiers in Physiology.

frontiers in PHYSIOLOGY

ORIGINAL RESEARCH ARTICLE
published: 12 June 2014
doi: 10.3389/fphys.2014.00222

Role of H-Ras/ERK signaling in carbon nanotube-induced neoplastic-like transformation of human mesothelial cells

Warangkana Lohcharoenkal[1], Liying Wang[2], Todd A. Stueckle[2], Jino Park[3], William Tse[3], Cerasela-Zoica Dinu[4] and Yon Rojanasakul[1,3]*

[1] *Department of Pharmaceutical Sciences, West Virginia University, Morgantown, WV, USA*
[2] *Health Effects Laboratory Division, Pathology and Physiology Research Branch, National Institute for Occupational Safety and Health, Morgantown, WV, USA*
[3] *Department of Medicine, Mary Babb Randolph Cancer Center, West Virginia University, Morgantown, WV, USA*
[4] *Department of Chemical Engineering, West Virginia University, Morgantown, WV, USA*

Edited by:
Sotirios G. Zarogiannis, University of Thessaly, Greece

Reviewed by:
Dimitra Mangoura, Biomedical Research Foundation of the Academy of Athens, Greece
Georgios T. Stathopoulos, University of Patras, Greece

Correspondence:
Yon Rojanasakul, Department of Pharmaceutical Sciences and Mary Babb Randolph Cancer Center, West Virginia University, 5706 Medical Center Dr., Morgantown, WV 26506, USA
e-mail: yrojan@hsc.wvu.edu

Rapid development and deployment of engineered nanomaterials such as carbon nanotubes (CNTs) in various commercial and biomedical applications have raised concerns about their potential adverse health effects, especially their long-term effects which have not been well addressed. We demonstrated here that prolonged exposure of human mesothelial cells to single-walled CNT (SWCNT) induced neoplastic-like transformation as indicated by anchorage-independent cell growth and increased cell invasiveness. Such transformation was associated with an up-regulation of H-Ras and activation of ERK1/2. Downregulation of H-Ras by siRNA or inactivation of ERK by chemical inhibitor effectively inhibited the aggressive phenotype of SWCNT-exposed cells. Integrin alpha V and cortactin, but not epithelial-mesenchymal transition (EMT) transcriptional regulators, were up-regulated in the SWCNT-exposed cells, suggesting their role in the aggressive phenotype. Cortactin expression was shown to be controlled by the H-Ras/ERK signaling. Thus, our results indicate a novel role of H-Ras/ERK signaling and cortactin in the aggressive transformation of human mesothelial cells by SWCNT.

Keywords: mesothelial cells, H-Ras, SWCNT, ERK, cortactin, cell transformation

INTRODUCTION

CNTs share some common properties with the carcinogenic asbestos fibers, including high aspect ratio, biopersistence and route of exposure, which raises a major concern about their potential carcinogenicity. A recent study by Sargent et al. indicated the tumor-promoting effect of CNTs (Sargent et al., 2014), while several other studies suggested the potential mesothelioma pathogenicity of this nanomaterial (Takagi et al., 2008, 2012; Sakamoto et al., 2009). At the cellular level, CNTs were shown to induce malignant transformation of human lung cells upon chronic exposure (Wang et al., 2011, 2014; Lohcharoenkal et al., 2013). In a recent study, we reported neoplastic transformation of human pleural mesothelial cells by chronic CNT exposure and demonstrated the role of matrix metalloproteinase (MMP)-2 in the process (Lohcharoenkal et al., 2013). Since our study has indicated the induction of proto-oncogenes by CNTs (Wang et al., 2014) and since *H-Ras* oncogene has been demonstrated to be involved in the DNA damage signaling induced by CNTs (Tong et al., 2011), we asked if H-Ras plays a role in the invasive transformation of CNT-exposed human mesothelial cells.

Ras oncogene family has been extensively studied during the past few decades. Ras protein is a major regulator of various pathological and physiological processes that control cell proliferation, differentiation and survival. Ras GTPase family proteins are critical players in many signaling networks, connecting a great variety of upstream signals to an even wider set of downstream effector pathways that control numerous cellular functions including cell cycle progression, growth, migration, cytoskeleton dynamic, apoptosis and senescence (Tong et al., 2011). Ras is a membrane-associated guanine nucleotide-binding protein that is normally activated in response to the binding of extracellular signals such as growth factors, receptor tyrosine kinases, T-cell receptors, and phorbol myristate acetate. It acts as a binary signal switch between ON and OFF states. In the resting state, Ras is tightly bound to guanosine diphosphate (GDP), which is exchanged for guanosine triphosphate (GTP) upon binding of extracellular stimuli to cell membrane receptors. In the GTP-bound form, Ras interacts specifically with effector proteins and initiates downstream cascades. To return to the inactive OFF state, Ras cleaves off the terminal phosphate moiety by the intrinsic GTPase reaction and the remaining GDP-bound Ras is no longer able to interact with effectors (Kolch, 2002). Reactive free radicals and cellular redox stress have also been proposed to directly activate Ras. Nitric oxide promotes the

Abbreviations: SWCNT, single-walled carbon nanotubes; ERK, extracellular signal-regulated kinases; MAPK, mitogen-activated protein kinases; PI3K, phosphatidylinositol 3-kinase; MMP, matrix metalloproteinase; EGF, epidermal growth factor; GSN, gene signaling network; IPA, ingenuity pathway analysis; E-cad, E-cadherin; N-cad, N-cadherin; FN, fibronectin; VIM, vimentin; FAK, focal adhesion kinase; uPA, urokinase-plasminogen activator; BEAS-2B, human bronchial epithelial cells; SAEC, human small airway epithelial cells; MeT-5A, immortalized human pleural mesothelial cells; LP-9, normal human peritoneal mesothelial cells.

direct post-translational modification of Ras by S-nitrosylation at Cys118. This modification results in stimulation of guanine nucleotide exchange, possibly by destabilization associated with other effectors, leading to transduction of Ras mediated signals (Diaz-Meco et al., 1994). Three members of the Ras family, Harvey-Ras (H-Ras), Kirsten-Ras (K-Ras), and N-Ras, are known to be activated in human tumors (Lowy and Willumsen, 1993; Stites and Ravichandran, 2009). The amino-terminal 85 amino acids are identical and the middle 80 amino acids exhibit an 85% homology between the Ras proteins, whereas the carboxyl-terminal sequence is highly divergent (Barbacid, 1987; Boguski and McCormick, 1993). Up to about 30% of all human tumors carry some forms of alteration in the canonical *Ras* genes. The biological effects of Ras proteins are mediated through the activation of several downstream effectors, including Raf, Rac, phosphatidylinositol 3-kinase (PI3K) and Ral (Marshall, 1996). Ras stimulates serine/threonine kinase Raf, followed by activation of the downstream kinase MAPK/ERK kinase (MEK), which in turn phosphorylates extracellular signal-regulated kinases (ERKs) (Kyriakis et al., 1992). In addition to the Ras/Raf/ERK pathway, the small GTPase Rac and PI3K are involved in the mitogenic and oncogenic effects of Ras (Joneson et al., 1996). PI3K is activated by G-protein-coupled receptors in response to extracellular stimuli or by direct interaction with Ras (Kapeller and Cantley, 1994; Rodriguez-Viciana et al., 1994).

Although these Ras proteins share many common signaling pathways leading to similar cellular responses, studies have clearly demonstrated the unique roles of Ras family members in physiological and pathological conditions. Moon *et al.* reported H-Ras, but not N-Ras, induced invasive and migrative phenotypes by activating p38 and ERK signaling pathways, whereas both induced transformed phenotype in human breast epithelial cells through an up-regulation of MMP-2 (Moon et al., 2000). In laryngeal carcinoma, a weaker tumorigenic effect of N-Ras vs. H-Ras and K-Ras was reported (Kiaris and Soandidos, 1995). In this study, we investigated the role of H-Ras in SWCNT-induced neoplastic transformation of human mesothelial cells and evaluated the downstream targets of H-Ras signaling in the transformed cells.

MATERIALS AND METHODS

CELL CULTURE AND SWCNT EXPOSURE

Human pleural mesothelial MeT-5A (ATCC® CRL9444) cells were acquired from American Type Culture Collection (Manassas, VA) and maintained in M199 medium (Life Technologies, Grand Island, NY) with 5% fetal bovine serum (FBS), 2 mM L-glutamine, 100 U/mL penicillin/streptomycin, 1 μg/mL EGF and 50 μg/mL hydrocortisone. Human peritoneal mesothelial LP-9 cells were obtained from NIA Aging Cell repository (Camden, NJ) at passage 5 and maintained in a medium containing a 1:1 ratio of M199 and Ham's F-12 nutrient mixture (Life Technologies, Grand Island, NY), supplemented with 10% FBS, 10 ng/mL EGF, 0.4 μg/mL hydrocortisone, 100 U/mL penicillin/streptomycin and 2 mM L-glutamine. Cell cultures were performed in a humidified atmosphere of 5% CO_2 at 37°C. SWCNT, synthesized by using a high-pressure carbon monoxide disproportionate process (HiPCO), were obtained from Carbon Nanotechnology (CNI, Houston, TX). Elemental analysis of the supplied CNT by nitric acid dissolution and inductively coupled plasma-atomic emission spectrometry (ICP-AES, NMAM #7300) showed that SWCNT were 99% elemental carbon and contained less than 1% w/w of contaminants.

Cells were continuously exposed to SWCNT at various surface area concentrations of 0.02, 0.06, and 0.2 μg/cm^2 for 2 months according to the method previously described (Sargent et al., 2014). Briefly, 0.1 mg/mL stocks of SWCNT in phosphate buffer saline (PBS) containing 1% FBS were sonicated and diluted in media (0.1 μg/mL) prior to cell exposure. Cultured MeT-5A and LP-9 cells were exposed to the dispersed CNT every 3 days following a PBS wash and passaged once per week.

SOFT AGAR COLONY FORMATION ASSAY

Soft agar assay was performed as previously described (Ottestad et al., 1988). SWCNT-exposed cells at 3×10^4 cells were mixed with the culture medium containing 0.5% agar to the final concentration of 0.33% agar. Cell suspension was immediately plated onto the dish coated with 0.5% agar in culture medium. Colonies were examined under a light microscope (Leica DM, IL) after 2 and 4 weeks.

CELL INVASION ASSAY

Cell invasion was determined in BD Matrigel® invasion chamber (BD Biosciences, NJ). Briefly, cells at the density of 3×10^4 cells per well were seeded into the upper chamber of the Transwell® unit in serum-free medium. The lower chamber of the unit was added with a normal growth medium containing 5% FBS. The unit was incubated at 37°C in a 5% CO_2 atmosphere for 48 h. The non-invading cells were removed from the inside of insert with a cotton swab. Cells that invaded to the lower side of the membrane were fixed and stained with Diff-Quik® (Dade Behring, Newark, DE). Inserts were visualized under a light microscope. The experiment was performed three times independently and the representative data of one experiment are shown.

WESTERN BLOT ANALYSIS

Cells at the density of 2.5×10^5 cells were seeded into each well of 6-well plates and cultured to confluence. They were washed twice with ice-cold PBS and incubated in lysis buffer containing 20 mM Tris-HCl (pH 7.5), 1% Triton X-100, 150 mM NaCl, 10% glycerol, 1 mM Na_3VO_4, 50 mM NaF, 100 mM phenylmethylsulfonyl fluoride, and a commercial protease inhibitor mixture (Roche Molecular Biochemicals, Indianapolis, IN) at 4°C for 20 min. Cell lysates were collected and analyzed for protein content using the BCA protein assay kit (Pierce Biotechnology, Rockford, IL). Samples containing 50 μg of cell lysate proteins per lane were resolved under denaturing conditions by 10% sodium dodecyl sulfate-polyacrylamide gel electrophoresis (SDS-PAGE) along with EZ-run pre-stained protein ladder (Fisher Scientific, Pittsburgh, PA) and transferred onto PVDF membranes (Invitrogen, Carlsbad, CA). The transferred membranes were blocked for 1 h in 5% nonfat dry milk in TBST (25 mM Tris-HCl, pH 7.4, 125 mM NaCl, 0.05% Tween 20) and incubated with the appropriate primary antibodies (Cell Signaling Technology, Danvers, MA or Santa Cruz Biotechnology, Dallas, TX) at 4°C overnight. Membranes were washed twice with TBST

for 10 min and incubated with horseradish peroxidase-coupled isotype-specific secondary antibodies (Cell Signaling Technology, Danvers, MA) for 1.5 h at room temperature. The immune complexes were detected by enhanced chemiluminescence detection system (Amersham Biosciences, Piscataway, NJ) and quantified using analyst/PC densitometry software (Bio-Rad Laboratories, Hercules, CA).

H-Ras siRNA TRANSFECTION

Cells were transfected with pre-designed human H-Ras siRNA (Santa Cruz Biotechnology, Dallas, TX: sc-29340) or control siRNA (Santa Cruz Biotechnology, Dallas, TX: sc-37007), according to the manufacturer's protocol. H-Ras expression in the H-Ras and control siRNA-transfected cells was determined by Western blotting as described above.

INHIBITION OF ERK MAPK SIGNALING PATHWAY

SWCNT-exposed cells at 2×10^5 cells were seeded into each well of 6-well plates and cultured for 48 h. Cells were then pre-incubated with the ERK inhibitor U0126 (Cell Signaling Technology, Danvers, MA) at different concentrations for 2 h prior to subjecting to cell invasion or Western blot assays as described above.

INGENUITY PATHWAY ANALYSIS

H-Ras-ERK invasion signaling network was generated using Ingenuity Pathway Analysis (IPA, version Fall 2012; Redwood City, CA) from whole genome expression data of SWCNT-treated mesothelial cells previously deposited on NCBI's Gene Expression Omnibus (GenBank ID: GSE48855) (Lohcharoenkal et al., 2013). Gene signaling networks (GSN) associated with cell invasion were created and mapped. Only genes that have the first order relationship with ERK were kept in the network. Genes were included in the GSN if they promoted invasion and were overexpressed or if they inhibited invasion and were underexpressed.

QUANTITATIVE REAL-TIME PCR OF EPITHELIAL-MESENCHYMAL TRANSITION (EMT) TRANSCRIPTIONAL REGULATORS

The expression of EMT transcriptional regulators including SnaI, Twist, E-cad, N-cad, FN1, and VIM was analyzed in control and SWCNT ($0.2\,\mu g/cm^2$)-exposed MeT-5A cells. Briefly, total RNA was isolated from cells using RNeasy mini kit (Qiagen, Valencia, CA), according to the manufacturer's instructions. The extracted RNA was then reverse transcribed into cDNA by high capacity RNA to cDNA kit (Applied Biosystems, Carlsbad, CA). After the reverse transcription reaction was finished, 10 μL of diluted cDNA product (final cDNA quantity 100 ng) was mixed with 10 μL of Taqman® master mix (Applied Biosystems) and transferred into Taqman® array plate (Applied Biosystems). Quantification of the PCR products was performed by NFQ-FAM® method using the Applied Biosystems 7500 Real-Time PCR system with the following profile: 1 cycle at 94°C for 2 min, 40 cycles at 94°C for 15 s, 60°C for 1 min, 72°C for 1 min. Data analysis was performed using the ABI sequence detection software (Applied Biosystems) by relative quantification. The threshold cycle (Ct), which is defined as the cycle at which PCR amplification reaches a significant value, is given as the mean value. The relative expression of each mRNA was calculated by the ΔCt method, where ΔCt is the value obtained by subtracting the Ct value of the housekeeping gene *18S* mRNA from the Ct value of the target mRNA. The amount of the target relative to *18S* mRNA was expressed as $2^{-\Delta Ct}$.

IMMUNOFLUORESCENCE STAINING

Cellular cortactin expression was visualized by immunofluorescence microscopy (Zeiss LSM 510 Axiovert 100 M, Zeiss, Thornwood, NY). Briefly, cells were cultured to confluence on glass cover slips and fixed in 4% paraformaldehyde in PBS. The samples were rinsed three times, permeabilized with 1.2% Triton X-100 for 5 min, rinsed three times and blocked with 1% bovine serum albumin (BSA) in PBS for 1 h before staining with 1:100 cortactin primary antibody (Cell Signaling Technology, Danvers, MA) followed by Alexa Fluor-conjugated secondary antibody (Invitrogen, Carlsbad, CA). The stained cells were mounted with ProLong® gold antifade reagent with DAPI (Invitrogen, Carlsbad, CA) and visualized by fluorescence microscopy. All microscopic exposure conditions were set the same between samples for fluorescence intensity comparison.

STATISTICAL ANALYSIS

All experiments were performed in triplicate. Difference between groups was assessed by One-Way analysis of variance (ANOVA). Differences were considered significant if P-values were < 0.05.

RESULTS

SWCNT EXPOSURE INDUCES AGGRESSIVE NEOPLASTIC-LIKE PHENOTYPE OF MESOTHELIAL CELLS

Cancer hallmark phenotypes were determined in SWCNT-exposed and control MeT-5A and LP-9 cells by established methods. Anchorage-independent cell growth was determined by assessing the size and number of isolated colonies on soft agar. Increased colony size was observed in the MeT-5A cells exposed to all doses of SWCNT with the highest dose ($0.2\,\mu g/cm^2$) inducing the biggest colonies (**Figure 1A**). At the same dose range, SWCNT had minimal effect on colony formation in LP-9 cells (**Figure 1A**), possibly due to their decreased susceptibility and limited lifespan under non-adherent conditions.

The invasiveness of SWCNT-exposed mesothelial cells was assessed by Transwell® invasion assay. SWCNT was able to increase the invasiveness of both MeT-5A and LP-9 cells in a dose-dependent manner as compared to their passage-matched control cells (**Figure 1B**). At the highest exposure dose ($0.2\,\mu g/cm^2$), significant increase in the number of invading cells was observed in both cell types. These results indicate the invasion-promoting activity of SWCNT in mesothelial cells.

H-Ras OVEREXPRESSION IN SWCNT-EXPOSED MESOTHELIAL CELLS

We hypothesized that H-Ras expression and its downstream targets may be activated and play a role in the neoplastic transformation of SWCNT-exposed mesothelial cells. To test this possibility, we analyzed H-Ras (also known as transforming protein p21) expression in SWCNT-exposed and control cells by Western blotting. Increased expression of H-Ras was observed in

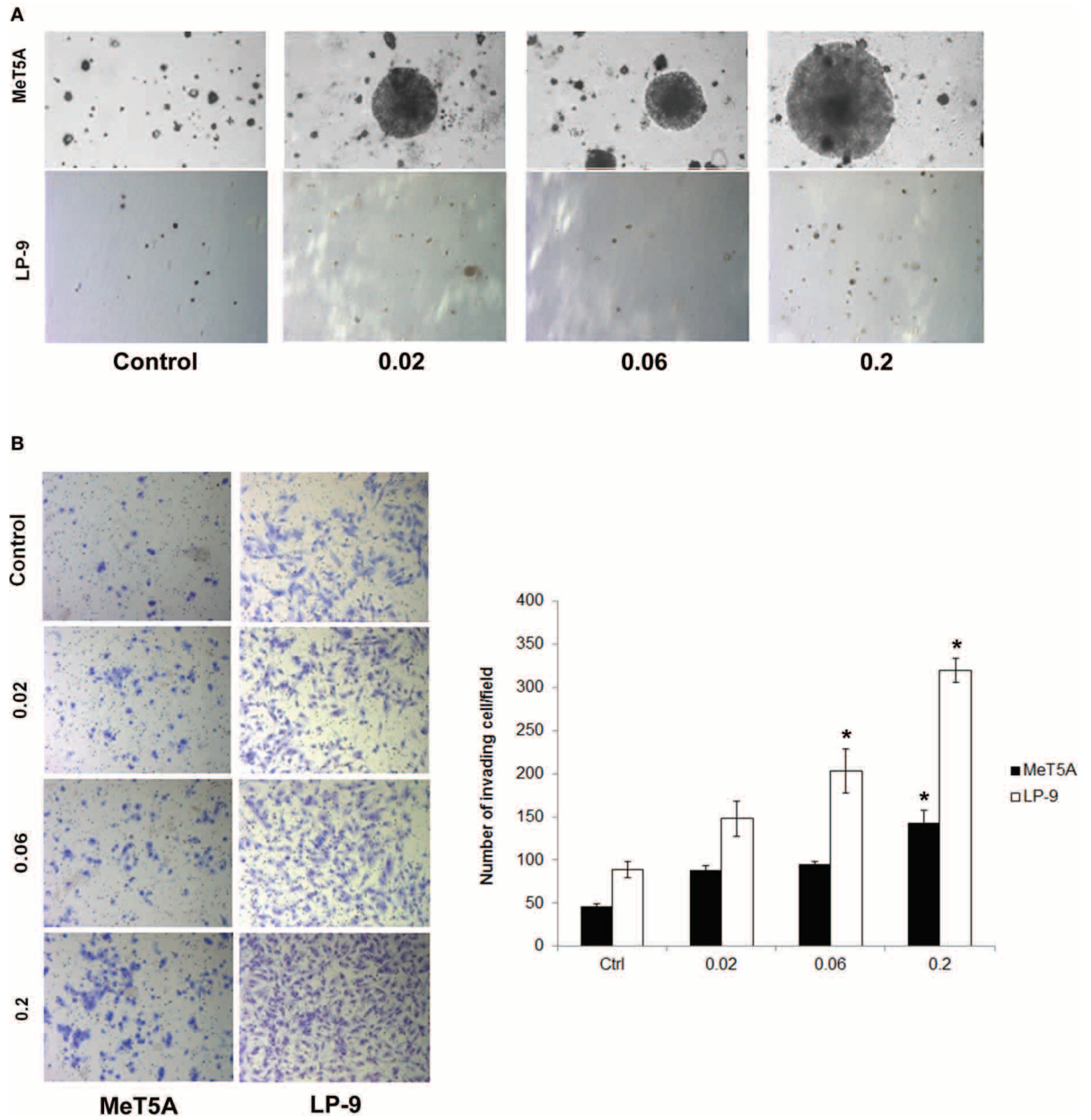

FIGURE 1 | Cancer hallmark transformation phenotypes of SWCNT-exposed MeT-5A and LP-9 cells. Anchorage-independent cell growth was determined by soft agar colony formation assay. Two-month exposed MeT-5A and LP-9 cells in culture medium containing 0.33% agar were plated onto the dish coated with 0.5% agar in culture medium. Colonies were examined by light microscopy after 4 weeks of incubation **(A)**. Invasion was assessed in the SWCNT-exposed cells using BD Matrigel® invasion chamber. Invading cells were fixed, stained and visualized under a microscope. The number of invading cells was counted and presented as a bar chart **(B)**. *Significantly difference from control with $P < 0.05$ ($n = 3$).

the SWCNT-exposed MeT-5A and LP-9 cells as compared to control cells (**Figure 2A**). The importance of H-Ras overexpression on the aggressive behavior of SWCNT-exposed cells was evaluated by siRNA silencing experiments. SWCNT-exposed MeT-5A and LP-9 cells were transfected with siRNA against H-Ras (siH-Ras) or control siRNA (siControl), and subjected to cell invasion assays. **Figures 2B,C** show that the siH-Ras treatment resulted in a substantial reduction of the H-Ras expression and a parallel decrease in cell invasion activity as compared to the siControl treatment.

ACTIVATION OF DOWNSTREAM SIGNALING PATHWAY OF H-Ras

To dissect the signaling pathway downstream of H-Ras that may be involved in the neoplastic phenotype of SWCNT-exposed cells, the activation of several known effectors of *Ras* including ERK, JNK, Akt, and NF-κB was investigated. Among

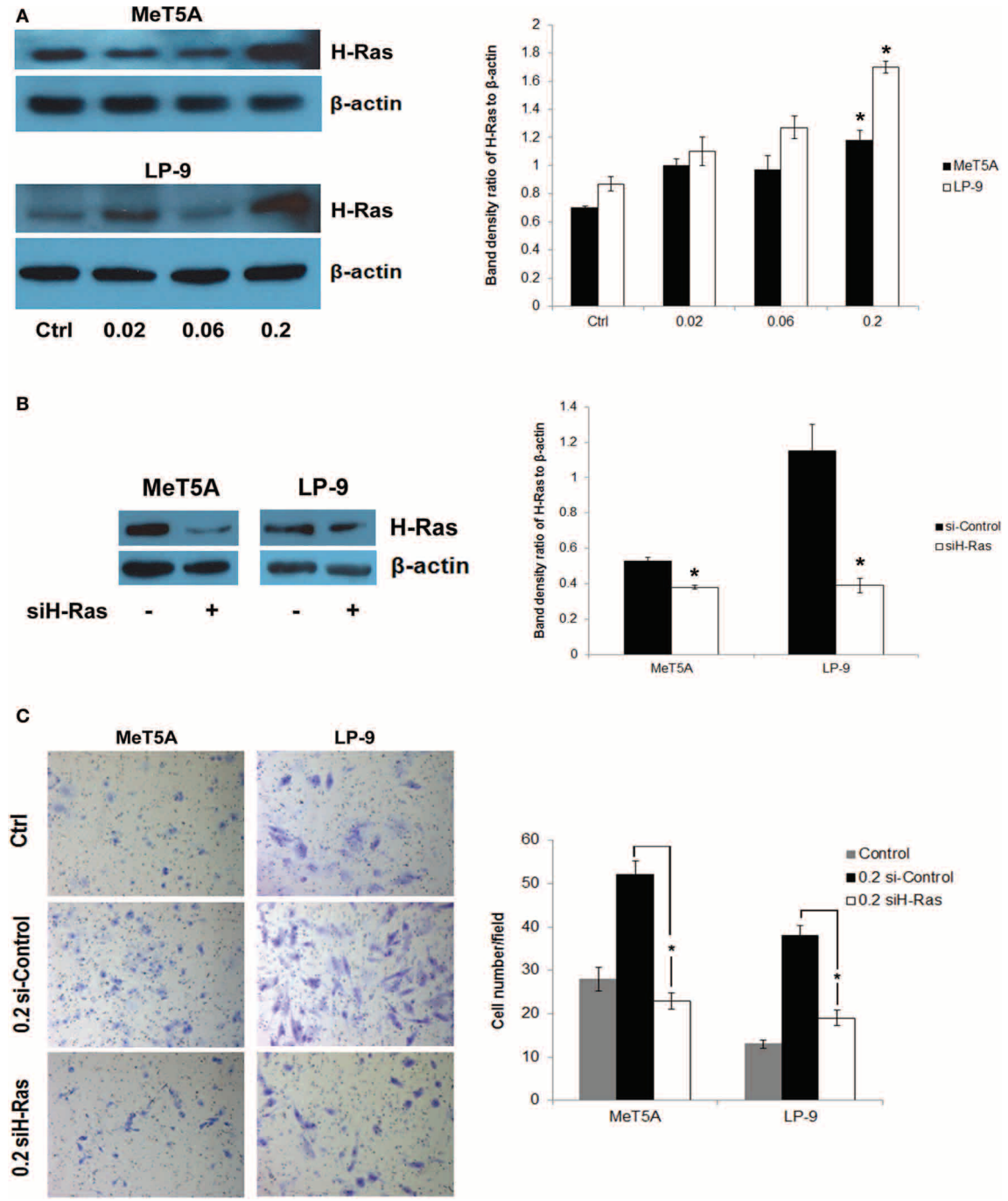

FIGURE 2 | Up-regulation of H-Ras in SWCNT-exposed mesothelial cells. Total H-Ras protein expression in SWCNT-exposed MeT-5A and LP-9 cells were analyzed by Western blotting. Band densities were determined and presented as a bar chart. Overexpression of H-Ras was observed in both SWCNT-exposed cell types at the high dose of 0.2 μg/cm^2 **(A)**. SWCNT (0.2 μg/cm^2)-exposed MeT-5A and LP-9 cells were transfected with siH-Ras or siControl RNA, and H-Ras protein expression was determined by Western blotting **(B)**. Cell invasion assays showed a reduced invasive capacity of the siH-Ras cells as compared to siControl cells **(C)**, *significantly difference with $P < 0.05$ ($n = 3$).

these, p44/42 (ERK1/2) was shown to be prominently activated in the SWCNT-exposed cells, suggesting the possible role of ERK signaling in the aggressive phenotype of these cells (**Figure 3A**).

To assess the functional importance of activated p44/42 in the aggressive phenotype, SWCNT-exposed cells were treated with non-cytotoxic doses of U0126, a selective ERK kinase inhibitor, and analyzed for cell invasiveness by Transwell® invasion assay.

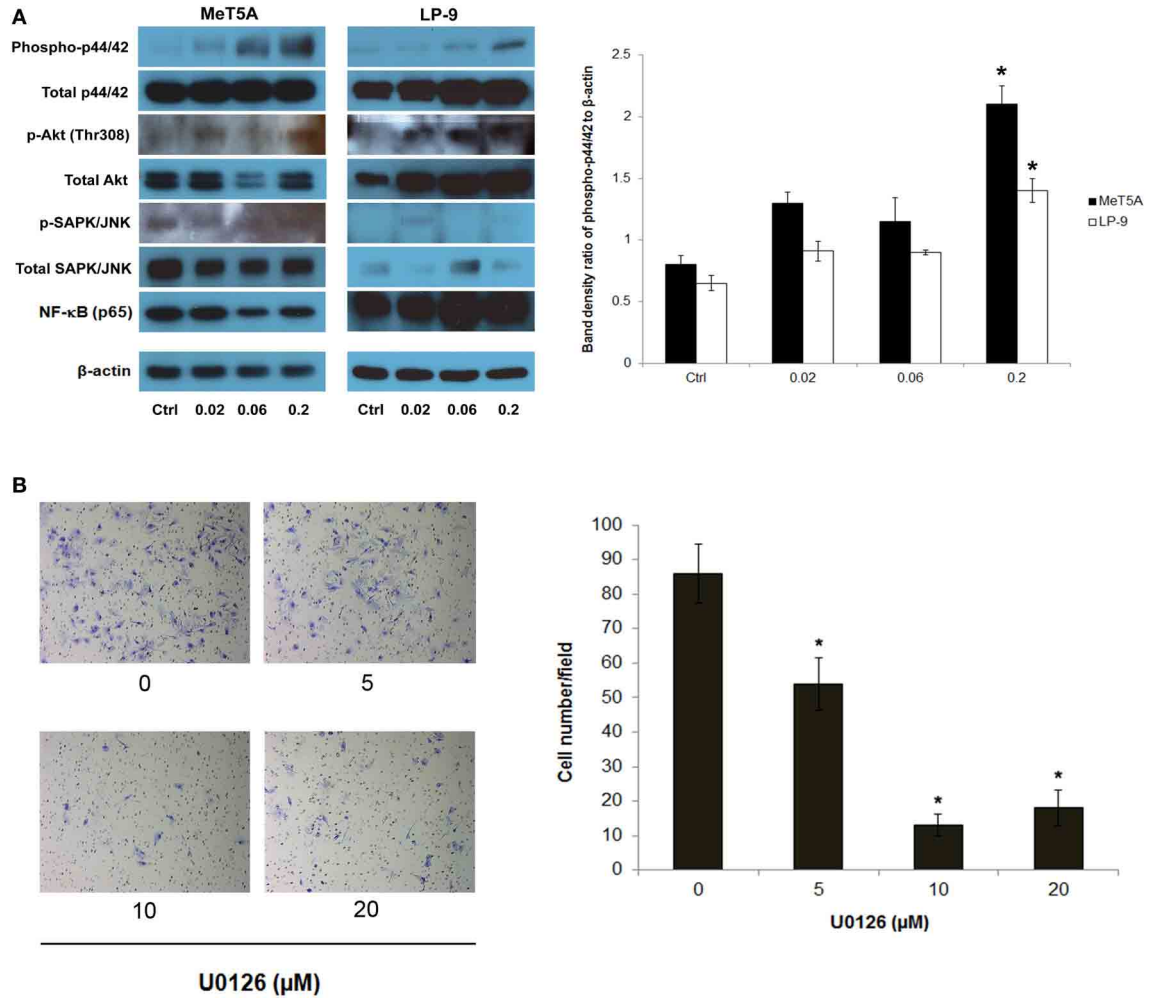

FIGURE 3 | Analysis of downstream effectors of H-Ras in SWCNT-exposed MeT-5A and LP-9 cells. A dose-dependent activation of p44/42 (ERK1/2) was evident in the SWCNT-exposed cells **(A)**. U0126, an ERK kinase inhibitor, was used to confirm the importance of ERK activation in the invasiveness of SWCNT-exposed cells. SWCNT (0.2 μg/cm^2)-exposed Met-5A cells were treated with various concentrations (5–20 μM) of U0126 for 2 h, after which they were washed and subjected to Transwell® invasion assay. A substantial and dose-dependent decrease in the number of invading cells was evident in the treatment groups **(B)**, *significantly difference from no treatment control with $P < 0.05$ ($n = 3$).

The results showed that the ERK inhibitor effectively inhibited the invasive activity of the cells in a dose-dependent manner (**Figure 3B**). These results support the role of ERK signaling downstream of H-Ras activation in SWCNT-induced cell invasiveness.

POTENTIAL GENES ASSOCIATED WITH ERK SIGNALING IN SWCNT-EXPOSED MESOTHELIAL CELLS

To determine the possible effectors of H-Ras-ERK signaling in the tested cells, whole genome expression data of SWCNT-exposed mesothelial cells from our previous study was subjected to IPA. Invasion GSN with first order relationship to ERK and a cross-section diagram for location of each gene within the cells are shown in **Figure 4**. Genes of potential interest to the SWCNT-induced cell invasiveness include some proteolytic enzyme-encoding genes (*MMP2*, *PLAU*), *AKT*, cyclin D1, integrin, several inflammatory genes, and EMT related genes (*TWIST*, *FN1*).

INTEGRIN ALPHA V AND CORTACTIN OVEREXPRESSION IN SWCNT-EXPOSED MESOTHELIAL CELLS

Further investigations on the genes from the invasion GSN were performed using Western blotting and quantitative real-time PCR. Western blot analysis showed a dose-dependent increase in integrin alpha V expression in SWCNT-exposed MeT-5A and LP-9 cells (**Figure 5A**). Cortactin, a protein known to be involved in cell motility and important in neoplasia development, was also overexpressed in the SWCNT-exposed cells. PCR analysis of EMT transcriptional regulators showed a repression of all EMT regulators examined in the exposed cells (**Figure 5B**). The relationship between cortactin and H-Ras-ERK activation was further evaluated by immunofluorescence staining. The results showed that cortactin was substantially induced in the SWCNT-exposed cells,

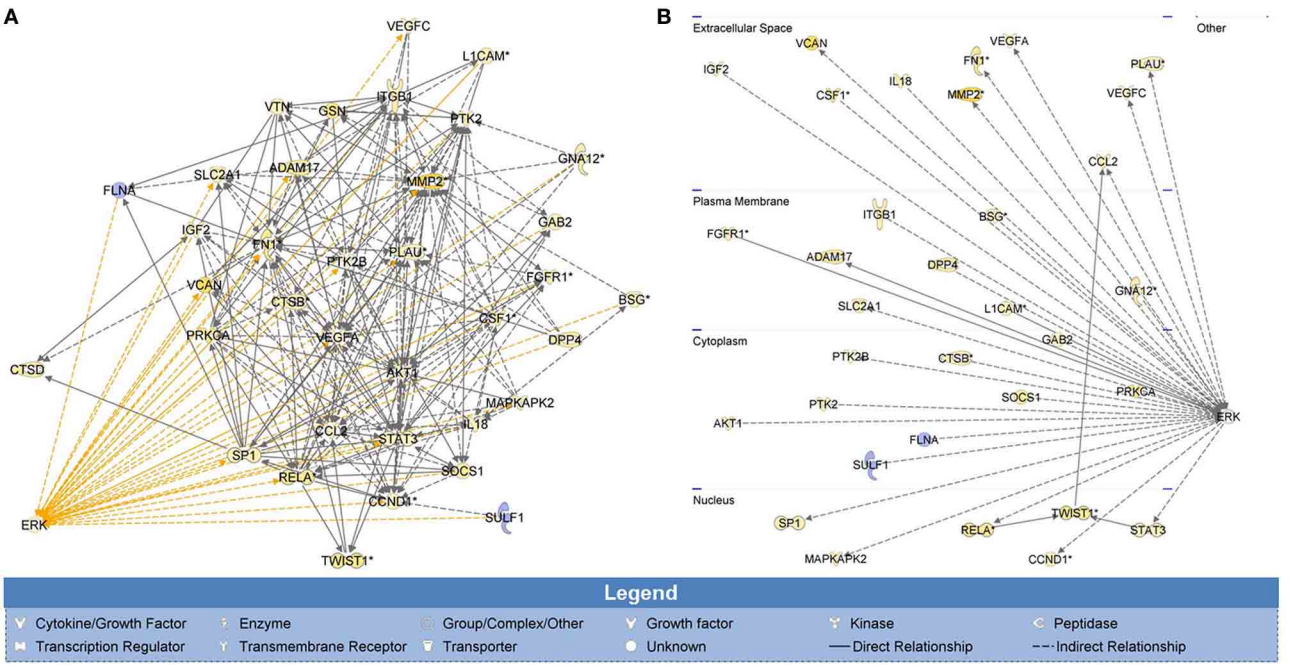

FIGURE 4 | Whole genome analysis of cell invasion network in SWCNT-exposed mesothelial cells. H-Ras-ERK invasion signaling network was created from whole genome expression data previously deposited on NCBI's Gene Expression Omnibus (GenBank ID: GSE48855) using IPA. Gene signaling networks (GSN) associated with cell invasion were created and mapped. Genes were included in the GSN if they promoted invasion and were overexpressed or if they inhibited invasion and were underexpressed. Invasion GSN with first order relationship to ERK **(A)** and a cross-section diagram for location of each gene within the cells **(B)** are shown. *MMP2, PLAU, AKT, CCND1, ITG,* several inflammatory genes and EMT-related genes (*TWIST, FN1*) were found to be the up-regulated genes with first relationship with ERK in the GSN. Most of these genes were reported to involve in cell motility and metastasis process.

consistent with the H-Ras/ERK data (**Figure 5C**). Overexpression of H-Ras in the MeT-5A cells also resulted in the up-regulation of cortactin (Supplementary Figure 1A), whereas siRNA downregulation of H-Ras decreased the cortactin expression in SWCNT-exposed cells (**Figure 5D**). In addition, the ERK kinase inhibitor U0126 mitigated the cortactin expression as analyzed by Western blotting (**Figure 5E**).

DISCUSSION

Rapid increase in CNT production and utility has raised a concern over the potential adverse effects of CNTs on human health and the environment. Both *in vivo* and *in vitro* studies have provided useful information on the biological and toxicological effects of CNTs; however, most of these studies have focused on short-term acute effects of the nanomaterials, which is due in part to the lack of appropriate experimental models for long-term studies. We have developed a chronic cellular exposure model to study the long-term biological effects of nanomaterials in various lung cell types including human bronchial epithelial cells (BEAS-2B), human small airway epithelial cells (SAEC), and human pleural mesothelial cells (MeT-5A) (Wang et al., 2011, 2014; Lohcharoenkal et al., 2013). Neoplastic transformation of these cells was demonstrated upon chronic exposure to low-dose CNTs as demonstrated by their anchorage-independent cell growth, apoptosis resistance, increased cell motility and angiogenesis. The induction of proto-oncogenes and cell division anomalies including centrosome fragmentation, mitotic spindle disruption, and aneuploidy has also been reported in CNT-exposed cells (Sargent et al., 2009; Wang et al., 2014). Despite its established importance in lung carcinogenesis, the role of H-Ras in CNT-induced carcinogenesis has not been reported, although a recent study indicated the involvement of H-Ras signaling in DNA damage caused by CNTs (Tong et al., 2011). Thus, the role of H-Ras in the neoplastic transformation of human mesothelial cells was focused in this study.

Two types of human mesothelial cells (MeT-5A and LP-9) were continuously exposed to different concentrations (0.02, 0.06, and 0.2 $\mu g/cm^2$) of SWCNT for 2 months and analyzed for cancer hallmark phenotypes. As shown in **Figure 1**, SWCNT induced colony formation and cell invasion in MeT-5A cells, whereas it induced mainly cell invasion with minimal effect on colony formation in LP-9 cells. Anchorage-independent cell growth is the most commonly used *in vitro* indicator of malignant transformation and it correlates well with *in vivo* tumorigenicity (Risser and Pollack, 1974; Shin et al., 1975). This indicates malignant transformation of SWCNT-exposed MeT-5A cells, although the control MeT-5A cells also formed slow-growing colonies on soft agar. This could be due to the fact that the cells were immortalized by transfection with the pRSV-T plasmid (an SV40 ori- construct containing the SV40 early region and sarcoma virus long terminal repeat). ATCC indicates that this cell line can form colonies in a semi-solid medium but is non-tumorigenic

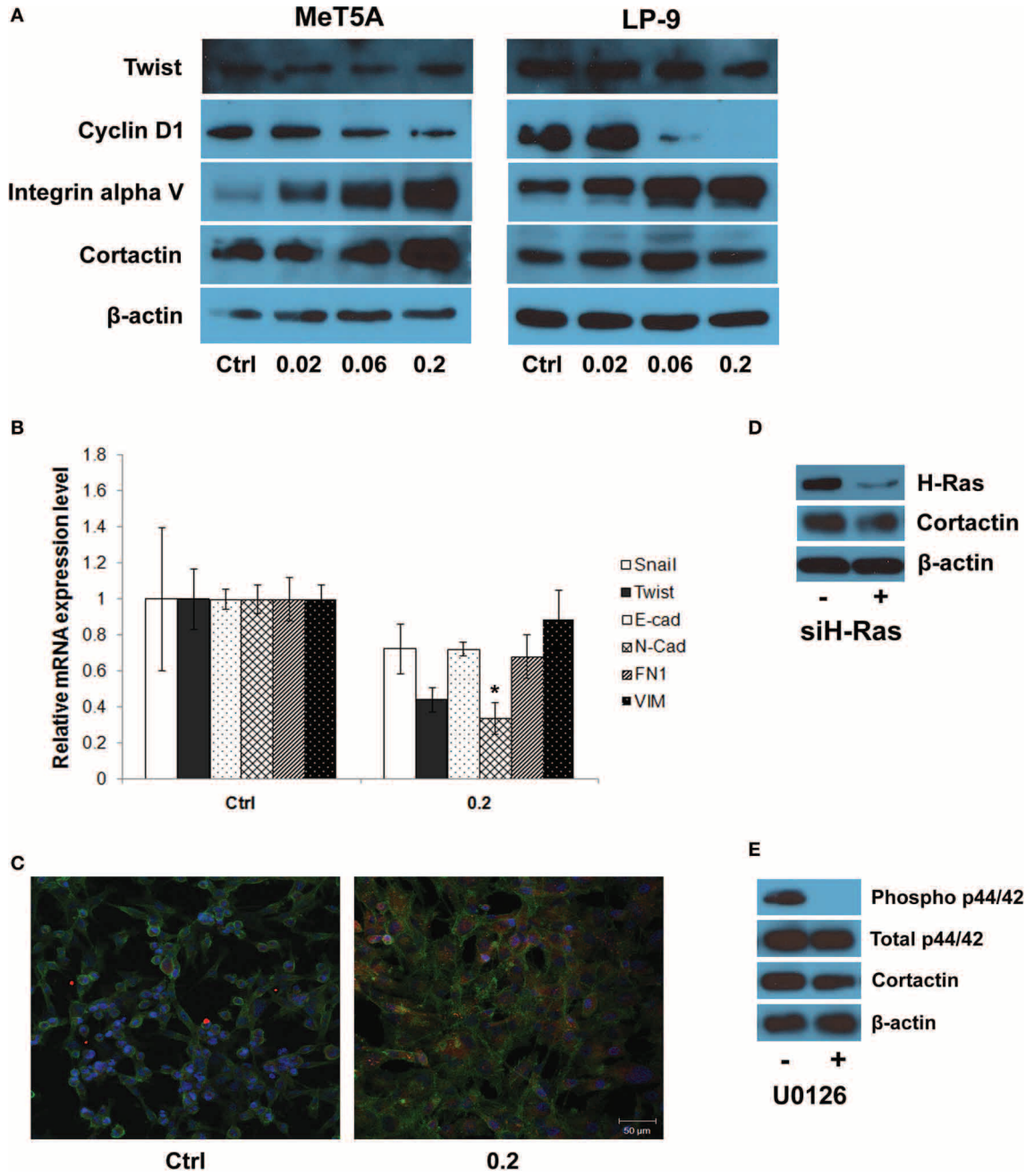

FIGURE 5 | Molecular and functional assays of genes in the gene signaling network. Western blot analysis showed a dose-dependent increase in integrin alpha V and cortactin expression in SWCNT-exposed MeT-5A and LP-9 cells **(A)**. Real-time PCR analysis showed a down-regulation of all EMT transcriptional regulators in SWCNT ($0.2\,\mu g/cm^2$)-exposed MeT-5A cells compared to control cells **(B)**. Immunofluorescence staining showed a substantial increase in cortactin protein expression in SWCNT ($0.2\,\mu g/cm^2$)-exposed MeT-5A cells compared to control cells **(C)**. Down-regulation of H-Ras by siH-Ras **(D)** and inactivation of ERK by U0126 **(E)** lowered the expression of cortactin in SWCNT-exposed MeT-5A cells. *Significantly difference from no treatment control with $P < 0.05$ ($n = 3$).

in immunocompromised mice. Therefore, the colony formation observed in the control cells is due to indigenous properties of the cells, and not because of their tumorigenicity. For normal cells, spontaneous colony formation was concentration dependent and the threshold for colony formation varied between cell types and some exogenous source of colony stimulating factor (CSF) may be needed. In case of normal mesothelial cells such as LP-9 cells, high concentrations of epidermal growth factor (EGF) and hydrocortisone in addition to fetal calf serum were required to induce colony formation in semi-solid medium

(La Rocca and Rheinwald, 1985). Cell invasion is a crucial step in many physiological processes and its impairment has been implicated in many pathological disorders such as tumor growth and metastasis. It has been used to assess the aggressive and malignant phenotypes of cells (Cho and Klemke, 2000). Our results demonstrated the induction of aggressive cancer phenotypes by SWCNT in mesothelial cells.

H-Ras expression was examined in SWCNT-exposed cells and was found to be elevated in both the SWCNT-exposed MeT-5A and LP-9 cells (**Figure 2A**). The functional importance of H-Ras overexpression was demonstrated by colony formation assay in H-Ras-transfected MeT-5A cells (Supplementary Figure 1B). Since overexpression of H-Ras has been shown to be important in cancer cell invasion and progression (Theodorescu et al., 1990), we hypothesized that H-Ras overexpression and the activation of its downstream targets may be crucial to the invasive transformation of SWCNT-exposed mesothelial cells. The results of our H-Ras knockdown experiments support this notion (**Figures 2B,C**).

Downstream effectors of *Ras* include members of the MAPK family comprising of JNK, ERK and stress-activated protein kinase-2 (p38). MAPKs are among the major kinases that transduce extracellular signaling into cellular responses and play a pivotal role in the regulation of cell proliferation, apoptosis, differentiation, cytoskeleton remodeling, and cell cycle regulation (Brunet and Pouyssegur, 1996; Foltz et al., 1997). Key effectors of Ras including ERK, JNK, AKT, and NF-κB were examined in SWCNT-exposed MeT-5A and LP-9 cells. An activation of ERK1/2 (p44/42) was prominent in these cells (**Figure 3A**), suggesting the possible role of H-Ras-ERK signaling in the invasiveness of SWCNT-exposed mesothelial cells. Our results on the inhibitory effect of U0126 ERK inhibitor on the invasivity of SWCNT-exposed MeT-5A cells support this notion (**Figure 3B**). Consistent with this finding, several studies have indicated the involvement of ERK in the migration and invasion of various forms of cancer including glioblastoma, pancreatic carcinoma and lung cancer (Lakka et al., 2000; Lu et al., 2011).

Invasion GSN obtained from the whole genome expression data of SWCNT-exposed mesothelial cells was created and filtered for ERK-related genes as shown in **Figure 4**. *MMP2*, *PLAU*, *AKT*, *CCND1*, *ITG*, several inflammatory genes and EMT-related genes (*TWIST*, *FN1*) were all up-regulated and exhibited the first relationship with ERK. *MMPs* are signature invasion marker genes that encode proteins involved in the degradation of ECM and are typically highly active during cancer development and progression (Passlick et al., 2000). MMPs belong to a family of zinc-dependent endopeptidases which are divided into different classes. MMP-2 (gelatinase A) has an important role in basement membrane turnover due to its specific activity to collagen type IV or gelatin. Its degradation plays a role in cell invasion of the vasculature and is considered to have a key role in metastasis. *MMP-2* expression has been associated with the invasiveness of many cancer cell lines and is elevated in high-grade tumors, specifically at the invasive front and in vascular invasion (Birkedal-Hansen et al., 1993; Coussens and Werb, 1996). Our previous study has demonstrated the importance of MMP-2 in cell invasion induced by chronic CNT and asbestos exposure (Lohcharoenkal et al., 2013). Urokinase-plasminogen activator or *PLAU* gene is known to encode uPA, the protease which degrades ECM and plays critical roles in cell migration, tissue remodeling, angiogenesis, tumor invasion, and metastasis (Suzuki et al., 2004). Plasminogen activators convert plasminogen to plasmin, which works efficiently in proteolysis of the fibrin. In addition, plasminogen activators activate several MMPs and could also facilitate the MMP activities. A positive feedback loop between the binding of uPA to uPA receptor (uPAR) and Ras-ERK signaling pathway activation has been reported in many cell types and implicated in cell migration and progression of cancer (Ma et al., 2001). AKT (also known as protein kinase B or PKB) is a serine/threonine kinase that is involved in mediating various biological responses, such as inhibition of apoptosis and stimulation of cell proliferation. There are three highly related isoforms of AKT (AKT1, AKT2, and AKT3) and these represent the major signaling arm of PI3K (Park et al., 2001). MEK/ERK and PI3K/AKT pathways are often concurrently activated by separate genetic alterations in cancer cells but it was reported that ERK and AKT signaling cooperate to translationally regulate metastatic progression of certain types of cancer, e.g., colorectal cancer (Ye et al., 2013). Integrins are cell surface receptors that interact with ECM and mediate intracellular signals that regulate many cellular processes including cell shape, mobility and progression through the cell cycle (Hynes, 2001). Integrins play an important role in cell signaling by affecting the cell signaling pathways of protein kinases including Ras-Raf-MEK-ERK pathway (Schlaepfer et al., 1994). Numerous studies have shown that integrin expression profiles are subject to change during cancer growth and progression and that such change contributes to the aggressive behavior of cancer cells (Danen and Sonnenberg, 2003; Danen, 2005). The enhanced expression of integrin is reported to be associated with EMT and poor prognosis of cancer (Bates et al., 2005).

Western blot and real-time PCR studies demonstrated the up-regulation of integrin alpha V, but not EMT transcriptional regulators, in SWCNT-exposed mesothelial cells (**Figures 5A,B**). Since integrin/focal adhesion kinase (FAK)/cortactin has been reported to regulate cell motility and proliferation, cortactin expression in the SWCNT-exposed cells was examined and found to be upregulated in the SWCNT-exposed MeT-5A and LP-9 cells (**Figure 5A**). Cortactin is a multidomain adapter protein, essentially contributing to cortical actin regulation. Regulation of this pool of actin is controlled by a variety of actin regulatory proteins at integrin or cadherin adhesion sites and is important in many normal and pathological cellular processes, such as adhesion, migration, morphogenesis, tumor progression and metastasis (Weed and Parsons, 2001; Clark et al., 2007). Cortactin functions in actin assembly via interaction with actin-related protein-2/3 (Arp2/3) complex, which is dependent on Src-mediated phosphorylation of cortactin (Schubert and Dotti, 2007).

Besides tyrosine phosphorylation, cortactin is a target for multiple serine/threonine kinases (Martin et al., 2006). Stimulation of tumor cells with EGF leads to phosphorylation of serine residues 405 and 418, coincident with a characteristic shift in cortactin electrophoretic mobility from 80 to 85 kDa

in SDS-PAGE. The mobility shift and phosphorylation of S405/S418 are impaired by pharmacologic inhibition of mitogen activated protein/extracellular signal regulated kinase (MEK)1/2. Biochemical evidence indicates that the MEK effector kinases ERK1/2 directly phosphorylate cortactin at these sites (Campbell et al., 1999). Thus, the relationship between cortactin and H-Ras-ERK activation in SWCNT-exposed cells was evaluated and the positive correlation between H-Ras and cortactin expression was observed (**Figure 5C** and Supplementary Figure 1A). In good agreement, knockdown of H-Ras or chemical inhibition of ERK kinase decreased the level of cortactin expression in the SWCNT-exposed cells (**Figures 5D,E**).

In summary, we demonstrated that prolonged exposure of human mesothelial cells to SWCNT induced aggressive neoplastic-like transformation in concomitant with H-Ras up-regulation. knockdown and overexpression studies indicated the relationship between H-Ras expression and the invasive phenotype of SWCNT-exposed cells. ERK1/2 was identified as an important effector for the aggressive phenotype of the cells as indicated by their reduced invasiveness by ERK kinase inhibitor. Whole genome microarray and Western blot analyses indicated the possible involvement of integrin alpha V in the H-Ras-ERK invasion signaling. Additionally, cortactin was shown to be a downstream target of H-Ras-ERK signaling in the SWCNT-exposed cells.

AUTHOR CONTRIBUTIONS

Warangkana Lohcharoenkal designed and performed cellular and molecular studies, and prepared the manuscript. Liying Wang prepared nanoparticle preparations and performed chronic exposure. Todd A. Stueckle performed microarray and Ingenuity Pathway Analysis. Jino Park performed real-time PCR experiments. William Tse participated in the design of the study and provided research reagents. Cerasela-Zoica Dinu characterized nanomaterials. Yon Rojanasakul designed and coordinated the project, and prepared the manuscript. All authors read and approved the final manuscript.

DISCLAIMER

The findings and conclusions in this report are those of the authors and do not necessarily represent the views of the National Institute for Occupational Safety and Health.

ACKNOWLEDGMENTS

This work was supported by grants from the National Institutes of Health (R01-HL095579 and R01-ES022968) and National Science Foundation (EPS-1003907). Imaging experiments were performed in the West Virginia University Imaging Facility, which is supported in part by the Mary Babb Randolph Cancer Center and NIH grants P20 RR016440, P30 RR032138/GM103488, and P20 RR016477.

SUPPLEMENTARY MATERIAL

The Supplementary Material for this article can be found online at: http://www.frontiersin.org/journal/10.3389/fphys.2014.00222/abstract

REFERENCES

Barbacid, M. (1987). Ras genes. *Annu. Rev. Biochem.* 56, 779–827. doi: 10.1146/annurev.bi.56.070187.004023

Bates, R. C., Bellovin, D. I., and Brown, C. (2005). Transcriptional activation of integrin β6 during the epithelial-mesenchymal transition defines a novel prognostic indicator of aggressive colon carcinoma. *J. Clin. Invest.* 115, 339–347. doi: 10.1172/JCI200523183

Birkedal-Hansen, H., Moore, W. G., and Bodden, M. K. (1993). Matrix metalloproteinases: a review. *Crit. Rev. Oral Biol. Med.* 4, 197–250.

Boguski, M. S., and McCormick, F. (1993). Proteins regulating Ras and its relatives. *Nature* 366, 643–654. doi: 10.1038/366643a0

Brunet, A., and Pouyssegur, J. (1996). Identification of MAP kinase domains by redirecting stress signals into growth factor responses. *Science* 272, 1652–1655. doi: 10.1126/science.272.5268.1652

Campbell, D. H., Sutherland, R. L., and Daly, R. J. (1999). Signaling pathways and structural domains required for phosphorylation of EMS1/cortactin. *Cancer Res.* 59, 5376–5385.

Cho, S. Y., and Klemke, R. L. (2000). Extracellular-regulated kinase activation and cas/crk coupling regulate cell migration and suppress apoptosis during invasion of the extracellular matrix. *J. Cell Biol.* 149, 223–236. doi: 10.1083/jcb.149.1.223

Clark, E. S., Whigham, A. S., Yarbrough, W. G., and Weaver, A. M. (2007). Cortactin is an essential regulator of matrix metalloproteinase secretion and extracellular matrix degradation in invadopodia. *Cancer Res.* 67, 4227–4235. doi: 10.1158/0008-5472.CAN-06-3928

Coussens, L. M., and Werb, Z. (1996). Matrix metalloproteinases and the development of cancer. *Chem. Biol.* 3, 895–904. doi: 10.1016/S1074-5521(96)90178-7

Danen, E. H. J. (2005). Integrins: regulators of tissue function and cancer progression. *Curr. Pharm. Des.* 11, 881–891. doi: 10.2174/1381612053381756

Danen, E. H. J., and Sonnenberg, A. (2003). Integrins in regulation of tissue development and function. *J. Pathol.* 201, 632–641. doi: 10.1002/path.1472

Diaz-Meco, M. T., Lozano, J., Municio, M. M., Berra, E., Frutos, S., Sanz, L., et al. (1994). Evidence for the *in vitro* and *in vivo* interaction of Ras with protein kinase C zata. *J. Biol. Chem.* 269, 31706–31710.

Foltz, I. N., Lee, J. C., Young, P. R., and Schrader, J. W. (1997). Hemopoietic growth factors with the exception of interleukin-4 activate the p38 mitogen-activated protein kinase pathway. *J. Biol. Chem.* 272, 3296–3301. doi: 10.1074/jbc.272.6.3296

Hynes, R. O. (2001). Integrins: bidirectional, allosteric signaling machines. *Cell* 110, 673–687. doi: 10.1016/S0092-8674(02)00971-6

Joneson, T., White, M. A., Wigler, M. H., and Bar-Sagi, D. (1996). Stimulation of membrane ruffling and MAP kinase activation by distinct effectors of RAS. *Science* 271, 810–812. doi: 10.1126/science.271.5250.810

Kapeller, R., and Cantley, L. C. (1994). Phosphatidylinositol 3-kinase. *Bioessays* 16, 565–576. doi: 10.1002/bies.950160810

Kiaris, H., and Soandidos, D. A. (1995). Analysis of H-ras, K-ras and N-ras genes for expression, mutation and amplification in laryngeal tumours. *Int. J. Oncol.* 7, 75–80.

Kolch, W. (2002). Ras/Raf signaling and emerging pharmacotherapeutic targets. *Expert Opin. Pharmacother.* 3, 709–718. doi: 10.1517/14656566.3.6.709

Kyriakis, J. M., App, H., Zhang, X. F., Banerjee, P., Brautigan, D. L., Rapp, U. R., et al. (1992). Raf-1 activates MAP kinase-kinase. *Nature* 358, 417–421. doi: 10.1038/358417a0

Lakka, S. S., Jasti, S. L., Kyritsis, A. P., Yung, W. K., Ali-Osman, F., Nicolson, G. L., et al. (2000). Regulation of MMP-9 (type IV collagenase) production and invasiveness in gliomas by the extracellular signal-regulated kinase and jun amino-terminal kinase signaling cascades. *Clin. Exp. Metastasis* 18, 245–252. doi: 10.1023/A:1006724826083

La Rocca, P. J., and Rheinwald, J. G. (1985). Anchorage-independent growth of normal human mesothelial cells: a sensitive bioassay for EGF which discloses the absence of this factor in fetal calf serum. *In Vitro Cell. Dev. Biol.* 21, 67–72. doi: 10.1007/BF02620917

Lohcharoenkal, W., Wang, L., Stueckle, T. A., Dinu, C. Z., Castranova, V., Liu, Y., et al. (2013). Chronic exposure to carbon nanotubes induces invasion of human mesothelial cells through matrix metalloproteinase-2. *ACS Nano* 7, 7711–7723. doi: 10.1021/nn402241b

Lowy, D. R., and Willumsen, B. M. (1993). Function and regulation of ras. *Annu. Rev. Biochem.* 62, 851–891. doi: 10.1146/annurev.bi.62.070193.004223

Lu, Z., Ding, L., Hong, H., Hoggard, J., Lu, Q., and Chen, Y. H. (2011). Claudin-7 inhibits human lung cancer migration and invasion through ERK/MAPK signaling pathway. *Exp. Cell Res*. 317, 1935–1946. doi: 10.1016/j.yexcr.2011.05.019

Ma, Z., Webb, D. J., Jo, M., and Gonias, S. L. (2001). Endogenously produced urokinase-type plasminogen activator is a major determinant of the basal level of activated ERK/MAP kinase and prevents apoptosis in MDA-MB-231 breast cancer cells. *J. Cell Sci.* 114, 3387–3396.

Marshall, C. J. (1996). Ras effectors. *Curr. Opin. Cell Biol.* 8, 197–204. doi: 10.1016/S0955-0674(96)80066-4

Martin, K. H., Jeffery, E. D., Grigera, P. R., Shabanowitz, J., Hunt, D. F., and Parsons, J. T. (2006). Cortactin phosphorylation sites mapped by mass spectrometry. *J. Cell Sci*. 119, 2851–2853. doi: 10.1242/jcs03034

Moon, A., Kim, M. S., Kim, T. G., Kim, S. H., Kim, H. E., Chen, Y. Q., et al. (2000). H-*ras*, but not N-*ras*, induces an invasive phenotype in human breast epithelial cells: a role for MMP-2 in the h-*ras*-induced invasive phenotype. *Int. J. Cancer* 85, 176–181. doi: 10.1002/(SICI)1097-0215(20000115)85:2%3C176::AID-IJC5%3E3.0.CO;2-E

Ottestad, L., Tveit, K. M., HÃifÃdt, H. K., Nesland, J. M., Vaage, S., HÃie, J., et al. (1988). Cultivation of human breast carcinoma in soft agar. Experience with 237 fresh tumour specimens. *Br. J. Cancer* 58, 8–12. doi: 10.1038/bjc.1988.151

Park, B. K., Zeng, X., and Glazer, R. I. (2001). Akt1 induces extracellular matrix invasion and matrix metalloproteinase-2 activity in mouse mammary epithelial cells. *Cancer Res*. 61, 7647–7653.

Passlick, B., Sienel, W., and Seen-Hibler, R. (2000). Overexpression of matrix metalloproteinase 2 predicts unfavorable outcome in early-stage non-small cell lung cancer. *Clin. Cancer Res*. 6, 3944–3948.

Risser, R., and Pollack, R. (1974). A non-selective analysis of SV40 transformation of mouse 3T3 cells. *Virol* 59, 477–489. doi: 10.1016/0042-6822(74)90457-7

Rodriguez-Viciana, P., Warne, P. H., Dhand, R., Vanhaesebroeck, B., Gout, I., Fry, M. J., et al. (1994). Phosphatidylinositol-3-OH kinase direct target of Ras. *Nature* 370, 527–532. doi: 10.1038/370527a0

Sakamoto, Y., Nakae, D., Fukumori, N., Tayama, K., Maekawa, A., Imai, K., et al. (2009). Induction of mesothelioma by a single intrascrotal administration of multi-wall carbon nanotube in intact male Fischer 344 rats. *J. Toxicol. Sci*. 34, 65–76. doi: 10.2131/jts.34.65

Sargent, L. M., Porter, D. W., Staska, L. M., Hubbs, A. F., Lowry, D. T., Battelli, L., et al. (2014). Promotion of lung adenocarcinoma following inhalation exposure to multi-walled carbon nanotubes. *Part. Fibre Toxicol.* 11, 3. doi: 10.1186/1743-8977-11-3

Sargent, L. M., Shvedova, A. A., Hubbs, A. F., Salisbury, J. L., Benkovic, S. A., Kashon, M. L., et al. (2009). Induction of aneuploidy by single-walled carbon nanotubes. *Environ. Mol. Mutagen*. 50, 708–717. doi: 10.1002/em.20529

Schlaepfer, D. D., Hanks, S. K., Hunter, T., and Van der Geer, P. (1994). Integrin-mediated signal transduction linked to Ras pathway by GRB2 binding to focal adhesion kinase. *Nature* 372, 786–791.

Schubert, V., and Dotti, C. G. (2007). Transmitting on actin: synaptic control of dendritic architecture. *J. Cell Sci.* 120, 205–212. doi: 10.1242/jcs.03337

Shin, S., Freedman, V. H., Risser, R., and Pollack, R. (1975). Tumorigenicity of virus-transformed cells in nude mice is correlated specifically with anchorage independent growth *in vitro*. *Proc. Natl. Acad. Sci. U.S.A.* 72, 4435–4439. doi: 10.1073/pnas.72.11.4435

Stites, E. C., and Ravichandran, K. S. (2009). A systems perspective of ras signaling in cancer. *Clin. Cancer Res*. 15, 1510–1513. doi: 10.1158/1078-0432.CCR-08-2753

Suzuki, M., Kobayashi, H., Kanayama, N., Saga, Y., Suzuki, M., Lin, C. Y., et al. (2004). Inhibition of tumor invasion by genomic down-regulation of matriptase through suppression of activation of receptor-bound pro-urokinase. *J. Biol. Chem*. 279, 14899–14908. doi: 10.1074/jbc.M313130200

Takagi, A., Hirose, A., Futakuchi, M., Tsuda, H., and Kanno, J. (2012). Dose-dependent mesothelioma induction by intraperitoneal administration of multi-wall carbon nanotubes in p53 heterozygous mice. *Cancer Sci.* 103, 1440–1444. doi: 10.1111/j.1349-7006.2012.02318.x

Takagi, A., Hirose, A., Nishimura, T., Fukumori, N., Ogata, A., Ohashi, N., et al. (2008). Induction of mesothelioma in p53+/- mouse by intraperitoneal application of multi-walled carbon nanotube. *J. Toxicol. Sci.* 33, 105–116. doi: 10.2131/jts.33.105

Theodorescu, D., Cornil, I., Fernandez, B. J., and Kerbel, R. S. (1990). Overexpression of normal and mutated forms of HRAS induces orthotopic bladder invasion in a human transitional cell carcinoma. *Proc. Natl. Acad. Sci. U.S.A*. 87, 9047–9051. doi: 10.1073/pnas.87.22.9047

Tong, L., Zhang, W., Hang, H., Yu, Z., Chu, P. K., and Hu, A. (2011). Toxicity of carbon nanotubes to p21 and hus1 gene deficient mammalian cells. *J. Nanosci. Nanotechnol*. 11, 11001–11005. doi: 10.1166/jnn.2011.3958

Wang, L., Luanpitpong, S., Castranova, V., Tse, W., Lu, Y., Pongrakhananon, V., et al. (2011). Carbon nanotubes induce malignant transformation and tumorigenesis of human lung epithelial cells. *Nano Lett.* 11, 2796–2803. doi: 10.1021/nl2011214

Wang, L., Stueckle, T. A., Mishra, A., Derk, R., Meighan, T., Castranova, V., et al. (2014). Neoplastic-like transformation effect of single-walled and multi-walled carbon nanotubes compared to asbestos on human lung small airway epithelial cells. *Nanotoxicol.* 8, 485–507. doi: 10.3109/17435390.2013.801089

Weed, S. A., and Parsons, J. T. (2001). Cortactin: coupling membrane dynamics to cortical actin assembly. *Oncogene* 20, 6418–6434. doi: 10.1038/sj.onc.1204783

Ye, Q., Cai, W., Zheng, Y., Evers, B. M., and She, Q. B. (2013). ERK and AKT signaling cooperate to translationally regulate surviving expression for metastatic progression of colorectal cancer. *Oncogene* 33, 1828–1839. doi: 10.1038/onc.2013.122

Conflict of Interest Statement: The authors declare that the research was conducted in the absence of any commercial or financial relationships that could be construed as a potential conflict of interest.

Received: 09 March 2014; accepted: 27 May 2014; published online: 12 June 2014.
*Citation: Lohcharoenkal W, Wang L, Stueckle TA, Park J, Tse W, Dinu C-Z and Rojanasakul Y (2014) Role of H-Ras/ERK signaling in carbon nanotube-induced neoplastic-like transformation of human mesothelial cells. Front. Physiol. **5**:222. doi: 10.3389/fphys.2014.00222*
This article was submitted to Membrane Physiology and Membrane Biophysics, a section of the journal Frontiers in Physiology.

Advantages of publishing in Frontiers

OPEN ACCESS
Articles are free to read for greatest visibility and readership

FAST PUBLICATION
Around 90 days from submission to decision

HIGH QUALITY PEER-REVIEW
Rigorous, collaborative, and constructive peer-review

TRANSPARENT PEER-REVIEW
Editors and reviewers acknowledged by name on published articles

Frontiers
Avenue du Tribunal-Fédéral 34
1005 Lausanne | Switzerland

Visit us: www.frontiersin.org
Contact us: info@frontiersin.org | +41 21 510 17 00

REPRODUCIBILITY OF RESEARCH
Support open data and methods to enhance research reproducibility

DIGITAL PUBLISHING
Articles designed for optimal readership across devices

FOLLOW US
@frontiersin

IMPACT METRICS
Advanced article metrics track visibility across digital media

EXTENSIVE PROMOTION
Marketing and promotion of impactful research

LOOP RESEARCH NETWORK
Our network increases your article's readership